

Structural and Functional Aspects of Metal Sites in Biology

Richard H. Holm,^{*,†} Pierre Kennepohl,[‡] and Edward I. Solomon^{*,‡}

Departments of Chemistry, Harvard University, Cambridge, Massachusetts 02138, and Stanford University, Stanford, California 94305

Received June 10, 1996 (Revised Manuscript Received September 3, 1996)

Contents

I. Introduction	2239
II. Metallobiomolecules as Elaborated Inorganic Complexes	2239
A. Coordinated Ligands	2240
B. Unique Properties of a Protein Ligand	2246
C. Physical Methods	2250
III. Active-Site Structure/Function Relationships	2251
A. Electron Transfer	2251
B. Dioxygen Binding	2263
C. Superoxide and Peroxide Dismutases and Non-Heme Peroxidases	2270
D. Oxidases and Oxygenases	2275
E. Hydrogenases and Nitrogenases	2287
F. Oxotransferases	2293
G. Transport and Storage Proteins	2296
H. Nonredox Enzymes	2300
IV. Prospectus	2306
V. References	2307

I. Introduction

The field of bioinorganic chemistry is at a propitious stage of development. Ever more complex metallobiomolecules are isolated and purified, physical methodologies and attendant theories probe even more deeply into the intricacies of electronic structure and structural dynamics, chemical syntheses of protein and metal coordination units become more sophisticated, and biochemical syntheses with site-directed mutagenesis disclose functions of specific amino acid residues. Inasmuch as explication of function is the ultimate investigative goal of any biological process, and function is inseparable from geometric structure, the ever-increasing crystallographic database of protein structure assumes an even greater significance. One need only contemplate the active-site structures of, *inter alia*, such complex molecules as nitrogenase,¹ cytochrome *c* oxidase,^{2,3} sulfite reductase,⁴ and ceruloplasmin⁵ reported within the last four years, to recognize that these can now be conceived at a molecular level of detail. For present purposes, a protein-bound metal site consists of one or more metal ions and all protein side chain and exogenous bridging and terminal ligands that define the first coordination sphere of each metal ion. Such sites can be classified into five basic types with the indicated functions:

(i) *structural*—configuration (in part) of protein tertiary and/or quaternary structure;

(ii) *storage*—uptake, binding, and release of metals in soluble form;

(iii) *electron transfer*—uptake, release, and storage of electrons;

(iv) *dioxygen binding*—metal-O₂ coordination and decoordination;

(v) *catalytic*—substrate binding, activation, and turnover.

We present here a classification and structure/function analysis of native metal sites based on these functions, where *v* is an extensive class subdivided by the type of reaction catalyzed (dismutases, oxidases and oxygenase, nitrogenases and hydrogenases, oxotransferases, hydrolases, and others). In order to restrict the scope of information presented to a manageable size, sites containing heme and corrin units have been excluded with only several exceptions. Here, structure refers primarily to crystallographic information. Not included in the tabulations of site structures which follow are (partial) structural deductions from X-ray absorption spectroscopy, NMR, and other spectroscopic techniques. Within this purview, coverage of the various site types is extensive, but not exhaustive. The purpose of this exposition is to present examples of all types of sites and to relate, insofar as is currently feasible, the structure and function of selected sites. Functional aspects of the latter and other sites are the subjects of accompanying contributions in this issue. We largely confine our considerations to the sites themselves, with due recognition that these site features are coupled to protein structure at all levels. In the next section, the coordination chemistry of metalloprotein sites and the unique properties of a protein as a ligand are briefly summarized. In section III, structure/function relationships are systematically explored and tabulations of structurally defined sites presented. Other compilations of metalloprotein structures have been made earlier.⁶ Finally, in section IV, future directions in bioinorganic research in the context of metal site chemistry are considered. Throughout, it will be evident that a high-resolution metalloprotein structure provides the initial point for penetrating the complexities of site function. But as such, it is only the beginning, and not the end, of any inquiry into function.

II. Metallobiomolecules as Elaborated Inorganic Complexes

Of the 4048 protein crystal structures contained in the Brookhaven Protein Data Bank as of December 1995, 2123 (52%) contain metals (excluding weakly bound metals such as sodium).⁷ This count includes proteins and enzymes with heme and corrin groups

[†] Harvard University.

[‡] Stanford University.

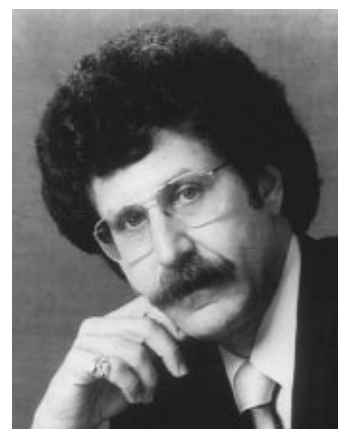


Richard H. Holm was born in Boston, MA, spent his younger years on Nantucket Island and Cape Cod, and graduated from the University of Massachusetts (B.S.) and Massachusetts Institute of Technology (Ph.D.). He has served on the faculties of the University of Wisconsin, the Massachusetts Institute of Technology, and Stanford University. Since 1980 he has been at Harvard University, where he has been Chairman of the Department of Chemistry, and since 1983 Higgins Professor of Chemistry. His research interests are centered in inorganic and bioinorganic chemistry, with particular reference to the synthesis of molecules whose structures and reactions are pertinent to biological processes.



Pierre Kennepohl was born Dec 12, 1970, in Scarborough, Canada, although he has spent most of his life in Montréal, Canada, which he considers home. Pierre completed his B.Sc. in chemistry at Concordia University in Montréal as a member of its Institute for Cooperative Education, which provided him with research opportunities in several areas including enzymology, solid-state chemistry, and pulse radiolysis. He was also fortunate to study under Professor Nick Serpone at Concordia, where he studied the photochemical and photophysical properties of surface-modified TiO_2 . Pierre is currently working toward his Ph.D. in inorganic chemistry at Stanford under the guidance of Professor Edward I. Solomon, with financial support from NSERC (Canada) in the form of a 1967 Science & Engineering Scholarship. His research interests include the elucidation of detailed electronic structure contributions to electron transfer processes in iron-sulfur centers and other redox-active metal sites in biology. He also enjoys any opportunity to involve himself in the teaching of chemistry and is presently a teaching consultant at Stanford. When not worrying about things like electronic relaxation and redox potentials, Pierre likes to spend time playing and writing music and getting involved in departmental affairs.

and is biased by the inclusion of mutated forms of certain metalloproteins and structures of the same enzyme with different substrates and inhibitors. Nonetheless, the pervasiveness of metals in biology is impressive. It has been variously estimated that approximately one-third of all proteins and enzymes purified to apparent homogeneity require metal ions as cofactors for biological function.



Edward I. Solomon grew up in North Miami Beach, FL, received his Ph.D. from Princeton University (with D. S. McClure), and was a postdoctoral fellow at the H. C. Ørsted Institute (with C. J. Ballhausen) and then at Caltech (with H. B. Gray). He was a professor at the Massachusetts Institute of Technology until 1982, when he moved to Stanford University, where he is now the Monroe E. Spaght Professor of Humanities and Sciences. His research is in the fields of physical-inorganic and bioinorganic chemistry with emphasis on the application of a wide variety of spectroscopic methods to elucidate the electronic structure of transition metal complexes and its contribution to physical properties and reactivity.

Metals which occur in the five types of sites above, or can be substituted for the native constituent, are "biological" metals. This set includes magnesium, calcium, all members of the first transition series (excluding scandium, titanium, and chromium), and molybdenum, tungsten, cadmium, and mercury. These metals and their ligands constitute *prosthetic groups* that usually are covalently bound to the polypeptide backbone by endogenous ligands provided by amino acid side chains. As initial examples, consider the structures of the electron-transfer proteins plastocyanin and rubredoxin in Figure 1. Shown are the single-chain protein structures and, in magnified form, the $[\text{Cu}^{\text{II}}(\text{N}\cdot\text{His})(\text{S}\cdot\text{Met})(\text{S}\cdot\text{Cys})]$ and $[\text{Fe}^{\text{III}}(\text{S}\cdot\text{Cys})_4]$ active sites. These depictions illustrate the protein structures which, although somewhat complicated, reduce in each case to a spatially correlated tetradentate ligand. Protein structure and environment modulate properties such as electronic structure, redox potential, and detailed stereochemistry, some or all of which in the general case will depart from the intrinsic value of the coordination unit removed from the protein and allowed to relax to its energy minimum. It is in this sense that a metallo-biomolecule is an elaborated metal complex. In this section, we focus on metal ion active sites and consider the properties of the protein as a unique ligand.

A. Coordinated Ligands

It is important first to recognize metalloproteins in which a metal is enclosed by a macrocyclic ligand that forms the equatorial plane of coordination. These include heme and corrin units, which may be either covalently or noncovalently (through hydrophobic interactions) bound to the protein. For these prosthetic groups, the intrinsic properties of the metal are strongly coupled to those of the macrocycle, primarily through extensive delocalization of d orbitals into the π -orbital network of the ring. In particular, the iron site in a heme can have very different

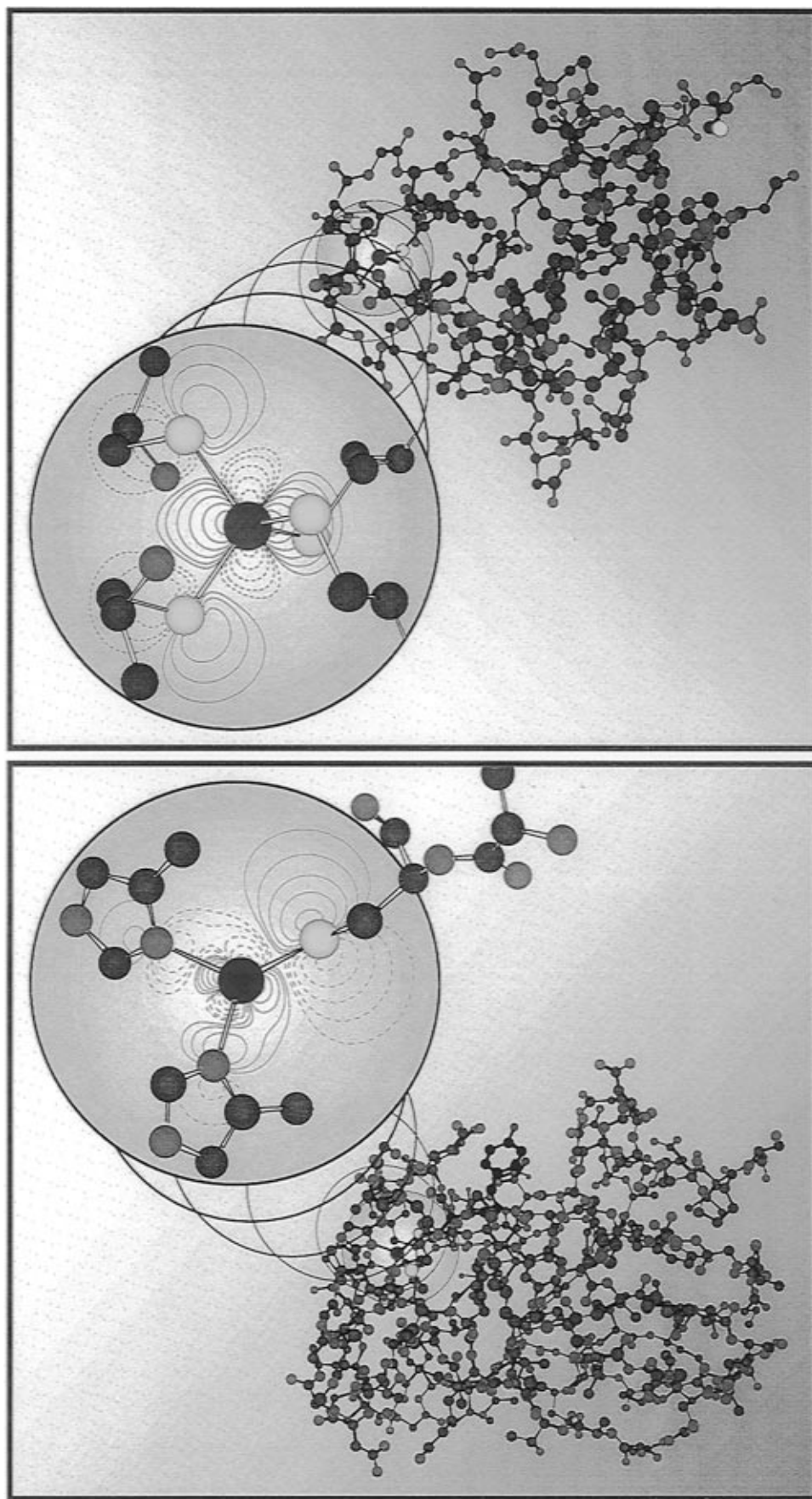
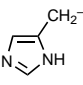
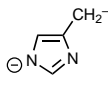
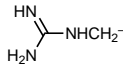
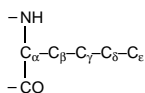


Figure 1. Expanded views of geometric and electronic structure of the active sites of plastocyanin (left) and rubredoxin (right). The expanded plastocyanin site is rotated such that the Met-S-Cu bond is out of the plane of the page. Contour values are set to ± 0.16 , ± 0.08 , ± 0.04 , ± 0.02 , and ± 0.01 (e/μ_B^3), with positive contours in solid red and negative values in dashed blue.

Table 1. Endogenous Biological Ligands[†]

coordinating group		nomenclature ^a (examples)	pK _a ^b
N-Donors			
amino:	side chain	H ₂ N ^c ·Lys	9–11 ^c
	N-terminus	H ₂ N·X (any residue)	
amido:	backbone (–NHC(O)–)	HN·X (any residue)	≈13
	side chain (–C(O)NH ₂)	HN ^γ ·Asn, HN ^δ ·Gln	
amidato:	backbone (–N–C(O)–) [–]	[–] N·X (any residue)	≈14 ^d
	side chain (–C(O)NH) [–]	[–] N ^γ ·Asn, [–] N ^δ ·Gln	
imidazolyl		N·His	
imidazolato		[–] N·His	
guanidine		H ₂ N ^δ ·Arg	>12 ^e
O-Donors			
carbamate		O ₂ CNH·Lys	
carboxylate:	side chain	O ₂ C ^γ ·Asp, O ₂ C ^δ ·Glu	4–5
	C-terminus	O ₂ C·X (any residue)	
carbonyl:	side chain	OC ^γ ·Asn, OC ^δ ·Gln	10
	backbone	OC·X (any residue)	
phenol		HO·Tyr	
phenolate		O·Tyr	
hydroxyl		HO·X (X = Ser, Thr)	≈14
olate		O·X (X = Ser, Thr)	
S-Donors			
thioether		S·Met	
thiol		HS·Cys	8–9
thiolate		S·Cys	
disulfide		SS·Cys (cystine)	

[†] In the text and Tables 5–13, coordinated ligands are designated using the above nomenclature. In formulas of metal coordination units, ligands are written with the donor atom near to the metal. When sites are bridged, terminal ligands are placed before and after the metals and bridging ligands between. Oxidation states of metals are indicated as necessary or when known. While certain protein ligands are negative, the inclusion of a negative charge in a formula is reserved for amidato and imidazolato ligands in order that they may be immediately distinguished from amido and imidazolyl, respectively. ^a X = amino acid residue; side chain C-atom designation:



^b Approximate values in proteins; actual values may vary with protein environment. ^c –NH₃⁺ form. ^d Imidazolium pK_a 6–7. ^e –HNC(NH₂)₂⁺ form.

electronic and reactivity properties relative to an iron center in a non-heme environment. Macrocyclic active sites which fulfill functions iii–v above are pervasive in biology and form a group of active sites so large and diverse as to require a separate treatment. Such sites are included here only when part of a larger metal-containing assembly with non-heme components.

Proteins coordinate metal ions with nitrogen, oxygen, and sulfur *endogenous* biological ligands, which are summarized in Table 1. Amido, amidato, amino, carbonyl, and carboxylate ligands are located at the C- or N-termini of the polypeptide chain, within the chain itself (except for amino and carboxylate), and in side chains. The remaining ligands occur exclusively in side chains. Protic acids coordinate as anions; from the tabulated pK_a values, only carboxylate is available in a substantially deprotonated

form around neutral pH. These values are generally expected to vary by about 1 log unit in proteins, owing to dielectric and local electrostatic effects (except if a protein conformational change is coupled to a deprotonation reaction).⁸ Metals can of course bind ligands at pH values well below their pK_a's. For example, coordination at the unprotonated nitrogen atom of the imidazolyl group lowers the pK_a of the protonated nitrogen by about 2 log units due to an inductive effect (*vide infra*). Competition of a second metal ion with the proton in CuZn superoxide dismutase results in proton displacement and metal binding. Imidazolato coordinates and bridges two metal atoms at pH ≈ 4, the effective pK_a of the ligand having been reduced to *ca.* 3.3.⁹

The ability of a metal ion to compete effectively with a proton in ligand binding is dictated in large measure by the strength of the metal–ligand bond. Extensive listings of stability constants for ligand molecules bearing the functionalities in Table 1 with different metal ions and oxidation states are available.¹⁰ The metal–ligand bond is dependent on the detailed nature of the valence orbitals of the ligands as well as the effective nuclear charge and coordination number and geometry of the metal ion. Presented in Table 2 is a listing of biological metals (excluding magnesium and calcium) and certain key properties, including size,¹¹ spin state, stereochemistry, and ligand field stabilization energy^{12,13} (LFSE) associated with these variables. Angular data for metal–ligand bonding and the key orbitals utilized in bonding by the most important endogenous ligands are set out in Figure 2.

Amino groups generally bond with the nitrogen lone pair oriented along the bond axis and have a strong σ -donor interaction with the metal ion through an a₁ MO comprised of nitrogen 2s and 2p_z character¹⁴ (Figure 2A). Imidazolyl can bind through either nitrogen atom, with the metal approximately in the ligand plane and along a trigonal direction of the coordinating atom.^{15,16} The dominant bonding interaction involves the σ orbital (Figure 2B), which is a somewhat weaker donor than an amino σ orbital. This property is reflected in the pK_a values for imidazolium and protonated amine (Table 1). Imidazolyl also has potential π -donor interactions through the out-of-plane π_1 and π_2 MO's;¹⁷ however, these are relatively limited interactions as the coefficient of the coordinating nitrogen orbital in the MO is small (particularly for π_1). Amides are usually found to coordinate through the carbonyl oxygen atom, although deprotonation at high pH can lead to amidato ligation.¹⁸ Metal ions tend to coordinate in the ligand molecular plane with a M–O–C angle of 140–170°. The dominant covalent interaction, which should increase as this angle decreases, involves σ donation from the π_{ip} MO (Figure 2C), which is mostly an oxygen p orbital perpendicular to the CO bond and in the molecular plane.¹⁹

Metal ions can coordinate to carboxylate in either a bidentate or *syn/anti* monodentate mode^{15,16,20} (Figure 2D). Of the monodentate possibilities, the *anti* arrangement is least frequently observed. The dominant σ -donor bonding interactions involve the 3b₁ and 4a₁ orbitals, which are the highest energy

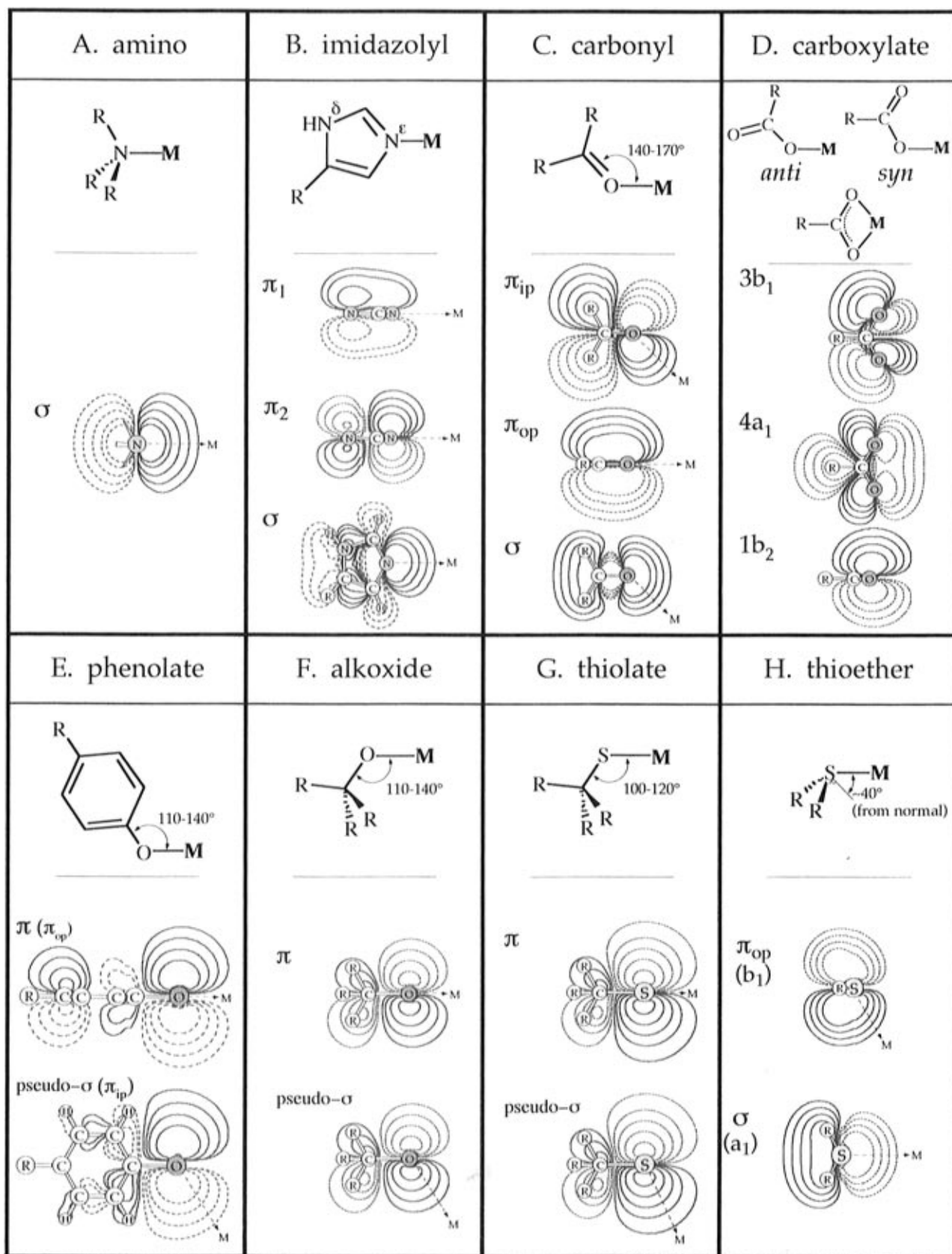


Figure 2. Bonding interactions for endogenous ligands: (top) typical metal–ligand angular orientations; and (bottom) important ligand valence orbitals involved in bonding; orbitals are shown in order of increasing energy.

valence orbitals. Their contributions vary with coordination mode. The $1b_2$ orbital can generate relatively strong π -donor interactions.²¹ Phenolate tends to bind metals with M–O–C bond angle of 110–140°. The bonding dominantly involves donor interactions

of the two oxygen p orbitals perpendicular to the C–O axis (π_{op} , π_{ip} , Figure 2E), the $2p_z$ orbital along the axis being strongly involved in σ bonding to the carbon atom. The two π -type orbitals are split in energy because of differences in conjugation to the ring. They

Table 2. Biologically Relevant Metal Ions

metal	common oxidation states	d ⁿ	d shell Z _{eff} ^a	common coord. no.	effective geometry ^b	spin state (S)	ionic radii ^c (Å)	LFSE ^d (Δ _o)			
V	+2	d ³	4.30	6	O _h	3/2	0.79	-1.200			
	+3	d ²	4.65	6	O _h	1	0.64	-0.800			
	[VO] ²⁺	+4	d ¹	5	C _{4v}	1/2	0.53	-0.400			
					O _h	1/2	0.58	-0.400			
[VO ₂] ⁺	+5	d ⁰	11.75 ^e	6	T _d	0	0.50	0.000			
Mn	+2	d ⁵	5.60	4	T _d	5/2	0.66	0.000			
				5	D _{3h}	5/2	0.75	0.000			
				6	O _h	1/2	0.67	-2.000			
				6	O _h	5/2	0.83	0.000			
				+3	d ⁴	5.95	5	C _{4v}	2	0.58	-0.914
							6	D _{3h}	2	0.58	-0.708
	6	O _h	1	0.58	-1.600						
	6	O _h	2	0.65	-0.600						
	+4	d ³	6.30	4	T _d	3/2	0.39	-0.356			
				6	O _h	3/2	0.53	-1.200			
	Fe	+2	d ⁶	6.25	4	T _d	2	0.63	-0.267		
					5	D _{4h}	2	0.64	-0.514		
5					C _{4v}	2		-0.457			
6					D _{3h}	2		-0.272			
6					O _h	0	0.61	-2.400			
6					O _h	2	0.78	-0.400			
+3		d ⁵	6.60	4	T _d	5/2	0.49	0.000			
				5	C _{4v}	5/2	0.58	0.000			
				6	O _h	3/2	0.55	-1.371			
				6	O _h	1/2	0.55	-2.000			
				6	O _h	5/2	0.65	0.000			
				6	O _h	1	0.59	-1.600			
Co	+2	d ⁷	6.90	4	T _d	3/2	0.58	-0.514			
				5	C _{4v}	3/2	0.67	-0.914			
				6	D _{3h}	3/2	0.67	-0.544			
	+3	d ⁶	7.25	6	O _h	1/2	0.65	-1.800			
					O _h	3/2	0.75	-0.800			
					O _h	0	0.55	-2.400			
6	O _h	2	0.61	-0.400							
Ni	+2	d ⁸	7.55	4	T _d	1	0.55	-0.800			
				5	D _{4h}	0	0.49	-2.684			
				5	C _{4v}	1		-1.000			
				5	C _{4v}	0	0.63	0.000			
				6	D _{3h}	1		-0.626			
				6	D _{3h}	0		0.000			
	+3	d ⁷	7.90	6	O _h	1	0.69	-1.200			
					4	D _{4h}	1/2		-2.684		
					5	C _{4v}	1/2		-1.914		
					6	O _h	1/2	0.56	-1.800		
					6	O _h	1/2	0.60	-0.800		
					6	O _h	3/2	0.48	-2.400		
Cu	+1	d ¹⁰	7.85	2	linear	0	0.46	0.000			
				3	trigonal	0		0.000			
				4	T _d	0	0.60	0.000			
				6	O _h	0	0.77	0.000			
	+2	d ⁹	8.20	4	T _d	1/2	0.57	-0.178			
					D _{4h}	1/2		-1.456			
					5	C _{4v}	1/2		-0.914		
					6	D _{3h}	1/2	0.65	-0.708		
+3	d ⁸	8.55	6	O _h	1/2	0.73	-0.600				
				O _h	1	0.54	-1.200				
Zn	+2	d ¹⁰	8.85	4	T _d	0	0.60	0.000			
				5	C _{4v}	0	0.68	0.000			
				6	D _{3h}	0		0.000			
				6	O _h	0	0.74	0.000			
Cd	+2	d ¹⁰	8.85	4	T _d	0	0.78	0.000			
				5	C _{4v}	0	0.87	0.000			
				6	D _{3h}	0		0.000			
				6	O _h	0	0.95	0.000			
Hg	+2	d ¹⁰	8.85	2	linear	0	0.69	0.000			
				4	T _d	0	0.96	0.000			
				6	O _h	0	1.02	0.000			
				6	O _h	0		0.000			

Table 2 (Continued)

metal	common oxidation states	d ⁿ	d shell Z _{eff} ^a	common coord no.	effective geometry ^b	spin state (S)	ionic radii ^c (Å)	LFSE ^d (Δ _o)
Mo	+3	d ³	5.30	6	O _h	3/2	0.69	-1.200
	+4	d ²	5.65	6	O _h	1	0.65	-0.800
	+5	d ¹	6.00	4	T _d	1/2	0.46	-0.600
[MoO] ³⁺				5	C _{4v}	1/2		
				6	O _h	1/2	0.61	-0.400
[MoO ₂] ²⁺	+6	d ⁰	12.75 ^e	4	T _d	0	0.41	0.000
				6	O _h	0	0.59	0.000
W	+4	d ²	5.65	6	O _h	1	0.66	-0.800
	+5	d ¹	6.00	5	C _{4v}	1/2		
				6	O _h	1/2	0.62	-0.400
[WO] ³⁺				4	T _d	0	0.42	0.000
	+6	d ⁰	12.75 ^e	5	C _{4v}	0	0.51	0.000
[WO ₂] ²⁺				6	O _h	0	0.60	0.000

^a Calculated using Slater's rules,^{11a} a more elaborate calculation of effective nuclear charges by Clementi and Raimondi^{11b} allows for the calculation of Z_{eff} for core orbitals as well. ^b Symmetry designations are used to denote usually observed geometries as follows: O_h, octahedral; T_d, tetrahedral; C_{4v}, square pyramidal; D_{3h}, trigonal bipyramidal; and D_{4h}, square planar. ^c Ionic radii as tabulated by Shannon.^{11c} "Effective ionic radii" are a more accurate measurement and can be obtained by adding 0.14 Å to the cation radii given in this table. ^d Δ_o = 10 D_q which is the splitting of the t_{2g}/e_g sets of d orbitals by an octahedral ligand field. These stabilization energies were obtained using the method of Ballhausen and Jørgensen¹² assuming B₂ = 2B₄. ^e Z_{eff} for an np electron.

are further affected by differences in bonding to the metal, which (as with alkoxide and thiolate) is dependent on the M–O–C angle. For both alkoxide (Figure 2F) and thiolate (Figure 2G), the dominant valence orbitals involved in bonding are also the two heteroatom p orbitals which are perpendicular to the C–O/S bond, the oxygen orbitals having more 2s character due to hybridization. These orbitals are degenerate in the free base, but split in energy into π and pseudo-σ levels upon bonding to a metal with a M–O/S–C angle less than 180°. The π orbital is perpendicular to the M–O/S–C plane, while the pseudo-σ orbital is in the plane with its lobe pointed toward the metal ion but not necessarily along the bond axis unless the M–O/S–C angle is close to 90°. The M–O/S–C angles of metal alkoxides are generally in the range 110–140° while those of metal thiolates are mainly 100–120°. Thioether ligands (Figure 2H) are often found to bind the metal ion below the molecular plane and approximately 40° off the plane normal.^{15,16} Two valence orbitals are involved in bonding. The b₁ and a₁ orbitals are p orbitals on the sulfur atom perpendicular to and largely in the ligand plane, respectively; the latter has significant amplitude in the direction of the bonding metal ion. Also included in the list of endogenous ligands (Table 1) is carbamylated lysine, which has recently been found in the active sites of a binuclear cadmium phosphoesterase²⁴ and in the binuclear nickel site of urease.²⁵ While occasionally postulated, there are no structurally proven cases of coordinated guanidine or disulfide.

Metal–ligand bonding in metalloproteins is dominated by ligand σ- and π-donor interactions, with neutral ligands behaving mostly as σ donors. Endogenous ligands are not π acceptors to any significant degree. For metal centers with low effective nuclear charges (Table 2), their d orbitals can be relatively high in energy and more extended spatially, thereby potentially available for π-bonding interactions with unoccupied low-lying valence orbitals on neutral ligands. Imidazolyl π* orbitals and thioether σ* orbitals might participate in back-

bonding, but such interactions lack convincing demonstration. Anionic ligands are stronger σ and π donors. In some instances, ligand–metal donor interactions can be highly covalent, with the covalency greatly influencing the reactivity of the metal center. Charge-transfer (CT) transitions are a direct probe of ligand–metal bonding. The presence of low-energy CT bands indicates that the ligand valence orbitals are close in energy to metal d orbitals, a situation that favors covalent bonding. (Note that the bonding interaction between metal and ligand orbitals is proportional to H_{ML}²/ΔE, where H_{ML} is the metal–ligand resonance integral, which increases with increasing orbital overlap, and ΔE is the energy difference between metal and ligand orbitals.) The extent of electron donor interactions of a ligand with a metal can be quantified by the intensity of the corresponding CT transition.²⁶ As the donor interaction of a ligand with a metal increases, the amount of metal character mixed into the occupied ligand orbital increases; i.e., Ψ'_L = (1 – α²)^{1/2}Ψ_L + αΨ_M, where α² quantitates the ligand donor strength. Reciprocally, the metal d orbital obtains ligand character due to covalency: Ψ'_M = (1 – α²)^{1/2}Ψ_M – αΨ_L. The ligand-to-metal CT transition corresponds to the Ψ'_L → Ψ'_M excitation (LMCT), which leads to a simple expression for the CT intensity as proportional to α². Metal sites with thiolate, phenolate, and the exogenous ligands oxide and sulfide exhibit intense low-energy CT transitions which dominate their absorption spectra. These are highly covalent sites, with attendant influences of covalency on physical properties and reactivity.

Ligands not derived from proteins are considered *exogenous* and are listed in Table 3 together with their pK_a values. The most ubiquitous ligands of this type are water, hydroxide, oxide, and sulfide. Also included are certain other ligands not necessarily found in native sites. These are buffer components that can ligate (acetate, phosphate), spectroscopic probes (azide, carbon monoxide, cyanide), and substitutes for native binding groups (ammonia, acetate, pyridine). Water is of course the most frequent

Table 3. Exogenous Biological Ligands

	ligand	$pK_a^{a,b}$
acid–base	H ₂ O/OH ⁻ /O ²⁻ ^c	14.0, ~34
	HCO ₃ ⁻ /CO ₃ ²⁻	10.3
	HPO ₄ ²⁻ /PO ₄ ³⁻	12.7
	HO ₂ /O ₂ ⁻	4.9
	HCO ₂ ⁻	3.8
	CH ₃ CO ₂ ⁻	4.7
	HO ₂ ⁻	11.6
	NH ₃	9.3
	imidazole	7.0
	pyridine	5.3
	N ₃ ⁻	4.8
	-NCO ⁻	3.7
	-NCS ⁻ , -SCN ⁻	1.0, -1.9
	NO ₂ ⁻	3.3
	HSO ₃ ⁻ /SO ₃ ²⁻	7.0
	HCN/CN ⁻	9.3
neutral	H ₂ S/HS ⁻ /S ²⁻ ^c	7.0, 12
	F ⁻ , Cl ⁻ , Br ⁻ , I ⁻	3.5, -7, -9, -11
neutral	O ₂ , CO, NO, RNC, N ₂	
N-heterocycles	chlorins, corrins, hemes, isobacteriochlorins	
	pterins, α-ketoglutarate	

^a Values refer to aqueous solution, 20–25 °C. ^b When a single species is listed, the value is that of the conjugate acid, which does not function as a ligand. ^c Oxide and sulfide usually occur as bridging ligands. In general, bridging ligands do not exchange, or exchange relatively slowly, with solvent or other exogenous ligands.

exogenous ligand. It is not uncommon in protein crystal structures to be unable to decide if water or hydroxide is coordinated to a metal. Provided the number and type of metal–oxygen interactions are not too large, M–O and M–OH bonds, whose bond length difference is usually 0.1–0.2 Å, can sometimes be distinguished by EXAFS. Coordination of water results in a substantial lowering of its pK_a value because the inductive effect of a bound cation further polarizes the O–H bond, a behavior that increases as the effective nuclear charge of the metal ion increases and its radius decreases (Table 2). For divalent ions of the first transition series, the first pK_a values of bound water are 8–11.²⁷ Exact data are dependent on ionic strength; typical values are 9.5 for [Fe(OH₂)₆]²⁺ and 8.0 for [Cu(OH₂)₆]²⁺. The trivalent ion [Fe(OH₂)₆]³⁺ is considerably more acidic, with a representative pK_a of 2.3.²⁷ Because of proton and metal ion competition for the conjugate base form of a ligand, at and below the ligand pK_a the observed binding constant K will be reduced relative to the stability constant K as the pH is lowered ($K' = K(1 + [H^+])/K_{HL}$, where K_{HL} is the acidity constant of the ligand).²⁸ While this behavior obviously applies to any monobasic ligand, it is worth noting that the extent of binding of an exogenous ligand added as, e.g., a metal site probe, will in general be pH dependent. The frequent occurrence of oxo and sulfido bridges and terminal ligands arises from the enhanced acidities of their conjugate acids when coordinated to sufficiently oxidized metal ions, together with the considerable bond strengths associated with binding these intensely nucleophilic dianions. Thus one finds in metalloproteins the bridging units Fe^{III}–O–Fe^{III} and Fe^{III}–S–Fe^{III,II}, *inter alia*. The terminal oxo and oxo–sulfido groups Mo^{IV,V,VI}O, Mo^{VI}O₂, and Mo^{VI}OS are expected to intervene in the catalytic cycles of molybdenum

oxotransferases.^{29,30} Oxo and sulfido ligands form multiple bonds with metal atoms and usually manifest intense low-energy LMCT absorptions; their bonding interactions should be considered as highly covalent. Finally, exogenous ligands of great importance are the substrate molecules in catalysis. Definition of enzyme–substrate complexes and identification of intermediates along the reaction coordinate to product are required for detailed elucidation of any catalytic mechanism on a molecular level.

B. Unique Properties of a Protein Ligand

Having considered features of proteins as ligands at localized metal sites, we turn attention to some of the unique aspects of protein structure as a whole that are critical to function. As may be seen even from the small proteins in Figure 1, protein molecular architecture is rather complex. Some or all of it has been evolved to promote function, which for metalloproteins is intimately coupled to the nature of the active site. Protein molecular weights usually fall in the 2–200 kD range, with the majority of metalloproteins and their subunits being under 100 kD. We consider next some of the more well-defined roles of protein structure in function, using as examples certain metalloproteins that are described in section III. Because this article deals primarily with metal sites in proteins, and not with protein structure and interaction at all levels, our considerations are necessarily illustrative and brief and are made with the aid of the schematic presentations in Figure 3.

1. Cooperativity and Allosteric Interactions

Arthropod hemocyanin (Figure 3A) contains one coupled binuclear copper center per 70 kD subunit. Six subunits α aggregate to form a hexamer, and eight hexamers combine to form the whole molecule with 48 binuclear copper sites. Salt bridges hold the hexamers together, affording the quaternary structure [α_6]₈.^{31,32} Dioxygen binding to the deoxy (Cu(I)) sites in a number of subunits changes the quaternary structure of whole protein such that the affinity of the remaining sites for dioxygen is enhanced (a homotropic allosteric effect). Calcium also binds to the protein, changing the intersubunit interactions and thus the O₂ affinity (a heterotropic allosteric effect). As in the case of hemoglobin, the cooperative interactions must be mechanically transmitted by protein quaternary and ternary structure, but exactly how this occurs is not well understood.

2. Organization of Sites in Multicenter Enzymes

Ascorbate oxidase catalyzes the reduction of dioxygen to water (O₂ + 4H⁺ + 4e⁻ → 2H₂O) using reducing equivalents derived from the oxidation of ascorbate to dehydroascorbate. The X-ray structure of the enzyme³³ reveals an electron transfer site and a trinuclear copper active site (Figure 3B). It indicates that electrons derived from the organic substrate enter the protein through a histidyl residue at the surface of the protein which is a ligand at a

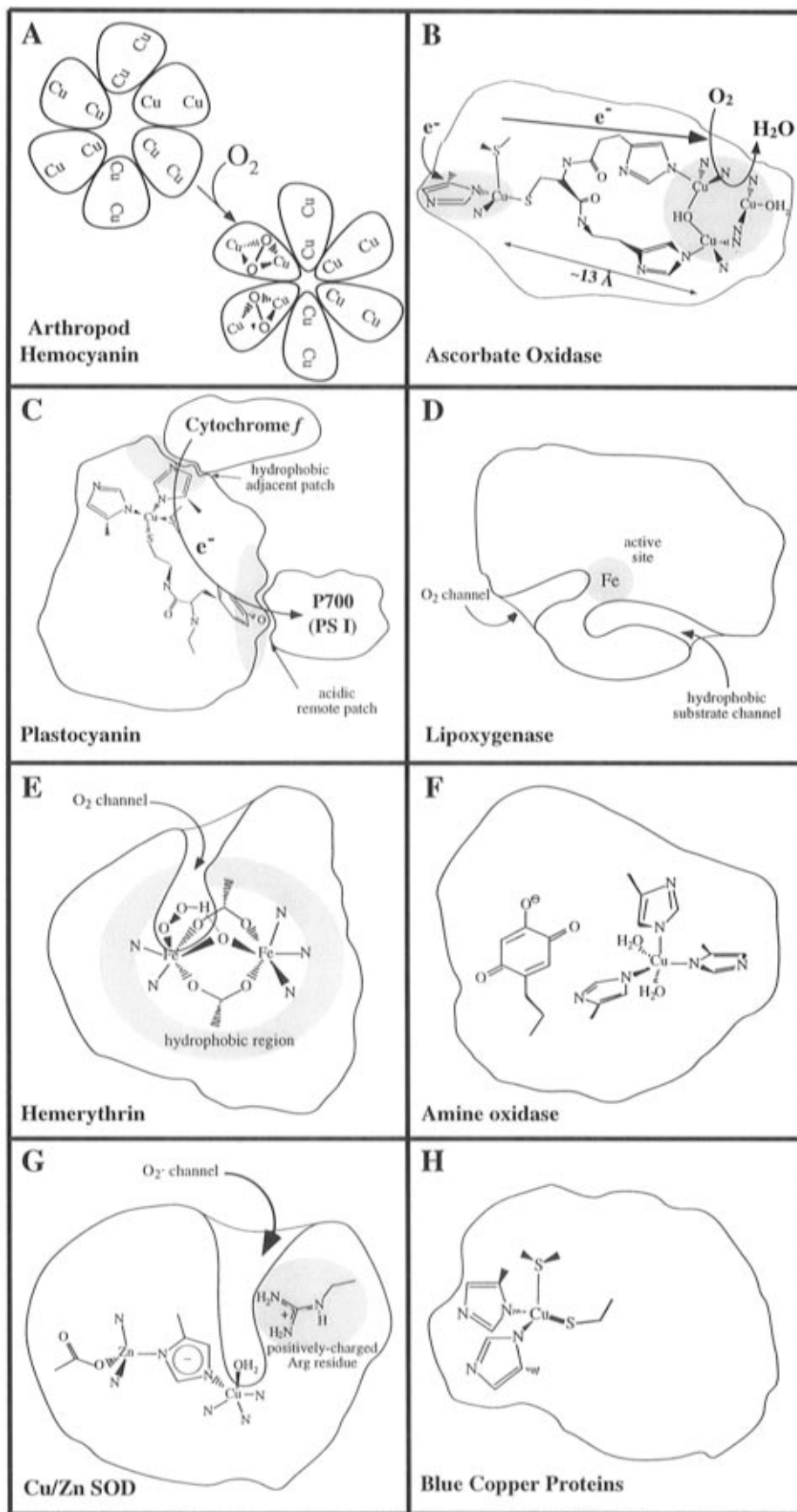


Figure 3. Illustrations of possible roles of protein ligands in biological function: (A) cooperativity and allosteric interactions; (B) organization of sites in multicenter enzymes; (C) specific surface recognition sites and superexchange pathways for electron transfer; (D) channels for substrate and small molecule access to active site; (E) hydrophobic environment; (F) additional residues in protein pocket for substrate binding and activation; (G) specific charge and hydrogen-bonding residues near the site to assist catalysis; (H) stabilization of reactive ligands and imposition of an entatic or rack state. For each role, a specific protein or enzyme is cited.

Table 4. Spectroscopic Methods in Bioinorganic Chemistry

method ^a	parameters	time scale ^b	information content	refs
magnetic susceptibility	molecular g value (g), axial (D) and rhombic (E) zero field splitting (ZFS), exchange interaction (J)		number of unpaired electrons/ground spin state; probes ground-state wave function at low resolution; defines antiferromagnetic and ferromagnetic interactions between metal centers; quantitates ground sublevel splittings on the order of kT	43–45
Mössbauer	quadrupole splitting (ΔE_Q), isomer shift (δ), metal hyperfine (A_i^m), J , g , D , E	10^{-7} s	for ^{57}Fe sites: oxidation and spin state; chemical environment; electric field gradient; occupation of d levels; degree of valence delocalization in mixed-valence systems	46,47
electron paramagnetic resonance (EPR)	g_i ($i = x, y, z$), A_i^m , ligand superhyperfine (A_i^l), D , E , J	10^{-8} s	usually for odd electron metal sites; probes ground-state wave function at high resolution; determination of atomic orbitals on metal and ligands contributing to the MO containing the unpaired e^- from electron-nuclear hyperfine coupling; LF splittings via anisotropic g and ZFS tensors; determines ligand bound to the metal site from superhyperfine coupling; probes exchange interaction in coupled systems by resonance line position ($J < kT$) or variable temperature and relaxation studies ($J > kT$)	48–50
electron-nuclear double resonance (ENDOR)	A_i^m , A_i^l , quadrupole tensor (P_i), nuclear Zeeman splitting ($g_n\beta_n H$)	10^{-7} s	combines the sensitivity of EPR and the high resolution of NMR to probe in detail the ligand superhyperfine interactions with the metal center and to identify the specific type of ligand	51,52
electron spin echo envelope modulation (ESEEM)	A_i^l , P_i^l	10^{-6} s	complementary technique to ENDOR for measuring very small electron-nuclear hyperfine couplings	53
nuclear magnetic resonance (NMR)	A_i^m , chemical shift, nuclear coupling (J)	10^{-1} – 10^{-8} s	for paramagnetic proteins: enhanced chemical shift resolution, contact and dipolar shifts; spin delocalization,	54,55
vibrational (Raman and IR)	energies (with isotope perturbation), intensities and polarizations	10^{-13} s	magnetic coupling from temperature dependence of shifts identification of ligands coordinated to a metal center; determination of M–L and intraligand vibrational modes; bond strengths from force constants	56
electronic absorption (ABS)	energies, intensities, and band shapes			
polarized single-crystal electronic absorption (linear dichroism)	same as ABS plus polarization information	10^{-13} – 10^{-15} s	direct probe of ligand field (LF) and charge transfer (CT) excited states; energies and intensities of LF transitions are a powerful probe of metal site geometry; CT intensity and energies directly relate to M–L orbital overlap and are thus a sensitive probe of M–L bonding	57
magnetic circular dichroism (MCD)	same as ABS plus circular polarization induced by applied magnetic field (A , B , and C -terms) and magnetic susceptibility	10^{-13} – 10^{-15} s	polarization information provides a direct determination of selection rules and allows for rigorous assignments based on group theory; allows correlation of spectral features with geometric structure providing detailed insight into the electronic structure of a metal ion active site	57
circular dichroism (CD)	same as ABS plus circular polarization due to asymmetric nature of metal site	10^{-13} – 10^{-15} s	greater sensitivity than ABS in observing weak transitions and greater resolution due to differences in circular polarization; complementary selection rules aiding in assignment of electronic transitions; variable temperature–variable field (VT/VH) MCD uses excited-state features to probe ground-state sublevel splittings; determination of ground spin state, ZFS, and g values	58–60
resonance Raman	A-term (F_A) and B-term (F_B), intensity profiles, depolarization ratios ($\rho = I_{\parallel}/I_{\perp}$)	10^{-13} – 10^{-15} s	CD dispersion is a signed quantity as in MCD leading to enhanced resolution over ABS; complementary selection rule involving magnetic dipole character of a transition; allows detection of transitions not readily observable in absorption	61,62
			excitation into an electronic absorption results in an intensity enhancement of normal modes of vibration which are coupled to the electronic transition either by Franck–Condon or Herzberg–Teller coupling; allows for study of chromophoric active sites in biological molecules at low concentrations; allows assignment of CT (and in some cases LF) transitions based on the nature of the excited-state distortion; can provide information on M–L bonding as described above for vibrational spectroscopy	63,64

X-ray absorption spectroscopy (XAS)	energies, intensities and polarizations	10 ⁻¹⁶ s	Core Excited-State Methods	atom specific and allows for study of closed shell systems which are inaccessible via valence excited state methods; extended X-ray absorption fine structure (EXAFS) involves ionized scattered e ⁻ and provides structural information (bond lengths and number of scatterers); X-ray absorption near-edge structure (XANES) involves transitions to bound states and is dependent on the type of edge; Metal K-edge: 1s→4p transitions are electric dipole allowed; energy and shape of the X-ray edge correlates with oxidation state and geometry; 1s→3d is electric quadrupole allowed and thus has some absorption intensity and noncentrosymmetric distortions can mix 1s→4p character into the electric dipole forbidden 1s→3d,4s transitions; the 3d/4p mixing probes a potential contribution to metal hyperfine; Metal L-edge: 3→4-fold higher resolution than metal K-edge; allowed 2p→3d transitions are observed; metal L-edge contains information on spin state, oxidation state, and the LF splitting of the d orbitals; intensity probes M-L covalency; L-edge MCD possesses similar information content to MCD described above (at lower resolution but more metal specific); Ligand K-edge: 1s→2p,3p transitions are electric dipole allowed; covalency mixes ligand p character into the partially occupied metal d orbitals; the intensity thus quantitates this mixing (as with superhyperfine described above) and the transition energy defines the energies of the ligand field states	57, 65–68
photoelectron spectroscopy (PES)	energies, polarizations, photoionization cross sections (intensity dependence on photon energy)	10 ⁻¹⁵ s	measures kinetic energy and number of electrons ejected from the sample, therefore is surface sensitive and is mostly applicable to active-site model complexes (note that in XAS one detects photons rather than electrons and therefore does not possess the surface sensitivity); X-ray photoelectron spectroscopy (XPS): involves core ionization which shows chemical shifts that are used to determine oxidation state and bonding information; probes exchange interactions between the metal d and core electrons which directly relate to the Fermi contact contribution to hyperfine; M-L bonding information from satellite structure; Ultraviolet photoelectron spectroscopy (UPS): involves ionization of valence electrons which probes metal-ligand bonding and its change with ionization (from resonance effects as the photon energy is scanned through the metal M-edge) thus directly studying redox processes in metal complexes; allows for study of closed-shell systems which are inaccessible via electronic absorption spectroscopy	57, 69	

^a These and other physical methods and their biological applications are available in specialized sources: Sauer, K., Ed. *Methods in Enzymology*; Academic Press: New York; 1995; Vol. 246. Riordan, J. F., Vallee, B. L., Eds.; *Methods in Enzymology*; Academic Press: New York, 1993; Vols. 226 and 227. ^b The experimental time scales are estimated from $\delta E\tau = \hbar$ where δE is the uncertainty in the energy of a state ($=\hbar\delta\nu$) and τ is its mean lifetime. To resolve two spectroscopic peaks separated by $\Delta\nu$, τ must be $\geq 1/(2\pi\Delta\nu)$ where $\Delta\nu(\text{MHz}) = 3 \times 10^4 \Delta\nu(\text{cm}^{-1})$. $\Delta\nu$ generally increases as the energy of the spectral feature increases allowing resolution of shorter lived species. ^c Not relevant since the observation time of the experiment is long.

type 1 or "blue copper" center (*vide infra*). The electrons are then transferred rapidly³⁴ over about 13 Å to the trinuclear site at which dioxygen is reduced to water. Evidently, the electron transfer and catalytic sites are favorably juxtaposed for efficient electron transfer, an apparently general organizational feature of redox protein structure.

3. Surface Recognition Sites and Electron-Transfer Pathways

On the surface of the blue copper protein plastocyanin there are two sites for docking with other proteins (Figure 3C). One is a hydrophobic patch adjacent to a histidine ligand. The other is an acidic patch (involving carboxylate residues) about 13 Å from the copper site and adjacent to a tyrosyl residue.³⁵ These patches interact strongly with complementary regions on the indicated proteins, which are involved in electron transfer. The rate of electron transfer by the copper site and the remote patch is fast,³⁶ indicating that an electron transfer pathway involving the cysteinyl ligand and the tyrosyl group is very efficient (*cf.* section III.A).

4. Access Channels to the Active Site

Lipoxygenase has a non-heme iron active site and oxygenates the C₁₈ substrate linoleic acid at a specific carbon atom. The crystal structure of the enzyme indicates the presence of two channels in the protein structure³⁷ (Figure 3D). One channel appears to allow access of dioxygen to a position near the iron center. The other, a long hydrophobic channel, presumably allows penetration and binding of substrate, with the correct carbon position oriented for interaction with the iron center and hydroperoxidation by dioxygen.

5. Hydrophobic Environment

Hemerythrin (Figure 3E) has a binuclear non-heme active site. When in the diferrous state it has a hydroxo bridge and reversibly binds dioxygen as hydroperoxide. This process involves no change in the local charge of the active site. The protein pocket in the vicinity of the site has only hydrophobic residues,³⁸ which stabilize the reactive bound dioxygen species with respect to loss as peroxide or hydroperoxide. Such an event would produce a diferric, or *met*, state which cannot bind dioxygen; hence, the reversible binding function of the site would be lost.

6. Substrate Binding and Activation by Residues in the Protein Pocket

Amine oxidase (Figure 3F) is a mononuclear copper enzyme which contains a topaquinone cofactor covalently bound to the polypeptide chain. This entity is thought to be formed from a tyrosyl residue which is oxygenated by the copper center to generate the active enzyme.³⁹ Topaquinone is required for enzyme activity. Together with the copper center, it is implicated in the two-electron oxidation of the substrate and stabilization of the intermediate.

7. Specific Charged and Hydrogen-Bonding Residues Near the Metal Site

Copper/zinc superoxide dismutase (Figure 3G) catalyzes the reaction $2\text{O}_2^- + 2\text{H}^+ \rightarrow \text{H}_2\text{O}_2 + \text{O}_2$ at

an extremely rapid rate, and has a high binding affinity for exogenous anions that inhibit catalysis. Mutation studies⁴⁰ have indicated that a positively charged arginine residue in the superoxide access channel near the copper site significantly contributes to both the catalytic interaction with superoxide and the high anion affinity.

8. The Entatic or Rack State

The *entatic*⁴¹ or *rack*⁴² state is an important concept in bioinorganic chemistry. The essence of this concept is that protein structure can impose an unusual (high energy) geometry at a metal site that enhances its reactivity in electron transfer or catalysis. The blue copper site (Figure 3H) has long been considered a classic example of an entatic state. Its [Cu^{II}(N·His)₂(S·Met)(S·Cys)] coordination unit has a distorted tetrahedral structure.³⁵ From Table 2, the preferred geometry of Cu(II) is planar and of Cu(I) tetrahedral. Therefore, it has been thought that Cu(I) geometry is imposed on the oxidized site for the purposes of creating a high redox potential (enhanced reducibility of Cu(II)) and a lessened extent of structural rearrangement attendant to electron transfer (reduced activation energy). The entatic nature of the blue copper site has now been studied in detail and will be discussed in section III.A.

C. Physical Methods

While we emphasize in this account crystallographically defined metal sites, it is important to recognize that much of our insight into site structure/function correlations derives from the application of spectroscopic and magnetic methods in combination with appropriate chemical perturbations. The latter include chemical modification of residues, anion and inhibitor binding, selective oxidation of metal centers, natural and artificial mutations, metal removal to form apoprotein, and reconstitution of apoprotein with a nonnative metal which acts as a structural or spectroscopic probe. Listed in Table 4⁴³⁻⁶⁹ are the key spectroscopic methods in bioinorganic chemistry in order of increasing energy. These cover 10 orders of magnitude in photon energy, with different energy regions providing complementary insight into properties of a metal site. Such insight is expressible through ligand field and molecular orbital theories,⁷⁰ which describe the electronic structures reflected by the spectroscopic properties. Often by correlation with well-defined model complexes, physical methods can be used to generate a *spectroscopically effective* working model of a protein-bound metal site. More importantly, spectroscopy can extend our understanding of a structurally defined active site by exposing substrate and small molecule interactions related to reaction mechanism, thus facilitating evaluation of geometric and electronic contributions of the site to reactivity. Certain types of sites, such as those containing Cu(I) or Zn(II) (d¹⁰), are transparent to many spectral probes, and new methods must be developed to study them. In some cases, spectroscopic features of protein sites are not approached in small molecules containing similar coordination units, indicating unique electronic structures that can make key contributions to electron transfer and catalysis.

In the sections which follow, we consider the structures and functions of biological sites containing the metals in Table 2. Prior to these more detailed considerations, some general functional aspects are noted. The nonredox ions Zn^{2+} , Cd^{2+} , and Hg^{2+} provide structural stability in some proteins; the first of these in particular is an effective Lewis acid catalyst in a wide range of transformations not involving electron transfer.⁷¹ Zinc sites have been probed by the insertion of a spectroscopically responsive ion such as Co^{2+} (d^7). Electron transfer and dioxygen binding, activation, and reduction occur at sites containing iron and copper. Molybdenum and tungsten in relatively high oxidation states catalyze oxidation–reduction reactions, perhaps largely by direct oxygen atom transfer.^{29,30} In apparently lower oxidation states, molybdenum and vanadium play as yet undefined roles in the reduction of dinitrogen to ammonia by nitrogenases. Divalent nickel is a Lewis acid catalyst in urease,²⁵ but is also involved in enzymes ([NiFe]-hydrogenases, carbon monoxide dehydrogenase) where redox activity is apparently required. The only structurally defined catalytic manganese site is Mn(II/III) in superoxide dismutase⁷² (iron and copper sites can also perform this function). In catalase, a μ -oxo dimanganese site is implicated in the disproportionation of H_2O_2 ,⁷³ and a tetranuclear high-valent oxomanganese center in the oxidation of water in photosystem II.⁷⁴ From this cursory examination, it is evident that known or proposed functions of metals involve those properties (redox flexibility, Lewis acidity, atom transfer) which are intrinsic to a particular element. However, in only few instances have these properties been manipulated such that the functional aspect is successfully duplicated outside of a biological system.

III. Active-Site Structure/Function Relationships

In this part, we examine crystallographically defined metal site structures and attempt to relate these to biological function. Structural information is reported in Tables 5–8 and 10–18. These contain coordination units specified using the notation of Table 1, origin of the protein, resolution of the X-ray data, literature citations, and the Brookhaven Protein Databank⁷ (PDB) code for use in accessing structures online. Resolution is roughly the minimum separation at which atoms can be distinguished. Whereas small molecules routinely afford electron density maps with resolutions of ≤ 0.8 Å, macromolecules infrequently diffract to a resolution better than 1.5 Å. The concept is discussed elsewhere.⁷⁵

Beyond the exclusion of heme- and corrin-containing biomolecules, there are further restrictions in the scope of the structural tables. One is the exclusion of the large body of magnesium- and calcium-containing proteins. Magnesium normally exhibits a structural and certain catalytic functions (e.g., ATPase, DNA polymerase). Calcium also functions as a structural metal and acts as a trigger in intracellular messenger systems controlling processes such as muscle contraction, secretion, glycolysis, and ion transport. The structure and function of calcium proteins have been examined at length elsewhere.^{76,77}

In addition, structures of enzymes considered here are nearly exclusively confined to those lacking substrates and inhibitors. Thus, a significant fraction of the total structural data available for certain hydrolytic enzymes is omitted. Selected structures of mutant molecules and of molecules with nonnative metal ions are, however, included. Owing to their complexity, crystallographically determined protein structures can and do exhibit certain limitations. Among the common difficulties for metal sites are substantial uncertainties in metric features (0.1–0.2 Å in some bond lengths), inexact stereochemistry, incomplete definition of the total ligand set (missing ligands), and the distinction between water and hydroxide. Several initial structure reports have been incorrect with respect to the pattern of ligation by sidechain ligands and the composition and structure of the metal site. These deficiencies, many of which have been ameliorated or corrected in subsequent studies, pale in comparison to the enormous volume of critical structural information delivered by protein crystallography.

Structures of most of the basic types of metal sites are exemplified in Charts 1–6. These depictions are rendered using crystallographic coordinates.⁷ Because structural sites are relatively simple, we shall not consider them at any length. The large majority of sites recognized as structural contain calcium or zinc. The classic example of a structural zinc site is tetrahedral $[\text{Zn}(\text{S}\cdot\text{Cys})_4]$ (Chart 6A) found in alcohol dehydrogenase.⁷⁸ This site has been most recently detected in bovine heart cytochrome *c* oxidase,³ where it presumably also fulfills a structural function. Examples of structural sites are included in the tables and will be noted as advisable in the discussions which follow.

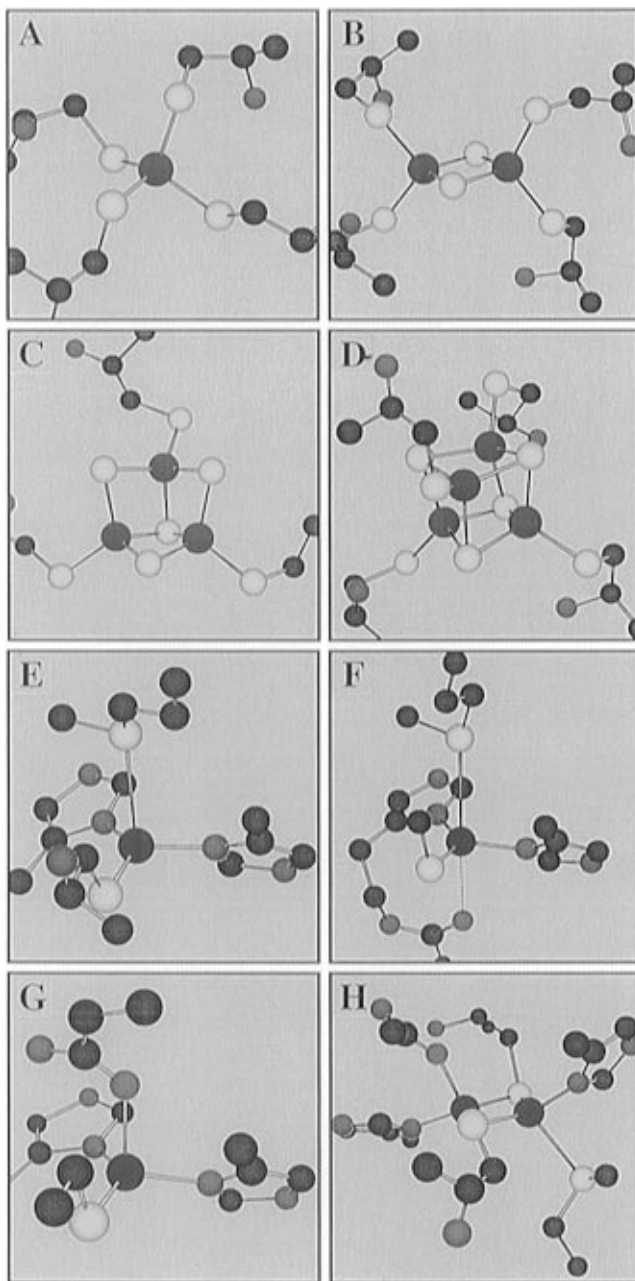
A. Electron Transfer

The three groups of metal-containing electron-transfer proteins are the cytochromes (containing heme groups), iron–sulfur proteins, and blue copper proteins. All structural types of sites present in the latter two groups are shown in Chart 1. Protein potentials are referenced to the normal hydrogen electrode.

1. Iron–Sulfur Proteins

Iron–sulfur proteins^{79–81} exhibit four sites (excluding the more complex “P-cluster” of nitrogenase): rubredoxins (A), rhombic Fe_2S_2 clusters (B), cuboidal Fe_3S_4 clusters (C), and cubane-type Fe_4S_4 clusters (D). Low molecular weight proteins containing the first and last three types are generically referred to as rubredoxins (Rd) and ferredoxins (Fd), respectively. In terms of formal oxidation states, all of these sites contain Fe(II) and/or Fe(III) in approximately tetrahedral FeS_4 coordination units. The sites are summarized in Figure 4 together with their physiological electron transfer reactions; redox potentials E_0' (pH 7) are given as approximate ranges; their values and variabilities are treated elsewhere (Stephens, P. J.; Jollie, D. R.; Warshel, A.; this issue). In some cases, electron and proton transfer are coupled, such that the potentials are pH dependent, accounting in part for the large ranges observed, especially for the

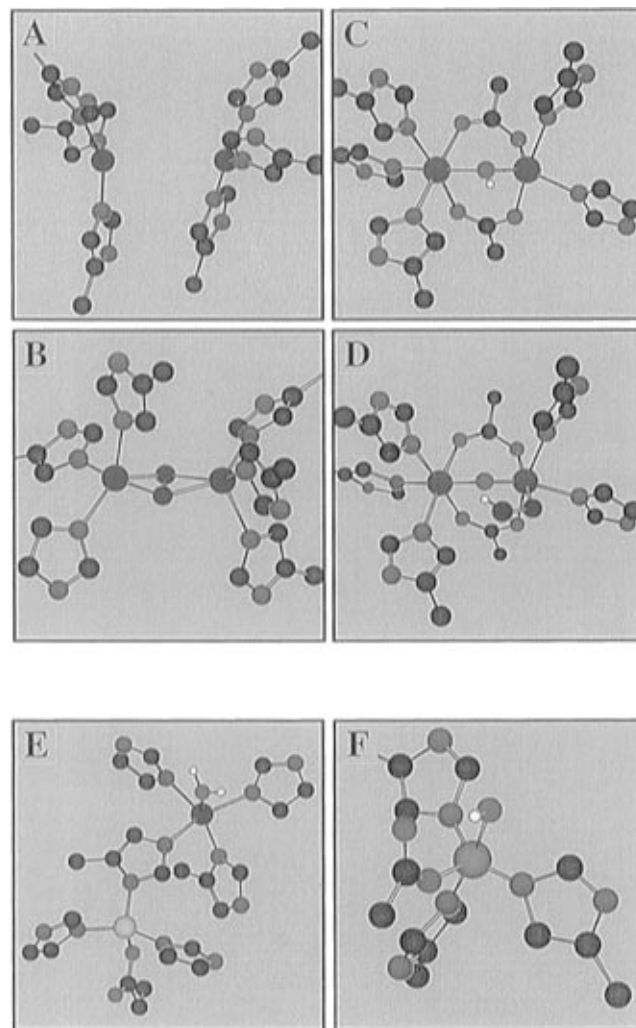
Chart 1. Structures^a of Redox Sites in Electron Transfer Proteins: (A) Rubredoxin (*Clostridium pasteurianum*); (B) Ferredoxin (*Equisetum arvense*); (C) Ferredoxin II (*Desulfovibrio gigas*); (D) Ferredoxin I (*Azotobacter vinelandii*); (E) Plastocyanin (*Chlamydomonas reinhardtii*); (F) Azurin (*Alcaligenes denitrificans*); (G) stellacyanin (cucumber); and (H) Cu_A Center in Cytochrome *c* Oxidase (Bovine Heart)



^a All structures depicted in these charts were created using crystallographic coordinates taken from the Brookhaven Protein Databank or by private communication. The color scheme for atoms is as follows: carbon (gray), oxygen (pink), nitrogen (cyan), sulfide and cysteine sulfur (bright yellow), methionine sulfur (light yellow), zinc (light purple), iron (red), copper (blue), other metals (gold), and hydrogen (white). Hydrogen atoms are not crystallographically defined but have been added to depict the nature of certain ligands when known. Structures are cross-referenced in Tables 5–8, 9, and 13–18.

polynuclear centers. In addition to discrete Rd and Fd electron transfer proteins, which often are the ultimate electron donors to enzymes, these centers may also be found within enzyme molecules them-

Chart 2. (I) Structures of Oxygen-Carrying Proteins [Hemocyanin (*Limulus polyphemus*) in Its Deoxygenated (A) and Oxygenated (B) Forms; Hemerythrin (*Themiste dyscrita*) in Its Deoxygenated (C) and Oxygenated (D) Forms] and (II) Structures of Superoxide Dismutases [(E) Cu/Zn Superoxide Dismutase (*Saccharomyces cerevisiae*); (F) Mn Superoxide Dismutase (Human Kidney)]

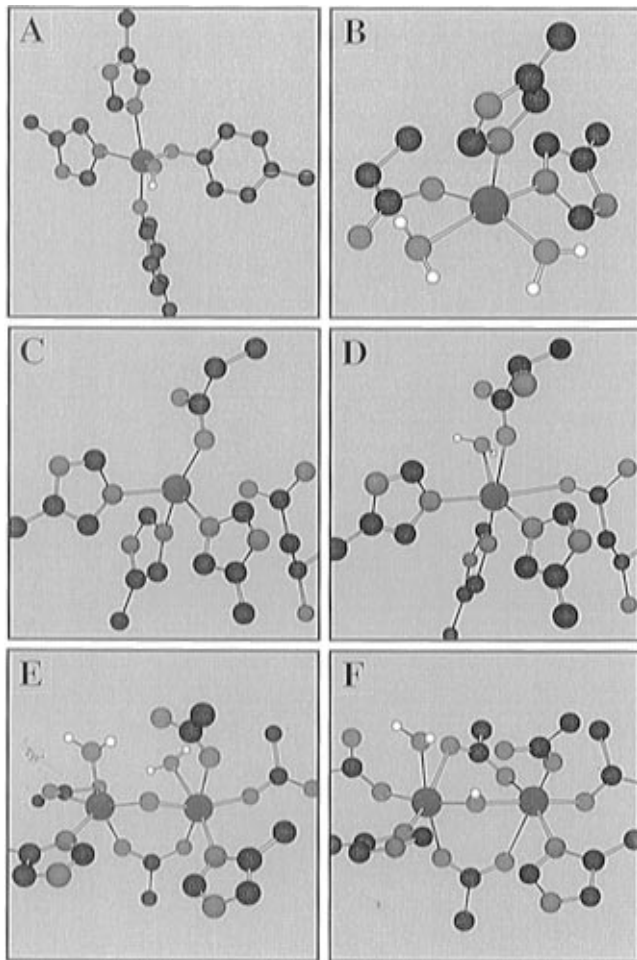


selves where they form part of the electron transfer conduit to the catalytic site.

Rubredoxins contain one iron atom, usually fall in the 6–7 kD range, and are the simplest of the iron–sulfur proteins. Reports of structures are collected in Table 5;^{82–86} the resolutions are some of the best achieved in protein crystallography. The high-spin FeS₄ cores of the [Fe^{II,III}(S·Cys)₄] coordination units are close to tetrahedral, but distortions of the entire unit tend to impose effective *D*_{2d} symmetry. The structures of *P. furiosus* Rd_{ox} and Rd_{red} have been obtained at 1.8 Å resolution, allowing an assessment of the structural changes pursuant to electron transfer. Mean Fe–S bond distances change by ≤0.05 Å and S–Fe–S bond angles by ≤5°.

Proteins containing [Fe₂S₂(S·Cys)₄] units are numerous; the Fe₂(μ₂-S)₂ cores approach *D*_{2h} symmetry. The structures of six proteins, listed in Table 6,^{87–97} have been determined in the oxidized state; no reduced protein structure is available. These pro-

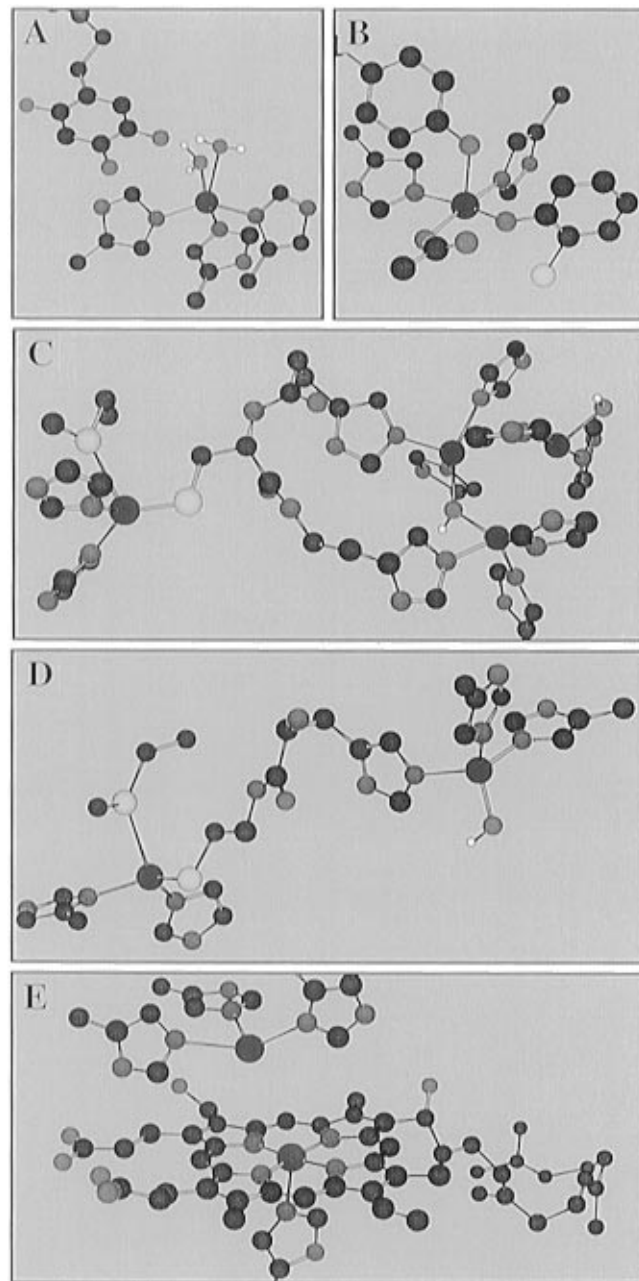
Chart 3. Active-Site Structures of Non-Heme Iron Oxygenases and Ribonucleotide Reductase: (A) Protocatechuate 3,4-Dioxygenase (*Pseudomonas aeruginosa*); (B) 2,3-Dihydroxybiphenyl 1,2-Dioxygenase (*Pseudomonas cepacia*); (C, D) Soybean Lipoxygenase; (E) Ribonucleotide Diphosphate Reductase^a (*Escherichia coli* - Protein R2); (F) Methane Monooxygenase (*Methylococcus capsulatus* at $-4\text{ }^{\circ}\text{C}$)



^a The redox-active tyrosyl radical in RDPR is $\sim 5\text{ \AA}$ from the binuclear iron site in the direction shown by the arrow.

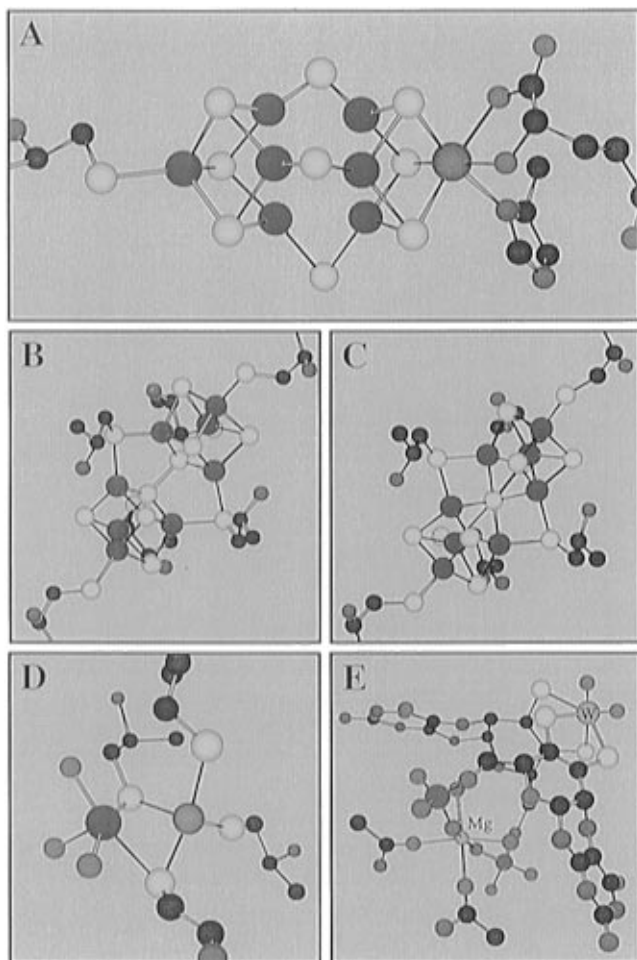
teins support a one-electron transfer reaction in which Fd_{ox} ($S = 0$ ground state) is reduced to Fd_{red} , a deeply valence-trapped $\text{Fe}^{\text{III}}\text{Fe}^{\text{II}}$ species with $S = 1/2$. For proteins of known structure and presumably others as well, one iron atom is closer to the surface (*ca.* 5 \AA), and it has been established by NMR that the added electron resides on that atom.^{98a} Despite the occurrence of two iron atoms, there is no known instance where a binuclear center acts as a physiological two-electron donor or acceptor. Recently, sequential one-electron reductions of several 2-Fe Fd proteins by a macrocyclic Cr(II) complex have been reported.^{98b} Binding of Cr(III) to the $[\text{Fe}_2\text{S}_2]^+$ protein redox level is essential to the second reduction, which can also be accomplished by dithionite. Neither this reagent nor Cr(II) is capable of reducing a protein past this level in the absence of bound Cr(III), whose presence indicates an inner-sphere reduction process. The potentials of the Cr(III)-bound Fd (-277 mV , -409 mV) reveal that the second reduction occurs at a value not atypical for the first reduction of a native

Chart 4. Active-Site Structures of Copper Oxidases and Related Enzymes: (A) Amine Oxidase (Pea Seedling); (B) Galactose Oxidase (*Dactylium dendroides*); (C) Ascorbate Oxidase (Zucchini); (D) Nitrite Reductase (*Alcaligenes faecalis*); (E) Cytochrome *c* Oxidase Cu_B -Heme a_3 Center (Bovine Heart)



2-Fe Fd. The only proven variation of primary coordination in the binuclear site is that found in the Rieske proteins, which occur mainly in the electron-transfer chains of mitochondria and photosynthetic bacteria. Spectroscopic results⁹⁹⁻¹⁰¹ have established the unit $[(\text{Cys}\cdot\text{S})_2\text{FeS}_2\text{Fe}(\text{N}\cdot\text{His})_2]$, in which two imidazolyl groups are bound to the same iron atom (Figure 4). This atom is the site of reduction, inasmuch as the presence of two neutral ligands raises the redox potential to values more positive ($\geq -100\text{ mV}$) than those for conventional 2-Fe Fd proteins. Increased redox potentials are among the most characteristic features of Rieske centers. A water-soluble fragment of a Rieske protein from bovine

Chart 5. Structures of Nitrogenase, Hydrogenase, and a Tungsten Oxotransferase: (A) Iron–Molybdenum Cofactor of Nitrogenase; P-Cluster of Nitrogenase from (B) Rees and (C) Bolin; (D) [NiFe]-Hydrogenase^a (*Desulfovibrio gigas*); (E) Aldehyde Ferredoxin oxidoreductase^b (*Pyrococcus furiosus*)



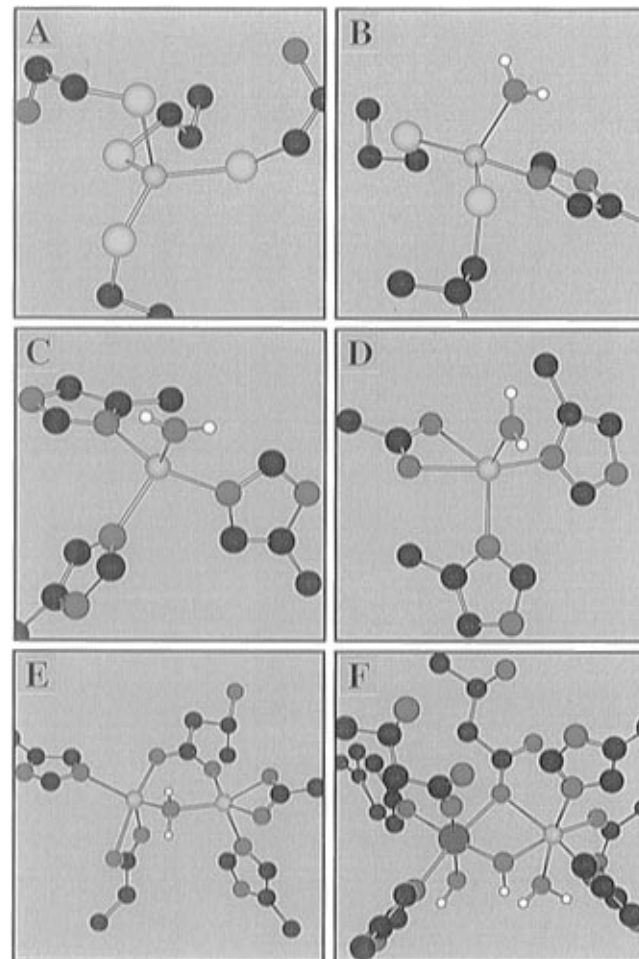
^a The three oxygen ligands on the iron have not been identified.

^b The two oxygen ligands on the tungsten atom are proposed to be one oxo and one glycerol (solvent) ligand.

heart is reported to show two reductions (at *ca.* +300 mV and –850 mV).¹⁰²

The structure of the trinuclear $[\text{Fe}_3\text{S}_4(\text{S}\cdot\text{Cys})_3]$ (Figure 4) has been demonstrated crystallographically for the two proteins in Table 6^{103–111} and for the inactive form of the enzyme aconitase¹¹² (*cf.* Table 14). The geometry of the $\text{Fe}_3(\mu_3\text{-S})(\mu_2\text{-S})_3$ core is cuboidal; i.e., a cube with one vacancy. Indeed, comparison of protein-bound $[\text{Fe}_3\text{S}_4]^+$ and $[\text{Fe}_4\text{S}_4]^{2+}$ cores reveals that the former is sensibly congruent with the latter; dimensional differences between the two are small. Further, the cuboidal structure does not owe its stability entirely to protein structure inasmuch as synthetic $[\text{Fe}_3\text{S}_4]^0$ clusters have now been prepared.¹¹³ Protein-bound Fe_3S_4 clusters are usually derived from $[\text{Fe}_4\text{S}_4(\text{S}\cdot\text{Cys})_3\text{L}]$ centers with $\text{L} = \text{H}_2\text{O}/\text{OH}^-$, a side chain carboxylate, or some other non-cysteinate ligand. Under oxidizing conditions, it is probable that the reaction $[\text{Fe}_4\text{S}_4]^{3+} \rightarrow [\text{Fe}_3\text{S}_4]^+ + \text{Fe}^{2+}$ occurs, the oxidized tetranuclear core being insufficiently basic to retain the ferrous ion, whose removal may be assisted by complexation with an

Chart 6. Structures of Catalytic and Structural Zinc Sites: (A) Alcohol Dehydrogenase—structural Site (Horse Liver); (B) Alcohol Dehydrogenase—catalytic Site (Horse Liver); (C) Carbonic Anhydrase II (Human); (D) Carboxypeptidase A (Bovine Pancreas); (E) Aminopeptidase (*Aeromonas proteolytica*); (F) Purple Acid Phosphatase (Kidney Bean)



exogenous ligand. An $[\text{Fe}_3\text{S}_4(\text{S}\cdot\text{Cys})_3]$ center formed in this way should be considered intrinsic to the protein, for it lacks the ability to stabilize, by tetracysteinate terminal ligation, an Fe_4S_4 center toward partial deconstruction. The cluster reconstitution reaction $[\text{Fe}_3\text{S}_4]^0 + \text{Fe}^{2+} \rightarrow [\text{Fe}_4\text{S}_4]^{2+}$ proceeds readily. The biological function of these centers remains unclear. One possibility is that the $\text{Fe}_4\text{S}_4/\text{Fe}_3\text{S}_4$ conversion is a switch for controlling metabolic reactions catalyzed by an Fe_4S_4 cluster. Another is electron transfer. The potential of the $[\text{Fe}_3\text{S}_4]^{+0}$ couple is notoriously variable, ranging over about 400 mV. Certain of these potentials are pH dependent,^{114,115} as are those linking the $[\text{Fe}_3\text{S}_4]^0$ state to lower oxidation level(s), and thus can be modulated by the medium. The most conspicuous chemical reaction discovered for trinuclear clusters is the formation of heteronuclear cubane clusters in the minimal reaction $[\text{Fe}_3\text{S}_4]^{0,+} + \text{M}^{2+,+} \rightarrow [\text{MFe}_3\text{S}_4]^{2+,+}$.^{116,117} The physiological significance (if any) of these reactions remains to be demonstrated. Many aspects of protein-bound Fe_3S_4 clusters, including their redox behavior and reactions with exogenous metal ions, are summarized elsewhere.^{116,118}

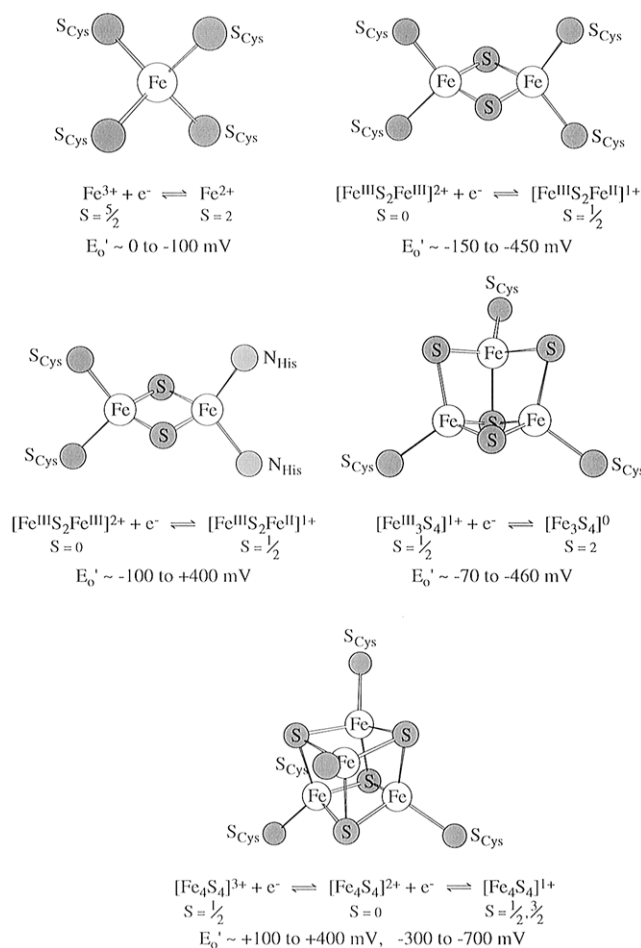


Figure 4. Schematic structures of Fe-S redox centers of nuclearities 1–4, and their electron-transfer reactions and approximate ranges of potentials. Individual iron atom oxidation states are not specified for delocalized clusters; spin states are indicated.

Proteins containing crystallographically defined cubane-type clusters with $\text{Fe}_4(\mu_3\text{-S})_4$ cores are listed in Table 6.^{105–110,119–129} Protein-bound clusters $[\text{Fe}_4\text{S}_4(\text{S}\cdot\text{Cys})_4]$ are known to exist in the three core oxidation states in Figure 4. Native proteins exhibit either the $[\text{Fe}_4\text{S}_4]^{2+,+}$ or the $[\text{Fe}_4\text{S}_4]^{3+,2+}$ redox couple; the three oxidation states have not been traversed in any one protein unless its tertiary structure is significantly disturbed. Proteins involved in the latter couple have been historically referred to as HiPIP (high-potential iron protein). Although the name persists, these proteins are best regarded as a subclass of Fd proteins that can sustain a higher oxidation state. The structures of the oxidized and

reduced forms of the *C. vinosum* protein provide the only opportunity to compare the metric features of protein-bound $[\text{Fe}_4\text{S}_4]^{3+,2+}$ states.^{121,122} However, with esd's on bond lengths of 0.03–0.08 Å, it is difficult to discern statistically meaningful changes in core dimensions and terminal Fe–S·Cys distances between the two states. As would be expected for $[\text{Fe}_4\text{S}_4]^{3+}$, which has more ferric character, the cluster appears to be smaller than the reduced form. Insofar as they can be compared, given the stated uncertainties in metric parameters, structures of eleven $[\text{Fe}_4\text{S}_4]^{2+}$ clusters in nine proteins exhibit no important differences. No structure of a protein in the $[\text{Fe}_4\text{S}_4]^{1+}$ state has been reported. When recourse is taken to synthetic clusters $[\text{Fe}_4\text{S}_4(\text{SR})_4]^{-,2-,3-,130,131}$ which contain the three physiological oxidation states, core volumes and mean Fe–S and Fe–SR bond lengths increase slightly but significantly upon reduction. While consideration of the electronic structures of these clusters is beyond our purview, these changes signify addition of electrons to antibonding molecular orbitals. With synthetic clusters, the $[\text{Fe}_4\text{S}_4]^{2+,+}$ reduction involves alteration of a tetragonally compressed core to a variety of distorted cubane geometries, suggesting that the reduced core enjoys a degree of plasticity not found in the oxidized form. A similar behavior can be anticipated in proteins.

All Rd and Fd proteins exhibit fairly well-resolved NMR spectra of α -CH and β -CH₂ protons of coordinated Cys residues, a feature which facilitates the study of redox reactions because the paramagnetically induced (isotropic hyperfine) shifts and their temperature dependencies are quite different in different oxidation states.^{55,132} Sequence-specific assignments of cysteinyl resonances have been derived for many proteins. Using this technique, the NMR information in Table 4 has been deduced in favorable cases. A key point for Fe_4S_4 clusters is that the intrinsic inequivalence of iron sites imposed by protein asymmetry is often resolved, owing to the enormous sensitivity of isotropic shifts to structure and environment. In particular, the $[\text{Fe}_4\text{S}_4]^{3+,2+}$ redox couple has been probed at a very high level of sophistication. The reduced cluster has a diamagnetic ground state and a low-lying triplet state which gives rise to isotropic shifts. Mössbauer spectroscopy of the oxidized cluster supports the presence of a pair of Fe^{3+} sites and two delocalized mixed valence ($\text{Fe}^{2.5+}$) sites. Antiferromagnetic coupling of the spins of the Fe^{3+} and $\text{Fe}^{2.5+}$ pairs leads to the cluster $S = \frac{1}{2}$ ground state. The spin-doublet oxidized clusters afford sharp lines with large isotropic shifts. Incisive

Table 5. Crystallographically Defined Coordination Units of Rubredoxins

unit/protein	resolution (Å)	references (PDB code) ^a
$[\text{Fe}^{\text{III}}(\text{S}\cdot\text{Cys})_4]$		
<i>Clostridium pasteurianum</i> Rd _{ox} ^{1(A) b}	1.2	82 (4RXN, 5RXN)
<i>Desulfovibrio desulfuricans</i> Rd _{ox}	1.5	83 (6RXN)
<i>Desulfovibrio gigas</i> Rd _{ox}	1.4	84 (1RDG)
<i>Desulfovibrio vulgaris</i> Rd _{ox}	1.0	85 (8RXN)
<i>Pyrococcus furiosus</i> Rd _{ox}	1.8	86 (1CAA)
$[\text{Fe}^{\text{II}}(\text{S}\cdot\text{Cys})_4]$		
<i>Pyrococcus furiosus</i> Rd _{red}	1.8	86 (1CAD)

^a References in parentheses are Brookhaven Protein Databank (PDB) reference codes for those structures which were available on Jan 1, 1996. ^b Brackets indicate that the active site of this protein/enzyme is shown in the color chart as indicated.

Table 6. Crystallographically Defined $\text{Fe}_2(\mu_2\text{-S})_2$, $\text{Fe}_3(\mu_3\text{-S})(\mu_2\text{-S})_3$, and $\text{Fe}_4(\mu_3\text{-S})_4$ Clusters in Iron-Sulfur Proteins and Enzymes

unit/protein	resolution (Å)	references (PDB code) ^a
$[(\text{Cys}\cdot\text{S})_4\text{Fe}_2\text{S}_2]$		
<i>Cyanobacterium anabaena</i> 7120 Fd vegetative	$[\text{Fe}_2\text{S}_2]^{2+}$ 2.5	87, 88 (1FXA)
heterocyst	$[\text{Fe}_2\text{S}_2]^{2+}$ 1.7	88, 89 (1FRD)
<i>Aphanothece sacrum</i> Fd	$[\text{Fe}_2\text{S}_2]^{2+}$ 2.2	90 (1FXI)
<i>Equisetum arvense</i> Fd ^(1B)	$[\text{Fe}_2\text{S}_2]^{2+}$ 1.8	91 (1FRR)
<i>Halobacterium</i> Fd	$[\text{Fe}_2\text{S}_2]^{2+}$ 3.2	92, 93
<i>Spirulina platensis</i> Fd	$[\text{Fe}_2\text{S}_2]^{2+}$ 2.5	94–97 (3FXC)
$[(\text{Cys}\cdot\text{S})_3\text{Fe}_3\text{S}_4]$		
<i>Desulfovibrio gigas</i> Fd II ^(1C)	$[\text{Fe}_3\text{S}_4]^+$ 1.7	103, 104 (1FXD)
<i>Azotobacter vinelandii</i> Fd I	$[\text{Fe}_3\text{S}_4]^{+0}$ 2.7–1.9	105–111 (1FDB, 1FDC)
$[(\text{Cys}\cdot\text{S})_4\text{Fe}_4\text{S}_4]$		
<i>Azotobacter vinelandii</i> Fd I ^(1D)	$[\text{Fe}_4\text{S}_4]^{2+}$ 2.7–1.9	105–110 (1FER, 5FDI, 1FDA-1FDC)
<i>Bacillus thermoproteolyticus</i> Fd	$[\text{Fe}_4\text{S}_4]^{2+}$ 2.3	119 (2FXB)
<i>Chromatium vinosum</i> HiPIP	$[\text{Fe}_4\text{S}_4]^{3+,2+}$ 2.0	120–122 (1HIP)
<i>Clostridium acididurici</i> Fd	$2[\text{Fe}_4\text{S}_4]^{2+}$ 1.8	123 (1FDN, 1FCA)
<i>Desulfovibrio africanus</i> Fd I	$[\text{Fe}_4\text{S}_4]^{2+}$ 2.3	124 (1FXR)
<i>Ectothiorhodospira halophila</i> HiPIP	$[\text{Fe}_4\text{S}_4]^{2+}$ 2.5	125 (2HIP)
<i>Ectothiorhodospira vacuolata</i> HiPIP	$[\text{Fe}_4\text{S}_4]^{2+}$ 1.8	126 (1HPI)
<i>Peptococcus aerogenes</i> Fd	$2[\text{Fe}_4\text{S}_4]^{2+}$ 2.8, 2.0	127, 128 (1FDX)
<i>Rhodocyclus tenuis</i> HiPIP	$[\text{Fe}_4\text{S}_4]^{2+}$ 1.5	129 (1ISU)

^a See footnote in Table 5.

analysis of these spectra has led to determination of spin distribution, detection of possible equilibria between clusters in which Fe^{3+} and $\text{Fe}^{2.5+}$ sites are differently placed in the cubane core fixed in the protein matrix, and estimation of microscopic redox potentials of individual sites in a cluster.¹³³

Lastly, esd's of crystallographically determined metric features of Rd and Fd sites do not permit tracking of structural changes pursuant to electron transfer to the accuracy of synthetic complexes. The latter are known to be excellent, albeit symmetrized, structural and electronic analogues of protein-bound sites. What has become abundantly clear, after more than 20 years of development of iron–sulfur chemistry and biochemistry, is that the sites in Figure 4 have been exquisitely evolved to encompass a large range of redox potentials for electron transfer reactions that require minimal structural reorganization energy.

2. Blue Copper Proteins

As the name indicates, blue copper sites (also called type 1 sites in multicopper oxidoreductases) have very different spectral features relative to other protein-bound $\text{Cu}(\text{II})$ sites and to synthetic $\text{Cu}(\text{II})$ complexes. Leading spectroscopic features are illustrated in Figure 5. Rather than weak ligand field transitions in the 600 nm region ($\epsilon_M \sim 50 \text{ M}^{-1} \text{ cm}^{-1}$; Figure 5A, left), blue copper proteins exhibit an extremely intense $\text{Cys}\cdot\text{S} \rightarrow \text{Cu}(\text{II})$ CT band ($\epsilon_M \sim 5000 \text{ M}^{-1} \text{ cm}^{-1}$, Figure 5B, right), resulting in their pronounced blue color. In the EPR spectrum, the parallel $^{63,65}\text{Cu}$ hyperfine splitting (A_{\parallel} in Figure 5B, right) is reduced to less than half the value observed in normal $\text{Cu}(\text{II})$ complexes (Figure 5A, right). These unique features are associated with a cysteinyl residue bound to $\text{Cu}(\text{II})$ in a distorted tetrahedral site with a highly covalent $\text{Cu}-\text{S}$ bond. As summarized in Table 7,^{2,3,35,134–161} the naturally occurring blue copper sites can be divided into four structural

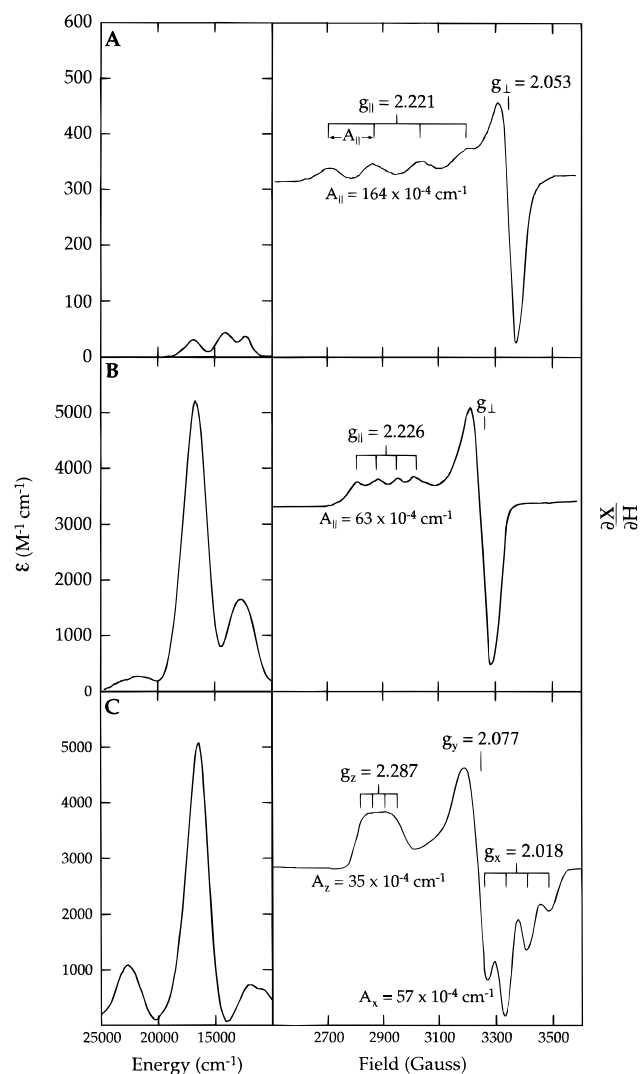


Figure 5. Low-temperature UV/vis absorption (left) and electron paramagnetic resonance (right) spectra of (A) a normal tetragonal copper complex, (B) poplar plastocyanin, and (C) stellacyanin.

Table 7. Crystallographically Defined Coordination Units of Blue Copper Proteins

unit/protein	resolution (Å)	references (PDB code) ^a
[Cu ^{II} (S·Cys)(N·His) ₂](S·Met) ^b		
poplar plastocyanin P _{Cox}	1.33, 1.6	35, 134 (1PLC, 1PND)
apoprotein	1.8	135 (2PCY)
Hg ^{II} -substituted	1.9	136 (3PCY)
reduced (P _{Cred}) – pH 3.8, ^c 7.8	1.7, 2.15	137 (6PCY, 5PCY)
<i>Chlamydomonas reinhardtii</i> P _{Cox} ^[1E]	1.5	138 (2PLT)
<i>Enteromorpha prolifera</i> P _{Cox}	1.85	139 (7PCY)
[Cu ^{II} (S·Cys)(N·His) ₂](S·Met) ^d		
Pseudoazurin Az _{ox}		
<i>Methylobacterium extorquens</i>	1.5	140 (1PMY)
<i>Alcaligenes faecalis</i> S-6	2.0, 1.55	141, 142 (2PAZ)
reduced form Az _{red} (pH 4.4; 7.8)	1.8	143 (1PZB, 1PZA)
cucumber basic blue	1.8	144 (1CBP)
nitrite reductase (type I site)		
<i>Alcaligenes faecalis</i> S-6 ^[4D]	2.0	145, 146 (1AFN)
Met150Glu mutant, Zn-substituted ^e	2.2	146
<i>Achromobacter cycloclastes</i>	2.3	147, 148 (1NRD)
NO ₂ ⁻ bound	2.2	148
Type II depleted	2.2	148
[Cu ^{II} (S·Cys)(N·His) ₂](S·Met)(OC·Gly) ^f		
azurin Az _{ox}		
<i>Pseudomonas aeruginosa</i> pH 5.5;9.0	1.93	149–151 (4AZU, 5AZU)
His35Gln, Leu mutants of Az _{ox}	2.1, 1.9	152 (3AZU, 2AZU)
Ni ^{II} -substituted ^g	2.05	153
Zn ^{II} -substituted ^g	2.1	154
<i>Alcaligenes denitrificans</i> ^[1F]	1.8	155, 156 (2AZA)
reduced form (Az _{red})	1.9	157
[Cu ^{II} (S·Cys)(N·His) ₂](OC ^δ ·Gln)]		
Stellacyanin (cucumber) ^[1G]	1.6	158
azurin (<i>Alcaligenes denitrificans</i>)		
Az _{ox} Met121Gln mutant	1.9	159
Az _{red} Met121Gln mutant ^h	1.9	159
apoprotein	1.8	160
[(His·N)(Met·S)Cu ^{II} (μ-S·Cys) ₂ Cu ^I (N·His)(OC·Glu)] ⁱ		
<i>E. coli</i> quinol oxidase, soluble fragment ^j	2.5	161
cytochrome oxidase		
<i>Pyrococcus denitrificans</i> (oxidized)	2.8	2
bovine heart (oxidized)	2.8	3

^a See footnote in Table 5. ^b Cu–S·Met distance ~ 2.9 Å. ^c Only one histidine ligand is bound in the low pH form of P_{Cred}. ^d Cu–S·Met distance ~ 2.6 Å. ^e Active-site structure of the mutant is [Zn(S·Cys)(N·His)₂](O₂C·Glu). ^f S·Met and OC·Gly are >3.0 Å from metal center. ^g M–(OC·Gly) distance shortens considerably in the metal-substituted forms. ^h This mutant becomes two-coordinate upon reduction. ⁱ Non-blue electron transfer center. ^j Engineered copper center.

classes, summarized in Figure 6, which cycle between the Cu(II) and Cu(I) states in electron transfer. The classic blue copper site is found in the plastocyanins (Chart 1E, p 2252). It has Cys·S, Met·S, and two His·N ligands bound in an elongated C_{3v} distorted tetrahedral stereochemistry,¹⁶² where the Cu^{II}–S·Met distance is quite long (~2.9 Å, forming the effective C₃ axis) and the metal is shifted toward the opposite trigonal N₂S plane. The Cu^{II}–S·Met bond involves sulfur 3p orbitals, which have an extended radial distribution function; thus there is some overlap with the unoccupied Cu 4p orbitals, resulting in a covalent bond with approximately one-third the bond strength of the Cu^{II}–N·His bonds.¹⁹ The Cu^{II}–S·Cys distance is quite short (2.1 Å), indicating a strong bond. Reduction of the blue copper center to the cuprous state results in the small structural changes diagrammed in Figure 7 except at low pH, where one His ligand is protonated and removed from the coordination sphere.¹³⁷ The small geometric change upon reduction, and retention of a long bond to Met·S upon substitution of copper with Hg(II) (despite the affinity of mercury for sulfur ligands), are prominent among the observations that have

been used to argue that the blue copper site is in an entatic or rack state.^{136,137}

The second blue copper structural class is comprised of the azurins (Az), which have an additional carbonyl oxygen *trans* to the axial Met·S ligand (Chart 1F, p 2252, Figure 6). The Cu^{II}–S·Met bond is somewhat longer (~3.1 Å) than in plastocyanin. The Cu^{II}···OC·Gly separation is too long for a covalent bond owing to the limited radial distribution of the oxygen 2p function.¹⁹ Rather, the interaction is weakly ionic, about one-fourth as strong as the limited covalent stabilization of the long Cu^{II}–S·Met bond.¹⁹ Substitution of Cu(II) by Zn(II) results in moderate structural rearrangement to a distorted tetrahedral coordination unit, with a Zn–OC·Gly distance of 2.3 Å and decoordination of the Met·S group to a position 3.4 Å from the metal. The former distance is reasonable for a Zn(II)–carbonyl interaction, which is significantly ionic in character. The third class of blue copper sites is the perturbed version depicted in Figure 6. The pseudoazurins, cucumber basic blue protein, and the type 1 centers in nitrite reductase all have the [Cu(S·Cys)(N·His)₂](S·Met)] coordination unit as in plastocyanins, but

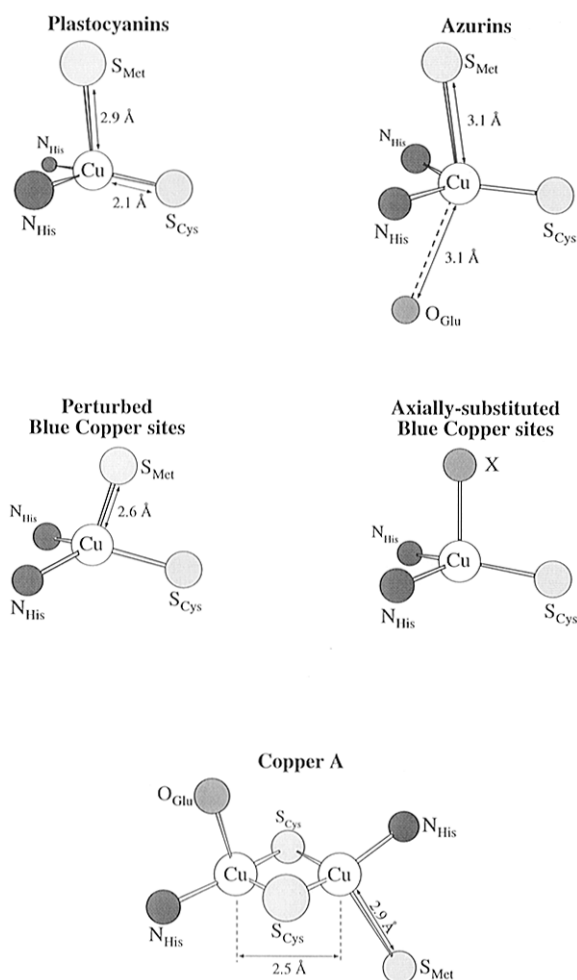


Figure 6. Structural classes of copper redox sites.

with a significantly shorter $\text{Cu}^{\text{II}}\text{-S}\cdot\text{Met}$ bond length of ~ 2.6 Å and additional angular changes (not evident in Chart 1F). These geometric differences are manifested by perturbed spectral features like those of stellacyanin (Figure 5C): a more rhombic EPR signal ($g_x \neq g_y$), hyperfine structure on the g_x signal, and enhanced intensity of an absorption band near 450 nm which is weak in plastocyanins. The latter is the most intense feature in the visible

spectrum of the type 1 site of nitrite reductase.¹⁴⁵ These changes reflect an alteration in the electronic structure of the perturbed blue copper site which should contribute to reactivity differences relative to the classic blue sites. The final class of blue copper proteins has coordinated Met-S substituted with other amino acid residues. The two best known examples are stellacyanin, which lacks methionine,¹⁶³ and Type 1 centers in fungal laccases where, on the basis of sequence alignments, noncoordinating residues replace methionine.¹⁶⁴ The X-ray structure of stellacyanin has recently become available.¹⁵⁸ It shows the coordination unit $[\text{Cu}^{\text{II}}(\text{S}\cdot\text{Cys})(\text{N}\cdot\text{His})_2(\text{OC}^{\circ}\cdot\text{Gln})]$, with the side chain glutamine carbonyl oxygen atom bound at a distance of 2.2 Å (Chart 1G, p 2252).

The last type of biological copper redox center is the so-called Cu_A site of cytochrome *c* oxidase and other heme-copper oxidases. While formulated for some time as a mononuclear site, it was first recognized as a binuclear copper center from ^{63}Cu EPR hyperfine splittings,¹⁶⁵ substantiated by Cu EXAFS,¹⁶⁶ and fully demonstrated by protein crystallography^{2,3,161} (Chart 1H, p 2252, Figure 6). The Cu_A site is a single electron donor and is the initial electron acceptor from cytochrome *c*. The most accurate structure is that of a soluble fragment of a quinol oxidase into which the binuclear site has been engineered by molecular biology techniques.¹⁶¹ The structure of this site consists of two distorted tetrahedral coordination units bridged by two Cys·S ligands. Terminal coordination is completed by one His·N ligand at each copper atom trans to each other, a Met·S ligand at one copper atom, and a backbone Glu·CO ligand at the other. The Cu–Cu distance is 2.5 Å, suggestive of a metal–metal bond. The oxidized site is a purple $\text{Cu}^{\text{II}}\text{Cu}^{\text{I}}$ chromophore, presently described as class III mixed valent;^{165–167} i.e., fully delocalized.

Two functionally significant properties of electron-carrying proteins are their redox potentials (E_0) and rates of electron transfer (k_{ET}). Active-site contributions to these properties are next considered for blue copper sites and rubredoxins, which, because of their simpler mononuclear structures, are more susceptible to analysis.

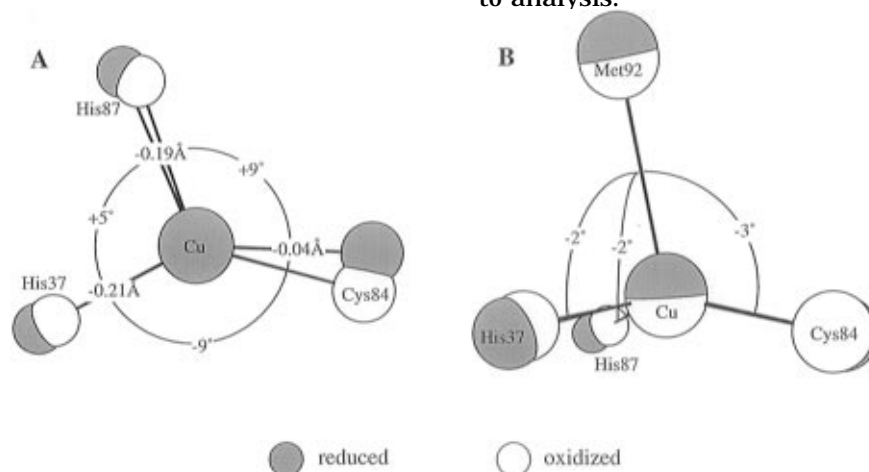


Figure 7. Geometric changes of the blue copper active site in plastocyanin upon oxidation (shaded circles, reduced; empty circles, oxidized): (A) in the bond lengths and angles in the NNS equatorial plane with the axial Met removed; (B) in the Met-S–Cu–ligand angles. (adapted from ref 137.)

3. Redox Potentials: Blue Copper and Rubredoxins

The reduction potential of an active site can be described by eq 1, where IE is the ionization energy

$$E_0(\text{V}) = \text{IE} - 4.5 + U \quad (1)$$

of the site, -4.5 eV is an additional constant to correct the potential to the normal hydrogen electrode (NHE, 240 mV more negative than the standard calomel electrode (SCE)), and U is a solvation term which accounts for reorganization of the active site environment upon reduction. The protein environment can significantly affect the potential of the metal site both through a general reduction of the dielectric relative to that of aqueous solution,¹⁶⁸ and through specific interactions with charged residues and hydrogen bonds,¹⁶⁹ which can selectively stabilize either the reduced or oxidized site. The difference in solvation between the reduced and oxidized sites can be approximated by the Born equation, $U = -(e^2/2r_0)[(\epsilon - 1)/\epsilon]$, where e is the unit charge, r is the radius of the solvent sphere around the site, and ϵ is the effective dielectric constant of the environment. In going from aqueous solution ($\epsilon \sim 80$) to a protein-bound site ($\epsilon \sim 5-10$), the contribution of this term is reduced, raising E_0 . The Cys·S ligands of both the iron-sulfur and blue copper sites have significant hydrogen-bonding interactions with amide NH groups of the protein, representative numbers of such bonds being 6, 1, and 2 for rubredoxin, plastocyanin, and azurin, respectively. These interactions will tend to reduce ligand electron density and increase the redox potential. As an example, the potential of the $[\text{Fe}(\text{SET})_4]^{-2-}$ couple is -1.08 V vs SCE in acetonitrile,¹⁷⁰ while that for the rubredoxin couple $[\text{Fe}(\text{S}\cdot\text{Cys})_4]^{-2-}$ is typically about -0.06 V vs SCE. Here the effect of the medium must be considered largely responsible for a potential shift of *ca.* 1 V. Charge interactions in the vicinity of the site can also shift potentials. The structurally equivalent type 1 sites in fungal laccases exhibit a range of 300 mV (from $+500$ to $+800$ mV) where there are amino acid variations in the protein sequence in the vicinity of the site.¹⁷¹

The IE term in eq 1 is governed by the electronic structure of the active site. There are three potential electronic contributions to the ionization energy. The first of these is the energy of the redox-active orbital, which is strongly affected by the geometry of the ligand field. Strong antibonding interactions with the ligands will raise the energy of this orbital and facilitate oxidation of the site (lowering E_0). The second is the change in the effective nuclear charge (Z_{eff}) of the metal upon complexation, and is determined by the total donor propensity of the ligand set.¹⁷² Lowering Z_{eff} raises the energy of the d-orbital manifold, making the site easier to oxidize. The third contribution involves electronic relaxation. Electrons in nonredox active orbitals (passive electrons) will shift in spatial distribution to compensate partially for the hole produced in the redox orbital upon oxidation.⁶⁹ Electron relaxation makes it easier to oxidize the site and is more effective when there is a significant change in electronic structure upon oxidation.

The blue copper proteins have relatively high reduction potentials; for example, the plastocyanin and azurin potentials are *ca.* $+350$ and $+250$ mV, respectively. These values are determined by the first two contributions above.¹⁷ The redox orbital is $d_{x^2-y^2}$. The distorted tetrahedral stereochemistry lowers the energy of this orbital relative to that for the tetragonal geometry generally observed for Cu(II) complexes, resulting in a significantly more positive potential than would be the case with the same ligand set in a tetragonal arrangement. Certain stereochemically unconstrained complexes with the $\text{Cu}^{\text{II}}\text{N}_4$ unit have $E_0 \sim -200$ mV,¹⁷³ while a constrained distorted tetrahedral complex with tetraakis(imidazolyl) coordination has $E_0 \sim +350$ mV.¹⁷⁴ These results (obtained in acetonitrile solution) suggest that the tetrahedral structure contributes about $+500$ mV to the potential. It is important to emphasize that relative to the tetrahedral species, substitution of one imidazolyl ligand with Cys·S at a bond length of 2.1 Å from Cu(II), would lower the potential of the site owing to the extensive charge donation of the thiolate ligand, thus lowering Z_{eff} .¹⁷ Replacing a second imidazolyl ligand with a normal Met·S–Cu^{II} bond at 2.3 Å would change the potential very little because that latter bond and a His·N–Cu^{II} bond at 2.1 Å involve similar charge donations. However, increasing the Met·S–Cu^{II} bond to 2.9 Å, as in plastocyanin, significantly reduces the charge donation of the ligand and is calculated to increase the potential by more than 1 V. Thus the potentials of blue copper proteins can be attributed to a combination of the distorted tetrahedral geometry and the reduced donor interaction of the long thioether–Cu(II) bond which destabilizes Cu(II) relative to Cu(I) and leads to the increased potential.¹⁷ In stellacyanin, Met·S is substituted by a carbonyl oxygen from a glutamine residue, leading to a Gln·CO–Cu^{II} bond at 2.2 Å (Chart 1G, p 2252) which has a stronger donor interaction and correlates with the lower potential ($+150$ mV) of this protein. In fungal laccases, the methionine of the Type 1 copper site is substituted by phenylalanine or leucine in the primary structures.¹⁶⁴ These noncoordinating residues eliminate the axial donor interaction, apparently contributing to the very high potentials of these sites, which can extend to *ca.* $+800$ mV.

Of all tetrahedral complexes of the type $[\text{Fe}^{\text{II}}\text{L}_4]^{2-}$, those with L = alkylthiolate have the lowest potentials.^{170,175} While the electronic contributions to these low potentials have yet to be systematically studied, it is important to recognize that for these redox centers, electronic relaxation can make a significant contribution to the redox potential. From both experiment and calculation, the electronic structure of high-spin Fe(II) complexes is normal, with the highest energy occupied orbitals being dominantly 3d in character,¹⁷⁶ as shown in Figure 8, left. For high-spin Fe(III), one finds an inverted bonding description.^{177,178} The large exchange interaction in high-spin d^5 leads to strong spin polarization and the half-occupied (spin up) d orbitals are greatly lowered in energy relative to the unoccupied (spin down) d orbitals. As shown in Figure 8, right, this places the occupied Fe 3d_i orbitals below the ligand valence

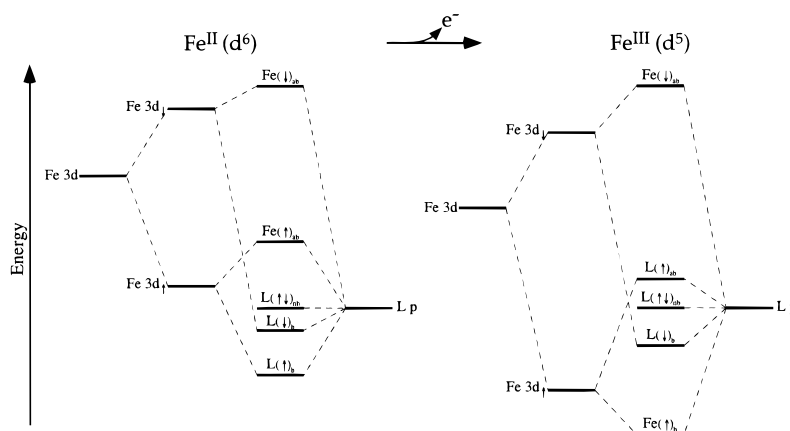


Figure 8. Bonding scheme for high-spin Fe(II) (left) and Fe(III) (right) $[\text{FeL}_4]^{2-}$ complexes. Electron exchange is large, which in a spin unrestricted (i.e., spin-polarized) description leads to a large energy splitting of the spin-up (\uparrow) orbitals relative to their spin-down (\downarrow) counterparts. In these diagrams, the spin-up orbitals are all occupied and b, nb, and ab correspond to bonding, nonbonding, and antibonding orbitals, respectively.

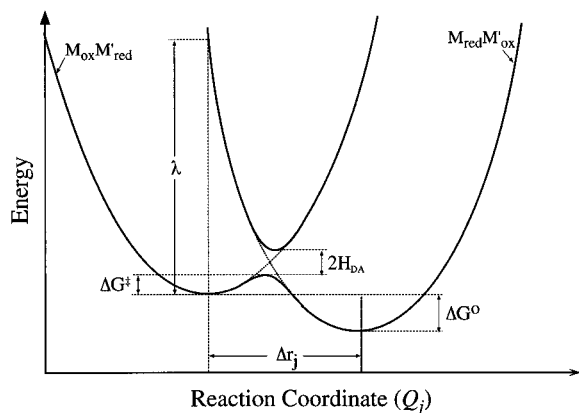


Figure 9. Potential energy diagram for electron transfer between two nearly equivalent complexes ($\Delta G^\circ \neq 0$ but is small).

orbitals, such that the highest occupied MO's have mostly ligand character. Thus, a large change occurs in electronic structure upon oxidation of high-spin Fe(II) complexes (i.e., electronic relaxation) owing to this change in electron exchange, which should contribute significantly to lowering the IE term and, therefore, the reduction potentials of such sites.

4. Electron Transfer Kinetics: Blue Copper and Rubredoxins

The kinetics of electron-transfer reactions are generally described by Marcus theory.¹⁷⁹ Two reactants come together, the environments of the two sites reorganize to facilitate electron transfer, and the electron is transferred from the reductant to the oxidant. A generic potential energy diagram for electron transfer is provided in Figure 9. In this model, the rate of electron transfer is given by eq 2, where Ao^2 is the collisional frequency conducive to electron transfer and the term $\exp(-\Delta G^\ddagger/RT)$ contains the activation energy. The quantity ΔG^\ddagger is defined by eqs 3a–d. In eqs 2 and 3a–d, w is the work required to bring two charged reactants together, ΔG° is the total free energy change for the electron-transfer reaction (zero for electron self-exchange), and λ is the energy required to reorganize the ligand (λ_i) and solvent (λ_o) environments (see Figure 9). The outer-sphere term λ_o involves reo-

larization of the solvent molecules as charge Δe is shifted from one center to the other; in eq 3c, a_1 and

$$k_{\text{et}} = Ao^2 \kappa_{\text{el}} \exp(-\Delta G^\ddagger/RT) = w + (1/4\lambda)(\lambda + \Delta G^\circ)^2 \quad (2)$$

$$\Delta G^\ddagger = w + \lambda/4(1 + \Delta G^\circ/\lambda)^2 \quad (3a)$$

$$\lambda = \lambda_o + \lambda_i \quad (3b)$$

$$\lambda_o = (\Delta e)^2 [1/2 a_1 + 1/2 a_2 - 1/r] [1/D_{\text{op}} - 1/D_s] \quad (3c)$$

$$\lambda_i = \sum_j k_j (\Delta r_j)^2 / 2 \quad (3d)$$

a_2 are the radii of the reactants, r is the radius of the solvent cavity around the reactants, and D_{op} and D_s are the optical (square of the refractive index) and static polarizabilities of the solvent. λ_o is estimated to be in the range of 10–20 kcal/mol for charge transfer in a low dielectric continuum.¹⁷⁹ In eq 3d, λ_i is the inner-sphere reorganization energy, where k_j is the force constant for the ligand–metal vibrational normal mode Q_j being distorted by bond length change Δr_j in the redox reaction. The quantity κ_{el} (the electron transmission coefficient) in eq 2 is a measure of the probability that the electron will transfer once the correct geometry is achieved. This is given in the Landau–Zener approximation¹⁸⁰ by eqs 4a–c, where h and k are the Planck and Boltz-

$$\kappa_{\text{el}} = 2P_o / (1 + P_o) \quad (4a)$$

$$P_o = 1 - \exp(-2\pi\gamma) \quad (4b)$$

$$2\pi\gamma = [H_{\text{DA}}^2 / h\nu_n] [\pi^3 / (4\Delta G^\ddagger / kT)]^{1/2} \quad (4c)$$

mann constants, ν_n is the frequency of the nuclear vibration associated with λ_i ($\sim 10^{12}$ – 10^{13} s⁻¹), P_o is the probability of going from the reactant to the product potential energy surface in Figure 9, and H_{DA} is the electronic matrix element that couples the electron donor (D) and acceptor (A) centers through the protein. When H_{DA} is small, eqs 4a–c give a value of κ_{el} proportional to H_{DA}^2 . (When H_{DA} is large, $\kappa_{\text{el}} \sim 1$ and the reaction is adiabatic.) For fixed internuclear distance ($w = 0$ in eqs 3a–d) and small electronic coupling as is often appropriate for electron

transfer studies in proteins, the first-order rate constant is expressed by eq 4d.

$$k_{\text{et}} = [(4\pi^3/h^2\lambda kT)^{1/2}]H_{\text{DA}}^2 \exp[-(\Delta G^\circ + \lambda)^2/4\lambda kT] \quad (4d)$$

Both the blue copper proteins and rubredoxin exhibit very rapid electron self-exchange. Rate constants are 10^4 – 10^6 $\text{M}^{-1} \text{s}^{-1}$ for blue copper sites¹⁸¹ and estimated at 10^9 $\text{M}^{-1} \text{s}^{-1}$ for rubredoxin on the basis of cross reaction rates,¹⁸² although the rubredoxin value may be somewhat overestimated.¹⁸³ From the above discussion, these rates require a small reorganization energy (λ_i); hence, electron transfer involves little geometric change (Δr_i), as previously noted, and a large electronic coupling matrix element (H_{DA}) between the two centers.

a. λ_i . The Entatic State. Both the $[\text{Fe}(\text{S}\cdot\text{Cys})_4]$ site in rubredoxins and the blue copper sites in plastocyanin and azurin exhibit little change in geometry on reduction. In rubredoxin there are two potential reasons for this behavior. First, the redox-active orbital is d_z ,¹⁸⁴ which is only weakly π interacting with the thiolate ligands. Second, the large electronic relaxation upon oxidation described above shifts charge from the ligand to the metal. This would reduce the net increase in the effective charge^{168,177} of the metal center on oxidation, which normally plays a major role in contracting the ligand–metal bonds.¹⁸⁵ This effect, however, needs to be evaluated experimentally. The small change in geometry upon redox in plastocyanin has been attributed to restriction of the active site by the protein in an entatic or rack state. The general concept has been that Cu(I) is normally tetrahedral, while Cu(II) is tetragonal because of the Jahn–Teller effect. A change in geometry leads to a large reorganization energy and, therefore, a large Franck–Condon barrier to electron transfer for small copper complexes. For plastocyanin, it has been believed that the protein imposes the reduced tetrahedral geometry on the oxidized site, thereby lowering the Franck–Condon barrier to electron transfer.

The entatic nature of the classic blue copper site in plastocyanin (Chart 1E, p 2252) has been analyzed in detail.¹⁷ First, with respect to the reduced site, it is found that the long thioether sulfur–Cu^I bond at ~ 2.9 Å is, in fact, imposed on the copper site by the protein (the minimum energy Met·S–Cu^I bond length should be ~ 2.3 Å). As described above, this reduces the donor interaction of the thioether with the copper, which is compensated for by the thiolate leading to the short Cys·S–Cu^I bond of 2.07 Å (the minimum energy Cys·S–Cu^I bond length should be ~ 2.2 Å). Oxidation of the reduced site produces a hole in the MO of $d_{x^2-y^2}$ character shown in Figure 10, which is strongly π antibonding with the cysteinate and weakly antibonding with the two imidazolyl ligands. Such a change in electronic structure upon oxidation produces distorting forces for the oxidized site in the reduced geometry so as to contract the Cys·S–Cu^{II} bond and two His·N–Cu^{II} bonds, consistent with the limited geometry change observed upon oxidation of the blue copper site in plastocyanin (Figure 7). Importantly, there is no distorting force present for the oxidized site along a bending mode; that situation

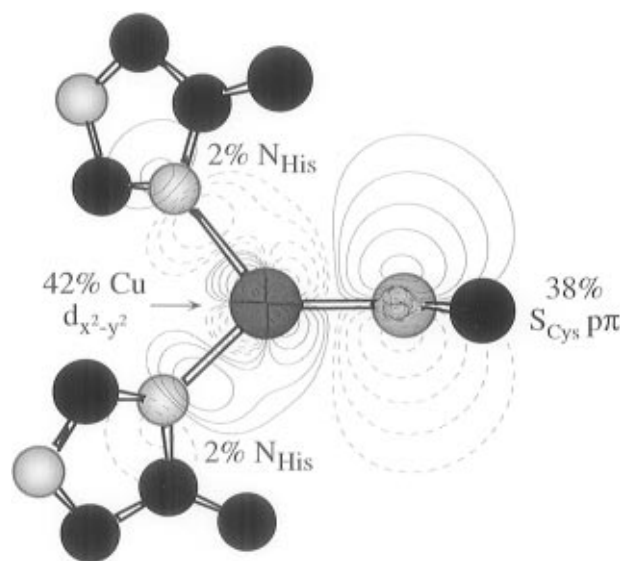


Figure 10. Redox-active orbital, of Cu $d_{x^2-y^2}$ character, in blue copper sites.

would have corresponded to a Jahn–Teller distortion of the oxidized site opposed by the protein. The electronic origin for the lack of a Jahn–Teller distortion of the oxidized blue copper site may be understood as follows. Starting with an idealized tetrahedral Cu(II) center, the ground state is 2T_2 and it is the orbital degeneracy of this state that is responsible for the Jahn–Teller distortion. For the blue copper site, the long Met·S–Cu^{II} bond lowers the effective symmetry to C_{3v} , resulting in a 2E ground state. The remaining orbital degeneracy is further eliminated by the C_s symmetry induced by contraction of the Cys·S–Cu^I bond to compensate for the long thioether–copper bond. In particular, the $d_{x^2-y^2}$ ground state and d_{xy} excited state are split by $> 10\,000$ cm^{-1} in the site environment;¹⁸⁶ it is the nuclear/electronic coupling between these levels that would normally lead to a Jahn–Teller distorting force for the Cu(II) site. Thus, the entatic nature of the classic blue copper site involves protein structure restricting the approach of the axial methionine sulfur atom to the copper center in both the reduced and oxidized states. This leads to little geometry change and a low Franck–Condon barrier to electron transfer ($\lambda/4$ in Figure 9).

b. H_{DA} : Electronic Coupling. In transferring an electron from a donor to an acceptor site in a biological system, there are three possible contributions to the electronic coupling matrix element reflecting orbital overlap between sites: (i) covalency of the ligand–metal bond, (ii) anisotropy in this covalency, and (iii) electron tunneling through the protein ligand. Most effort has been directed toward understanding contribution iii. The rate of electron tunneling through the protein matrix is expected to decay exponentially with increasing distance r_{DA} between the donor and the acceptor according to $\exp[-\beta(r_{\text{DA}} - r_{\text{van der Waals}})]$, where β , a parameter reflecting the effectiveness of the protein in mediating electron transfer, is generally found to be in the range of 0.8–1.5 \AA^{-1} .^{179,187,188} Recent studies focus on specific superexchange pathways for the electron through the protein,¹⁸⁸ where the total electronic coupling is a product of contributions from individual steps. An

Table 8. Crystallographically Defined Coordination Units of Dioxygen-Binding Proteins

protein/unit	resolution (Å)	references (PDB code) ^a
hemocyanin (Arthropod) [(His·N) ₃ Cu ^{II} (μ-η ² :η ² -O ₂ ²⁻)Cu ^{II} (N·His) ₃] oxy form (<i>Limulus polyphemus</i>) ^[2-1B]	2.4	199 (1OXY)
[(His·N) ₃ Cu ^I ···Cu ^I (N·His) ₃] deoxy form (<i>Limulus polyphemus</i>) ^[2-1A]	2.2	200 (1LLA)
deoxy form (<i>Panulirus interruptus</i>)	3.2	201–203 (1HCZ)
hemerythrin (<i>Themiste dyscrita</i>) [(His·N) ₃ Fe ^{III} (μ-η ¹ :η ¹ -O ₂ C ^δ ·Glu)(μ-η ¹ :η ¹ -O ₂ C ^γ ·Asp)(μ-O)Fe ^{III} (N·His) ₂ L] oxy form (L = OOH ⁻) ^[2-ID]	2.0	204, 205 (1HMO)
azidomet form (L = N ₃ ⁻)	1.66; 1.7/1.3	206, 38, 207; 208 ^b (2HMZ)
hydroxomet form (L = OH ⁻)	2.0	209
met form (L absent)	1.66	38, 206, 207 (2HMQ)
[(His·N) ₃ Fe ^{II} (μ-η ¹ :η ¹ -O ₂ C ^δ ·Glu)(μ-η ¹ :η ¹ -O ₂ C ^γ ·Asp)(μ-OH)Fe ^{II} (N·His) ₂] deoxy form ^[2-1C]	2.0	204, 205 (1HMD)

^a See footnote in Table 5. ^b From *Themiste zostericola* (both organisms are sipunculids).

self-exchange of spinach ferredoxin is apparently $\sim 10^{10}$ smaller.¹⁹² Little structural change is expected on reduction of the binuclear site. This site may be less accessible to a redox partner than the rubredoxin site. It is also possible that electronic coupling of the redox-active iron atom to the second iron atom contributes to these redox differences. Calculations indicate that there is a large exchange contribution to the lower potentials, and predict the presence of new low-energy charge-transfer transitions that could alter the superexchange pathways for electron transfer.¹⁹³ It is apparent that, at least with some two-iron ferredoxins of known structure, large differences in redox potentials do not correlate with differences in hydrogen bonding to the clusters.⁸⁸ Unlike the binuclear site, mixed-valence Fe₄S₄ clusters (Chart 1D, p 2252) are electronically delocalized, a property which appears to arise from exchange coupling within and between Fe₂S₂ fragments.¹⁹³ The [Fe₄S₄]^{3+,2+} redox couple is found in proteins where the cluster exists in a hydrophobic environment, apparently amenable to the stabilization of that cluster unit ([Fe₄S₄(S·Cys)₄]⁻), having the lowest net charge of any accessible oxidation state. Despite the fact that the cluster is ≥ 5 Å from the protein surface, electron transfer is facile, k_{et} being $\sim 10^5$ M⁻¹ s⁻¹.¹⁹⁴ There is as yet no systematic development of electron transfer rates of the [Fe₄S₄]^{2+,+} redox couple in relation to structural properties of the proteins.

Other than the iron–sulfur clusters, the only polynuclear biological redox center of known structure is the binuclear Cu_A site of cytochrome *c* oxidase (Chart 1H, p 2252, Figure 6). This site is in redox equilibrium with the heme *a* center which is ~ 19 Å away.^{2,3} Electrons are then transferred from heme *a* to the heme *a*₃–Cu_B binuclear site, where dioxygen is reduced to water. Electron transfer from Cu_A to heme *a* is exceptionally fast; a particularly efficient electron-transfer pathway through the protein structure has been identified.¹⁹⁵ It has been proposed that the delocalized Cu_A site might facilitate electron transfer both through limiting the geometric change with reduction and providing a somewhat extended pathway for electron transfer through the binuclear unit.¹⁹⁵

B. Dioxygen Binding

In addition to the heme protein dioxygen carriers hemoglobin and myoglobin, two other dioxygen car-

riers have evolved. These are the hemerythrins and hemocyanins, both of which contain binuclear active sites and neither of which contains a heme group. Hemerythrins^{196,197} are found in several phyla of invertebrates; they bind dioxygen in the stoichiometry O₂:2Fe. Hemocyanins^{31,32,198} are large multisubunit proteins found in arthropods and mollusks; they bind dioxygen cooperatively with the stoichiometry O₂:2Cu. We next consider the active site structure and function of these respiratory proteins.

1. Structural Aspects

Sites that have been structurally defined by protein crystallography are collected in Table 8.^{38,199–209} The deoxy and oxy forms of hemerythrin (Hr) and hemocyanin (Hc) are depicted in Chart 2,I (p 2252). DeoxyHr is characterized by the [Fe^{II}₂(μ-OH)(μ-η¹:η¹-O₂C·X)₂] bridge unit containing high-spin metal sites.²¹⁰ One Fe(II) atom is six-coordinate with three terminal His·N ligands; the other Fe(II) atom is five-coordinate with two terminal His·N ligands (Chart 2,IC, p 2252). Dioxygen reacts at the open coordination site, and is reduced to the level of peroxide as the two Fe(II) atoms are oxidized to high-spin Fe(III), which are antiferromagnetically coupled through the bridging oxo atom²¹¹ (Chart 2,ID, p 2252). The Fe^{III}–O–Fe^{III} bridge is ubiquitous in synthetic iron chemistry and occurs in at least two proteins;^{212,213} it is always found to be strongly antiferromagnetically coupled. Reduced dioxygen is bound as hydroperoxide; the proton of this group is apparently derived from the hydroxide bridge and is hydrogen bonded to the resultant oxo bridge atom.^{214,215}

Two structures of deoxyHc have been reported. The better resolved structure is that of the *L. polyphemus* (horseshoe crab) hexameric protein. The dioxygen-binding site consists of two distorted trigonal, nearly coplanar [Cu^I(N·His)₃] units whose imidazole rings are staggered across a Cu···Cu separation of 4.6 Å (Chart 2,IA, p 2252). No bridging ligand could be detected. The same basic arrangement emerges from the less accurate structure of *P. interruptus* (spiny lobster) hemocyanin. At the lower resolution, the individual [Cu^I(N·His)₃] units appear to be more distorted from trigonal-planar stereochemistry, and the Cu···Cu distance is much shorter (3.5 ± 0.3 Å). Reaction with dioxygen generates a blue chromophore and engenders substantial rearrangement of the coordination units. The symmetric

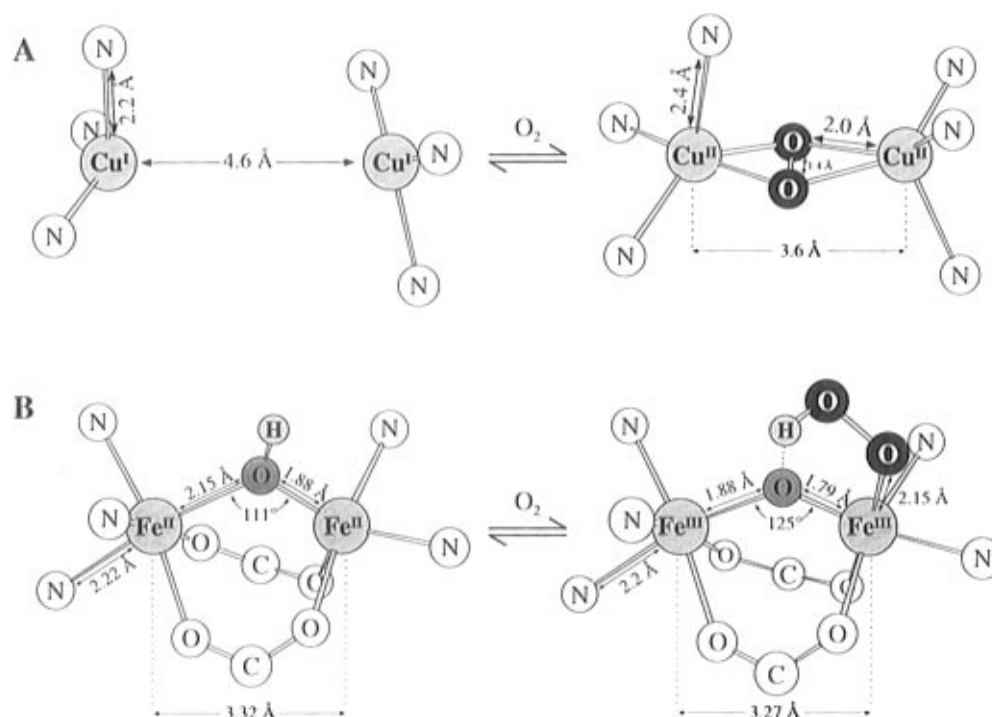


Figure 12. Effects of O_2 binding on the active sites of (A) *L. polyphemus* hemocyanin and (B) *T. dyscrita* hemerythrin.

bridge unit $[Cu^{II}(\mu-\eta^2:\eta^2-O_2)Cu^{II}]$, with a side-on coordinated peroxo group and a $Cu^{II}\cdots Cu^{II}$ distance of 3.6 Å, is formed (Chart 2,IB, p 2252). Two of the three His·N ligands at each copper remain to afford an approximately planar $Cu^{II}_2O_2N_4$ arrangement. Square-pyramidal coordination is completed at each Cu^{II} site by an axial His·N ligand; these are arranged in a trans configuration across the bridge. The coordination geometries present in deoxyHc and oxyHc are conventional for Cu(I) and Cu(II), respectively. However, the side-on peroxide–Cu(II) bridge binding is not, having been first observed by crystallography in 1989.²¹⁶

The deoxy forms of hemerythrin and hemocyanin both function as two-electron reservoirs in their action as dioxygen carriers, reducing substrate to the peroxide level with one-electron oxidation of the metal centers. Because of the different modes of binding of reduced dioxygen, the active site structural changes attendant to binding, summarized in Figure 12, are much more extensive with hemocyanin. Two functionally significant features of these active sites are next considered: the relation of structural change to cooperativity, and the nature of the metal–dioxygen bond that contributes to the reversible binding of dioxygen by these proteins.

2. Molecular Basis for Cooperativity

In hemoglobin, dioxygen binds to the five-coordinate high-spin heme Fe(II) site, causing oxidation to $Fe^{III}-O_2^-$ (limiting formulation) and movement of low-spin Fe(III) by *ca.* 0.5 Å into the porphyrin plane. This affects the iron–nitrogen bond distance and the orientation of the proximal histidine Fe–N vector relative to the porphyrin plane, producing a structural change which is propagated through the protein to the salt bridges at contacts between the four subunits of the protein.²¹⁷ The binding constant of the first dioxygen molecule is considerably lower than

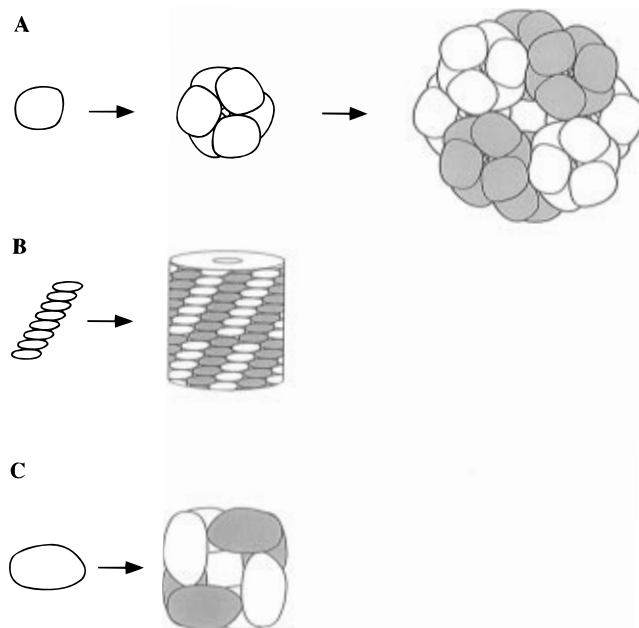


Figure 13. Quaternary structures of (A) *L. polyphemus* hemocyanin, (B) *Busycon* hemocyanin, and (C) *Golfingia gouldii* hemerythrin.

that of the last, owing to protein structural changes which tend to configure the heme site increasingly toward that in the oxygenated form.

Although no X-ray structure is yet available, spectroscopic studies indicate that the active site of mollusk hemocyanins is very similar to that of proteins from arthropods.²¹⁸ As seen in Figure 13, the quaternary structures of proteins from arthropods (A) and mollusks (B) are very different.^{31,32} The arthropod proteins have one binuclear copper site per ~70 kD subunit. Six of these aggregate to form a trigonal antiprismatic hexamer, which is the basic building block of the arthropod hemocyanins. Depending on conditions, the hexamers exist as ag-

gregates of one, two, four, six, or eight in the holoprotein. *L. polyphemus* hemocyanin has 48 subunits, which divide into five heterogeneous fractions.²¹⁹ The X-ray structure of this protein is that of a reassembled hexamer of subunit II, whose dioxygen binding can be cooperative. *P. interruptus* hemocyanin has three different subunits which form hexamers.²²⁰ For the mollusk hemocyanins, a single subunit has about eight binuclear active sites, each in a ~50 kD domain. These are linked covalently to form a "string of beads".²²¹ Twenty of these ~400 kD subunits aggregate to form the holoprotein with 160 binuclear sites and a molecular weight of ~8000 kD. Hemerythrins have one binuclear iron site per 13.5 kD subunit. These form aggregates of one, two, three, four, or eight, depending on the species from which the proteins were isolated. The octamer is often observed; it has the subunits arranged in the form of a square prism of D_4 symmetry¹⁹⁷ (Figure 13C). Hemerythrins are most commonly found in the sipunculid and brachiopod phyla. Crystal structures exist only for proteins from sipunculids, but spectroscopic similarities insure that the binuclear site is the same in proteins from both phyla. Only the brachiopod proteins, which are octameric, have been found to be cooperative in dioxygen binding.^{222,223} This may relate to the fact that these proteins have two different types of subunits ($\alpha_4\beta_4$) with additional inter-subunit contacts.²²⁴ Alternatively, there may be allosteric effector molecules present *in vivo* in the sipunculids that have not been identified.

As is the case for hemoglobin, the complicated quaternary structures of hemocyanin and hemerythrin lead to the possibility of cooperative dioxygen binding by interactions of the binding sites through protein structure. Dioxygen binding to an isolated site (with an equilibrium constant $K = [\text{MO}_2]/[\text{M}]\text{P}_{\text{O}_2} = 1/\text{P}_{1/2}$, where $\text{P}_{1/2}$ is pressure of dioxygen at which one-half of the binding sites M are oxygenated) is usually described by eq 5, which leads to a hyperbolic dioxygen saturation curve, plotted as the dashed line in Figure 14A.

$$Y = [\text{MO}_2]/([\text{M}] + [\text{MO}_2]) = KP_{\text{O}_2}/(1 + KP_{\text{O}_2}) \quad (5)$$

Alternatively, in aggregated proteins there can be cooperative interactions that lead to a sigmoidal binding curve (Figure 14A). The fraction Y of oxygenated sites is lower at low O_2 pressures than in the noncooperative case, but shows a larger change in the number of bound sites with small change in pressure, allowing for extremely efficient dioxygen uptake, delivery, and regulation.

Dioxygen binding curves are often presented as Hill plots ($\log(Y/(1 - Y))$ vs $\log P_{\text{O}_2}$). In Figure 14B, the linear behavior at low pressures has unit slope and extrapolates to an intercept corresponding to the $\text{P}_{1/2}$ value (i.e., $\log(Y/(1 - Y)) = 0$ when $Y = 0.5$) of the low-affinity site, $\text{P}_{1/2}^{\text{T}}$. The high-pressure region of the Hill plot also has unit slope, and correspondingly extrapolates to an intercept corresponding to the value of the high-affinity site, $\text{P}_{1/2}^{\text{R}}$. The difference between these two $\text{P}_{1/2}$ values leads to the site-site interaction energy, $\Delta G_{\text{O}_2}^{\text{R}} - \Delta G_{\text{O}_2}^{\text{T}} = \delta\Delta G = -RT \ln K^{\text{T}}/K^{\text{R}} = RT \ln(\text{P}_{1/2}^{\text{R}}/\text{P}_{1/2}^{\text{T}})$. The Hill curve for a

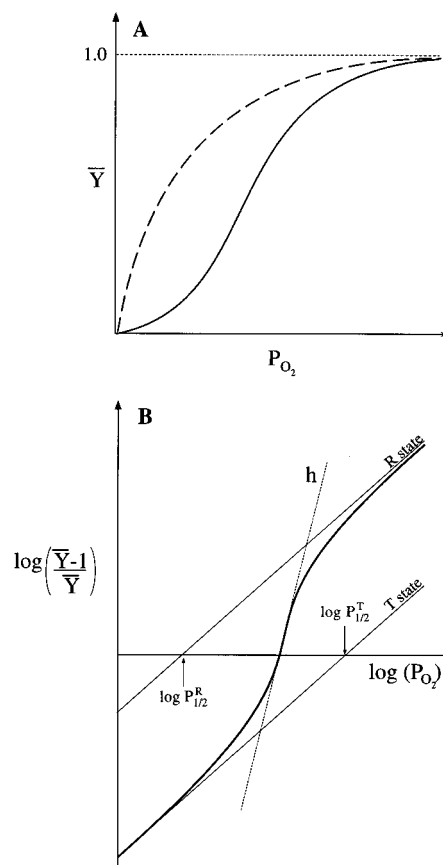


Figure 14. (A) O_2 saturation plots for cooperative (solid) and noncooperative (dashed) systems; (B) Hill plot of cooperative O_2 binding.

Table 9. Properties Relating to Cooperativity in Oxygen-Binding Proteins

property ^a	hemoglobin	hemocyanin ^b	hemerythrin ^c
$\text{P}_{1/2\text{rep}}^{\text{T}}$ (torr)	9	45	20
$\text{P}_{1/2\text{rep}}^{\text{R}}$ (torr)	0.25	2	2
$\delta(\Delta G)_{\text{max}}$ (kcal/mol)	3	5	1.4
h_{rep}	2.8	4	2

^a Properties shown in this table are representative values in all cases except for $\delta(\Delta G)$ which gives maximum values. ^b Reference 225. ^c Reference 222.

cooperative protein is nonlinear for pressures between the high- and low-affinity limits, and the slope at the $\text{P}_{1/2}$ value of the protein gives the Hill coefficient h . A value of $h = 1$ indicates a noncooperative protein aggregate, while a slope equal to the number of subunits in the aggregate corresponds to a completely cooperative protein assembly. Listed in Table 9 are representative values of the cooperativity parameters and the maximum observed site-site interaction energies for hemoglobin, hemocyanin,²²⁵ and a brachiopod hemerythrin.²²² The values indicate that the binding sites in the latter two proteins have a somewhat lower intrinsic dioxygen binding affinity than is the case for hemoglobin. The site-site interaction energy is smallest for hemerythrin and largest for hemocyanin, consistent with the latter showing the largest site structural change on dioxygen binding. Finally, the empirical values of the Hill coefficients indicate that there is cooperativity, but it does not extend over all subunits.

Physical insight into the origin of cooperativity and the number of subunits involved in the cooperative unit is given by the Monod, Wyman, Changeux (MWC) two-state model.²²⁶ This allows for a “tense” (T) and a “relaxed” (R) quaternary structure related by the equilibrium constant $L = [T]/[R]$, with all subunits changing in a concerted fashion between these states such that they have either low affinity, *tense* ($K^T = 1/P_{1/2}^T$), or high affinity, *relaxed* ($K^R = 1/P_{1/2}^R$), equilibrium constants for dioxygen binding to the active site. Solving the coupled equilibria associated with binding to these sites in the aggregated protein in the two conformations gives eq 6, where $\alpha = P_{O_2}/P_{1/2}^R$ and $c = P_{1/2}^R/P_{1/2}^T$, which must

$$\bar{Y} = \frac{\alpha(1 + \alpha)^{n-1} + L\alpha(1 + \alpha\alpha)^{n-1}}{(1 + \alpha)^n + L(1 + \alpha\alpha)^n} \quad (6)$$

be <1 for positive cooperativity in dioxygen binding. Fitting eq 6 to the data in a Hill plot as in Figure 14B provides the equilibrium constant

$$L = \left[\frac{\alpha_{1/2} - 1}{1 - c\alpha_{1/2}} \right] \cdot \left[\frac{1 + \alpha_{1/2}}{1 + c\alpha_{1/2}} \right]^{n-1}$$

where $\alpha_{1/2}$ is the O_2 concentration required for half-saturation and n is the number of interacting subunits in the cooperative unit. Consistent with the quaternary structure, the number of interacting sites in hemoglobin is four. For arthropod hemocyanins, the interacting unit is the hexamer, for mollusk hemocyanins this appears to involve a constellation of ~ 12 domains, and for hemerythrin it is four subunits, which is half the octameric protein.^{32,222,227} It should be noted that heterotropic allosteric effectors involved in the regulation of dioxygen binding act by changing the equilibrium constant L between the tense and relaxed quaternary structures. For hemocyanins, these include pH (the normal Bohr effect which shifts the Hill plot in Figure 14B to the right with decreasing pH, stabilizing the tense quaternary structure) and Ca^{2+} (which also stabilizes the tense quaternary structure). The Eu^{3+} ion has been substituted for Ca^{2+} as a spectroscopic probe. Luminescence lifetime studies of the allosteric effector site have shown that it is ~ 32 Å from the binuclear copper site.²²⁸ This effector site binds one less water molecule when the equilibrium is shifted to the tense quaternary structure, indicating that Ca^{2+} stabilizes this T state by binding an additional residue (possibly carboxylate) to crosslink the protein.

The site–site interaction energy in Table 9 should relate to the change in geometry of the active site on dioxygen binding, which is more difficult in the tense quaternary structure due to the restraints associated with inter-subunit interactions. In hemoglobin, there are six salt bridges between the α and β subunits in the deoxy structure, which are no longer present in the oxy structure. In hemerythrin, all structures available are for noncooperative sipunculids; therefore, the subunit interactions leading to cooperativity are not yet defined. From Figure 12B, the geometry change of the hemerythrin active site on binding is rather limited, consistent with the relatively low site–site interaction energy of 1.4 kcal/mol. In

contrast to hemoglobin, exogenous ligand binding to both the reduced (deoxy) and oxidized (met) forms of the hemerythrin site is not cooperative, indicating that either the oxidation of the binuclear site or the specific hydroperoxide–site interaction is the feature of the site subject to allosteric regulation.²²² The site–site interaction energy would correspond to a change in redox potential of the binuclear iron site of only 30 mV, which could easily be associated with the limited structural change. Alternatively, the ease of transfer of a proton from the bridging hydroxide to the peroxide and its stabilization by hydrogen bonding to the resultant oxo bridge could be strongly affected by changes in the Fe–O–Fe bond. While crystallography indicates little change in the Fe–Fe distance in hemerythrin on oxygenation, EXAFS data reveal that this distance changes by more than 0.3 Å (oxy, 3.24 Å; deoxy, 3.57 Å).²²⁹ This effect should significantly change the Fe–O–Fe angle, and hence, the nature of the bridge unit.

For hemocyanin, it was determined early on that the peroxide derived from dioxygen bridges the two copper atoms, and thus the dioxygen affinity could be subject to allosteric regulation by variation in the Cu–Cu distance.²³⁰ This is now supported by the two crystal structures of deoxyHc¹⁹⁸ (Table 8). As indicated above, the Cu–Cu distance in deoxy *L. polyphemus* hemocyanin is 4.6 Å, while that in the *P. interruptus* protein is 3.6 Å. Given the crystallization conditions and the presence of chloride, the former structure is thought to be in the tense state while the latter structure is believed to be relaxed. The 1 Å change in Cu–Cu distance could greatly affect the dioxygen affinity, providing a large site-site interaction energy (Table 9). This would also explain the lack of cooperativity in CO binding to the deoxyHc site,²³¹ as this ligand has been found to bind terminally to one Cu(I) atom.²³² Alternatively, there is a redox change upon dioxygen binding to hemocyanin that leads to a significant alteration in the geometry at each copper center (the Jahn–Teller effect); this could also be subject to allosteric control.

3. Nature of the Dioxygen-Metal Bond: Contributions to Reversible Dioxygen Binding

The bent, end-on structure of the Fe– O_2 unit in hemoglobin and myoglobin is well defined from X-ray crystallography on proteins and synthetic complexes.^{217,233} The iron atom lies approximately in the porphyrin plane, the Fe–O–O angle is variable (115–130°), and the Fe–O–O plane tends to bisect two adjacent nitrogen ligands of the porphyrin. The electronic structure of the oxygenated heme complex is less well understood. Many spectroscopic studies suggest that the dioxygen is bound as superoxide to a low-spin Fe(III) center; these two $S = 1/2$ entities would be antiferromagnetically coupled to give the diamagnetic ground state observed experimentally.²³³ Alternatively, electronic structure calculations suggest that this bond may be described better by an ozone-type model where dioxygen is coupled to an intermediate-spin Fe(II) site, with significant perturbations within the O_2 bond relative to the free dioxygen molecule.²³⁴ Part of the difficulty in studying heme systems is that electron delocalization over

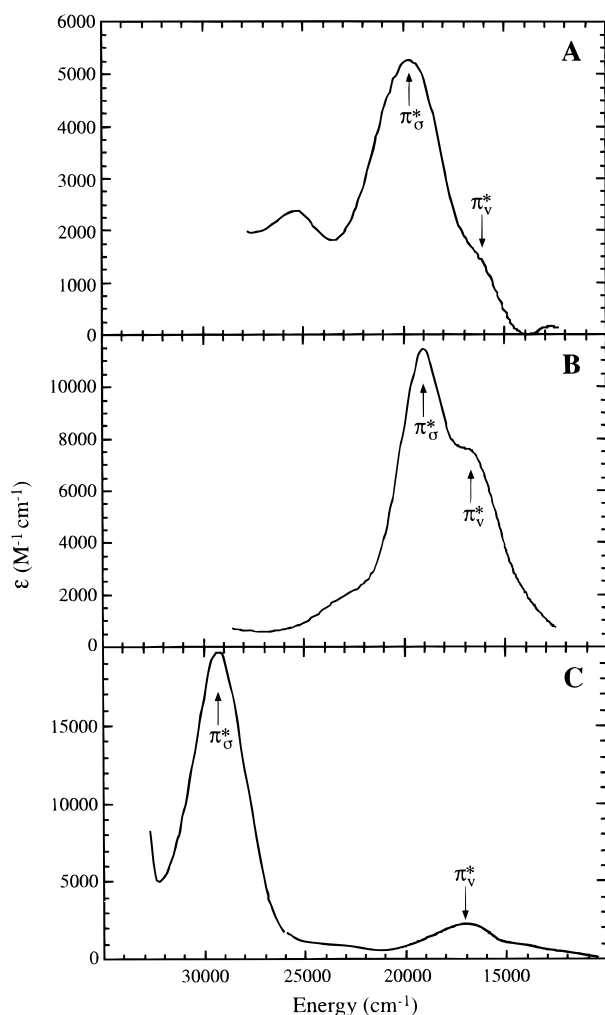


Figure 15. Peroxide \rightarrow Cu(II) charge transfer spectra: (A) an end-on peroxide monomer; (B) an end-on bridged dimer; (C) oxy-hemocyanin, a side-on bridged peroxide structure. The π^*_σ and π^*_v labels indicate the CT assignments at each site.

the porphyrin complicates the electronic structure description. In hemocyanin and hemerythrin, an initial valence description of bonding is more accessible from a variety of spectroscopies.^{212a,235} Both oxygenated proteins exhibit intense low-energy CT transitions. As already emphasized, CT transition intensities and energies sensitively probe ligand-metal bonding interactions. Thus both proteins have sites whose covalency must make a major contribution to reversible dioxygen binding. For hemocyanin, this contribution is quite well understood.

Compared in Figure 15 are the peroxide-to-Cu(II) CT absorption spectrum of oxy-hemocyanin (C) and that of a mononuclear model complex²³⁶ which has peroxide end-on bound to a single Cu(II) atom (A). The absorption band in the oxyHc spectrum ($h\nu = 29\,000\text{ cm}^{-1}$; $\epsilon_M = 20\,000$) is far more intense and at much higher energy than that of the model complex ($h\nu = 20\,000\text{ cm}^{-1}$; $\epsilon_M = 5000$).²³⁷ Also, the O–O stretching frequency of the mononuclear model complex is 803 cm^{-1} while that of oxyHc is 750 cm^{-1} . These spectral features of oxyHc are unique and reflect a novel electronic structure for the side-on peroxide-bridged structure in Figure 12A. For peroxide bonded to Cu(II), the appropriate valence

orbitals are the half-occupied $d_{x^2-y^2}$ orbital and the π^* set on the peroxide which are its highest occupied molecular orbitals. Shown in Figure 16 are orbitals and energy level schemes for three bonding modes of peroxide with Cu(II). In Figure 16A, the π^* set splits into two nondegenerate orbitals on bonding to Cu(II); π^*_σ shifts to deep binding energy owing to its σ -bonding interaction with the metal; π^*_v (vertical to the Cu–O₂ plane) is less stabilized as it is only weakly π bonding with the metal. As the intensity of the CT transition is dependent on the extent of overlap of the ligand and metal orbitals involved, the $\pi^*_v \rightarrow \text{Cu(II)}d_{x^2-y^2}$ excitation should produce a lower energy, weak CT transition, and the $\pi^*_\sigma \rightarrow \text{Cu(II)}d_{x^2-y^2}$ CT transition should be at higher energy and more intense. This predicted CT band pattern is, in fact, observed for the model complex which has peroxide end-on bound to a single Cu(II) (Figure 15A).²³⁷ It should be noted that the wave function of the occupied π^*_σ orbital acquires significant Cu $d_{x^2-y^2}$ character due to this σ -bonding interaction, and thus the peroxide ligand acts as a σ donor to the Cu(II) center.

For peroxide bridged between two Cu(II) atoms, one must take plus and minus combinations of the $d_{x^2-y^2}$ orbitals on the two copper atoms and allow these to interact with the valence orbitals on the peroxide ligand. As shown in Figure 16B, the bonding is very similar to that for the end-on monomer. The π^*_σ orbital becomes stabilized (destabilizing the LUMO) due to σ overlap and again produces a high-energy, intense CT transition. The difference between the end-on bridged case and the end-on monomer case is that there are now two σ -donor bonding interactions, one with each of the two Cu(II) atoms (note the LUMO contour). Thus the CT intensity should go up by a factor of about two, as is experimentally observed for an end-on bridged binuclear Cu(II) model complex (Figure 15B).²³⁸ The CT energy should also increase; however, this is opposed by the very large excited-state antiferromagnetism in CT transitions of bridged dimers.²³⁹ It should also be noted that the σ -donor interaction shifts electron density out of the π^*_σ orbital, which is antibonding with respect to the peroxide O–O bond. Therefore, this bond should be stronger in the end-on bridged case; indeed, the experimental O–O stretching frequency of the end-on peroxide-bridged binuclear model complex is 830 cm^{-1} .

Next, consider the electronic structure of the side-on bridged peroxide of oxy-hemocyanin in Figure 16C.²⁴⁰ First, the peroxide π^*_σ orbital is greatly stabilized in energy, indicating a *very strong* σ -donor interaction with the two Cu(II) atoms. From the LUMO contour, this occurs because there are four σ -donor interactions in the side-on bridged structure. The strong σ -donor bond is the origin of the extremely high intensity and energy of the $\pi^*_\sigma \rightarrow \text{Cu(II)}d_{x^2-y^2}$ CT transition, at $29\,000\text{ cm}^{-1}$, in the oxy-hemocyanin spectrum (Figure 15C). Further, the strong σ -donor interaction greatly destabilizes the LUMO, which is the positive combination of $d_{x^2-y^2}$ orbitals on the two Cu(II) atoms. Only in the case of the side-on bridged peroxide structure is the HOMO (the negative combination of $d_{x^2-y^2}$ orbitals) stabilized, owing to a

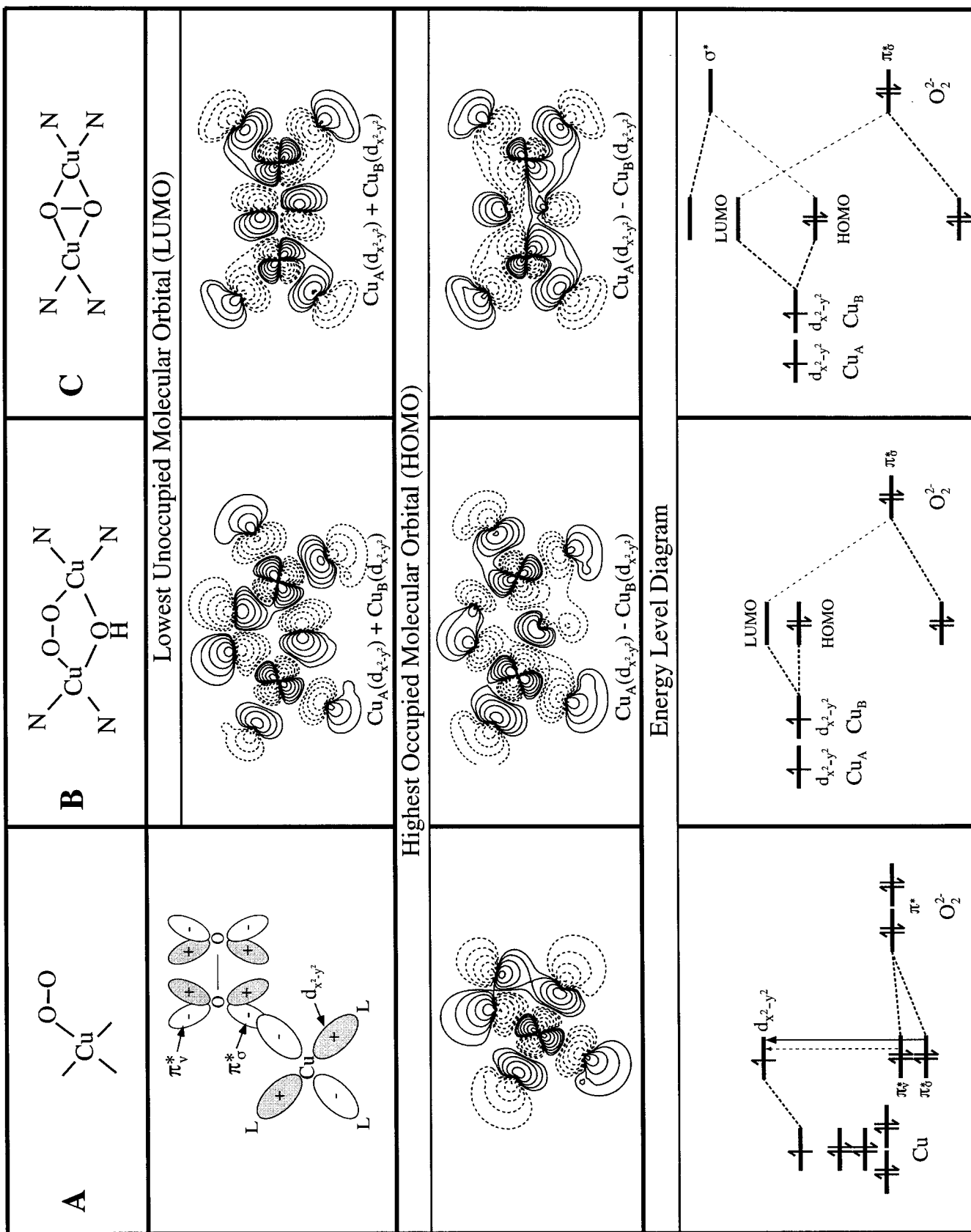


Figure 16. Electronic structures of the peroxide-Cu(II) bond: (A) end-on monomer; (B) end-on bridged dimer; (C) side-on bridged dimer site in oxy-hemocyanin.

bonding interaction with a high-energy, unoccupied σ^* orbital on the peroxide. Thus, the occupied copper $d_{x^2-y^2}$ orbitals gain some peroxide character which shifts electron density into the σ^* orbital of the peroxide (a π -acceptor interaction). This orbital is highly antibonding with respect to the O–O bond and should greatly weaken it. Given the very strong σ -donor interaction of the peroxide in the side-on bridged structure described above, one would expect the O–O bond to be stronger than for the end-on bridged case (i.e., more electron density is shifted out of the peroxide π^*_{σ} orbital). Yet, as indicated above, the O–O stretching frequency is reduced to ~ 750 cm^{-1} , a result attributed to the back-bonding interaction of the peroxide σ^* level with the two Cu(II) atoms.²⁶ The combination of strong σ -donor and π -acceptor bonding interactions leads to a correspondingly strong peroxide–binuclear Cu(II) bond. This effect is important in oxyHc as it stabilizes the site from loss of dioxygen as peroxide, which would produce a binuclear Cu(II) (met) site that is inactive in further dioxygen binding.

OxyHr also exhibits intense ligand-to-Fe(III) CT transitions in its solution and single-crystal absorption spectra,²¹⁴ presented in Figure 17, indicating a highly covalent electronic structure. At this time its electronic structure has not been well defined; however, preliminary insights are available which may be correlated with reactivity. In the hemerythrin octamer, all Fe–Fe vectors are approximately aligned,²⁴¹ and polarized single-crystal spectra can be obtained with the E vector of light parallel and perpendicular to the Fe–Fe vector of the oxy site in Figure 12B. These data²⁴² are shown in Figure 17B, where the parallel spectrum corresponds to the CT transitions of the oxo bridge and the perpendicular spectrum (with correction for a small oxo-CT contribution) gives the peroxide-to-Fe(III) charge-transfer transitions. The two spectra exhibit low-energy bands, indicating that both structural features of the oxyHr site contribute to its electronic structure, the oxo bridge being dominant on the basis of its high CT intensity. In contrast to Cu(II) with one hole in its $d_{x^2-y^2}$ orbital, high-spin Fe(III) has five half-occupied d orbitals available as electron-acceptor levels for CT transitions. The peroxide π^*_{σ} orbital should have σ overlap with one iron orbital of the e_g set and produce an intense high-energy CT transition, while π^*_{ν} should overlap one orbital of the iron t_{2g} set to produce a lower energy, weaker π CT transition as in Figure 18A. However, the peroxide-to-Fe(III) CT spectrum of oxyHr (perpendicular spectrum in Figure 17B) exhibits two sets of two transitions with only moderate CT intensity,²¹⁵ indicating that the π^* orbitals of the peroxide are not much split in energy and have comparable CT transition probabilities to both sets of iron d orbitals. These spectral features reflect protonation of the end-on peroxide as in Figure 18B, which (depending on the Fe–O–O/O–O–H dihedral angle) would interact strongly with both π^* orbitals. This would reduce their splitting, mix their wave functions, and distribute intensity over the CT transitions.²⁴³ The net effect of this protonation should be to greatly reduce the donor interaction of the peroxide with Fe(III) (causing

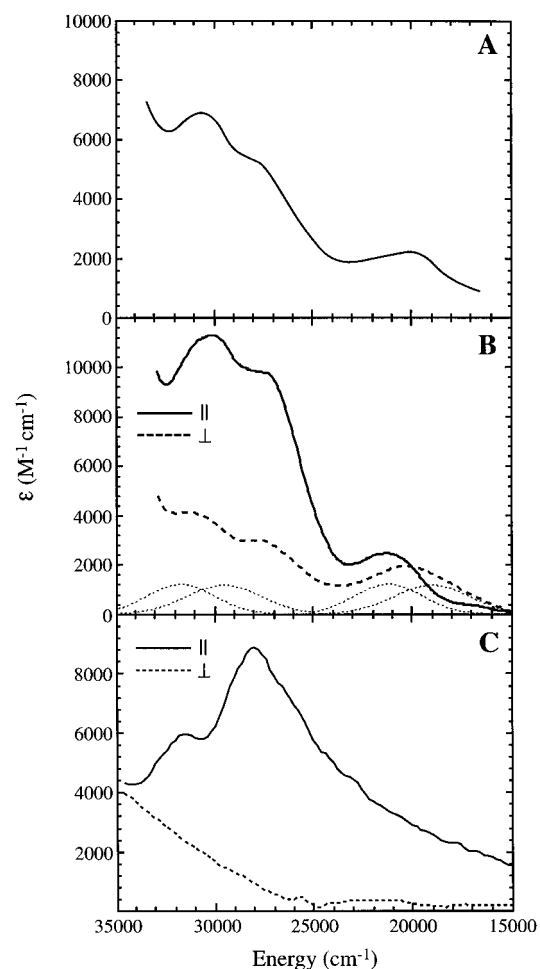


Figure 17. Charge transfer spectra: (A) oxy-hemerythrin in solution; (B) polarized single crystal of oxy-hemerythrin (\parallel = along Fe–Fe vector, gives oxo-Fe(III) CT; \perp gives peroxide-Fe(III) CT transitions—these must be corrected for a small oxo CT contribution in the high-energy region giving the two sets of two Gaussian-resolved peroxide-Fe(III) CT bands indicated with dotted lines); (C) polarized single crystal of [(HEDTA)Fe]₂O, an approximately linear Fe^{III}–O–Fe^{III} complex.

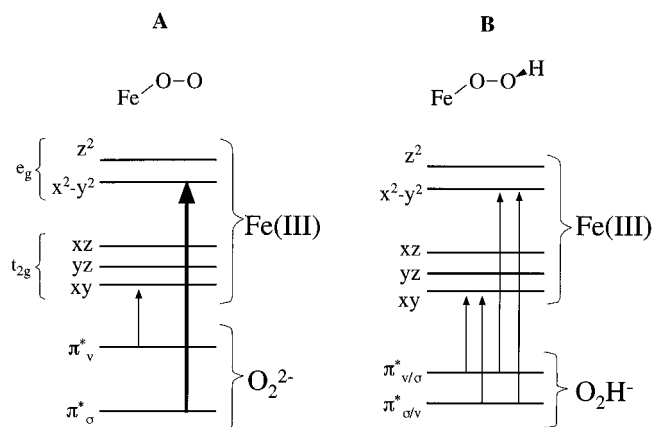


Figure 18. Electronic structure of (A) Fe^{III}–O₂²⁻ and (B) Fe^{III}–OOH⁻ with the peroxide ligands bound end-on.

the relatively low peroxide-to-Fe CT intensity in the perpendicular spectrum of Figure 17B) and the strength of the peroxide–Fe bond.

The electronic structure of μ -oxo iron(III) dimers has been studied in detail.²¹³ The CT transitions

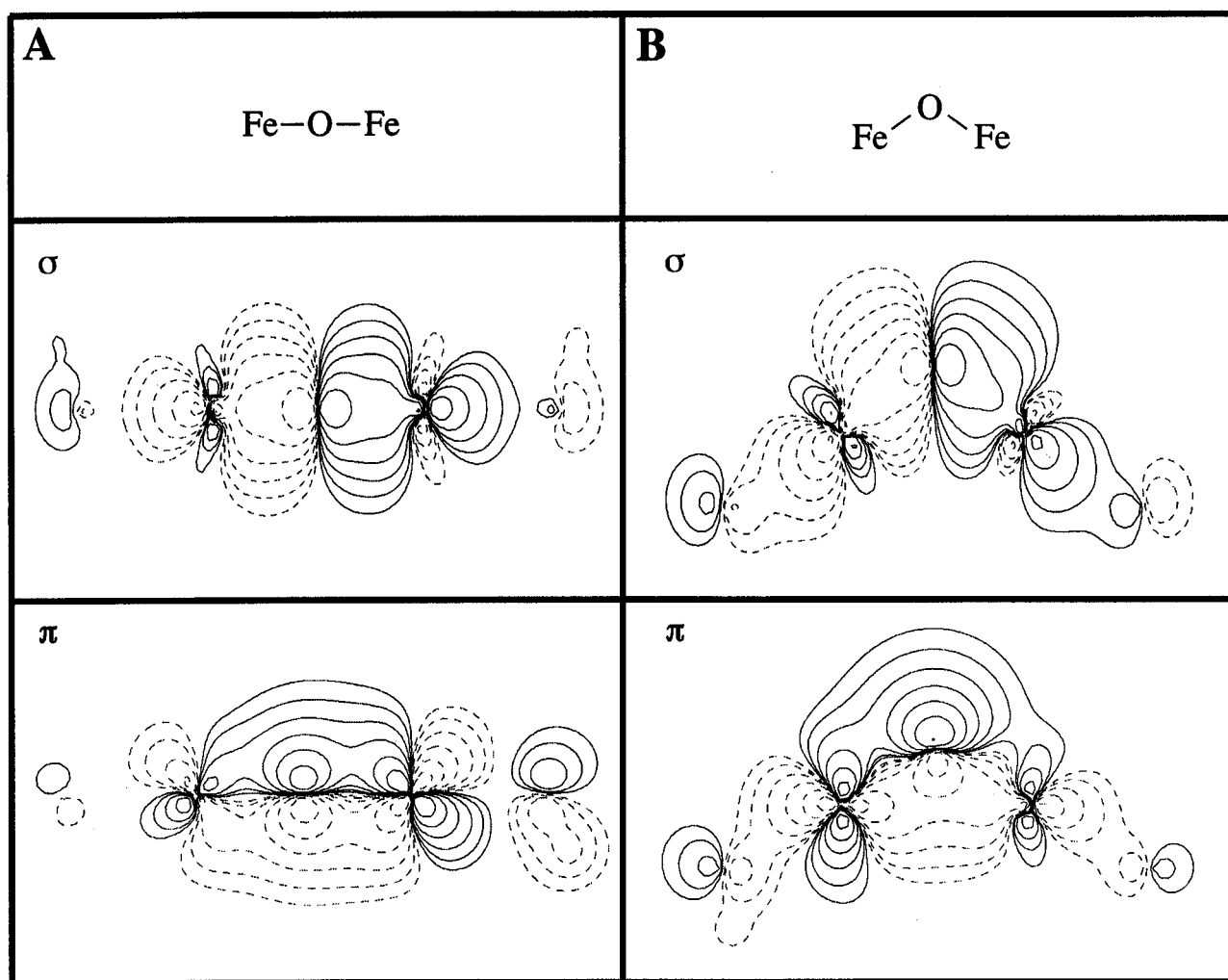


Figure 19. Electronic structure of the $\text{Fe}^{\text{III}}\text{—O—Fe}^{\text{III}}$ unit: (A) linear; (B) bent (120°) structures.

associated with the $\text{Fe}^{\text{III}}\text{—O—Fe}^{\text{III}}$ group (parallel spectrum, Figure 17B) show a remarkable temperature dependence which derives from an extremely large antiferromagnetism in the oxo \rightarrow $\text{Fe}(\text{III})$ CT excited states, and directly relates to the superexchange pathways for ground-state exchange coupling in these binuclear complexes. The assignment of the $\mu\text{-oxo} \rightarrow \text{Fe}^{\text{III}}_2$ CT spectrum in Figure 17B and its relevance to superexchange are presented elsewhere.²¹³ Here we emphasize that this oxo- $\text{Fe}(\text{III})$ CT spectrum greatly changes on going from a linear Fe—O—Fe structure (Figure 17C) to the $\sim 120^\circ$ bent structure of hemerythrin. Because the CT spectrum reflects the oxo-iron bond, this bond is significantly affected by the Fe—O—Fe angle imposed on it by the bridging carboxylates (Figure 12B). In the linear Fe—O—Fe case, the dominant bonding interaction involves the oxygen $2p_z$ orbital σ -donor bonding to the $\text{Fe}(\text{III})$ atoms, as depicted in Figure 19A. In addition to Fe 3d character, this bond has significant contributions from Fe 4s and 4p orbitals, resulting in a strong, short bond. The σ -bonding interaction does not change significantly on going to the 120° bent structure of hemerythrin (Figure 19B). The linear structure also has a doubly degenerate set of oxygen $2p_{x,y}$ orbitals (perpendicular to the Fe—O—Fe bond) involved in π -bonding interactions with the appropriate $d\pi$ orbitals on the iron. The out-of-plane oxygen π bond also does not change significantly on

going to the bent structure. However, as shown in Figure 19B, in the 120° bent structure of oxyHr and metHr the in-plane oxygen π bond loses Fe d character and becomes more localized on the oxo bridge. This increases the net electron density on the oxo ligand, which would raise its pK_a value (increased stability of the protonated over the deprotonated form).

These preliminary bonding considerations suggest possible electronic structure contributions to dioxygen binding in hemerythrin. Protonation of the peroxide reduces its donor interactions with iron and the strength of the $\text{Fe}^{\text{III}}\text{—OOH}$ bond; however, this site is stabilized from loss of peroxide (preventing irreversible production of met-hemerythrin) by the strong hydrogen bonding to the bent oxo bridge. This interaction will also facilitate deprotonation of hydroperoxide, which would concertedly increase the peroxide donor interaction with the $\text{Fe}(\text{III})$ atoms, favoring reduction of the site and reversible loss as dioxygen. These proton interactions would be affected by structural changes in the site, providing a possible contribution to the allosteric control of dioxygen binding.

C. Superoxide and Peroxide Dismutases and Non-Heme Peroxidases

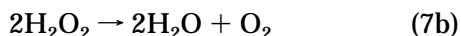
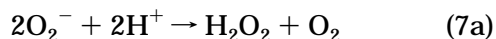
In the course of aerobic metabolism, reduced forms of dioxygen, superoxide, and peroxide, are generated

Table 10. Crystallographically Defined Coordination Units of Superoxide Dismutases and Vanadium Chloroperoxidase

enzyme/unit	resolution (Å)	references (PDB code) ^a
iron SOD [Fe ^{III} (N·His) ₃ (O ₂ C ^γ ·Asp)(OH ₂)]		
<i>Escherichia coli</i>	1.85	249, 250 (1ISB, 0SDE)
azide-bound form	1.8	249 (1ISC)
reduced (Fe ^{II})	1.8	249 (1ISA)
<i>Mycobacterium tuberculosis</i>	2.0	251, 252 (1IDS)
<i>Pseudomonas ovalis</i> (no H ₂ O ligand)	2.1	253, 254 (3SDP)
apoprotein	2.9	254
azide-bound form	2.9	255
manganese SOD[Mn ^{III} (N·His) ₃ (O ₂ C ^γ ·Asp)(OH ₂)]		
<i>Thermus thermophilus</i>	1.8	72, 256 (3MDS)
reduced (Mn ^{II})	2.3	72
azide-bound form	1.8	249 (1MNG)
<i>Bacillus stearothermophilus</i> (no H ₂ O ligand)	2.4	257
human [2-IIF]	2.2	258 (1ABM, 1MSD)
copper–zinc SOD [(His·N) ₃ (H ₂ O)Cu ^{II} (μ-η ¹ :η ¹ -N ⁻ ·His)Zn ^{II} (N·His) ₂ (O ₂ C ^γ ·Asp)]		
spinach	2.0	259 (1SRD)
<i>Saccharomyces cerevisiae</i> (yeast) [2-III]	2.5	260, 261 (1SDY)
<i>Xenopus laevis</i>	1.49	262 (1XSO)
human erythrocyte	2.4	263, 264 (1SPD)
Cys6Ala and Cys111Ser double mutant	2.5	264 (1SOS)
bovine erythrocyte	2.0	265, 266 (2SOD)
reduced (Cu ^I)	1.9	267, 268 (1SXA-C)
reduced (Cu ^I) ^b (no H ₂ O ligand)	1.7	269
cyanide-bound form	c	269
nitrated at Tyr 108	2.5	270 (1SDA)
Cys6Ala mutant	2.1	271 (3SOD)
Co ^{II} -substituted (for Zn ^{II})	2.0	272 (1COB)
vanadium chloroperoxidase [V ^V (N·His)(O) ₃ (OH)]		
<i>Curvularia inaequalis</i>	c	273
azide-bound form	2.1	273

^a See footnote in Table 5. ^b Cu^I center is three-coordinate due to protonation of bridging His ligand and loss of H₂O. ^c This structure is from a preliminary analysis.

in cells. Either directly, or indirectly through subsequent reactions, these species can be toxic; several mechanisms have evolved to eliminate them or repair the damage inflicted.^{244,245} The superoxide dismutases (SODs) and catalases catalyze the disproportionation reactions of superoxide (eq 7a) and peroxide (eq 7b), respectively. Peroxide can also be biologically



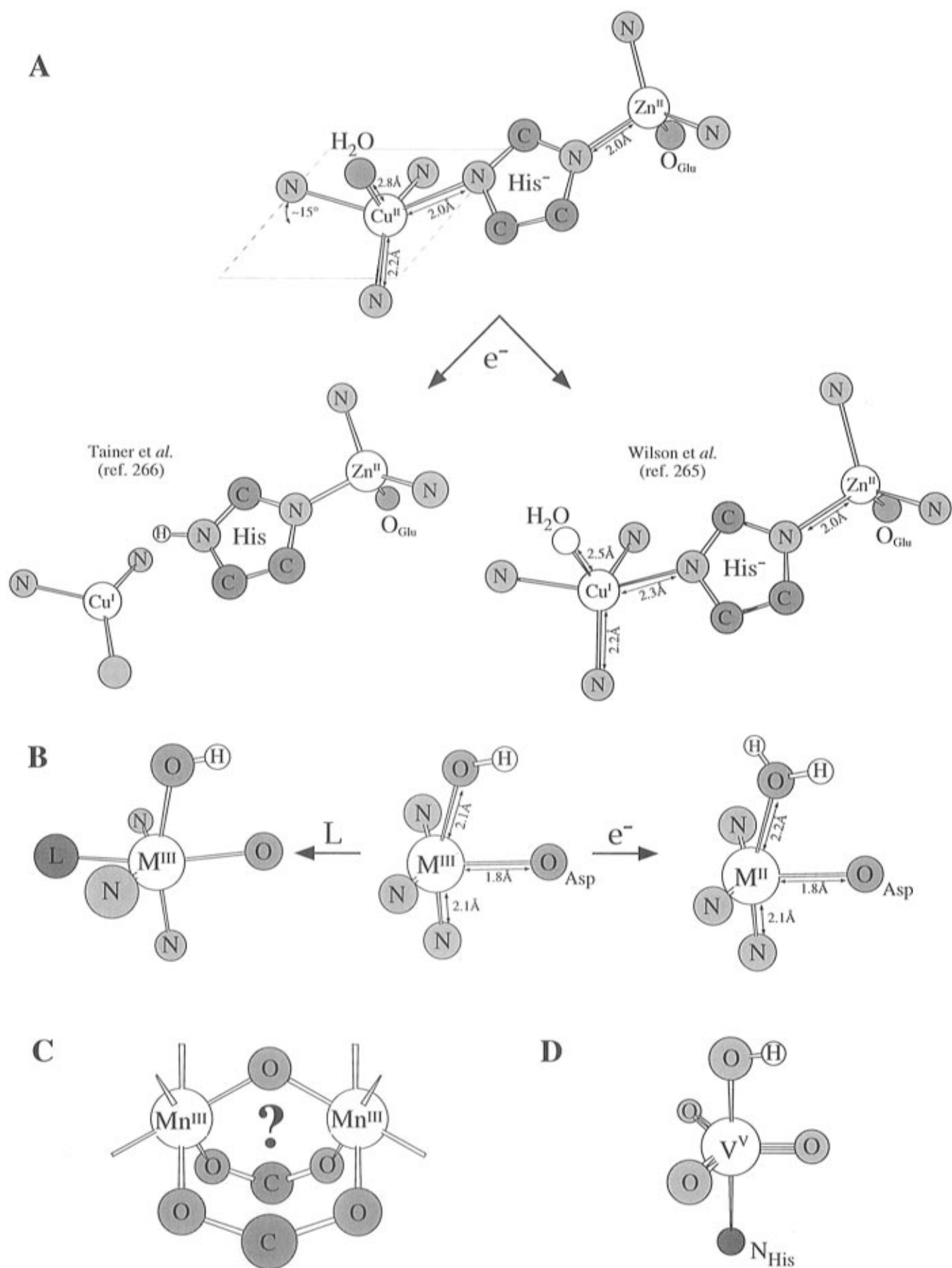
useful as a reactant in oxygenation and oxidation catalysis (peroxidase activity). In addition to the ubiquitous heme-containing peroxidases, there are non-heme vanadium-dependent haloperoxidases which halogenate organic substrates.^{246–248} Interestingly, activation of superoxide and peroxide is achieved utilizing a large range of metals (V, Mn, Fe, Cu), oxidation states (1+ to 5+), and modes of reaction (redox and Lewis acid).

1. Structural Aspects

A large body of structural information is available for SODs and is assembled in Table 10.^{72,249–273} These enzymes can be divided into two classes based on the active site structures in Chart 2,II (p 2252). The Cu/Zn SODs, mostly found in eukaryotic cells, cycle between the Cu(II) and Cu(I) states in catalysis. The structure of the oxidized site (Chart 2,II E, p 2252) is elaborated in Figure 20A. The Cu(II) center has a distorted square pyramidal structure with a

D_{2d} distortion toward tetrahedral for the four His·N ligands in the equatorial plane. Trans Cu–N vectors make an angle of 15° above or below the mean N₄ plane. The axial water ligand is weakly coordinated to Cu(II); the inductive effect on the pK_a of water is such that it binds as the neutral ligand.²⁷⁴ The imidazole group of one of the histidine ligands (His-61 in bovine SOD) is deprotonated, owing to its additional bridging interaction with Zn(II). This is the only example of an imidazolate-bridged site in a metalloprotein. The zinc atom is buried in the protein and fulfills a structural role.²⁷⁵ It is tetrahedrally coordinated, the additional ligands being two His·N and monodentate Asp·CO₂ which binds in the *syn* configuration (Figure 2D). The role of the bridging imidazolate in enzyme function has been an important question. Two structural reports have appeared for the reduced bovine enzyme; these disagree as to whether the bridge ligand is protonated and thus no longer bound to Cu(I). Spectral data for the reduced protein in solution²⁶⁷ (particularly X-ray absorption K-edge data²⁷⁶) strongly support a three-coordinate Cu(I) site. Copper(I) is not an effective competitor with the proton for the unbound site of the ligand. Crystallographic information for the cyanide-bound oxidized form shows that this exogenous ligand displaces axial water at the copper site with retention of the imidazolate bridge.

The manganese and iron superoxide dismutases, which are found in prokaryotes (Mn, Fe), mitochondria (Mn), and plants (Fe), have very similar active



site structures. The relevant oxidation states for catalysis are Fe(III,II) and Mn(III,II). The structure of the oxidized sites of both enzymes is trigonal bipyramidal (Chart 2, IIF, p 2252, Figure 20B), with two His·N and a monodentate *syn* carboxylate oxygen in the equatorial plane and axial His·N and water ligands. Two points should be noted about the axial water ligands. First, two structures, Fe SOD from *P. ovalis* and Mn SOD from *B. stearothermophilus*, do not indicate the presence of an axial water ligand. This apparent disagreement has been suggested to be due to structural disorder in the crystals.^{249,277} Second, on the basis of bond lengths and active site charge, it is thought that the water is deprotonated and binds as hydroxide to the oxidized site in both enzymes. On reduction, little overall structural change occurs; however, the bond lengths increase and from the effective pK_a it is thought that the axial hydroxide ligand is protonated to water. A structure also exists for the azide-bound form of oxidized *T. thermophilus* Mn SOD. Interestingly, rather than compete with the axial hydroxide, the exogenous ligand binds between the two equatorial His·N ligands to form a six-coordinate distorted octahedral structure.

The catalase reaction (eq 7b) is catalyzed by enzymes having either heme or non-heme active sites. The non-heme enzyme has a binuclear manganese active site that cycles between the 2Mn(II) and 2Mn(III) oxidation states in catalysis.²⁷⁸ Only preliminary structural information is available for the manganese catalase from *T. thermophilus*.²⁷⁹ From the 3 Å structure of the reduced protein, a manganese pair with a 3.6 Å metal–metal distance has been reported. The overall protein fold (four antiparallel α helices) is similar to that of hemerythrin. This, combined with the absorption spectrum of the oxidized site, which looks like those of μ -oxo, bis(μ -carboxylato) binuclear Mn(III) complexes, has led to the idea that a similar site structure may be present in manganese catalase²⁸⁰ (Figure 20C).

The structure of a vanadium chloroperoxidase (capable of oxidizing chloride, bromide, and iodide) from the fungus *Curvularia inaequalis* has been reported (Table 10). Sequence homology comparisons strongly indicate that the structural motif of this enzyme should be applicable to other vanadium-containing haloperoxidases.^{248,273} A pentavalent vanadium atom is covalently linked to the protein by His·N at one of the axial positions of the trigonal bipyramidal active site (Figure 20D). The other axial position is occupied by hydroxide. Three oxo ligands are located in the equatorial plane. Although the site is covalently linked to the protein at only one position, the coordination unit is stabilized by extensive hydrogen bonding to the equatorial oxo ligands by the protein moiety. The axial hydroxide ligand is accessible to solvent and can be replaced by other exogenous ligands such as azide.

2. Molecular Mechanisms

The disproportionation of superoxide by redox-active metal ions is generally thought to occur in two one-electron steps via a “ping-pong” mechanism as in eqs 8a,b.²⁸¹ The aqueous Cu(II) ion catalyzes this

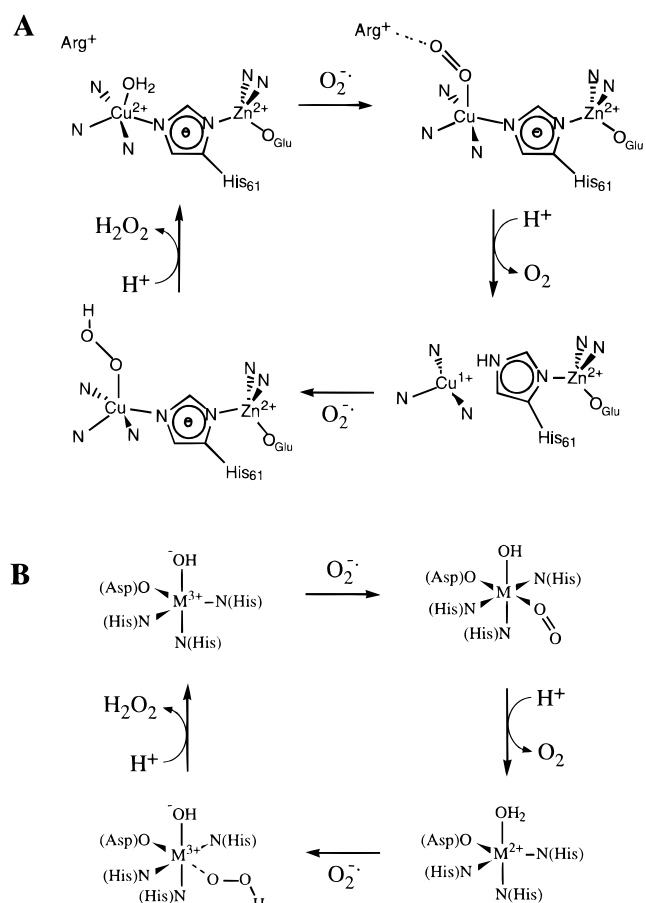
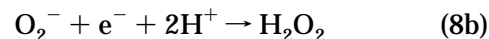


Figure 21. Mechanistic proposals for (A) Cu/Zn and (B) Fe or Mn superoxide dismutases under physiological conditions.

disproportionation through one-electron oxidation and reduction cycles about 10^4 faster than the uncatalyzed reaction ($k_{\text{uncat}} = 2.5 \times 10^5 \text{ M}^{-1} \text{ s}^{-1}$ at pH 7,^{282a} $k_{\text{Cu}} = 8 \times 10^9 \text{ M}^{-1} \text{ s}^{-1}$ ^{282b}). However, when Cu(II) is bound to most chelate ligands or adventitiously to proteins, its activity is reduced or eliminated.²⁸³



The bimolecular rates of enzymatic disproportionation of superoxide are $2 \times 10^9 \text{ M}^{-1} \text{ s}^{-1}$ for Cu/Zn SOD,²⁸⁴ $3 \times 10^8 \text{ M}^{-1} \text{ s}^{-1}$ for Fe SOD²⁸⁵ and $5.6 \times 10^7 \text{ M}^{-1} \text{ s}^{-1}$ for Mn SOD.²⁸⁶ In order to achieve these high catalytic rates, the active site must provide (i) a high rate of access of superoxide to the site and rapid release of product (dioxygen and, in particular, peroxide which can bind to metal ions leading to product inhibition), (ii) an open or exchangeable coordination position at the metal ion if an inner-sphere electron transfer mechanism is involved, (iii) rapid protonation of the peroxide anion, and (iv) the appropriate thermodynamic driving force (redox potential).

The molecular mechanisms that have been developed for the Cu/Zn²⁶⁶ and Mn and Fe²⁷⁷ SODs, set out in Figure 21, allow for these reactivity requirements. For Cu/Zn SOD, electrostatic²⁸⁷ and molecular dynamics²⁸⁸ calculations have shown that there

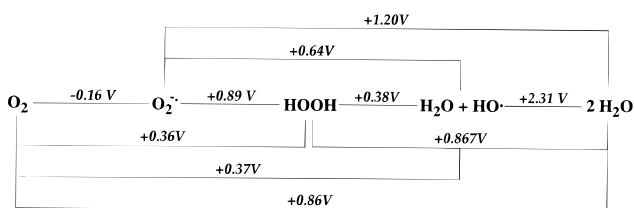


Figure 22. Latimer diagram for O_2 in aqueous solution at unit activity. (Adapted from ref 293.)

is a network of positively charged residues along the channel described in Figure 3G which steer the superoxide and enhance its rate of access to the Cu(II) center. From density functional calculations,²⁸⁹ it is thought that the superoxide must bind to the Cu(II) center, displacing the axial water for electron transfer. This binding is assisted by a positive arginine residue at about 5 Å from the Cu(II) atom and by the weak binding of the axial water ligand. Electron transfer results in loss of dioxygen and creates a Cu(I) center that is three-coordinate with the imidazolate being protonated and bound only to the zinc ion. A second superoxide would then bind to the open coordination position on Cu(I), followed by inner-sphere electron transfer to generate peroxide which is protonated by re-forming the imidazolate bridge. Additional protonation would lead to rapid loss of H_2O_2 and further turnover. The reaction sequence is depicted in Figure 21A. It should be noted that there are problems with this mechanism in terms of breaking and forming the imidazolate bridge; the turnover rate is too high under saturating superoxide conditions,²⁹⁰ and, if the zinc ion is removed, there is still dismutation with only a limited reduction in the turnover rate.²⁹¹ It is thought that the reduced Cu/Zn SOD structure with the imidazolate bridge intact (Figure 20A) may be relevant to catalysis at high superoxide concentration (i.e., non-physiological conditions) where a Cu(II)– O_2 complex could form and be reduced by the second superoxide,²⁶⁸ as observed for superoxide disproportionation by nonredox active metal ions.²⁸¹

The mechanism for the manganese and iron enzymes shown in Figure 21B is similar to that of Cu/Zn SOD. The major difference is that water is bound as hydroxide to the oxidized site and thus would not be displaced by superoxide; instead, superoxide binds to increase the coordination number of the metal. Reduction then leads to protonation of the bound hydroxide to form water, which upon oxidation by a second superoxide transfers its proton to the resultant peroxide. It is important to note that the hydroperoxide formed could have a fairly high affinity for trivalent metal ions, leading to product inhibition. At least in the case of the Fe SOD, it is found that exogenous ligands do not bind to the reduced site.²⁹² If this can be extended to the superoxide substrate, it would support an outer-sphere mechanism for the reduction of O_2^- which would result in a noncoordinated hydroperoxide product and no inhibition.

From the Latimer diagram in Figure 22,²⁹³ the reduction potential of superoxide dismutases should be between -0.16 V and $+0.89$ V, and preferentially near the middle of this range to afford maximum thermodynamic driving force for rapid one-electron oxidation and reduction of superoxide. The reduction

potentials of the superoxide dismutases are $+0.40$ V for Cu/Zn SOD,²⁹⁴ $+0.26$ V for Fe SOD,²⁹⁵ and $+0.31$ V for Mn SOD²⁹⁶ at pH values near 7, and decrease with increasing pH (by ~ 0.059 V/log unit) indicating that protonation of the site occurs with reduction. It is interesting to compare these values to the standard reduction potentials of the aquo ions: $[Cu(OH_2)_n]^{+/2+}$, $+0.16$ V; $[Fe(OH_2)_6]^{2+/3+}$, $+0.77$ V; $[Mn(OH_2)_6]^{2+/3+}$, $+1.5$ V.²⁹⁷ Thus, only the aquo copper ion should be an efficient superoxide disproportionation catalyst. The low potential of the copper couple relative to those of the iron and manganese complexes derives from the fact that it involves ionization of a monovalent rather than a divalent metal ion. The trend between the manganese and iron reduction potentials is associated with the added stability of the high-spin d^5 configuration due to electron exchange which lowers the energy of the oxidized iron and reduced manganese states. For all three metal ions, coordination to the donor ligand set of the protein should markedly stabilize the oxidized over the reduced sites because of coordination to anionic ligands. Such stabilization lowers the redox potential, although the lower dielectric of the protein environment would tend to decrease the stabilization of the oxidized site. From the above potentials, one would expect that Fe(III) bound to the three His·N, Asp·CO₂, and OH⁻ ligands of the Fe SOD site would have its potential lowered into the middle of the region for superoxide dismutation. Indeed, $[Fe(EDTA)]^-$, with $E^\circ = +0.12$ V, does catalyze superoxide disproportionation.²⁹⁸ However, the potential of aqueous manganese is considerably higher than that of aqueous iron, and $[Mn(EDTA)]^-$, with $E^\circ = +0.82$ V, does not catalyze superoxide dismutation.²⁹⁹ This difference in intrinsic reduction potentials may contribute³⁰⁰ to the fact that even though the iron and manganese SOD active sites are very similar, substitution of the manganese into the iron site and iron into the manganese site usually leads to inactive enzyme.³⁰¹ Protein differences outside the first coordination sphere may correlate with this difference in metal ion activation.^{254,255}

Alternatively, $[Cu(OH_2)_6]^{2+}$ has a relatively low reduction potential; coordination to a ligand set of three His·N, water, and imidazolate should lower it further. Thus the $+0.40$ V potential for Cu/Zn SOD is surprisingly high for the Cu(II) site structure (Chart 2, IIE, p 2252). However, a change in coordination number on reduction to a three-coordinate Cu(I) structure would stabilize the reduced site and raise the potential into the required region for efficient superoxide dismutation by eqs 8a,b. Thus, an important role of the bridging imidazolate–zinc unit, and one possible reason for the large structural difference between the active sites of Cu/Zn and Mn and Fe SODs (Chart 2, II, p 2252), is to allow for a decrease in coordination number of the redox-active metal center on reduction. This appears to be required for Cu(II) to increase its potential into the active range with protein donor ligands, but not for the Mn(III) or Fe(III) ions, which have intrinsically higher reduction potentials.

Because detailed structural insight on manganese catalases is not yet available, discussion of the

reaction mechanism on a molecular level is necessarily limited. From kinetics studies,²⁷⁸ the disproportionation of peroxide also involves a ping-pong mechanism as given in eqs 9a,b. From the Latimer

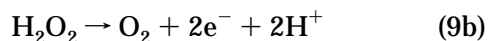
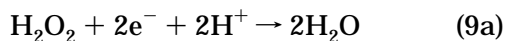


diagram in Figure 22, the net peroxide disproportionation reaction (eq 7b) must involve two-electron steps with a fairly high two-electron reduction potential midway between +0.36 V and +1.35 V. In the heme enzymes, the two-electron reduction of peroxide is accomplished by an Fe^{III}–protoporphyrin IX center with an axial tyrosinate ligand.³⁰² This generates compound I which is reasonably well characterized as a ferryl (Fe^{IV}=O) species bound to a porphyrin monoanion radical. The two-electron oxidation of the active site is thought to be assisted by the strong donor interaction of the distal axial phenolate and by Arg and His residues in the protein pocket on the proximal side, which heterolytically polarize the peroxide to give H₂O and the [Fe^{IV}O(por⁻)]⁺ intermediate. This species oxidizes a second peroxide to dioxygen in catalase, or oxidizes substrates in the case of the heme peroxidases. For Mn catalase, the two-electron reduction of peroxide is accomplished by a binuclear Mn(II) site being oxidized to two Mn(III) ions. The binuclear Mn(II) site is antiferromagnetically coupled, perhaps through a bridging hydroxide.³⁰³ The two-electron reduction of peroxide could be assisted by the formation of an oxo bridge at the oxidized binuclear Mn(III) site. The putative oxo bridge could be derived from peroxide or from the hydroxide bridge proposed to be present in the reduced structure. It is clear from EXAFS³⁰⁴ and MCD³⁰⁵ results that further oxidation of the site leads to a di(μ -oxo) Mn^{III}Mn^{IV} structure, which, however, is not active in catalysis. If the μ -oxo, bis(μ -carboxylato) structure (Figure 20C) is correct, the second peroxide would bind terminally to one Mn(III) atom of the oxidized site. This could produce a peroxy intermediate similar to the oxyHr structure (Figure 12B). Interaction of the hydroperoxide proton with an oxo bridge would increase charge donation to the binuclear manganese center, leading to its reduction and loss of dioxygen. As with hemerythrin, such an event would require a two-electron transfer, one electron to each metal ion, from the peroxide bound to one metal center and thus an efficient superexchange pathway to the adjacent metal ion. At present, accurate structural information for the oxidized and reduced forms of the manganese catalase active site is required to eliminate speculation and allow the development of a molecular mechanism for this interesting two-electron catalytic cycle.

In contrast to the manganese or heme catalases, the vanadium haloperoxidases are not redox-active during catalytic turnover.³⁰⁶ Peroxide is believed to bind to V(V) at an axial position, substituting the hydroxide ligand. Pentavalent vanadium is a strong Lewis acid and can activate bound peroxide for nucleophilic attack by halide ions, ultimately produc-

ing hypohalous acid (HOX or possibly vanadium-bound OX⁻), which can halogenate organic substrates.^{306–308} In the absence of suitable substrates, hypohalous acid can react with a second molecule of hydrogen peroxide, producing dioxygen and water (a net peroxide dismutation reaction).³⁰⁸

Biological systems have evolved a multitude of ways to deal with toxic molecules. The dismutation of superoxide and peroxide, as well as the coupling of peroxide degradation with useful chemical catalysts, are examples. Interestingly, and as already noted, the methods of activation span a large range of metals, oxidation states, and two general activation modes. All of this constitutes another elegant display of the ability of nature to harness and control the properties of bioavailable metals for specific purposes.

D. Oxidases and Oxygenases

Dioxygen reduction (oxidase activity) and activation for incorporation into organic substrates (oxygenase activity) are catalyzed by non-heme iron and copper active sites. These reactions, which are also catalyzed by flavin and heme enzymes, are listed in Table 11. The oxidases couple the one-, two-, or four-electron oxidation of substrates to the two- or four-electron reduction of dioxygen to hydroperoxide or water. The oxygenases incorporate either one (monooxygenases) or two (dioxygenases) atoms of oxygen into organic substrates. In the monooxygenases, the nonincorporated oxygen atom is reduced to water either by an additional two-electron reductant (RH₂ in Table 11) in the case of the external monooxygenases, or by the substrate itself in the internal (or mixed function) monooxygenases. It should be noted that in the case of poor substrates (S' in Table 11), the reaction can be uncoupled in the sense that the reductant is still oxidized but O₂ is reduced to peroxide rather than incorporated into the substrate. This emphasizes the connection between oxygenase and oxidase activity. In the dioxygenases, either both oxygen atoms are incorporated into the substrate (intramolecular dioxygenases) or one oxygen atom is incorporated into substrate and the second into an additional organic cofactor (intermolecular dioxygenases). The intermolecular dioxygenases lead to the apparent monooxygenation of substrate. This situation again emphasizes the parallels between the different categories of dioxygen reactivity. The non-heme oxidases and oxygenases can be classified as mononuclear and binuclear non-heme iron and mononuclear, binuclear and trinuclear copper enzymes. A list of many of these enzymes and the reactions they catalyze is given in Table 12. These enzymes and the Cu_B–heme *a*₃ site of cytochrome *c* oxidase are discussed elsewhere in this issue. Here we summarize the known structural features of these enzymes and make some general observations concerning structure/reactivity correlations.

1. Structural Aspects

a. Mononuclear Non-Heme Enzymes. Of the mononuclear non-heme iron enzymes listed in Table 12, structures are available for the intradiol and extradiol dioxygenases, lipoxigenase, and isopenicillin N-synthase. Active-site structures are collected in

Table 11. Oxidase and Oxygenase Reactions^a

oxidases	2 electron	$2RH + O_2 \rightarrow 2R + H_2O_2$
		$RH_2 + O_2 \rightarrow R + H_2O_2$
monooxygenases	4 electron	$4RH + O_2 \rightarrow 4R + 2H_2O$
		$2RH_2 + O_2 \rightarrow 2R + 2H_2O$
	external	$RH_4 + O_2 \rightarrow R + 2H_2O$
	(uncoupled)	$S + RH_2 + O_2 \rightarrow SO + R + H_2O$
dioxygenases	internal	$S' + RH_2 + O_2 \rightarrow S' + R' + H_2O_2$
	intramolecular	$SH_2 + O_2 \rightarrow SO + H_2O$
	intermolecular	$S + O_2 \rightarrow SO_2$
		$S + C_o + O_2 \rightarrow SO + C_oO$

^a RH_n = reductant; S = substrate; S' = poor substrate; C_o = cofactor.

Table 13.^{2,3,33,37,309–328} The intradiol and extradiol dioxygenases demonstrate that active sites with very different geometric and electronic structures can be employed to execute similar reactivity, in this case the incorporation of both oxygen atoms into *o*-diphenol substrates which results in ring cleavage between or external to the diol.^{329,330} The structures of intradiol and extradiol dioxygenases are compared in Chart 3 parts A and B (p 2253). The intradiol dioxygenase has a trigonal-bipyramidal geometry with His·N, Tyr·O, and hydroxide equatorial ligands and His·N and Tyr·O axial ligation. The extradiol dioxygenase has a square-pyramidal structural with equatorial His·N, carboxylate, and two *cis*-water ligands and an axial His·N ligand. As indicated in section II.A, Tyr·O is a strong donor ligand; here it stabilizes the Fe(III) state in the intradiol dioxygenases. Thus, the intradiol dioxygenases are active as high-spin iron(III), while the extradiol dioxygenases are active in the high-spin iron(II) state.^{329,330} This difference in electron structure determines their mode of reactivity; the intradiol dioxygenases function by substrate activation, while the extradiol dioxygenases function by dioxygen activation (*vide infra*). For both subclasses of mononuclear non-heme iron enzymes, the mechanism is sequential, with substrate coordination required for dioxygen reactivity. The high effective nuclear charge of Fe(III) in the intradiol dioxygenases leads to water ligand ionization, producing bound hydroxide. As shown in Figure 23A, this is thought to assist in substrate coordination as the dianion; the substrate protonatively replaces the equatorial hydroxide and axial tyrosine ligands. In the extradiol dioxygenases (Figure 23B), the catechol substrate replaces the two equatorial water ligands and is thought to bind as a monoanion with inequivalent Fe^{II}–O(substrate) bond lengths.³³¹

Two structures have recently been reported for soybean lipoxygenase, and are given in Chart 3, parts C³⁷ and D³¹⁴ (p 2253). In one, three His·N and the C-terminal carboxylate oxygen from an Ile residue bind to the Fe(II) site with a geometry described as octahedral with two open *cis* coordination positions.³⁷ In the other, these *cis* positions are occupied by two additional ligands, a distant carbonyl oxygen atom of Asn and a water ligand. Spectroscopic data on lipoxygenase indicate that there is an equilibrium mixture of five- and six-coordinate protein sites present in solution which becomes six-coordinate on binding fatty acid substrate.³³² These crystallographic and spectral studies are on the reduced form, while the oxidized form is the active catalyst.³³³ As shown in Figure 23C, oxidation of lipoxygenase is

believed to result in a similar six-coordinate high-spin Fe(III) structure with ionization of the bound water to hydroxide.^{334,335} The fatty acid substrate is thought to react by hydrogen atom abstraction to reduce the Fe^{III}–OH[–] to an Fe^{II}–OH₂ center, indicating a high reduction potential for this site in the presence of substrate.

All the remaining mononuclear non-heme enzymes in Table 12 are active as high-spin Fe(II) centers and are involved in dioxygen activation. While no crystal structure is yet available for phthalate dioxygenase or related *cis*-hydroxylation enzymes, a fair amount of spectroscopic information is available from XAS³³⁶ and MCD.^{337,338} The Fe(II) center is six-coordinate, but upon binding substrate in the protein pocket with the aromatic ring adjacent to the iron the coordination number decreases to five, leading to an open coordination position at the Fe(II) center for O₂ reactivity (Figure 23D). Very little structural information is presently available for ω -hydroxylase³³⁹ or any pterin- or α -ketoglutarate-dependent dioxygenase. For both of the latter classes of enzymes, one oxygen atom is incorporated into substrate and the other into the organic cofactor bipterin or α -ketoglutarate. In the case of the α -ketoglutarate-dependent enzymes, cofactor oxygenation leads to succinate, which contains the second atom of dioxygen, and CO₂. For the pterin-dependent enzymes, oxygenation of the organic cofactor produces a transient 4 α -hydroxypterin species that dehydrates to the oxidized dihydropterin.³⁴⁰ Thus the net reaction is that of an external monooxygenase, and the pterin-dependent enzymes are often classified as such. Clavaminate synthase is used as the example of an α -ketoglutarate-dependent enzyme in Table 12 because, in addition to the usual hydroxylation chemistry of this class of enzymes,³⁴¹ it also catalyzes oxidative ring closure³⁴² similar to the reactivity of isopenicillin N-synthase (IPNS),³⁴³ which is not α -ketoglutarate-dependent.

The recent crystal structure of the manganese-substituted IPNS enzyme³¹⁵ has been adapted to Fe(II) coordination and is illustrated in Figure 23E. The site is six-coordinate with two His·N, Gln·N, and monodentate Asp·CO₂ endogenous ligands and two *cis* water ligands. The thiolate group of the ACV substrate is known to bind to the Fe(II) center,³⁴⁴ and it is thought that this binding induces a structural change at the site such that O₂ attacks at the Gln·N coordination position. Bleomycin is included in Table 12 as it is a histidine-containing glycopeptide antibiotic which catalyzes a reaction very similar to that of cytochrome P-450 by use of a mononuclear non-

Table 12. Iron and Copper Oxidases and Oxygenases and Related Enzymes^a

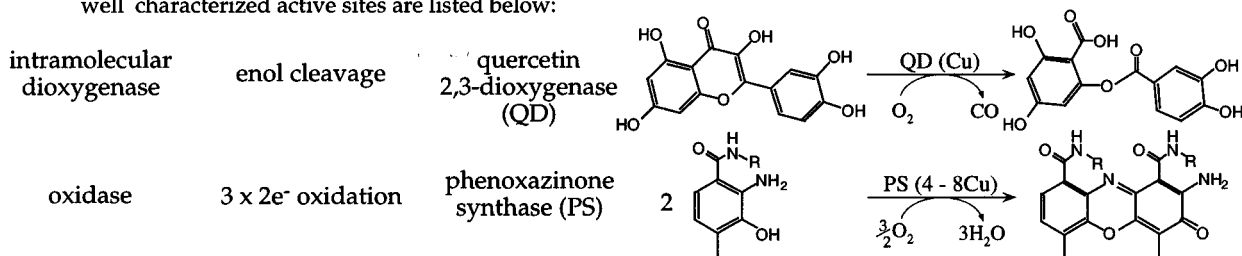
Enzyme Type	Reaction Type	Representative Enzyme ^b	Catalytic Reaction ^c
<i>mononuclear non-heme iron enzymes</i>			
intramolecular dioxygenase	intradiol dioxygenation	protocatechuate 3,4-dioxygenase (PCD) ^d ✓	$\text{3,4-PCD (Fe}^{\text{III}}\text{)} \xrightarrow{\text{O}_2}$
	extradiol dioxygenation	catechol 2,3-dioxygenase (CTD) ^e ✓	$\text{2,3-CTD (Fe}^{\text{II}}\text{)} \xrightarrow{\text{O}_2}$
	hydroperoxidation	lipoxygenases (LO) ✓	$\text{LO (Fe}^{\text{III}}\text{)} \xrightarrow{\text{O}_2}$
	<i>cis</i> -hydroxylation	phthalate dioxygenase (PDO) ^{f,g}	$\text{PDO (Fe}^{\text{II}}\text{ + Rieske)} \xrightarrow{\text{O}_2, \text{NADH} \rightarrow \text{NAD}^+}$
external monooxygenase	hydroxylation	ω -hydroxylase (ω H)	$\omega\text{H (Fe}^{\text{II}}\text{)} \xrightarrow{\text{O}_2, 2\text{Rd}_{\text{red}} \rightarrow \text{H}_2\text{O}, 2\text{Rd}_{\text{ox}}}$
intermolecular dioxygenase	pterin-dependent hydroxylation	phenylalanine hydroxylase (PAH) ^{h,i}	$\text{PAH (Fe}^{\text{II}}\text{)} \xrightarrow{\text{O}_2, \text{H}_4\text{biopterin} \rightarrow \text{H}_2\text{O}, \text{H}_2\text{biopterin}}$
	α -ketoglutarate-dependent hydroxylation	clavaminate synthase (CS) ^j	$\text{CS (Fe}^{\text{II}}\text{)} \xrightarrow{\text{O}_2, \alpha\text{-KG} \rightarrow \text{CO}_2, \text{succinate}}$
oxidase	α -ketoglutarate-dependent 4e ⁻ oxidation	clavaminate synthase	$\text{CS (Fe}^{\text{II}}\text{)} \xrightarrow{\text{O}_2, \alpha\text{-KG} \rightarrow \text{H}_2\text{O}, \text{CO}_2, \text{succinate}}$
	4 e ⁻ oxidation		isopenicillin N-synthase (IPNS) ✓
	H [•] abstraction	bleomycin (BLM) ^k	$\text{BLM (Fe}^{\text{II}}\text{)} \xrightarrow{\text{O}_2, \text{e}^-}$
<i>binuclear non-heme iron enzymes</i>			
external monooxygenase	hydroxylation	methane monooxygenase (MMO) ✓	$\text{MMO (Fe}^{\text{II}}\text{Fe}^{\text{II}}\text{)} \xrightarrow{\text{O}_2, \text{NADH} \rightarrow \text{H}_2\text{O}, \text{NAD}^+}$
oxidase	4 x 1e ⁻ oxidation/ 4e ⁻ reduction of O ₂	ribonucleotide diphosphate reductase (RDPR) ✓	$\text{RDPR (Fe}^{\text{II}}\text{Fe}^{\text{II}}\text{)} \xrightarrow{\text{O}_2, \text{e}^-} 2\text{H}_2\text{O}$
	2e ⁻ oxidation	Δ^9 desaturase (Δ^9)	$\Delta^9 \text{ (Fe}^{\text{II}}\text{Fe}^{\text{II}}\text{)} \xrightarrow{\text{O}_2, \text{AH}_2 \rightarrow 2\text{H}_2\text{O}, \text{A}}$

Table 12 (Continued)

Enzyme Type	Reaction Type	Representative Enzyme ^b	Catalytic Reaction ^c
mononuclear copper enzymes^l			
oxidase	2e ⁻ oxidation/ 2e ⁻ reduction of O ₂	amine oxidase (AmO) ✓	$\text{R-CH}_2\text{-NH}_2 \xrightarrow[\text{O}_2]{\text{AmO (Cu}^{\text{II}} + \text{TOPAQ)}} \text{R-CHO} + \text{NH}_3$
		galactose oxidase (GO) ✓	$\text{Galactose} \xrightarrow[\text{O}_2]{\text{GO (Cu}^{\text{II}} + \text{Tyr-SR)}} \text{Galactonolactone}$
reductase	1e ⁻ oxidation of PsAz/ 1e ⁻ reduction of NO ₂ ⁻	nitrite reductase (NiR) ✓	$\text{NO}_2^- \xrightarrow[\text{2H}^+, \text{PsAz}_{\text{red}}]{\text{NiR (Cu}^{\text{I}} + \text{Cu}^{\text{I}})} \text{NO}$
uncoupled binuclear copper enzymes			
external monooxygenase	hydroxylation	dopamine β-hydroxylase (DBH)	$\text{Dopamine} \xrightarrow[\text{O}_2, \text{2AscH}_2, \text{2AscH}^+]{\text{DBH (Cu}^{\text{I}} + \text{Cu}^{\text{I}})} \text{3,4-Dihydroxyphenylethylamine}$
		peptidylglycine α-hydroxylating monooxygenase (PHM) ^m	$\text{Peptidylglycine} \xrightarrow[\text{O}_2, \text{2AscH}_2, \text{2AscH}^+]{\text{PHM (Cu}^{\text{I}} + \text{Cu}^{\text{I}})} \text{α-Hydroxy-peptidylglycine}$
coupled binuclear copper enzymes			
internal monooxygenase	hydroxylation & 2e ⁻ oxidation	tyrosinase	$\text{Tyrosine} \xrightarrow[\text{O}_2, \text{H}_2\text{O}]{\text{Tyr (Cu}^{\text{I}}\text{Cu}^{\text{I}})} \text{3,4-Dihydroxyphenylpyruvate}$
trinuclear copper enzymes			
oxidase	4 x 1e ⁻ oxidation/ 4e ⁻ reduction of O ₂	ascorbate oxidase (AO) ✓	$4 \text{ Ascorbate} \xrightarrow[\text{O}_2, \text{2H}_2\text{O}]{\text{AO (3Cu}^{\text{I}} + \text{Cu}^{\text{I}})} 4 \text{ Ascorbyl radical}$
		ceruloplasmin (CEP) ⁿ ✓	$4 \text{ Fe}^{2+} \xrightarrow[\text{O}_2, \text{2H}_2\text{O}]{\text{CEP (3Cu}^{\text{I}} + \text{3Cu}^{\text{I}})} 4 \text{ Fe}^{3+}$
		laccase (LC)	$4 \text{ HO-C}_6\text{H}_4\text{-OH} \xrightarrow[\text{O}_2, \text{2H}_2\text{O}]{\text{LC (3Cu}^{\text{I}} + \text{Cu}^{\text{I}})} 4 \text{ HO-C}_6\text{H}_4\text{-O}^\bullet$
external monooxygenase	hydroxylation	copper methane monooxygenase (MMO) ^o	$\text{CH}_4 \xrightarrow[\text{O}_2, \text{NADH}]{\text{MMO (3Cu}^{\text{I}})} \text{CH}_3\text{OH}$
copper-heme enzymes			
oxidase	4 x 1e ⁻ oxdn of cyt c/ 4e ⁻ redn of O ₂	cytochrome c oxidase ✓	$4 \text{ cyt } c \xrightarrow[\text{O}_2, \text{2H}_2\text{O}]{\text{Cyt } c \text{ Ox } ((\text{Cu}^{\text{I}}\text{Cu}^{\text{I}})_A, \text{heme}_A^{2+}, \text{Cu}^{\text{I}}\text{-heme}_{A3}^{2+})} 4 \text{ cyt } c^+$

Footnotes to Table 12

^a this table includes only enzymes which have been sufficiently well characterized. Other copper enzymes with less well characterized active sites are listed below:



^b ✓ indicates that the enzyme has been crystallographically defined (see Table 13).

^c abbreviations used: NADH = nicotinamide dinucleotide, Rd = rubredoxin, PsAz = pseudoazurin, AscH₂ = ascorbate, α-KG = α-ketoglutarate, TOPAQ = TOPA quinone.

^d other intradiol dioxygenases include catechol 1,2-dioxygenase, 7,8-dihydroxykynurenate 8,8α-dioxygenase, ascorbate 2,3-dioxygenase, caffeate 3,4-dioxygenase and 2,3-dihydroxyindole 2,3-dioxygenase.

^e other extradiol dioxygenases and related enzymes include procatechuate 4,5-dioxygenase, 2,3-dihydroxybenzoate 3,4-dioxygenase, and 3,4-dihydroxyphenylacetate 2,3-dioxygenase. Enzymes active on monodisols and/or meta or para disols are gentisate 1,2-dioxygenase, 3-hydroxyanthranilate 3,4-dioxygenase, and 2,5-dihydroxypyridine 5,6-dioxygenase.

^f other *cis*-dihydrodiol dioxygenases include benzene dioxygenase, benzoate dioxygenase, naphthalene dioxygenase, pyrazon dioxygenase, and toluene dioxygenase.

^g several enzymes with similar non-heme ferrous active sites do not yield dihydrodiol products. These include 4-chlorophenyl-acetate 3,4-dioxygenase (chloride elimination yielding catechols), vanillate demethylase (biodegradation of lignin), and 4-methoxybenzoate *O*-demethylase (putidamonooxin, hydrolysis of 4-methoxybenzoic acid to 4-hydroxybenzoic acid).

^h often listed as a monooxygenase.

ⁱ other pterin-dependent hydroxylases include tyrosine *o*-hydroxylase, tryptophan 5-hydroxylase, and benzoate 4-hydroxylase.

^j other α-ketoglutarate-dependent hydroxylases include deoxyuridine-1'-hydroxylase, deoxyuridine-2'-hydroxylase, hyoscyamine 6β-hydroxylase, deacetoxyvindoline 4-hydroxylase, deacetoxycephalosporin C synthase, deacetylcephalosporin C synthase, proline 4-hydroxylase, thymine hydroxylase, prolyl hydroxylase, and lysyl hydroxylase. A similar class of non-heme iron enzymes, known as ethylene-forming enzymes (EFEs), do not require α-KG, using ascorbate as a stoichiometric reductant instead.

^k bleomycin is a glycopeptide antibiotic composed of a β-aminoalanine-pyrimidine-β-hydroxyhistidine metal-binding domain directly bound to a DNA-binding bithiazole-terminal amine tail and a disaccharide glucose-mannose region at the β-hydroxyhistidine. Hydrogen abstraction is the first step of a multistep process which cleaves DNA and produces base propenals.

^l phenylalanine hydroxylase (PAH) is often classified as a mononuclear pterin-dependent copper enzyme; recent literature shows, however, that copper is not required for activity (see Carr, R. T.; Benkovic, S. J. *Biochemistry* 1993, 32, 14132).

^m this is one functional component of the enzyme petidylglycine α-amidating monooxygenase (PAM).

ⁿ ceruloplasmin is highly unspecific in its oxidative function; Fe²⁺ is one of several demonstrated substrates for this enzyme.

^o EPR and magnetic data presently support the possibility that CuMMO contains a trinuclear copper cluster.³⁶⁶

heme Fe(II) active site.³⁴⁵ Spectroscopic information is available on this site, indicating that it is six-coordinate with a weak axial ligand position available for dioxygen reactivity.³⁴⁶ The oxy-bleomycin complex accepts an additional electron to generate activated bleomycin,³⁴⁷ which reacts with DNA by H-atom abstraction from the C4'-position of the deoxyribose sugar.³⁴⁵

In summary, the intradiol dioxygenases and lipoxygenases react with substrate at the high-spin Fe(III) level, while all other mononuclear non-heme iron enzymes are active for catalysis in their Fe(II) states.

b. Binuclear Non-Heme Enzymes. Of these enzymes listed in Table 12, structures are now available for methane monooxygenase (MMO) and ribonu-

Table 13. Crystallographically Defined Iron and Copper Oxidases and Oxygenases and Related Enzymes

enzyme/unit	resolution (Å)	references (PDB code) ^a
Mononuclear Iron		
protocatechuate 3,4-dioxygenase (<i>Pseudomonas aeruginosa</i>) ^[3A] [Fe ^{III} (N·His) ₂ (O·Tyr) ₂ (OH)]	2.15	309, 310, 311 (2PCD)
2,3-dihydroxybiphenyl 1,2-dioxygenase [Fe ^{II} (N·His) ₂ (O ₂ C ^δ ·Glu)(OH) ₂] <i>Pseudomonas cepacia</i> ^[3B] <i>Pseudomonas</i> sp. strain KKS102 oxidized (Fe ^{III})	1.9 1.8 1.8	312 (1HAN) 313 313
lipoxygenase-1 (Soybean) ^c [Fe ^{III} (N·His) ₃ (O ₂ C·Ile ^δ)(OC ^γ ·Asn)(OH) ₂] ^[3D] [Fe ^{III} (N·His) ₃ (O ₂ C·Ile ^δ)] ^[3C]	2.6 2.6	37 314 (2SBL)
isopenicillin N-synthase Mn substituted [Mn ^{II} (OC ^γ ·Gln)(N·His) ₂ (O·Asp)(OH) ₂]	2.5	315
Binuclear^e Iron		
methane monooxygenase (<i>Methylococcus capsulatus</i> -Bath) ^[3F] oxidized (+4 °C) [(H ₂ O)(Glu· ^δ CO ₂)(His·N)Fe ^{III} (μ-η ¹ :η ¹ -O ₂ C ^δ ·Glu) (μ-η ¹ :η ¹ -O ₂ Ac)(μ-OH)Fe ^{III} (N·His)(O ₂ C ^δ ·Glu) ₂]	2.2	316, 317 (1MMO)
oxidized (-160 °C) [(H ₂ O)(Glu· ^δ CO ₂)(His·N)Fe ^{III} (μ-η ¹ :η ¹ -O ₂ C ^δ ·Glu) (μ-OH ₂)(μ-OH)Fe ^{III} (N·His)(O ₂ C ^δ ·Glu) ₂]	1.7	318
fully reduced (-160 °C) [(H ₂ O)(Glu· ^δ CO ₂)(His·N)Fe ^{II} (μ-η ¹ :η ² -O ₂ C ^δ ·Glu) (μ-η ¹ :η ¹ -O ₂ C ^δ ·Glu) Fe ^{II} (N·His)(O ₂ C ^δ ·Glu)]	1.7	318
ribonucleotide reductase (<i>Escherichia coli</i> -Protein R2) ^[3E] [(H ₂ O)(Asp· ^γ CO ₂)(His·N)Fe ^{III} (μ-η ¹ :η ¹ -O ₂ C ^δ ·Glu) (μ-O ²⁻)Fe ^{III} (N·His)(O ₂ C ^δ ·Glu) ₂ (OH) ₂]	2.2	319 (1RIB)
Mn substituted	2.2	320 (1MRR)
apoenzyme	2.5	321
Mononuclear Copper		
amine oxidase [Cu ^{II} (N·His) ₃ (OH) ₂] <i>Escherichia coli</i> active form	2.0 2.0 2.4	322 322 323
inactive form pea seedling ^[4A]		
galactose oxidase (<i>Dactylium dendroides</i>) [Cu ^{II} (N·His) ₂ (O·Tyr)(O·TyrS·Cys ^δ)(X)] pH 4.7 ^[4B] (X = AcO ⁻) pH 7.0 (X = H ₂ O) apoprotein	1.7 1.9 2.2	324, 325 (1GOF) 324, 325 (1GOG) 324 (1GOH)
nitrite reductase (type II site) ^g [Cu ^{II} (N·His) ₃ (OH) ₂] <i>Alcaligenes faecalis</i> S-6 ^[4D] Met150Glu mutant, Zn-substituted <i>Achromobacter cycloclastes</i> NO ₂ ⁻ bound type II depleted	2.0 2.2 2.3 2.2 2.2	145, 146 (1AFN) 146 147, 148 (1NRD) 148 148
Trinuclear Copper		
ascorbate oxidase (zucchini) ^g oxidized form ^[4C] type III [(His·N) ₃ Cu ^{II} (μ-OH)Cu ^{II} (N·His) ₃] type II [Cu ^{II} (N·His) ₂ (OH)]	1.9	33, 326 (1AOZ)
peroxide form type III [(His·N) ₃ Cu ^{II} (O ₂ H)···Cu ^{II} (N·His) ₃] type II [Cu ^{II} (N·His) ₂ (OH)]	1.9	327 (1ASP)
azide form type III [(His·N) ₃ Cu ^{II} (N ₃ ⁻) ₂ ···Cu ^{II} (N·His) ₃] type II [Cu ^{II} (N·His) ₂ (OH)]	1.9	327 (1ASQ)
reduced form type III [(His·N) ₃ Cu ^I ···Cu ^I (N·His) ₃] type II [Cu ^I (N·His) ₂ (OH/OH ₂)] type II depleted ^h	1.9	327 (1ASO) 328

Table 13 (Continued)

enzyme/unit	resolution (Å)	references (PDB code) ^a
Trinuclear Copper (continued)		
ceruloplasmin human (oxidized) ⁱ type III [(His·N) ₃ Cu ^{II} (μ-L)Cu ^{II} (N·His) ₃] type II [Cu ^{II} (N·His) ₂ (L')]	3.1	5
Mononuclear Iron and Copper		
cytochrome <i>c</i> oxidase ^j <i>Paracoccus denitrificans</i> (oxidized)	2.8	2
bovine heart (oxidized) ^[4E] [Fe ^{III} (heme _A)(N·His) ₂] [(His·N) ₃ Cu ^{II} ···Fe ^{III} (heme _{A3})(N·His)] [Zn(S·Cys) ₄] (bovine) [Mg(N·His)(O ₂ C ⁻ ·Asp)(O ₂ C ^{δ-} ·Glu)(OH ₂)] (bovine)	2.8	3

^a See footnote in Table 5. ^b 2,3-Dihydroxybiphenyl and 3-methylcatechol. ^c Two X-ray structures differ with respect to OC^γ-Asn and H₂O ligation, see text. ^d C-terminal carboxylate group. ^e Binuclear rather than dinuclear is used throughout as both *bi* and *nucleus* have latin roots. ^f 3'-Cysteinylytyrosine bound to the copper through the tyrosine oxygen. ^g A blue copper (type I) center is also present in this enzyme (see Table 7). ^h The structure is an averaged structure with partial depletion of all Cu at the trinuclear site. ⁱ There are also three blue copper (type I) centers in this enzyme, one of them lacks the axial methionine. The bridging ligand (L) of the type III site and the third ligand of the type II site (L') are both believed to be non-protein water-derived ligands as in ascorbate oxidase. ^j A binuclear copper_A site is also present in this enzyme (see Table 7).

cleotide diphosphate reductase (RDPR). In RDPR, the binuclear Fe(II) site plus an additional electron reacts with dioxygen to generate the active site,³⁴⁸ which has a tyrosyl radical within approximately 5 Å of the resulting binuclear ferric center (Chart 3E, p 2253). In MMO, the binuclear ferrous site activates dioxygen for hydroxylation.³⁴⁹ In contrast to the binuclear non-heme iron active site in hemerythrin (Chart 2, parts C and D, p 2252), MMO (oxidized resting enzyme in Chart 3F, p 2253) and RDPR have two, rather than five, His·N ligands. The remaining positions are occupied by carboxylate and water-derived ligands, which are better donors and contribute to the difference in reactivity of reversible dioxygen binding in hemerythrin versus dioxygen activation in MMO and RDPR. The structures of the oxidized sites for MMO and RDPR are shown in Figure 24, left. Note that in MMO at low temperature, the exogenous acetate ligand bridge (from the crystallization buffer) in Chart 3F (p 2253) is absent and a water bridge appears, affording what is probably the active site structure in solution. Owing to the increased donor ligation, the effective nuclear charge on the iron atoms should be lowered relative to that of the oxidized (2Fe(III)) hemerythrin site, and one might expect the p*K*_a of the water-derived bridging ligand to be increased. Thus, instead of the bridging oxo group in oxyhemerythrin in Chart 2D (p 2252), a hydroxide bridge is present at the binuclear ferric site of MMO.³⁵⁰ However, there is an oxo bridge present in oxidized RDPR.³⁵¹ The major structural difference between met RDPR and MMO (Figure 24, left) is that the bidentate Asp·CO₂ of Fe₁ in RDPR is replaced by a monodentate Glu·CO₂ in MMO. A position on Fe₁ is opened and the terminal water ligand on Fe₂ in RDPR becomes a bridging ligand in MMO. It has also been noted that both His·N ligands of MMO are hydrogen-bonded to Asp residues, while only one His·N is hydrogen-bonded to Asp in RDPR.³¹⁷ Some combination of structural differences appears to decrease the net charge donated to the iron atoms in RDPR (relative to MMO)

leading to its oxo (rather than hydroxo) bridge.

On reduction, one five- and one four-coordinate Fe(II) atoms are present in RDPR from MCD studies, which indicate that both iron atoms are coordinatively unsaturated and available for reaction with dioxygen.³⁵² Two possible structures for reduced RDPR are given in Figure 24B, right. The top structure corresponds to that of the manganese-substituted enzyme,³²⁰ while the lower structure would derive from loss of all water-related ligands and a carboxylate shift³⁵³ of the Glu·CO₂ ligand on Fe₂ to a μ-η¹:η¹ bridging position. Consistent with open coordination positions on both Fe(II) centers, the μ-oxo bridge of the oxidized site derives from dioxygen.³⁵⁴ In the case of reduced MMO, the low-temperature crystal structure shows two inequivalent five-coordinate Fe(II) centers, consistent with MCD results.³⁵⁵ The hydroxide bridge of the oxidized site is replaced by a second carboxylate bridge, whereby a terminal Glu·CO₂ on Fe₂ in the oxidized site becomes bidentate to that iron atom in the reduced structure with one of its oxygen atoms bridging to the other Fe(II). The terminal water ligand on Fe₁ in the oxidized structure no longer coordinates in the reduced structure, and the water bridge is replaced by a terminally bound water molecule at that iron atom. It is assumed that the bridging water position of the oxidized structure is the site of dioxygen and substrate reactivity.

c. Mononuclear Copper Enzymes. Crystal structures are available for the mononuclear copper enzymes listed in Table 12 (see Table 13). Nitrite reductase is included here since it has a mononuclear copper center (called type 2 or normal) in addition to a blue copper center. The normal copper center catalyzes the one-electron reduction of NO₂⁻ to NO.³⁵⁶ Amine oxidase and galactose oxidase are particularly interesting enzymes in that they have a single copper center, yet catalyze the two-electron oxidation of substrates coupled to the two-electron reduction of dioxygen to hydrogen peroxide. This is accomplished by utilizing an additional organic cofactor covalently

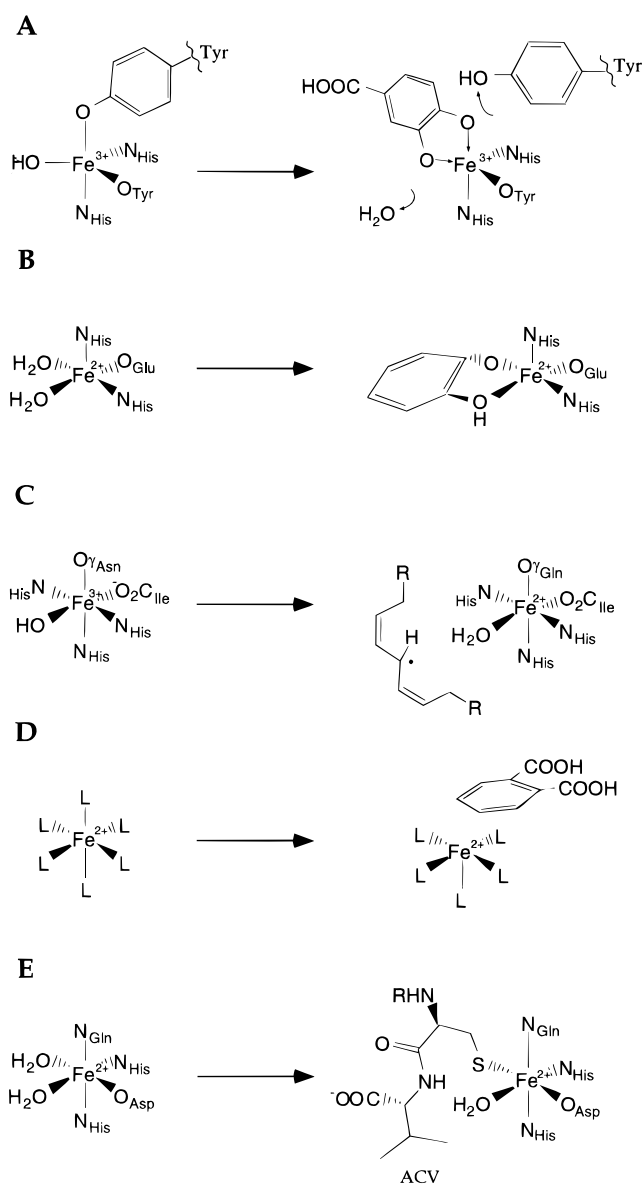


Figure 23. Proposed active-site structures of mononuclear non-heme iron enzymes and their interactions with substrates: (A) intradiol dioxygenase; (B) extradiol dioxygenase; (C) lipoxygenase; (D) phthalate dioxygenase (no specific ligation information is presently available); (E) isopenicillin *N*-synthase based on Mn^{II} structure, no coordinates available in PDB (the substrate ACV is δ -(*L*-amino adipoyl)-*L*-cysteinyl-*D*-valine).

bound to the site (see section II.B.6). For both enzymes, the copper center appears to be required for the post-translational modification of a tyrosyl residue to form the cofactor. For amine oxidase, that residue is hydroxylated to generate a topa (hydroxyphenylalanine) quinone³⁵⁷ which is approximately 5 Å from the copper atom (Chart 4A, p 2253). The resting enzyme has a square-pyramidal $\text{Cu}(\text{II})$ center with three His·N ligands and one water ligand in the equatorial plane and an axial water ligand. As seen in Figure 25A, the primary amine substrate reacts with the topaquinone to generate the aminoquinol of the cofactor and the aldehyde product.³⁵⁸ The copper center is not involved in this chemistry, but is required for the reoxidation of the cofactor by O_2 to produce the amine and H_2O_2 . The aminoquinol- $\text{Cu}(\text{II})$ form of the enzyme is thought to be in a redox

equilibrium with the $\text{Cu}(\text{I})$ -iminosemiquinone, which is observed by EPR. This $\text{Cu}(\text{I})$ center may be the site for the dioxygen reaction. In the case of galactose oxidase, the copper center appears to catalyze the covalent coupling of a Tyr·O ligand to a cysteinyl residue to form 3'-cysteinyltyrosine.³²⁵ This is one of the ligands in the equatorial plane of a square-pyramidal $\text{Cu}(\text{II})$ center; the remaining ligands are two His·N and an acetate (from the crystallization buffer) in the plane and an axial Tyr·O ligand (Chart 4B, p 2253). The resting $\text{Cu}(\text{II})$ form of the enzyme must be activated by one-electron oxidation of the cysteinyl tyrosine, whose potential is significantly lowered due to the covalent sulfur and a stacking interaction with a tryptophan which can provide further electron delocalization. As the resultant tyrosyl radical is covalently bound to $\text{Cu}(\text{II})$, there is no EPR signal observed for either center.³⁵⁹ As indicated in Figure 25B, this $\text{Cu}(\text{II})$ -O·TyrS·Cys site will react with substrate at the exchangeable equatorial position, leading to its oxidation and the elimination of aldehyde. The resulting $\text{Cu}(\text{I})$ center is three-coordinate³⁶⁰ and reacts with dioxygen to regenerate the fully oxidized active site with the elimination of hydrogen peroxide.

d. Binuclear Copper Enzymes. The binuclear copper monoxygenases in Table 12 are divided into two groups dependent upon whether the site, at the binuclear $\text{Cu}(\text{II})$ oxidation level, is coupled or uncoupled. Here, "coupled" refers to the antiferromagnetic interaction between the two $S = 1/2$ $\text{Cu}(\text{II})$ atoms to produce an $S_{\text{total}} = 0$ ground state that is EPR silent. This coupling requires a strong covalent pathway between the two $\text{Cu}(\text{II})$ centers through a bridging ligand (i.e., a superexchange pathway). The uncoupled binuclear copper enzymes dopamine β -hydroxylase and peptidylglycine α -hydroxylating monoxygenase exhibit normal $\text{Cu}(\text{II})$ EPR signals,³⁶¹ indicating that the two metal atoms are greater than 6 Å apart and have no direct bridging ligand. Thus they are often classified as mononuclear copper enzymes. However, two copper atoms are required for activity.^{362,363} One is the site for substrate and dioxygen reaction and the second provides an additional electron that is rapidly transferred to the reactive center. No crystallographic information is yet available for the uncoupled binuclear copper enzymes.

Crystallographic results are also not available for the coupled binuclear copper site in tyrosinase (no EPR signal, strong antiferromagnetic coupling); however, this site exhibits striking spectral similarities²¹⁸ to the coupled binuclear copper site in the oxygen-binding protein hemocyanin (*vide supra*). The major difference between the hemocyanin and tyrosinase active sites appears to be the much higher accessibility of the coupled binuclear copper site in tyrosinase to exogenous ligands.³⁶⁴ It has been found that substrates bind directly to the copper center and undergo an associative rearrangement into the equatorial plane for hydroxylation. Presented in Figure 26 is a structural model for the monoxygenase and oxidase reactivity of tyrosinase in terms of the deoxy and oxy (side-on or μ - η^2 : η^2 -peroxy) structures of hemocyanin (Chart 2.I, parts C and D, p 2253). Phenolic substrates coordinate to one copper center

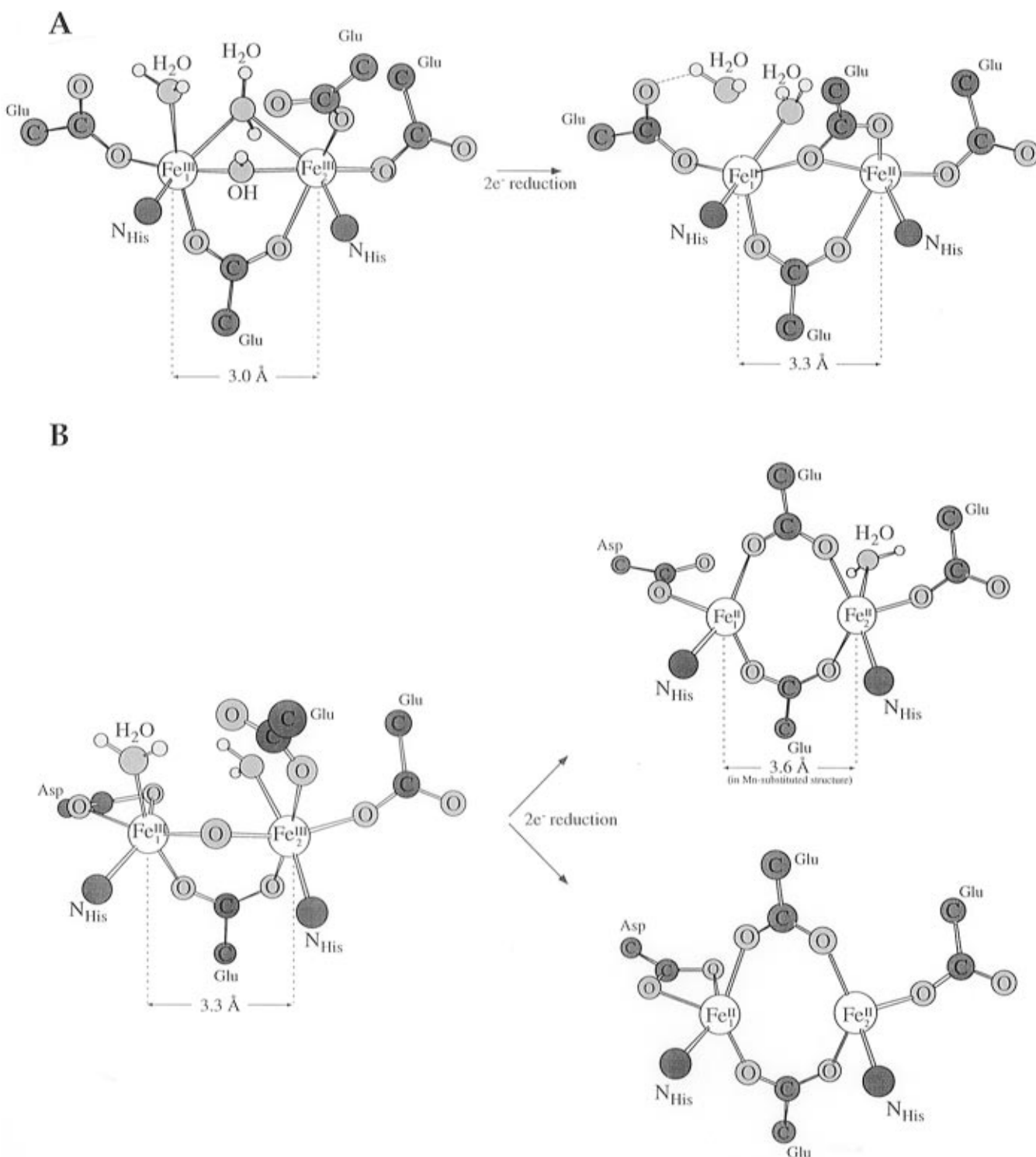


Figure 24. Active-site structures of two binuclear non-heme iron enzymes and their changes upon reduction: (A) methane monooxygenase at low temperature ($-160\text{ }^{\circ}\text{C}$) and (B) ribonucleotide diphosphate reductase.

of the oxy site and undergo a rearrangement with *ortho* hydroxylation to produce equatorially bound catecholates. The latter undergo a further two-electron oxidation, resulting in loss of quinone and formation of a reduced site with open coordination positions on both Cu(I) centers for further dioxygen reactivity to reform the oxy site.

e. Trinuclear Copper Cluster Enzymes. Trinuclear copper cluster sites are known to be present in laccase (LC),³⁶⁵ ascorbate oxidase (AO),³³ and ceruloplasmin (CEP),⁵ and are thought to exist in copper MMO³⁶⁶ and perhaps in phenoxazinone synthase³⁶⁷

(Table 12). For LC, AO and CEP, together with additional copper center(s), these copper sites couple four one-electron oxidations of substrate to the four-electron reduction of dioxygen to water. Crystallographic results are available for AO and a number of its derivatives, and at lower resolution for CEP (Table 13). The oxidized trinuclear copper cluster site shown in Chart 4C (p 2253) parallels the structure anticipated from spectroscopy.³⁶⁵ Three copper atoms are within $\sim 3.7\text{ }\text{\AA}$ of one another. Two are bridged by a hydroxide ligand forming an antiferromagnetically coupled site referred to as a type 3

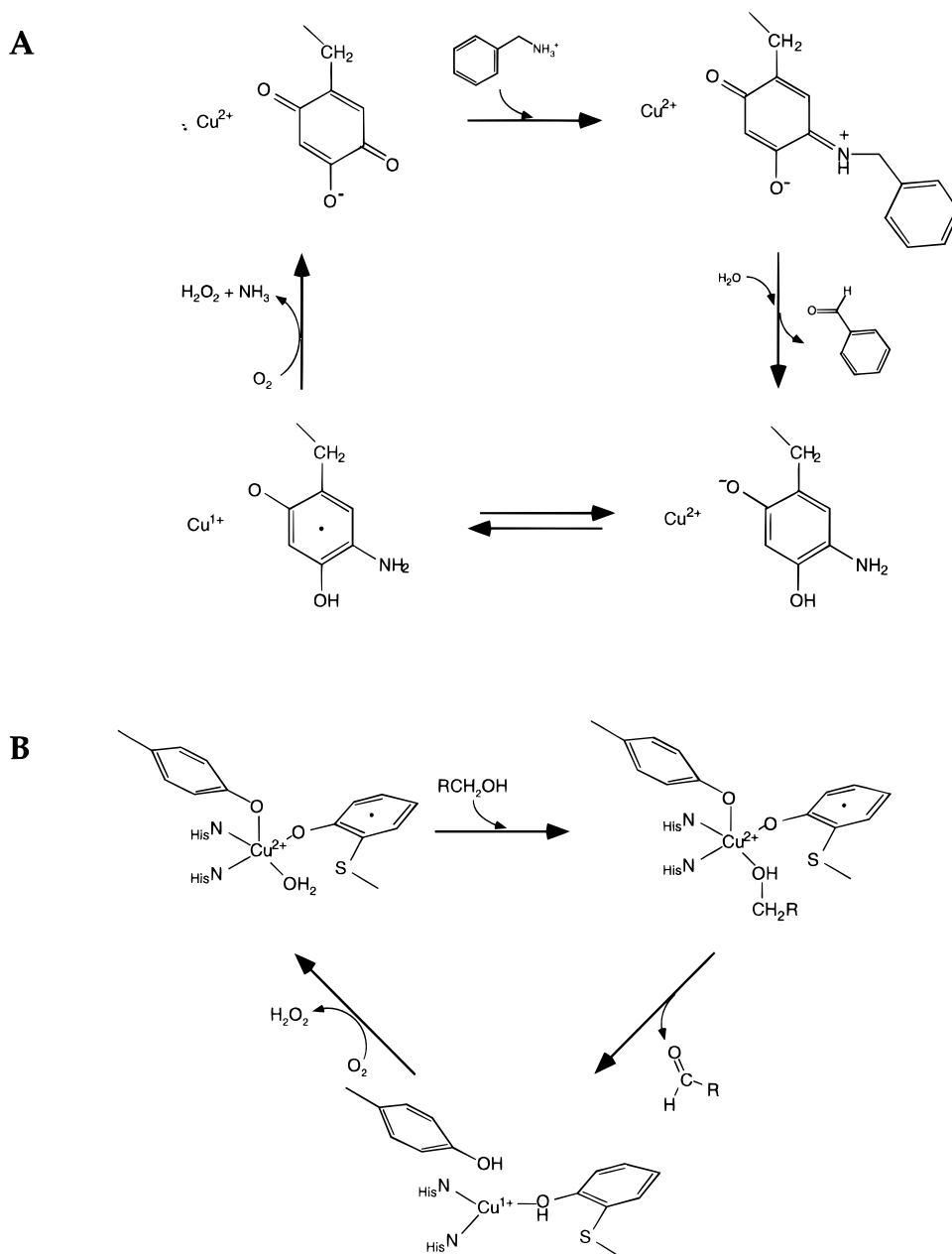


Figure 25. Proposed molecular mechanisms of mononuclear copper oxidases: (A) amine oxidase and (B) galactose oxidase.

center. There are also three His·N ligands on each type 3 copper. The third copper atom of the cluster, called type 2, has no bridging ligands to the type 3 center, but is required for reactivity.³⁶⁸ It has a surprising trigonal planar structure with two His·N and a hydroxide ligand, the latter oriented away from the cluster. As depicted in Figure 27, on reduction there is little change in the type 2 center but the type 3 copper atoms lose their hydroxy bridge and become three-coordinate with a Cu–Cu distance of >5 Å. The trinuclear copper cluster is the site of dioxygen reduction and several intermediates are observed. Electrons from the substrate enter at the blue (type 1) center, which is close to the surface but ~ 13 Å from the trinuclear cluster. However, the thiolate ligand at the type 1 center is flanked on both sides in the sequence by His·N ligands to the type 3 center of the type 2/type 3 trinuclear cluster. This provides an efficient superexchange pathway for rapid electron transfer (see section III.A). A similar type 1-tri-

nuclear cluster arrangement is also present in LC and CEP,^{5,369} the latter enzyme having two additional copper centers whose role in reactivity is unclear. Chart 4, parts C and D (p 2253), compare the type 1-trinuclear structural motif with that of nitrite reductase, which also has a type 1 copper atom bridged through a Cys–His pathway to the type 2 center, the site of nitrite reduction. Nitrite replaces the hydroxide ligand and binds in a bidentate mode by utilizing both oxygen atoms.

*f. The Cu_B –Heme a_3 Site in Cytochrome *c* Oxidase.* Cytochrome *c* oxidase^{370–372} also catalyzes the four-electron reduction of dioxygen to water. This reduction is coupled to proton translocation across a cell or inner mitochondrial membrane to generate an electrochemical gradient for ATP synthesis. The structures of the bovine heart and bacterial oxidases have recently become available. Instead of a type 1 copper center for substrate oxidation and a trinuclear copper cluster for dioxygen reduction, cytochrome *c*

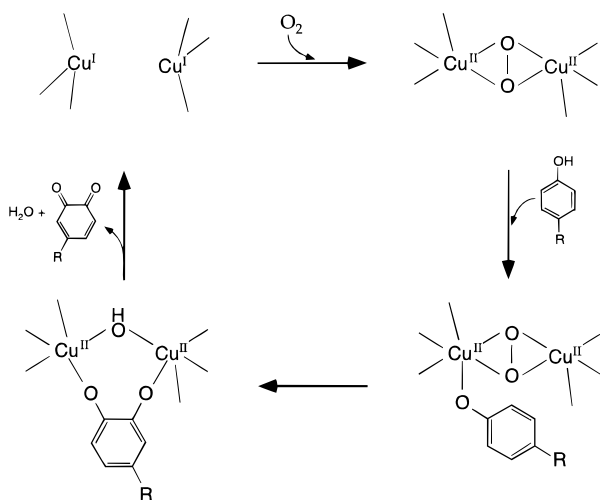


Figure 26. Proposed molecular mechanism of the coupled binuclear copper site in tyrosinase based on structures of deoxy and oxyhemocyanin (see section III.B and text for details).

oxidase utilizes a binuclear Cu_A center (see section III.A) for the oxidation of cytochrome *c*. Electrons then pass across 19 Å to a standard heme *a* center (with two axial His-N ligands), which transfers them to the nearby Cu_B -heme a_3 center; the two heme groups are separated by ~5 Å edge-to-edge. This is the site of dioxygen reduction (and likely proton translocation²). As shown in Chart 4E (p 2253), this center has open coordination positions on both the Cu_B and heme- a_3 centers, which are facing each other, presumably to promote dioxygen binding and reactivity. The metal centers are 4.5 Å (bovine heart) and 5.2 Å (bacterial) apart in the two structures, with the copper atom shifted by ~1 Å off the heme normal at the iron center. Surprisingly, there is no bridging ligand observed at the present resolution and refinement, which is inconsistent with the antiferromagnetic coupling reported for this center in the resting enzyme.³⁷³ Cytochrome *c* oxidase is treated in detail elsewhere (Babcock, G. T.; Ferguson-Miller, S.; this issue).

2. Intermediates

All the reactions listed in Table 12 are thermodynamically favorable, but kinetically very slow, and

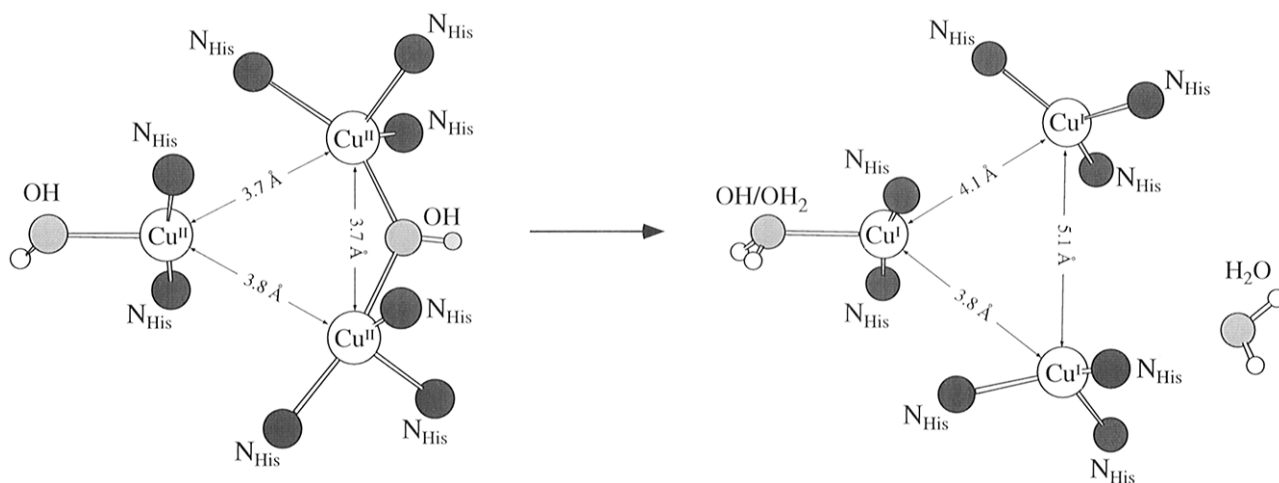


Figure 27. Active-site structure of the trinuclear copper cluster in oxidized ascorbate oxidase and its change upon reduction.

must be catalyzed by the metalloenzymes listed. Because dioxygen has a $(1\pi_g^*)^2$ valence configuration which gives a high-spin $^3\Sigma_g^-$ ground state, all reactions listed are spin forbidden. In addition, the exchange stabilization of this high-spin configuration makes one-electron reduction of dioxygen difficult, leading to a low reduction potential for this reaction (Figure 22) and a kinetic barrier. However, one-electron reduction eliminates this exchange stabilization, making the second electron addition a higher potential process. Metalloenzymes often overcome the barriers involved in dioxygen reactions either by (i) substrate activation by an oxidized metal center to induce radical character, or (ii) dioxygen activation by a reduced metal site through two-electron reduction to the peroxide level.

a. Substrate Activation. Of the enzymes listed in Table 12, only the intradiol dioxygenases and lipoxygenases are characterized as utilizing a mechanism involving substrate activation by their oxidized high-spin Fe(III) active sites. For lipoxygenases (Figure 23C), fatty acid substrate binding in the protein pocket near the iron (see section II.B.4) leads to reduction of the metal center (and protonation of the bound hydroxide; therefore, a net H-atom abstraction) and formation of a substrate radical ($S = 1/2$). This undergoes a rapid spin-allowed reaction with triplet oxygen to generate the peroxy substrate radical.³⁷⁴ The alternative of substrate deprotonation and direct coordination of the carbanion to the Fe(III) center has also been suggested.³⁷⁵ In the case of the intradiol dioxygenases, the catechol substrate coordinates in a bidentate mode directly to the Fe(III) center (Figure 23A).³³⁰ The resultant enzyme-substrate complex exhibits a very intense, low-energy catecholate-to-Fe(III) CT transition, indicating that the substrate-Fe(III) bonding is very covalent. This interaction is thought to donate electron density from the substrate to the iron, resulting in partial reduction of the metal and some semiquinone radical character on the substrate.³⁷⁶ Accordingly, the substrate would be activated for direct attack by dioxygen, generating a peroxy-substrate intermediate that converts to the product complex.

b. Dioxygen Activation. In the remaining reactions listed in Table 12, the two-electron reduction of dioxygen to the peroxide level is accomplished either

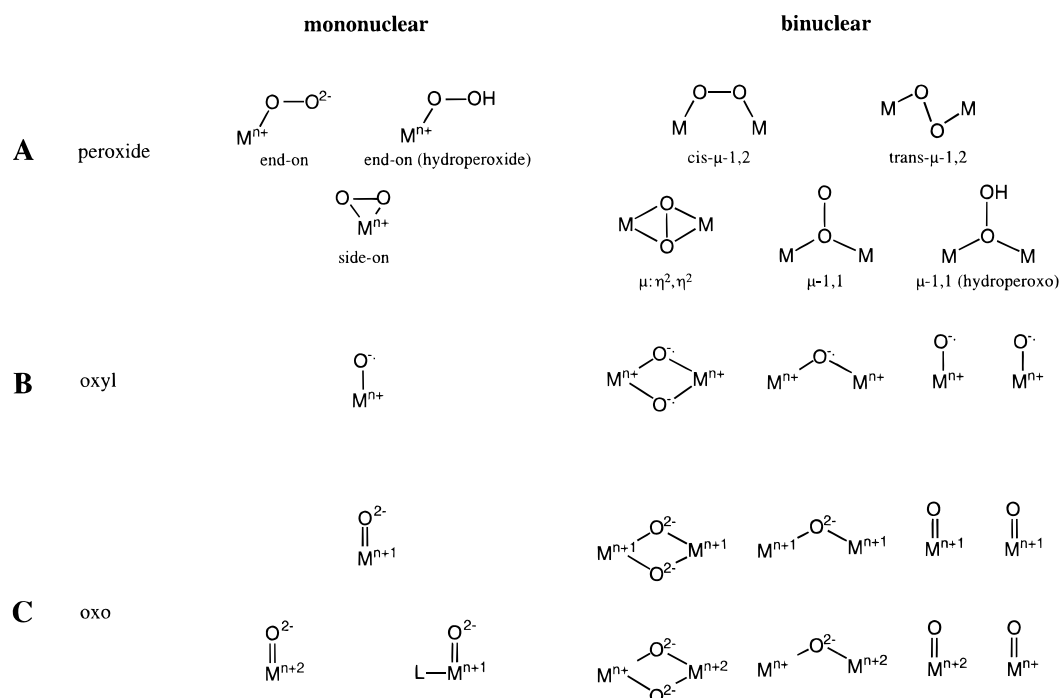


Figure 28. Possible peroxide level intermediates: (A) retention of O–O bond; (B) homolytic cleavage of O–O bond to produce oxyl species; (C) homolytic cleavage with metal oxidation (upper) and heterolytic cleavage of O–O (lower).

by having more than one reduced metal center or, in the mononuclear enzymes, having the second electron donated by a protein-bound organic cofactor (topaquinone and cysteinyl tyrosine), an exogenous cofactor (pterin, α -ketoglutarate), or some other source (e.g., a Rieske center, substrate, etc.). In heme enzymes, the peroxy-Fe(III) level intermediate is generally thought to undergo heterolytic cleavage of the O–O bond to generate a high-valent iron-oxo (ferryl) species, which either oxygenates substrate in the case of cytochrome P-450 or is further reduced to water in cytochrome *c* oxidase. A major concern has been whether non-heme iron and copper sites in enzymes with innocent imidazole and carboxylate ligation can generate analogous high-valent metal-oxo intermediates, or whether some form of bound peroxide or its homolytically cleaved oxyl form is the active species in catalysis (Figure 28). Peroxide-level intermediates have now been observed and studied in five non-heme iron and copper enzymes: tyrosinase, laccase, bleomycin, ribonucleotide reductase, and methane monooxygenase.

In the coupled binuclear copper enzyme tyrosinase and the trinuclear copper cluster enzyme laccase, the oxygen intermediates observed are fundamentally different from the high-valent oxo-heme species. The peroxide O–O bond is present in both observed enzyme intermediates, and each binds peroxide in a mode with differing geometric and electronic structures. In oxy-tyrosinase, the side-on (μ - η^2 : η^2) peroxy structure (Figure 28A, right) leads to an extremely weak O–O bond owing to back-bonding of the copper electron density into the σ^* orbital of the peroxide, which activates it for cleavage and oxygen atom transfer in the reaction shown in Figure 26.²⁴⁰ In laccase, an intermediate best described as an end-on (μ - η^1 : η^1) hydroperoxide is observed which promotes its further reduction to water at the trinuclear copper cluster site.^{34,377}

From XAS,³⁷⁸ mass spectrometry,³⁷⁹ and EPR³⁸⁰ studies, the peroxide-level intermediate of bleomycin (activated bleomycin), which is kinetically competent to cleave DNA, is best described as a low-spin ferric peroxide species with one of the structures in Figure 28A, left. The coordinating portion of this molecule, the β -aminoalanine–pyrimidine–histidine region, has particularly covalent pyrimidine-deprotonated amide ligation. This produces low-energy CT transitions in the absorption spectra of reduced and oxidized Fe-bleomycin that are not present in the absorption spectra of the other non-heme iron enzymes and indicate significant electron delocalization. Thus, the bleomycin site might be expected to have an electronic structure and reactivity more similar to that of heme enzymes, yet a ferryl species is not observed. This suggests that the latter possibility is even less likely for the other mononuclear non-heme iron enzymes which have more innocent ligation.

Oxygen intermediates have been observed at the binuclear non-heme iron sites in MMO and RDPR. For MMO, the first intermediate (called L or P) has been demonstrated to be a peroxide with one of the symmetric bridging structures in Figure 28A, right.³⁸¹ It converts to compound Q, which from Mössbauer spectroscopy is described as a binuclear Fe^{IV}-oxo species,³⁸² as in Figure 28C, right. In RDPR, a three-electron reduced intermediate called X is observed (an intermediate U is also observed that was originally thought to be a peroxy complex, but is now assigned as a tryptophan radical).³⁸³ Analysis of the Mössbauer data on X has led to its description as a binuclear Fe(III)-bridging oxyl species³⁸⁴ (Figure 28B, right), although anisotropic iron hyperfine coupling in its ENDOR spectrum has been used to argue for some Fe^{IV}-oxo character.³⁸⁵ MMO appears to be more reactive toward forming a high-valent oxo-intermediate. This may relate to the structural difference between MMO and RDPR described above; i.e., the

Table 14. Crystallographically Defined Coordination Units in Iron-Sulfur Enzymes

enzyme	cluster core	resolution	references (<i>PDB Code</i>) ^a
Nonredox			
aconitase (beef heart mitochondrial)			
active [(Cys·S) ₃ Fe ₄ S ₄ (OH ₂ /OH ⁻)]	[Fe ₄ S ₄] ²⁺	2.5	387 (<i>6ACN</i>)
inactive [(Cys·S) ₃ Fe ₃ S ₄]	[Fe ₃ S ₄] ⁺	2.1	112 (<i>5ACN</i>)
endonuclease III (<i>E. coli</i>) [(Cys·S) ₄ Fe ₄ S ₄]	[Fe ₄ S ₄] ²⁺	2.0	388 (<i>1ABK</i>)
glutamine PRPP amidotransferase (<i>Bacillus subtilis</i>) ^b [(Cys·S) ₄ Fe ₄ S ₄]	[Fe ₄ S ₄] ²⁺	3.0	389 (<i>1GPH</i>)
Redox			
[NiFe]-hydrogenase ^c (<i>Desulfovibrio gigas</i>) [(Cys·S) ₂ Ni(μ-S·Cys) ₂ FeL ₃] ^[5D]	[Fe ₃ S ₄] ⁺ , ^e 2[Fe ₄ S ₄] ²⁺ , ^e	2.85	390
nitrogenase			
<i>Azotobacter vinelandii</i>			
Fe protein [(Cys·S) ₄ Fe ₄ S ₄]	[Fe ₄ S ₄] ²⁺	2.9	391 (<i>1NIP</i>)
MoFe protein (P-cluster) ^{[5B],d}	[Fe ₈ S ₈] ^f	2.7	1, 392 (<i>1MIN</i>)
MoFe protein (cofactor) ^[5A]	[MoFe ₇ S ₉] ^f	2.2	1, 392 (<i>1MIN</i>)
<i>Clostridium pasteurianum</i>			
MoFe protein (P-cluster) ^{[5C],d}	[Fe ₈ S ₈] ^f [Fe ₈ S ₇] ^f	3.0	393 (<i>1MIO</i>) 394, 395
MoFe protein (cofactor) ^[5A]	[MoFe ₇ S ₉] ^f	3.0	393 (<i>1MIO</i>) 394, 395
phthalate dioxygenase reductase ^g (<i>Pseudomonas cepacia</i>) [(Cys·S) ₄ Fe ₂ S ₂]	[Fe ₂ S ₂] ²⁺	2.0	396 (<i>2PIA</i>)
sulfite reductase (<i>E. coli</i>)	[Fe ₄ S ₄] ²⁺ -(μ-S·Cys)-(siroheme)	1.6	4, 397 (<i>M12</i>)
W3A1 trimethylamine dehydrogenase [(Cys·S) ₄ Fe ₄ S ₄]	[Fe ₄ S ₄] ²⁺	2.4	398

^a See footnote in Table 5. ^b PRPP = 5-phosphoriboxyl-1-pyrophosphate. ^c Oxidation states of clusters are unclear; ligands L are unidentified. ^d Two conflicting X-ray structures presently exist for the P-clusters of nitrogenase. ^e Electron-transfer centers with standard Cys·S terminal ligation. ^f Terminal ligation as in Figure 29 where the two Mo-bound oxygens are from homocitrate (homocitric acid: HO₂CCH₂CH₂C(COOH)(OH)CH₂CO₂H). ^g Electron-transfer protein (not an enzyme).

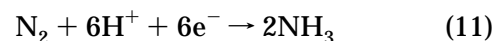
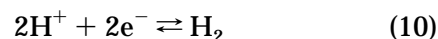
absence of an oxo bridge in MMO at the binuclear ferric level (Figure 24, left). Reaction of reduced MMO with dioxygen would produce a hydroxide-bridged binuclear Fe(III)-peroxide intermediate that should be unstable toward further oxidation to form a μ-oxo ferryl species, presumably stabilized by the strong Fe–O–Fe bond.

From this summary, only the intermediate Q of MMO appears to have some parallels to heme chemistry. The other peroxy intermediates are either the active form of the enzyme or convert to a more reactive, short-lived species in the reaction with organic substrate.

E. Hydrogenases and Nitrogenases

Complex iron–sulfur proteins have been defined by the International Union of Biochemistry as those which contain additional prosthetic groups and generally have enzymatic activity.^{80,386} These proteins may be further classified according to the prosthetic groups present, these including flavins, pterins, siroheme, and others. In contrast, electron-transfer proteins containing the sites in Figure 4 and other proteins that have a nonredox catalytic function are regarded as *simple* iron–sulfur proteins. Rubredoxins, ferredoxins, and aconitase (Beinert, H.; Kennedy, M. C.; Stout, C. D.; this issue) are examples of simple proteins. The Fe–S clusters present in those complex proteins that are redox enzymes can assume the following roles: (i) electron transfer only, (ii) catalytic only, and (iii) electron transfer and catalytic (two or more clusters present). An extensive tabulation of simple and complex iron–sulfur proteins is available.⁸⁰ Structurally defined cluster units in nonredox and redox enzymes are available in Table

14.^{1,4,112,387–398} Examples of i are numerous; in particular, enzymes containing one or more Fe–S clusters and a flavin active site are rather common. A structurally characterized example is the bacterial enzyme trimethylamine dehydrogenase, which catalyzes the oxidative N-demethylation of trimethylamine: Me₃N + H₂O → Me₂NH + CH₂O + 2H⁺ + 2e⁻. The active site is a flavin; during catalysis it is reduced to the dihydro form and reoxidized by the [Fe₄S₄]²⁺ cluster present in the same subunit. Electrons are then passed to a flavoprotein, which is the natural electron acceptor. Other examples are found with the molybdenum oxotransferases (Hille, R.; this issue), in which the molybdenum site is catalytic and clusters within the enzyme molecule form part of the electron transfer conduit. Sulfite reductase contains an assembly in which the site of catalysis (siroheme) and the Fe₄S₄ electron transfer unit are intimately coupled through a Cys·S bridge. There are as yet no proven examples of ii, in which a redox-catalytic Fe–S center is not accompanied by an electron-transfer cluster in the same molecule. Phthalate dioxygenase reductase is included in Table 14 because it is the electron-donor protein to the enzyme phthalate dioxygenase, which contains a Rieske center (Figure 4) and an Fe(II) catalytic site. Our concern here is with hydrogenases and nitrogenases, which are examples of iii and catalyze reactions 10 and 11, respectively. Pertinent structural depictions of metal sites in these enzymes are included in Chart 5 (p 2254) and Figure 29.



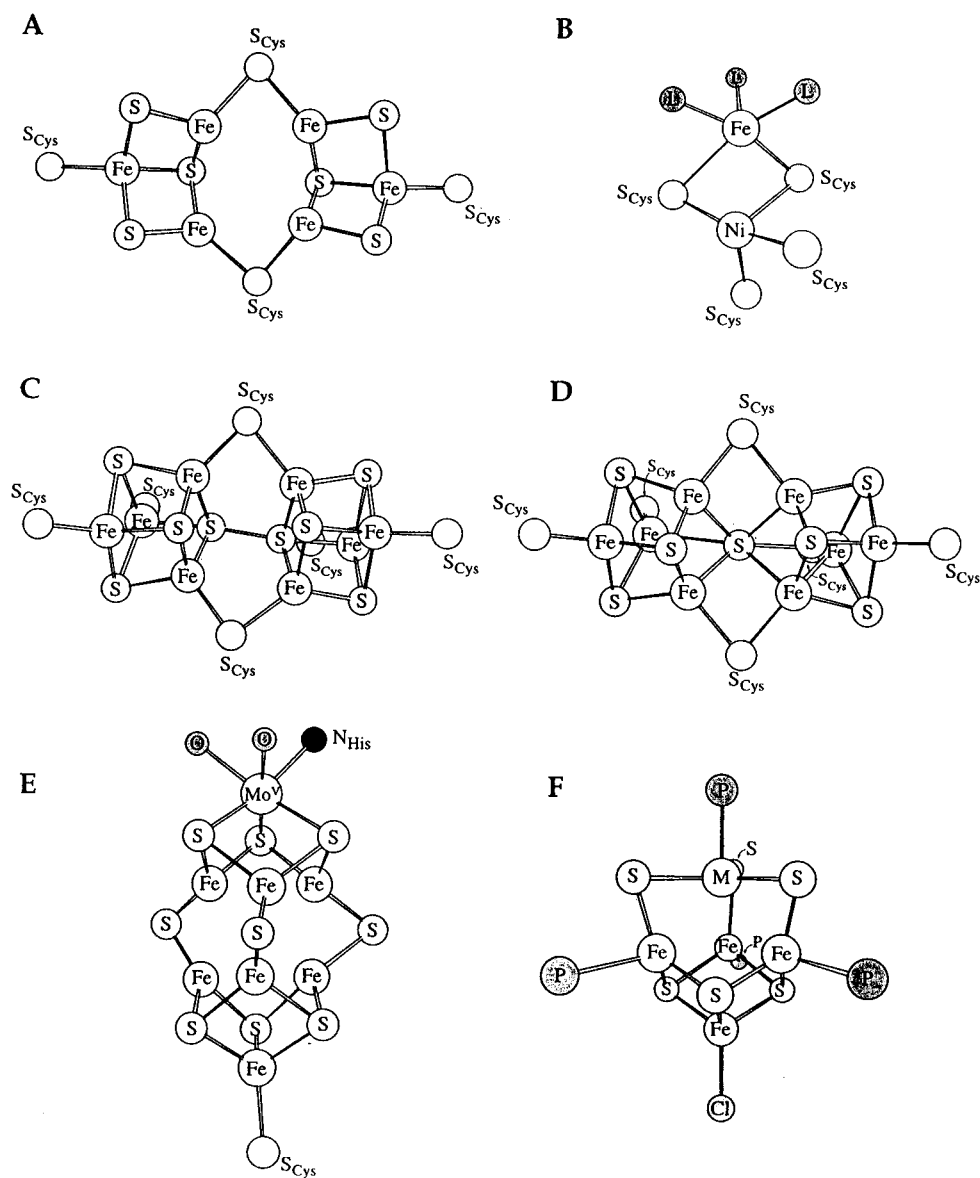


Figure 29. Schematic structures of (A) a proposed 6-Fe cluster in [Fe]-hydrogenase, (B) the binuclear site in *D. gigas* hydrogenase, (C) the P cluster of nitrogenase (Rees), (D) the P cluster of nitrogenase (Bolin), (E) the cofactor cluster of nitrogenase, and (F) $[\text{MFe}_4\text{S}_6(\text{PEt}_3)_4\text{Cl}]$ ($\text{M} = \text{V}, \text{Mo}$).

1. Hydrogenases

Excluding the metal-free enzymes described elsewhere (Thauer, R. K.; Klein, A. R.; Hartman, C.; this issue), hydrogenases^{399–402} may be classified according to whether they contain iron, or nickel and iron, as the only metal component(s). The number of purified [NiFe]-hydrogenases is so large compared to [Fe]-hydrogenases that it is incumbent on the investigator to show that a newly isolated enzyme does *not* contain nickel. All hydrogenases are bacterial enzymes. Although this article emphasizes structure/function relationships, we include [Fe]-hydrogenases, for which there are no structures, to provide one illustration of the difficulty of structure deduction from noncrystallographic information for a complicated metalloprotein.

a. [Fe]-Hydrogenases. Iron-only hydrogenases have been isolated from only a few genera of bacteria. Early research on these enzymes was hampered in particular by uncertainties in iron content, some of

which still persist. The most thoroughly investigated [Fe]-hydrogenases are those of the anaerobe *Clostridium pasteurianum*. This organism produces two enzymes, *CpI* (M_r 61 kD) and *CpII* (M_r 46 kD with a 10 kD subunit).⁴⁰¹ *CpI* contains about 20 iron atoms and 18 sulfide atoms, which now appear to be organized in three Fe_4S_4 clusters (“F clusters” in hydrogenase nomenclature), one Fe_2S_2 cluster, and an additional uncharacterized cluster. We proceed on the basis of this cluster composition. The binuclear site was detected in 1993 by resonance Raman spectroscopy.⁴⁰³ In earlier work, it apparently eluded detection by EPR because of anomalous relaxation properties, and was difficult to resolve by MCD and Mössbauer techniques against a background of three Fe_4S_4 clusters and the active-site cluster. When the enzyme is reduced by dithionite or by incubation with dihydrogen, the three F clusters are reduced to the $[\text{Fe}_4\text{S}_4]^+$ state; two have $S = 1/2$ and the other appears to be in a mixed spin $S = 1/2 + 3/2$ state. When

oxidized, the F clusters become EPR-silent ($[\text{Fe}_4\text{S}_4]^{2+}$), and another type of paramagnetic center exhibits a rhombic $S = 1/2$ EPR spectrum ($g = 2.10, 2.04, 2.00$) not found in any other iron-sulfur protein. The three F clusters, all of which have indistinguishable midpoint potentials $E_m = -420$ mV, function as standard ferredoxin-type electron carriers. The remaining redox center, which consists of three or six iron atoms and has $E_m = -400$ mV, is termed the "H cluster" and is, or constitutes the major part of, the catalytic site. It is the origin of the rhombic $g = 2.10$ spectrum, which accounts for nearly 1 spin/mol. The second hydrogenase, *Cp2*, contains about 14 iron atoms and 11 sulfide atoms. EPR and MCD results indicate the presence of two Fe_4S_4 clusters with different potentials $E_m = -180$ mV and < -300 mV. The remaining six iron atoms occur as the H cluster, with an EPR spectrum nearly identical to that of *Cp1* and corresponding to 1.0 spin/mol. For this cluster, $E_m = -400$ mV. Both enzymes are irreversibly inhibited by CO, and when treated with CO or O_2 quantitatively replace their rhombic $g = 2.10$ spectra with new axial or rhombic EPR spectra.

The structure of the H cluster is unknown. We briefly consider certain information pertinent to its composition and structure.⁴⁰¹ From the collective analytical and spectroscopic data of the *Cp* enzymes, the H cluster apparently contains three or six iron atoms. Analytical data further suggest that the sulfide content may be slightly lower than the iron content. The atom ratio Fe:S > 1 has never been found in any structurally characterized native cluster,⁸⁰ and while occasionally represented among synthetic clusters of known structure,⁴⁰⁴ it is a minority condition. Spectroscopic studies have provided a modicum of structural information. *Cp1* obtained from cells grown in the presence of ^{57}Fe exhibited two well-resolved ^{57}Fe ENDOR resonances in the rhombic $g = 2.10$ EPR spectrum of the oxidized enzyme,⁴⁰⁵ proving that the H cluster contains two magnetically inequivalent types of iron atoms which are spin coupled. It was further demonstrated by ENDOR that ^{13}C binds to the oxidized H cluster of *CpI*, that the ^{13}C - ^{57}Fe coupling constant is within the range of iron carbonyl clusters, and that the electron distribution within the cluster is substantially altered upon inhibitor binding.⁴⁰⁶ The observation of two ^{57}Fe resonances in oxidized *CpI* and its CO adduct demonstrates that the cluster remains intact upon CO binding.

A corresponding ENDOR study of oxidized *CpII* has revealed a strong structural similarity between the H clusters of the two enzymes.⁴⁰⁷ A detailed Mössbauer investigation of oxidized and reduced *CpII* and its CO adduct established a 2:1 ratio of spin-coupled iron atoms and a diamagnetic ground state in the reduced form.⁴⁰⁸ Further, the reduced enzyme exhibited two quadrupole doublets corresponding to two nearly equivalent pair-delocalized $\text{Fe}^{2.5+}$ sites and one Fe^{3+} site. This is just the situation in synthetic¹¹³ and native⁴⁰⁹ $[\text{Fe}_3\text{S}_4]^0$ clusters (Figure 4) which, however, possess an $S = 2$ ground state. Evidently, the cuboidal structure of the latter cluster does not extend, at least with corresponding metric features, to a putative 3-Fe H cluster. However, with a content

of 14 Fe atoms which includes two Fe_4S_4 clusters, and the observation that the rhombic $g = 2.10$ spectrum corresponds to one spin/mol, it has been concluded that the H cluster probably contains six spin-coupled iron atoms.⁴¹⁰ It might also be noted that with the $3\text{Fe}_4\text{S}_4 + \text{Fe}_2\text{S}_2$ composition of *CpI*⁴⁰³ and a total of 20 iron atoms, six iron atoms can be apportioned to the H cluster. The nature of ligation of these atoms is unclear. Beyond the bridging function of sulfide, it has been adduced from MCD results⁴¹¹ and apparent negligible enhancement in resonance Raman spectra⁴⁰³ that the iron atoms are engaged in substantial oxygen/nitrogen coordination. Coordination of the H cluster of oxidized *CpI* by two nitrogen atoms has been reported from pulsed ESEEM spectroscopy.⁴¹² The primary structure of *CpI* contains 574 amino acids, of which 22 are Cys residues.⁴¹³ One large domain includes 17 Cys residues, of which 16 would be required for the $3\text{Fe}_4\text{S}_4 + \text{Fe}_2\text{S}_2$ clusters assuming conventional terminal ligation. Five other Cys residues are located in the presumptive H cluster bonding domain and might function as terminal ligands, providing an opportunity for non-cysteinylligation as well. Alternatively, the total 22 Cys residues could be fully utilized if the H cluster contains six iron atoms, each with one terminal Cys-S ligand.

The function of hydrogenases is expressed by reaction 10. A model for the functioning of *CpI* and *CpII* has been proposed,⁴¹⁰ which is based on F clusters as intramolecular electron transfer centers and preceded the report of an Fe_2S_2 center in *CpI*. Dihydrogen binds to the oxidized H cluster. In *CpI*, the potentials of the F clusters (-420 mV), the H cluster (-400 mV), and the H^+/H_2 couple at pH 7 (-414 mV) are nearly the same. Consequently, electrons can be caused to flow from or to the H cluster in the presence of suitable oxidized or reduced electron carriers, respectively, consistent with the observed bidirectional function of the enzyme. Because in *CpII* the F cluster potentials (< -300 mV, -180 mV) are considerably more positive than those of the H cluster (-410 mV) and the H^+/H_2 couple around physiological pH, transfer of electrons from H_2 to the H cluster, and then to an external acceptor through the F clusters is the thermodynamic direction of electron flux. Consequently, *CpII* is an uptake hydrogenase. When examined by X-ray absorption spectroscopy,⁴¹⁴ the overall shapes of the iron edges of oxidized and reduced *CpII* resemble those of synthetic and native clusters having tetrahedral FeS_4 coordination units (Figure 4). In the oxidized form of the enzyme, EXAFS analysis affords mean Fe-S and Fe-Fe distances of 2.27 and 2.76 Å, respectively, well within the range of usual values for clusters. Upon reduction, these distances do not change significantly, but a new EXAFS peak appears corresponding to an Fe-Fe separation of 3.3 Å. Because the dimensions of Fe_4S_4 clusters change only slightly upon reduction,^{130,131} the new feature is associated with the H cluster. Iron-iron distances in this range are preceded only in Fe_4S_4 clusters in which one or more iron sites are occupied by low-spin Fe(II), as in $[\text{Fe}_4\text{S}_4(\text{SPh})_2(\text{CNBu}^t)_6]$, where the sites are separated by 3.46 Å.⁴¹⁵ Apparently, reductive electron transfer to an H cluster is coupled to a significant

core structural change, which is unprecedented for synthetic and native iron–sulfur clusters.

Despite the incisive application of a wide range of spectroscopic techniques over more than a decade since it was recognized that [Fe]-hydrogenases contain an unusual cluster, the structure of the H cluster remains unresolved. One proposed structure, by Kim and Rees,⁴¹⁶ is illustrated in Figure 29A. It is based on the composition [Fe₆S₆(S·Cys)₄], implicates four Cys residues that are conserved in the H cluster binding domain,⁴¹³ and contains iron sites in a 4:2 ratio, with the three-coordinate iron sites similar to those crystallographically demonstrated in the cofactor cluster of nitrogenase^{1,392–395} (*vide infra*). These coordinatively unsaturated iron atoms are possible binding sites for H₂ and the inhibitor CO. Kim and Rees⁴¹⁶ note that nitrogenase simultaneously reduces N₂ and evolves H₂, leading to the possibility that the two enzymes have some structural features in common. Whatever are the merits of this proposal, an imperative must be placed on crystallographic structure determination of the most conspicuously undefined cluster structure in iron–sulfur biochemistry. In this connection, we note the putative Fe₆S₆ clusters in several bacterial proteins which have been assigned the prismane core structure,⁴¹⁷ but are also crystallographically unestablished.

This discussion has focussed on only two enzymes. For a penetrating analysis of the general status of [Fe]-hydrogenases through 1990 together with mechanistic proposals of enzyme action, the treatment by Adams⁴⁰¹ should be consulted. The collective spectroscopic evidence for different enzymes suggests that their H clusters are basically similar, as in a recently discovered protozoan enzyme.⁴¹⁸ However, a [Fe]-hydrogenase has been isolated from a hyperthermophilic bacterium that does not exhibit the rhombic $g = 2.10$ EPR spectrum diagnostic of the oxidized H cluster.⁴¹⁹

b. [NiFe]-Hydrogenases. This class of hydrogenases has been extensively reviewed.^{399,400,402, 420,421} We largely confine our attention to the active-site structure determined for the hydrogenase from the sulfate-reducing bacterium *Desulfovibrio gigas*³⁹⁰ (Chart 5D, p 2254, Figure 29B). This enzyme is rather typical of its class, and it, together with hydrogenases from *Chromatium vinosum* and *Thiocapsa roseopersicina*, are among the most extensively studied and exhibit many similarities. We consider briefly some of the leading properties of the *D. gigas* enzyme,^{399,402,421,422} for which four redox states, some or all involving nickel, have been detected. The enzyme is composed of two subunits with masses of 63 kD and 26 kD and contains 1 g-atom of nickel and 11–12 g-atoms of iron and sulfide/89 kD. The iron content was deduced from EPR and Mössbauer spectroscopies to be organized into one Fe₃S₄ and two Fe₄S₄ clusters, a matter confirmed by crystallography. The aerobically isolated enzyme exhibits two rhombic $S = 1/2$ EPR spectra (Ni-AB) generally agreed to arise from low-spin Ni(III) which, from EXAFS analysis⁴²³ and crystallography, is in a dominantly sulfur coordination environment. The two spectra arise from different forms of the enzyme, one of which (Ni-B) is much more rapidly activated by H₂ than the other.

When reduced under H₂, the two spectra are superimposed at different rates, first by an EPR-silent form possibly containing Ni(II), and then by a new rhombic spectrum (Ni-C). An inactive EPR-silent form (Ni-R) is attained under prolonged incubation with H₂. Redox titrations indicate that, compared with Ni-AB spectra, the Ni-C and Ni-R forms are reduced by two and three electrons,^{422b,424,425} respectively. These properties are representative of other [NiFe]-hydrogenases.^{399,402,421}

The Ni-C state is directly generated from the “ready” Ni-B form of the enzyme by partial reduction with H₂. Its formation occurs in two one-electron steps whose potentials exhibit a pH dependence, indicating incorporation of two hydrogenic equivalents in Ni-C.^{422b} Recent redox titration results are consistent with the consumption of two electrons in forming Ni-C, which has been variously formulated as Ni^I-2H⁺ (implying protonation of ligands or other contiguous basic sites), Ni^{III}-H⁻, Ni^{III}-H₂, or perhaps a Ni^{II} ligand radical species.⁴²⁴ The Ni-C state in related enzymes is light sensitive.^{422b,425,426} When the enzyme is irradiated in this state, a different rhombic spectrum is elicited indicative of a metal-based $S = 1/2$ system but with an altered coordination environment. The rate of this process is nearly six times slower in D₂O than H₂O, suggesting that the reaction involves breaking of a Ni-H/D bond. Further, an exchangeable hydrogen originating from H₂ has been detected in the Ni-C form of two enzymes by ENDOR,^{426,427} consistent with, but not requiring, the existence of a ligated “Ni-H” species.

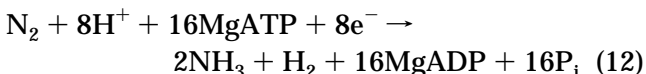
Given the foregoing results and other observations,^{399,402,421,428} the mechanistic proposals for the pathway of reaction 10 have consistently (and understandably) implicated a mononuclear nickel site. There had been some suspicion that another metal atom of uncertain location, exclusive of nickel and iron–sulfur clusters and probably iron, might be present.⁴²¹ Analysis of Ni K-edge EXAFS of *T. roseopersicina* hydrogenase poised in the Ni-C state led to the proposal of Ni-Fe distances of 4.3 and 6.2 Å and the presence of an Fe-S cluster–Ni bridged array.⁴²⁹ However, the actual bridged binuclear structure established in oxidized *D. gigas* hydrogenase (crystallographically examined as a mixture but mainly in the Ni-A state) was not clearly anticipated in any published account prior to the report of the structure in 1995.³⁹⁰ The iron–sulfur clusters are located in the smaller subunit, and the catalytic center, in which the other metal is now known to be iron, is present in the larger subunit. The subunits interface such that a coordinated cysteinyl sulfur atom at the active site is 6 Å from a similar atom on the proximal Fe₄S₄ cluster. This and the other two clusters are separated by nearest Cys·S distances of 5–6 Å. The array of three clusters forms the electron transfer conduit for the enzyme, which is an uptake hydrogenase and hence requires disposal of two electrons per substrate molecule. The natural electron acceptor is cytochrome *c*₃. At 2.85 Å resolution and with some possible disorder in the structure, reliable metric details of the active site have not yet emerged and not all atoms are identified. The nickel atom is bound by four Cys·S ligands, two of which

are terminal and two bridging to the iron atom (Figure 29B). The stereochemistry at nickel appears to correspond to square pyramidal but with one basal ligand absent. The Ni–Fe distance is 2.7 Å. In addition to the two Cys·S bridges, the iron atom carries three unidentified exogenous ligands L.

The existence of the binuclear site raises more questions than it answers. Among these questions are the extent to which spectroscopic results previously attributed to nickel have to be reinterpreted, and whether the site functions as a concerted two-atom unit or, in the localized limit, one metal is passive and perhaps structural only. A further question involves the ramifications of Cys·S ligands beyond metal-binding itself and recalls the observation by Bagyinka *et al.*⁴³⁰ that in X-ray absorption spectra neither the position and shape of the nickel K-edge XANES nor the EXAFS change appreciably over five oxidation states of *T. roseopersicina* hydrogenase. This of course implies that redox events are confined largely or exclusively to a locale other than the nickel atom, perhaps the thiolate ligands as has been suggested,⁴³⁰ or the iron site. The latter has been detected in *C. vinosum* hydrogenase by Mössbauer spectroscopy.⁴³¹ Delineation of the mechanism of action of the hydrogenase site, the most intimately bridged heterometal catalytic site in biology, continues to be a major challenge in bioinorganic enzymology. Lastly, we note that the complexities of the [NiFe]-hydrogenase problem extend even further to include enzymes with properties not typical of the class. As one example, the oxidized enzyme from the thermophile *Pyrococcus furiosus* does not show the rhombic Ni(III)-type EPR spectrum, contains an Fe₂S₂ cluster, and preferentially catalyzes H₂ evolution rather than uptake.⁴³² It appears to be a new type of hydrogenase.

2. Nitrogenase

The complex enzyme nitrogenase (Howard, J. B.; Rees, D. C.; this issue)^{416,433–436} consists of the iron protein and the molybdenum–iron protein within which is the catalytic center, an entity dissociable from the protein and called the iron–molybdenum cofactor⁴³⁷ (FeMoco). Reaction 11 is a simplified expression of nitrogenase activity. The overall stoichiometry of the nitrogenase-catalyzed process is that of reaction 12, in which, additionally, ATP is hydrolyzed and H₂ is evolved; P_i is inorganic phosphate.



Structure determination of the two components of nitrogenase (Table 14) provides the microscopic basis for all further investigations of the enzymes and the ultimate evolution of mechanism. Not only have the structures of the nitrogenase components immensely clarified the nature of the enzyme itself, their knowledge has had the more general salutary effect of reinvigorating the field of iron–sulfur biochemistry. Mechanistic aspects of the enzyme are dealt with elsewhere (Burgess, B. K.; Lowe, D. J.; this issue); we concentrate on the structures of metal clusters of the enzyme complex.

a. Iron Protein. The Fe protein has the α₂-subunit structure with an [Fe₄S₄(S·Cys)₄] cluster symmetrically bonded by Cys-97 and Cys-132 and located near one end of each subunit. Because it is placed between subunits, the cluster is exposed to solvent and is very sensitive to attack by dioxygen. The cluster is the ultimate electron donor to the MoFe protein and cycles between the [Fe₄S₄]^{2+,+} states with a potential E₀' ~ -300 mV. When reduced, the cluster exists in a mixture of S = 1/2 and 3/2 spin states as determined by EPR and Mössbauer spectroscopies and magnetization behavior.⁴³⁸ The proportion of states is subject to changes in the solvent medium, a likely consequence of the exposed nature of the cluster. Spin-state mixtures of [Fe₄S₄]⁺ clusters are no longer uncommon; spin states of the synthetic clusters [Fe₄S₄(SR)₄]³⁻ have been shown to be quite sensitive to extrinsic factors.⁴³⁹ When MgATP binds to the reduced Fe protein, a conformational change ensues and the redox potential is lowered by about 100 mV. An electron is then transferred from the Fe to MoFe protein and two MgATP's are hydrolyzed. The Fe protein itself is reducible by flavodoxin or a conventional ferredoxin *in vivo* and by viologens and dithionite *in vitro*. In dinitrogen reduction, the rate-determining step is apparently dissociation of the Fe and MoFe proteins after electron transfer and MgATP hydrolysis.⁴⁴⁰ Electron transfer between the two proteins is then a gated process initiated by MgATP binding to the reduced Fe protein.⁴⁴¹ The MoFe protein must store electrons one at a time prior to the reduction of substrate. Thus far, among chemical and biological electron carriers, the Fe protein is the entirely specific reductant of the MoFe protein.

b. Molybdenum–Iron Protein. This component of the nitrogenase complex has an α₂β₂-subunit structure with M_r ~ 230 kD and about two molybdenum atoms, 30–34 iron atoms (in the most active preparations), and an equivalent amount of sulfide per molecule. The metal content is distributed over two “P clusters” and two “M clusters”, or cofactor clusters, which contain the molybdenum atoms and are the catalytic sites for N₂ reduction. As originally shown by Bolin *et al.*,^{394,442} the cofactor and P clusters are separated by an edge-to-edge distance of 14 Å, and the cofactor clusters by 70 Å in the α₂β₂ protein. It is now known from crystallography^{392,393} that the cofactor cluster is located in the α subunit and the P clusters at the interface of the α and β subunits. When isolated in the dithionite-reduced condition, the protein contains the cofactor clusters in the M^N state with S = 3/2 and the P-clusters are diamagnetic. The former can be reversibly oxidized to the M^{ox} state with S = 0. The transient reduced state M^{red} appears under turnover conditions where the M^N EPR signal is nearly absent; this super-reduced state of the cluster may correspond to the catalytically active form. In a breakthrough experiment in 1977, Shah and Brill⁴⁴³ demonstrated that the cofactor cluster could be removed intact from the protein and reinserted into a mutant form of the MoFe protein lacking this cluster, restoring the enzyme complex to full activity. MoFe proteins from two organisms (*A. vinelandii*, *C. pasteurianum*) have been investigated crystallographically (Table 14).

While P-clusters in MoFe proteins from different sources appear to be spectroscopically identical, the two available structures differ (Chart 5, p 2254, parts B and C). Both structures contain two Fe_4S_4 cubane-type units and six Cys·S ligands, with one bridging and two terminal ligands contributed by each subunit at the α/β interface. The structure favored by Rees and co-workers^{1,392,393,416,436} has an Fe_8S_8 core composition and implicates a direct S–S bond between subclusters (Figure 29C). One of the iron atoms not bridged by Cys·S groups is coordinated by a serine residue (not shown). The structure deduced by Bolin³⁹⁵ has an Fe_8S_7 core and a μ_6 -S atom at the center of an Fe_6 trigonal prism (Figure 29D). Spectroscopic results indicate that in the as-isolated protein most or all of the iron atoms are in the ferrous state.⁴⁴⁴ When oxidized, P-clusters appear to exist as a mixture of spin states.⁴⁴⁴ Despite the apparent compositional and structural differences at present, it is clear that P-clusters represent a new type of cluster structure not known in any other other protein and not yet realized by synthesis. It has proven possible to link synthetic Fe_4S_4 clusters through one μ_2 -S bridge⁴⁴⁵ and by two intercluster Fe-(μ_3 -S) bonds generating an Fe_2S_2 rhomb-like bridge.⁴⁴⁶ Intercluster cysteinate bridging and S–S bonds between clusters remain unknown in nonnative clusters.

The structure of the cofactor cluster, apparently in the M^{N} state, has been determined with two MoFe proteins at different resolution (Table 14). The structure of the FeMo protein of *A. vinelandii* determined in 1992 at 2.7–2.8 Å resolution provided the first model of cofactor structure. Thereafter, the protein structure was acquired at 2.2 Å resolution, rendering more certain most aspects of the cofactor cluster structure. Despite numerous published predictions, the actual structure (Chart 5A, p 2254, Figure 29E) was not fully anticipated. The cluster may be described as a bridged assembly in which cuboidal Fe_4S_3 and MoFe_3S_3 units are connected by three μ_2 -S atoms. The MoFe_7S_9 core has idealized C_{3v} symmetry, with an Fe_6 trigonal prism capped on the C_3 axis by an iron and a molybdenum atom, and is covalently bound in the α subunit by a Cys·S ligand at the unique iron atom and by a His·N ligand at the molybdenum site. Six-coordination is completed at the molybdenum atom by formation of a five-membered chelate ring involving hydroxyl and carboxylate oxygen atoms of homocitrate. This species was identified prior to the structure as an essential component of the cofactor.⁴⁴⁷

The cofactor cluster structure has two, and perhaps three, notable features. (i) The core topography is unprecedented. It is similar to the Ni_8S_9 core of $[\text{Ni}_8\text{S}(\text{SBU})_9]^-$,⁴⁴⁸ in which the triangular faces of a Ni_6 trigonal prism are capped by two nickel atoms. However, the nickel cluster contains a μ_6 -S atom centered in the trigonal prism and all thiolate sulfur atoms are doubly bridging along the nine edges of the Ni_8 construct. In the cofactor cluster, a sulfur atom would not fit in the trigonal Fe_6 cavity, and, in any case, no electron density was located at the site of a putative interstitial atom. The native cluster is more closely approached structurally and composi-

tionally by another type of synthetic cluster. Of the 17 core atoms of the cofactor cluster, the clusters $[\text{MFe}_4\text{S}_6(\text{PET}_3)_4\text{L}]$ ($\text{M} = \text{V}, \text{Mo}$; $\text{L} = \text{Cl}^-, \text{RS}^-$; Figure 29F) present the 10 atoms $\text{Fe}_4\text{S}_3(\mu_2\text{-S})_3$ with analogous bond connectivity and spatial disposition.^{449,450} (ii) The iron atoms of the Fe_6 trigonal prism are three-coordinate, occurring in the units $\text{Fe}(\mu_2\text{-S})(\mu_3\text{-S})_2$. An FeS_3 coordination unit has otherwise been achieved only with sterically encumbered thiolate ligands and only with Fe(II).⁴⁵¹ While no trigonal unit with sulfide ligands has been prepared, it is relevant to observe that in the FeS_3P units of $[\text{MFe}_4\text{S}_6(\text{PET}_3)_4\text{L}]$ the FeS_3 fragments are approximately trigonal planar, with the Fe–P bond normal to the S_3 plane. (iii) In the more accurately determined cofactor structure (*A. vinelandii* FeMo protein¹) the distances between three-coordinate iron atoms are variable (2.4–2.6 Å) and average to ~ 2.5 Å. These values are possibly smaller than are found in native and synthetic Fe_2S_2 , Fe_3S_4 , and Fe_4S_4 clusters in any oxidation state, where Fe–Fe distances are typically 2.65–2.80 Å. Associated with these distances are displacements of iron atoms from their S_3 planes toward the interior of the trigonal prism. The mean Fe–Fe distance deduced from EXAFS analysis^{452,453} is somewhat longer (2.6 Å) than the crystallographic mean value, but contains contributions from the P-clusters. On balance, three-coordinate Fe–Fe separations appear to be somewhat smaller than those between tetrahedrally coordinated iron atoms in other clusters. This implies a modicum of direct metal–metal bonding and a means of partially alleviating electron deficiency at the three-coordinate sites.

When liberated from acid-denatured MoFe protein by extraction into basic *N*-methylformamide (NMF), the Mo·N·His and Fe·S·Cys bonds of the cofactor cluster are broken, but homocitrate binding and the $S = 3/2$ state are maintained. In NMF solution, on the basis of the small-angle X-ray scattering studies, the cofactor is aggregated.⁴⁵⁴ By the detection of both first- and second-shell scattering, the Mo K-edge EXAFS results make clear that the cofactor core structure is maintained upon removal from the protein.⁴⁵⁵ In solution, the cofactor binds exogenous ligands, among them PhSe^- at an iron site⁴⁵⁶ and cyanide at the molybdenum site.⁴⁵⁵ These results were obtained by Se and Mo K-edge EXAFS. The existence of an Fe–Se bond strongly implies that thiolate binding to cofactor established earlier involves iron and not molybdenum; the unique iron atom, ligated by Cys·S in the protein, is the likely binding site. By use of acidic methyl ethyl ketone, it is possible to extract from the MoFe protein a different cluster, termed the MoFe cluster, which has the metal content MoFe_6 and an $S = 3/2$ EPR spectrum, but lacks homocitrate.⁴⁵⁷ EXAFS results indicate that the molybdenum atom retains six-coordination, as it does in the cofactor, but that at least one of the iron atoms in the first shell of molybdenum has been lost. Further, the second shell scattering around 5 Å is absent, suggesting that the MoFe cluster does not have the long-range order of the cofactor structure. Evidently, the MoFe cluster is a structural derivative of the cofactor cluster. Insertion of the cluster into a mutant MoFe protein followed by addition of Fe protein and MgATP results

in ATP hydrolysis at 28% of the rate of the wild-type enzyme.⁴⁵⁷ Not surprisingly, the MoFe cluster does not reconstitute H₂ evolution or acetylene reduction activity.

Although it cannot be said to be proven in its entirety, sequence 13 is the consensus order of electron flow in nitrogenase. The difficulty in relat-

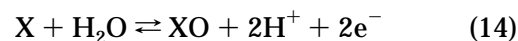
Fe protein → P-clusters →
cofactor → substrate (13)

ing the structures of the metal clusters in the MoFe protein to function is the uncertainty of their fidelity to actual structures under turnover conditions. Further, the fine details of protein structure in the fixing enzyme are unknown. It has been proposed that electron transfer through a P-cluster results in the breaking and making of the S–S bond between subclusters.⁴³⁶ Fe and Mo K-edge EXAFS of the MoFe protein in three oxidation levels, ranging from the indigo disulfonate oxidized form to that present under slow turnover conditions (effected with limiting Fe protein) indicate that metal–metal distances contract slightly upon addition of each electron.⁴⁵³ In particular, the Mo–Fe distance is shortened by *ca.* 0.06 Å upon two-electron reduction of the M^{ox} state. The only relevant comparison is with cubane-type [MoFe₃S₄]^{3+,2+} cores; examples of both expansion and contraction of Mo–Fe distances by ≤ 0.05 Å have been found upon reduction.^{458–460} Nothing is yet known about the nature of the interaction of any substrate with the cofactor cluster. The most obvious points of interaction between substrate and cluster are the coordinatively unsaturated iron atoms. One initial realization was that the cavity of the cofactor is far too small to accommodate a dinitrogen molecule.¹ If this or another substrate were to reside within the cluster structure, Fe–S bond breakage and/or expansion of cavity size is required. One estimate is that Fe–Fe distances of the Fe₆ trigonal prism must reach *ca.* 3 Å in order to contain dinitrogen.⁴⁶¹ In the Thorneley–Lowe mechanism,⁴⁶² the cofactor binds dinitrogen in a state more reduced than M^N. The idea of cofactor cavity occupation should be continued, given a possible synergy between cluster reduction, cavity expansion, and the formation of Fe–N bonds which would be part of the activation process. However, this notion is problematic; exterior binding modes of dinitrogen to the cluster have been examined theoretically.^{461,463} Despite its six-coordination, the molybdenum atom also remains a possible site of dinitrogen binding. When the cluster is further reduced, it is likely that the electron density on the molybdenum atom will increase to some extent, weakening in particular bonds to anionic ligands. The homocitrate chelate ring might open and dinitrogen bind to a coordination position previously occupied by a carboxylate oxygen atom.⁴⁶⁴ The current resolution of the MoFe protein X-ray structures does not permit a distinction between the hydroxyl group or its deprotonated form as one of the homocitrate binding sites. If the ligand is alkoxide, cluster reduction could lead to protonation and displacement by dinitrogen. If the ligand is hydroxyl, it could be displaced by substrate upon reduction.

Synthetic systems based on MFe₃S₄ cubane-type clusters (M = V, Mo) have been developed which reduce hydrazine to ammonia or acetylene to ethylene in the presence of proton and electron sources.⁴⁶⁵ Reduction activity was empirically correlated with the presence of labile coordination sites (occupied by solvent) on the M atom, implying that the heterometal was the site of substrate binding. Such clusters remain the best *structural* models of the MFe₃S₃ cuboidal fragment of the native cluster. Examination of the interaction of cofactor cluster and substrates as dependent on cluster oxidation level is an attractive proposition which might assist in defining binding modes. However, any such study must await solution of the formidable problem of the synthesis of FeMoco, or a reasonable analogue thereof, in tractable form. Alternative nitrogenases, not containing molybdenum, are considered elsewhere (Eady, R.; this issue).

F. Oxotransferases

Oxotransferases^{29,466,467} and nitrogenase are the only enzymes that utilize molybdenum. However, any resemblance between the two enzyme types ends there. While many oxotransferases contain iron–sulfur clusters as electron transfer centers, all such clusters appear to be of a standard type (Figure 4). Further, because all molybdenum sites are mononuclear, the catalytic centers in oxotransferases are unrelated to that in nitrogenase. Oxotransferases catalyze overall reaction 14, in which X and XO are generalized oxygen atom acceptors and donors, respectively. All reactions of these enzyme involve



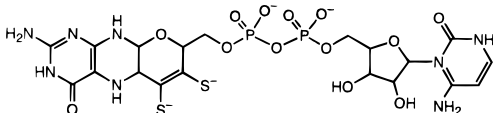
substrates and products whose oxygen content differs by one atom; hence, the name “oxotransferase” which, however, does not necessarily carry a mechanistic implication. In past²⁹ and present accounts (this issue), Hille has presented comprehensive treatments of the types of enzymes, reactions and mechanisms, and active-site structures obtained by crystallography and XAS. In addition, the current state of tungsten enzymes, some of which are oxotransferases, has been summarized (Adams, M. W. W.; Johnson, M. K.; Rees, D. C.; this issue). We limit our consideration here to structure and, in selected cases, its relation to reactivity.

Until 1995, structural information on the active sites of oxotransferases was deduced from spectroscopy, principally molybdenum EXAFS analysis and EPR results. In that year two protein crystal structures were reported; structural information is summarized in Table 15.^{468,469} The first published structure was that of the oxidized tungsten-containing aldehyde ferredoxin oxidoreductase from the hyperthermophile *Pyrococcus furiosus*. This enzyme contains four metal sites. The tungsten site (Chart 5E, p 2254) consists of two dithiolene chelate rings from two pterin cofactor molecules. The remaining two coordination sites are occupied by two oxygen ligands thought to be oxo and/or glycerol (from the protein storage buffer). There is no protein ligand. The chelate rings are disposed at a dihedral angle of about

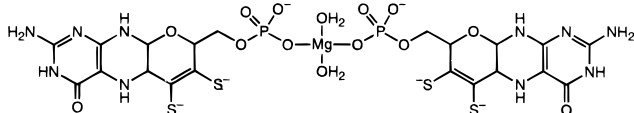
Table 15. Crystallographically Defined Coordination Units of Molybdenum and Tungsten Oxotransferases

enzyme/unit	resolution (Å)	references (PDB code) ^a
aldehyde oxidoreductase (<i>Desulfovibrio gigas</i>) inactive form [MoO(S ₂ ·pterin)L ₂] ^{c,d} 2[Fe ₂ S ₂ (S·Cys) ₄]	2.2, 1.8	468, <i>b</i>
partially sulfided form [MoOS(S ₂ ·pterin)(OH ₂)] ^c 2[Fe ₂ S ₂ (S·Cys) ₄]		<i>b</i>
aldehyde ferredoxin oxidoreductase ^e (<i>Pyrococcus furiosus</i>) [W(S ₂ ·pterin) ₂ L ₂ Mg(OH ₂) ₂ (OC·Ala)(OC·Asn)] ^f [Fe ₄ S ₄ (S·Cys) ₄]	2.3	469a
DMSO reductase (<i>Rhodobacter sphaeroides</i>) oxidized [MoO(S ₂ ·pterin) ₂ (O·Ser)] ^g reduced [MoO(S ₂ ·pterin)(O·Ser)] ^h	2.2	469b

^a See footnote in Table 5. ^b Hille, R., this issue. ^c S₂·pterin:



^d L = unidentified oxygen ligand. ^e Also contains tetrahedral iron atom (structural). ^f (S₂·pterin)₂Mg(OH₂)₂:



L = oxo and/or glycerol oxygen ligands. ^g S₂·pterin contains a guanine group; one dithiolene group is asymmetrically coordinated (Mo–S 2.4, 3.1 Å). ^h One S₂·pterin is in the active site region but interacts weakly with the Mo atom (Mo–S 2.9, 3.7 Å).

97° and the WO₂S₄ unit has distorted trigonal prismatic stereochemistry. Prior to the X-ray structure determination, two oxo ligands were proposed from analysis of the tungsten EXAFS.⁴⁷⁰ All oxotransferases contain a pterin cofactor,⁴⁷¹ which was originally thought to consist of a pterin nucleus with a four-carbon side chain carrying an ene-1,2-dithiolate fragment, one hydroxyl group, and a terminal phosphate group which may or may not be bonded to guanine or cytosine dinucleotide. However, the crystal structure reveals that the cofactor contains an additional six-membered ring closed by a C–O bond at C(7) involving the oxygen atom initially thought to be present as hydroxyl. This pyran-type ring is decidedly nonplanar, and the pyrazine-type ring of the pterin is also nonplanar, indicating that it is in the reduced (dihydro) form. As seen in Table 15, the two cofactors are connected through a structural Mg(II) ion coordinated to two phosphate oxygen atoms, two water molecules, and two backbone carbonyls. One [Fe₄S₄(S·Cys)₄] cluster is hydrogen bonded to the cofactor and is located about 10 Å from the tungsten atom. Its function doubtless is to provide a pathway for electron flow from the catalytic center where reaction 14 (X = RCHO, XO = RCO₂H) occurs to the physiological electron acceptor, which is a ferredoxin. The pathway may involve the pterin nucleus. The fourth metal center is tetrahedrally coordinated and thought to involve iron on the basis of anomalous scattering.

It is about 25 Å removed from the other metal center and probably has a structural role.

The aldehyde oxidoreductase from *D. gigas* contains a molybdenum site and two [Fe₂S₂(S·Cys)₄] clusters, the same metal composition as in xanthine oxidase where the iron–sulfur clusters have an electron transfer function. In the inactive form investigated crystallographically, the molybdenum atom was found in distorted square-pyramidal coordination and is displaced ~0.5 Å toward the axial position. One dithiolene chelate ring lies in the equatorial plane together with an oxo ligand. The remaining two positions are occupied by unidentified oxygen ligands. As for the tungsten enzyme, there is no protein ligand. When the enzyme is partially converted to a sulfided form, the coordination unit undergoes a significant change. The electron density at an axial position increases and is displaced ~0.4 Å away from the metal atom. This observation is entirely consistent with the conversion Mo=O (1.7 Å) → Mo=S (2.1 Å), the indicated distances having been established in enzymes by EXAFS^{472,473} and in numerous synthetic compounds by X-ray diffraction. The equatorial Mo=O group is maintained in the sulfided form; the other equatorial ligand has been assigned as a water molecule of the basis of a Mo–O bond distance of 2.4 Å.

Following Hille (this issue), most molybdenum oxotransferases can be placed in the families indicated in Figure 30, these being named for their prototypic enzymes. Structures and metric features have been taken from X-ray and EXAFS^{472–477} investigations and are intended as current consensus depictions of active sites. Mo(IV) and Mo(VI) sites are shown because, under the oxo transfer hypothesis in Figure 31A, the indicated oxidation states are those involved in direct oxygen abstraction from or donation to substrate, respectively. Other enzymes in the xanthine oxidase family include xanthine dehydrogenase, aldehyde oxidase, and CO dehydrogenase. Members of this family are characterized by the presence of one pterin cofactor, the Mo^{VI}OS group in the oxidized enzymes, and an apparent terminal hydrosulfide ligand in the reduced form. Oxygen atom transfer in the oxidation of xanthine to uric acid by milk xanthine oxidase has been proven by labeling the oxidized enzyme with ¹⁸O and demonstrating that under single turnover conditions 79% of the label appeared in the product when the reaction was performed in unlabeled water.⁴⁷⁸ The 21% isotope dilution must have arisen from exchange with solvent over the course of reaction; controls showed that this exchange did not occur with uric acid. Hence, the oxygen atom transferred to the product originated with the molybdenum atom and not with solvent. In light of the active-site structure (Figure 30), it is probable that the oxo atom is transferred inasmuch as ligated water (or hydroxide) would be expected to exchange with bulk solvent. Water enters into overall reaction 14 because it is the ultimate source of the oxo ligand in all enzymes (Figure 31A). Mechanistic considerations of xanthine oxidase catalysis are extensive and complex (Hille, R.; this issue). Treatment of the enzyme with cyanide removes sulfide as thiocyanate and completely deacti-

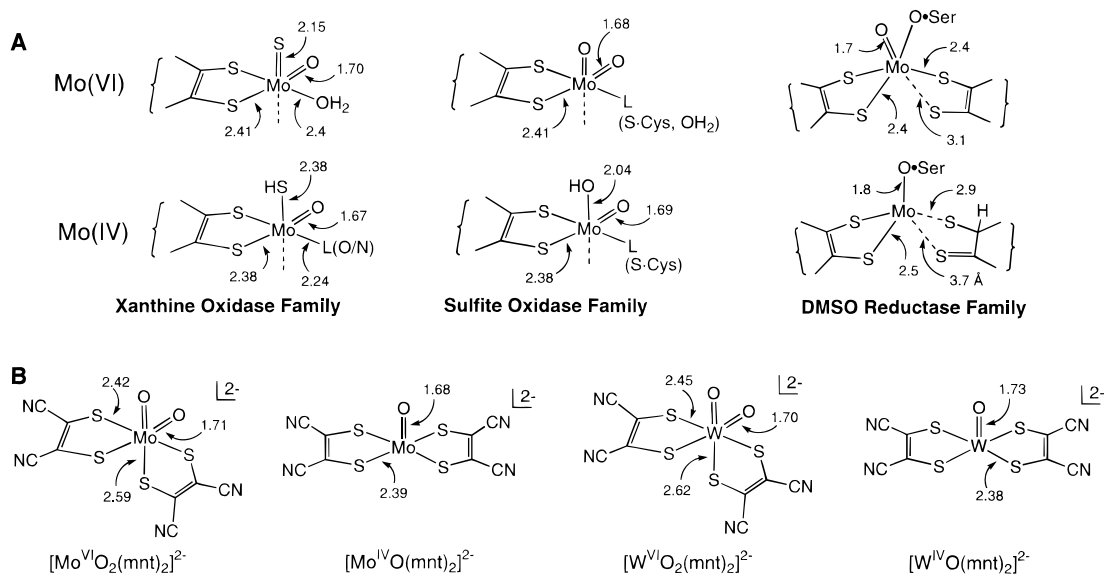


Figure 30. Structures of molybdenum sites and complexes. (A) Structures of Mo(VI) and Mo(IV) sites in the indicated families of oxotransferases as determined from crystallography and Mo EXAFS, with the bracketed portions being the pterin cofactors. All bond distances (Å) given to three figures are from EXAFS; others are crystallographic values. (B) Schematic structures of the dithiolene complexes $[\text{MO}_2(\text{mnt})_2]^{2-}$ ($\text{M} = \text{Mo}, \text{W}$) showing selected bond lengths.

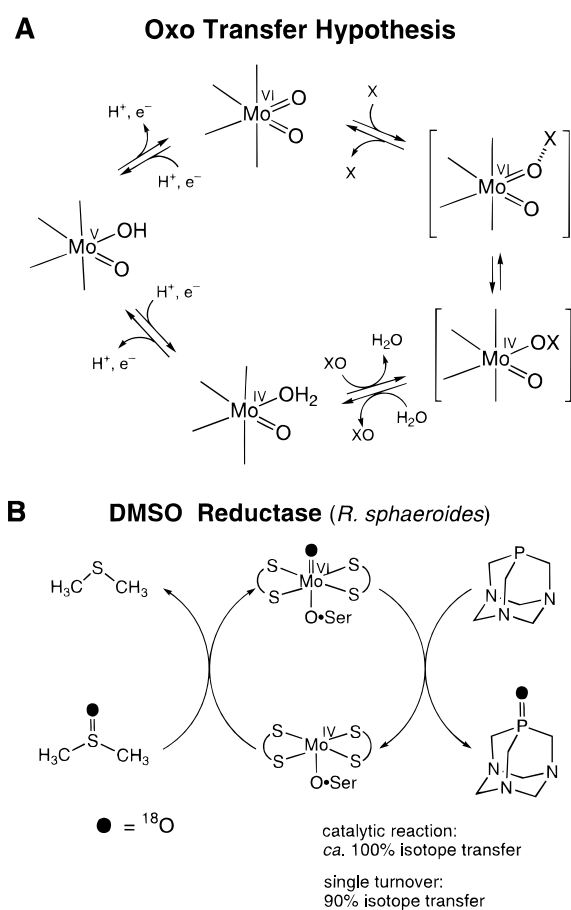


Figure 31. Reaction schemes: (A) the oxygen atom (oxo) transfer reaction hypothesis for molybdenum oxotransferases; (B) the double oxo transfer reaction demonstrated for a DMSO reductase. The asymmetric coordination of one dithiolene group found crystallographically (Figure 30A) is not depicted here.

vates the enzyme. Consequently, the sulfido ligand is essential to activity. While in certain other enzymes molybdenum-mediated direct atom transfer from or to substrate is probable and in one instance

established, this is not the case for the xanthine oxidase family. Proposed mechanisms frequently involve more steps and utilize water or protons as a reactant; hence, these enzymes are frequently described as hydroxylases.

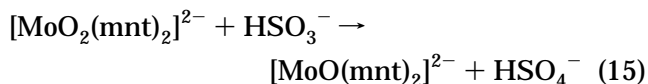
The sulfite oxidase family also includes assimilatory nitrate reductase. All available structural information (Figure 30A) has derived from molybdenum XAS.^{472,475} For oxidized chicken liver sulfite oxidase, the EXAFS data are most consistent with the Mo^{VI}O₂ group and 2–3 coordinated sulfur atoms, indicating the presence per molybdenum atom of one pterin cofactor, which has otherwise been detected.⁴⁷¹ In the reduced states, the results are in accord with a Mo^{V,IV}O(OH) unit. Remaining ligands may be Cys•S from a conserved cysteinyl residue and/or water. The EXAFS of nitrate reductase from *Chlorobacterium vulgaris* in the oxidized and reduced states are very similar to those of sulfite oxidase.⁴⁷⁴

The DMSO reductase family is considerably larger, and encompasses enzymes such as biotin-S-oxide reductase, trimethylamine-N-oxide reductase, dissimilatory nitrate reductase, and formate dehydrogenase. XAS results for *Rhodobacter sphaeroides* DMSO reductase lead to structures that are somewhat surprising because of the monooxo Mo^{VI}O group in the oxidized form and no terminal oxo ligands in the Mo(V,IV) states.⁴⁷⁷ The dissimilatory nitrate reductase from *E. coli* also has a monooxo Mo^{VI}O group, significant thiolate ligation, and no Mo^{IV}O group.⁴⁷⁶ While synthetic molybdenum complexes with these characteristics are not unknown, they are relatively infrequent compared to species with the Mo^{VI}O₂ and Mo^{V,IV}O groups, especially in the aqueous chemistry of the element. The 2:1 pterin:Mo ratio, taken as a defining feature of this family, has also been established by direct analysis of the enzyme.⁴⁷⁹

Very recently, the X-ray structure of DMSO reductase from *Rhodobacter sphaeroides* in two oxidation states has become available (Table 15). It reaffirms the Mo^{VI}O unit and the absence of an oxo ligand in

the Mo(IV) state, and shows tight bidentate coordination of one pterin dithiolene grouping in both oxidation states. However, the dithiolene of the second cofactor behaves in a most unexpected manner, described schematically in Figure 30A. In the oxidized form, the molybdenum atom is firmly coordinated by five ligands, including the presumably deprotonated serine side chain. The potential sixth ligand is a sulfur atom of an asymmetrically bound dithiolene group located at 3.1 Å from the molybdenum atom. In the reduced form, only three strongly bound ligands have been identified, two sulfur atoms in a dithiolene ring and Ser·O(H). The second cofactor has moved away from the metal, such that the Mo···S separations are long (2.9 and 3.7 Å) and nonbonded. Furthermore, the distant dithiolene appears to have become protonated, creating a chiral center, with attendant formation of a thione group. Whether these bizarre structural effects extend to other members of the DMSO reductase family in an enzymatically active condition remains to be determined.

The oxo-transfer hypothesis (Figure 31A) was originally presented for enzymes thought at the time to contain the Mo^{VI}O₂ and Mo^{V,IV}O groups,^{480,481} the presence of the Mo^{VI}O and the absence of Mo^{IV}O group in enzymes not having been anticipated. It is founded on an extensive body of reaction chemistry in synthetic systems demonstrating the general reactions Mo^{VI}O₂L_n + X ⇌ Mo^{IV}OL_n + XO.^{467,480–484} Among these, the sulfite oxidase analogue reaction system 15 involving complexes of known structure⁴⁸³ (Figure 30B) suggests that the hypothesis is applicable to the sulfite oxidase family. As yet, there



are no isotope labeling experiments that prove atom transfer from the molybdenum center to substrate in this family of enzymes. However, results such as reaction 15 and many others make clear that the Mo^{VI}O₂ and Mo^{IV}O groups, with a variety of coligands which often include thiolate, are well suited to oxo-transfer reactions. The sulfite oxidase family appears to utilize these groups in both oxidation and reduction processes.

A thermodynamic scale for oxygen atom transfer reactions has been developed.^{481,485} A series of reactions (or couples) X + 1/2O₂ → XO is arranged in the order of decreasing ΔH, such that the reduced member Y of a couple Y/YO is thermodynamically competent to reduce the oxidized member XO of a couple X/XO with a larger ΔH. With the extensive database available,⁴⁸⁵ the directions of many reactions X + YO can be predicted. Given the values ΔH(HSO₃⁻/HSO₄⁻) = -62 kcal/mol and ΔH(NO₂⁻/NO₃⁻) = -24 kcal/mol in aqueous solution, it follows that ΔH exceeds -62 kcal/mol for the Mo^{IV}O/Mo^{VI}O₂ couple of sulfite oxidase and for the complexes in reaction 15 in order that bisulfite function as an oxo acceptor. Similarly, it is required that ΔH be less than -24 kcal/mol for the Mo^{IV}O/Mo^{VI}O₂ couple of assimilatory nitrate reductase in order that nitrate behave as an oxo donor. If, as seems likely, the ΔH

values for both enzymes are within these limits, then on thermodynamic grounds reduced sulfite oxidase should be capable of reducing nitrate, and oxidized nitrate reductase capable of oxidizing bisulfite. We are unaware of any experiments designed to test the activities of these enzymes toward the two potential cross-substrates.

In the DMSO reductase family, the double oxo transfer experiment in Figure 31B has been performed with *R. sphaeroides* enzyme using ¹⁸O labeling.³⁰ The labeled substrate was incubated with the enzyme and the water-soluble tertiary phosphine under both single-turnover and catalytic conditions where the reaction is Me₂SO + R₃P → Me₂S + R₃PO. Isotope transfer was ≥90%, showing at once that the Mo^{VI}O group is competent as an oxo donor and the non-oxo Mo(IV) center as an oxo acceptor, the natural function of the enzyme. If the correlation between two bound pterin cofactors and an M^{VI}O group extends to the foregoing tungsten aldehyde oxidoreductase, it would be placed in the DMSO reductase family. In that event, the structurally defined bis(dithiolene) W^{VI}O₂/W^{IV}O complexes⁴⁸⁶ in Figure 30B would not strictly apply as models of the enzyme site. Hille (this issue) has also placed Mo-containing formate dehydrogenases in this family, with recognition that there may be a subclass containing the Mo=S group. While the tungsten enzymes have yet to be classified in a similar scheme, we note the powerful oxo-acceptor ability of [WO-(mnt)₂]²⁻, which has been reported to effect the transformation HCO₃⁻ → HCO₂⁻.⁴⁸⁷ On the thermodynamic scale, this places ΔH(W^{IV}O/W^{VI}O₂) for these complexes below -64 kcal/mol, in the range of such avid oxo acceptors as cyanide and tertiary phosphines. Lastly, should catalytic centers containing one M^{IV}O/M^{VI}O₂ group (M = Mo, W) bound by two pterin cofactors appear, the complexes in Figure 30B and related species⁴⁸⁸ provide intrinsic structures, including the oxo trans effect on dithiolene coordination. As yet, no bis(dithiolene)monooxo complexes of Mo(VI) or W(VI) have been prepared.

G. Transport and Storage Proteins

Three types of proteins are considered. *Transferrins* solubilize, transport, and deliver Fe(III) to cells. *Ferritins* store Fe(III) intracellularly in exceptionally large iron-oxo aggregates surrounded by a protein sheath. *Metallothioneins* sequester Zn(II), Cd(II), and Cu(I) by means of their remarkably high cysteinyl content. Metal site structures are summarized in Table 16.^{489–501}

1. Transferrins

These monomeric glycoproteins^{502,503} are found in all vertebrates and some invertebrates. Like siderophores, they solubilize Fe(III) by binding, thus avoiding the formation of Fe(OH)₃. Transferrins bind two Fe(III) atoms tightly but reversibly and synergistically bind two carbonate ions as bidentate ligands to the metals. They deliver Fe(III) to cells during which process they pass through cell walls and are encapsulated in endosomes. ATP-driven proton pumps on the surface of the endosome lower the interior acidity (pH ~5.5) resulting in the release of Fe(III) which is

Table 16. Crystallographically Defined Coordination Units in Transport and Storage Proteins

protein	resolution (Å)	references (<i>PDB code</i>) ^a
Iron		
transferrin [Fe ^{III} (N·His)(O ₂ C·Asp)(O·Tyr) ₂ (CO ₃)] ^b		
serum transferrin		
rabbit	3.3	489 (<i>ITFD</i>)
N-terminal half-molecule	2.3	490
lactotransferrin		
human	2.2, 2.0	491, 492 (<i>ILFG, ILCT</i>), 493
N-terminal half-molecule	2.0	494
Cu(II)-substituted form ^c	2.1	495 (<i>ILFI</i>), 493
apoprotein	2.8	496 (<i>ILFH</i>)
ovotransferrin		
duck, quarter-molecule	2.3	497
hen, N-terminal half-molecule	2.1	498
ferritin [Fe(N·His)(O ₂ C·Glu)(OH ₂)]		
apo form (human H-chain, mutant)	2.4	499 (<i>IFHA</i>)
Zinc–Cadmium		
metallothionein (Cd ₅ Zn ₂ isoform 2, rat liver)	2.0	500, 501 (<i>4MT2</i>)
[Cd ₄ (μ-S·Cys) ₅ (S·Cys) ₆ , (Cys·S) ₂ Cd(μ-Cys·S) ₂ Zn ₂ (μ-S·Cys)(S·Cys) ₄]		

^a See footnote in Table 5. ^b Carbonate acts as a bidentate ligand. ^c Two inequivalent Cu sites.

taken up by other iron-binding proteins including ferritin. Apotransferrin is subsequently released from the cell, and the process is repeated. Transferrins impede bacterial growth and survival. Iron metabolism is regulated by transcription and subsequent destruction of transferrin receptor mRNA. High iron levels within cells promote degradation of this mRNA, hindering synthesis of the receptor via translation. Low iron levels stabilize transferrin receptor mRNA, promoting the synthesis of the transferrin receptor and thus increasing iron uptake. Transferrins also protect cells from the toxic effects of free iron by sequestration, thereby preventing the formation of injurious hydroxyl radicals in Fenton reactions. There are three main types of transferrins: serum transferrin, located mainly in the blood plasma; ovotransferrin, in hen egg white, and lactotransferrin, in milk. Structural information is available for all three types (Table 16), although not always for an intact transferrin molecule.

Transferrins typically consist of a single polypeptide with 670–700 residues and a molecular weight of *ca.* 80 kD. Protein folding affords N- and C-terminal halves or lobes, with one iron binding site in each lobe. Each half exhibits up to about 40% sequence homology, and the protein structural features of each, where known, are quite similar. The two lobes are connected by a short α helix, generating a bilobate structure. Transferrin half-molecules can be prepared by proteolytic reactions or recombinant DNA techniques; structures of several such species have been determined. The Fe(III) binding sites in the two halves are separated by ~ 42 Å (in human lactotransferrin) and are practically identical. They display distorted octahedral coordination with the ligation pattern illustrated in Figure 32A. Carbonate (or bicarbonate) fits efficiently into a strongly hydrogen-bonded site and coordinates as a bidentate ligand; the aspartate carboxyl group is unidentate. Coordination is completed by His·N and two Tyr·O ligands arranged facially. In this set of weak-field ligands, Fe(III) is bound in the high-spin condition. For reactions at fixed pH and partial pressure of CO₂, the effective formation constants K_1' and K_2' (eq 16)

can be defined. These have been found to be of similar magnitude and in the range 10^{17} – 10^{20} M⁻¹.^{502a}

$$K_1' = [\text{FeTfn}]/[\text{Fe}^{3+}][\text{Tfn}]$$

$$K_2' = [\text{Fe}_2\text{Tfn}]/[\text{Fe}^{3+}][\text{FeTfn}] \quad (16)$$

As befits such high Fe(III) affinity, the ligands are hard anions and imidazole—just those known to bind high-spin Fe(III) effectively in nonprotein circumstances. The total ligand charge of 5– is matched by the metal charge and the nearly 2+ charge of the protein binding pocket.⁵⁰³ The redox potential of about –500 mV⁵⁰⁴ reveals that the anionic ligand environment strongly favors Fe(III) over Fe(II).

Nonnative metals can be substituted for iron in transferrins. As recently noted by Baker,⁵⁰⁵ Aisen⁵⁰⁵ has proposed three criteria for binding at the native iron sites: (i) no more than two metals bound per transferrin molecule; (ii) no binding to iron-saturated transferrin; (iii) one (bi)carbonate or other appropriate anion bound with each metal ion. By these criteria the ions VO²⁺, Cr³⁺, Mn³⁺, Co³⁺, Cu²⁺, and Ga³⁺ bind specifically,⁵⁰⁵ but others may also bind in this way.^{502,503} However, while the binding constants (eq 16) for Ga³⁺, a trivalent ion with nearly the same radius as Fe³⁺ (0.62 Å¹¹), also are 10^{17} – 10^{20} M⁻¹,⁵⁰⁶ those for divalent ions such as Fe²⁺ and Zn²⁺ under conditions comparable to Fe³⁺ binding are much less (10^4 – 10^6 M⁻¹).⁵⁰⁷ Evidently, the site was evolved to stabilize trivalent ions. When Cu(II) is substituted into human lactotransferrin, two inequivalent sites are observed. In the N-lobe, the [Cu(N·His)(O₂C·Asp)(O·Tyr)₂(CO₃)] coordination unit is square pyramidal with the carboxylate and carbonate groups unidentate in the equatorial plane and an axial Tyr·O ligand (at 2.8 Å). In the C-lobe, carbonate is bidentate and the metal is six-coordinate with one long Cu–O·Tyr bond (2.4 Å). The overall protein structure is the same as the native form, the different coordination units arising from small movements of Cu(II) and carbonate in the binding site. This local flexibility presumably allows the binding of the much larger trivalent lanthanides, although the extent to

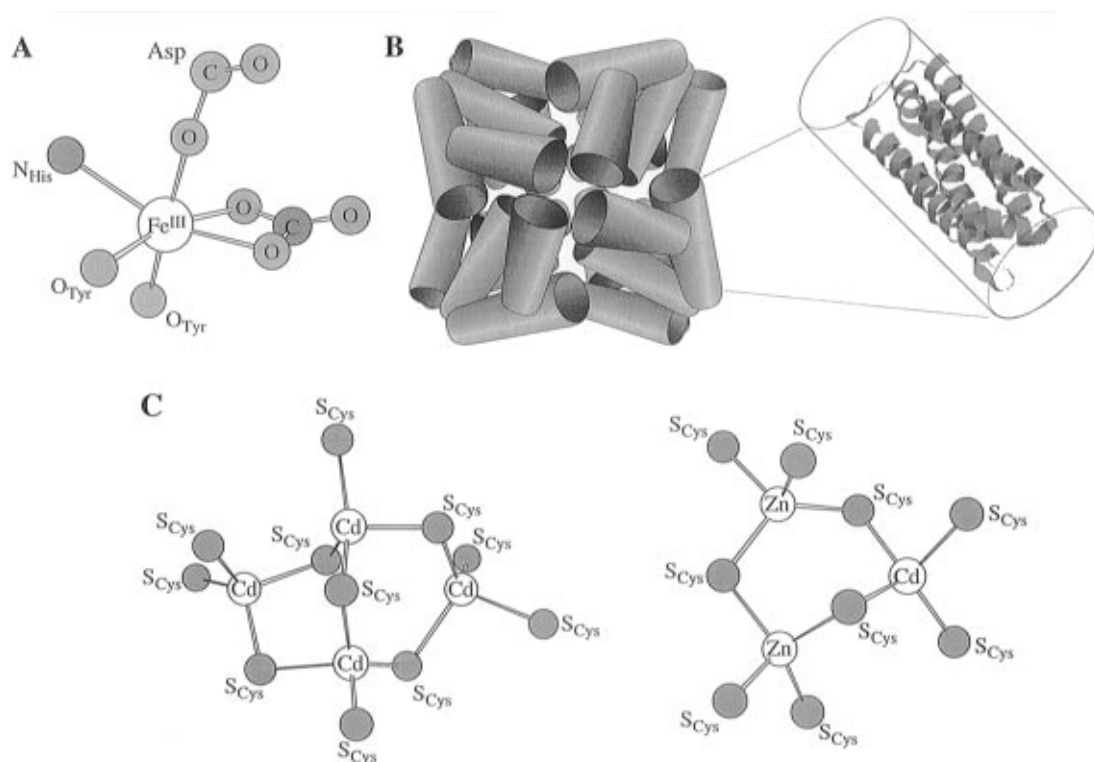


Figure 32. Structural features of iron transport and storage proteins: (A) the binding site of transferrin; (B) quaternary structures of horse spleen ferritin showing the arrangement of 24 subunits and structure of one subunit; (C) the tetranuclear (α domain) and trinuclear (β domain) structures in rate liver Cd_5Zn_2 metallothionein-2.

which protein structure is preserved is not known in such cases.

The binding of Fe(III), and also Cu(II), contributes to tertiary structure. In apolactotransferrin, the N- and C-lobes are rotated around intervening protein structure by 53° compared to the holoprotein. Further, the N-lobe undergoes a large conformational change while the C-lobe is little changed. These results demonstrate a substantial conformational change which is intimately coupled to Fe(III) binding and release, reactions which are examined in more detail elsewhere.^{502,503} The function of transferrins has been aptly encapsulated by Baker: "The most striking feature of transferrin chemistry is that iron is bound with extraordinary avidity, yet it can be released without any denaturation and the protein can be recycled through many cycles of uptake and release."⁵⁰³ The view that emerges for the binding sites of transferrins is that they have been beautifully engineered to bind their native metal Fe(III), but possess sufficient conformational flexibility to coordinate other ions of different size and lower charge, albeit with reduced affinity.

2. Ferritin

These proteins, found in vertebrates, invertebrates, higher plants, fungi, and bacteria, function as iron storage vehicles in aerobic cells and have been extensively studied.^{508–510} Horse spleen ferritin is the most thoroughly examined member of this family of proteins and is prototypic among mammalian ferritins. Ferritins are very large proteins, typically 100–110 Å in outside diameter and containing a protein coat about 10 Å thick that envelops a core of hydrous ferric oxide with variable amounts of phos-

phate. The core has an effective diameter of *ca.* 75 Å and contains up to 4500 iron atoms; ferritins with highly variable iron contents have been isolated. The protein coat, or shell, is built up of 24 subunits. Each subunit consists of a single polypeptide chain with *ca.* 170 residues. A given ferritin molecule includes two different types of chains, termed H and L, of similar sequence and size. Each subunit of horse spleen ferritin, for example, contains 174 amino acids; about 85% of these subunits consist of L chains and the remainder H chains. Following Harrison *et al.*,^{509,510} each subunit is a 4- α -helix bundle involving two antiparallel helix pairs (AB, CD). A fifth shorter helix (E) lies at the end of the bundle at an acute angle to the other helices; 129 residues are included in the five helices. A long loop positioned on the outside surface of the bundle joins the C-terminus of helix B to the N-terminus of helix C. As shown schematically in Figure 32B, the subunits are arranged in the manner of a rhombic dodecahedron (an example of the rare point group *O* if all subunits are taken as identical). This spatial disposition of subunits produces channels into the core along C_3 and C_4 axes of the molecule. The six 4-fold channels are substantially lined with Leu residues and are considered hydrophobic. The eight 3-fold channels are relatively hydrophilic because of Asp and Glu residues and, to a lesser degree, His and Tyr residues. The inside shell of the ferritin molecule is also hydrophilic. The arrangement of subunits and the size of the molecule are basically the same in apo- and holoproteins. Iron is stored nearly exclusively as Fe(III); treatment of the holoprotein with dithionite or ascorbate in the presence of a chelating agent with affinity for Fe(II) results in formation of the

apoprotein. The latter may be reconstituted *in vitro* by aerobic treatment with an Fe(II) salt in a solution at pH \sim 7.

The foregoing structural results were obtained by X-ray diffraction using samples crystallized from solutions containing salts of ions such as Ca^{2+} and Cd^{2+} , a technique that has proven effective for molecules with mainly L-chain subunits. In such cases, individual ferritin molecules are linked by metal bridges involving coordination to Asp and Gln residues. The metals execute a (nonbiological) structural function. However, in the case of certain H-chain ferritins this method failed to afford crystalline protein because coordinating Gln residues were not conserved. Site-directed mutagenesis of recombinant human H-chain ferritin (Lys \rightarrow Gln) allowed the desired bridges to form, producing crystals from CaCl_2 solutions suitable for X-ray structure determination.⁴⁹⁹ The bridges were formed by the coordination units $[\text{Ca}(\text{O}_2\text{C}\cdot\text{Asp})_2(\text{O}^\delta\cdot\text{Gln})_2]$. The recombinant form retains activity in iron uptake and is an otherwise normal ferritin. Also discovered in the structural analysis was the tetrahedral $[\text{Fe}(\text{N}\cdot\text{His-B})(\text{O}_2\text{C}\cdot\text{Glu-A,B})_2(\text{OH}_2)]$ coordination unit located within the helical bundle of each subunit and 7–10 Å from the cavity surface. Ligating groups are located in the A and B helices; the coordinated water molecule is hydrogen-bonded to Glu-C and Gln-D residues.^{499,510} This unit is thought to be the “ferroxidase” center,⁵¹¹ at which Fe(II) is catalytically oxidized to Fe(III) attendant to its entry into the protein cavity. Iron(II) may reach the ferroxidase site via the hydrophilic 3-fold channels. However, the structural results for human H-chain ferritin suggest a more direct route through the subunit itself.⁵¹⁰ The ferroxidase center accelerates the rate of iron uptake and core formation, but is not essential to it inasmuch as L-chain ferritins, lacking this redox center, can take up iron slowly and develop cores. Iron(II) may also bind at other sites in the protein.

While details remain obscure, ferritin core formation is an example of biomineralization. The “mineral” in this case is the core, which is rendered soluble by encapsulation within the protein shell. The reaction $4\text{Fe}^{2+} + \text{O}_2 + 6\text{H}_2\text{O} \rightarrow 4\text{FeO}(\text{OH}) + 8\text{H}^+$ is a simplified representation of the formation of hydrous Fe(III) oxide which, together with variable amounts of phosphate, makes up the core. Oxidation may occur at ferroxidase sites or at the surface of the nucleating core, with dioxygen being the ultimate electron acceptor. The core is built up by hydrolysis of aquo Fe(III), formation of oligomeric $\text{Fe}^{\text{III}}\text{—O—Fe}^{\text{III}}$ species, and then separation from solution as core crystallites. On the basis of strong X-ray⁵¹² and electron diffraction⁵¹³ reflections, the core is none of the crystalline forms of $\text{FeO}(\text{OH})$ minerals or of Fe_2O_3 . The best match is the hydrous ferric oxide mineral ferrihydrite,⁵¹⁴ of approximate composition $5\text{Fe}_2\text{O}_3\cdot 9\text{H}_2\text{O}$ and containing octahedral $\text{Fe}^{\text{III}}\text{O}_6$ units. EXAFS results for ferritin (2000 iron atoms) have demonstrated octahedral coordination with a mean $\text{Fe}^{\text{III}}\text{—O}$ bond distance of 1.95 Å.⁵¹⁵ The core is the “active site” of ferritin, both taking up and releasing iron in response to cellular demands. Of the many challenges that remain in this aspect of active-site

chemistry, certainly none exceeds elucidation of the mechanism of iron entry to the protein cavity and the formation of the core. Two other related proteins are known but are crystallographically undefined. Bacterioferritins resemble mammalian ferritins and apparently contain a four-helix bundle,⁵¹⁰ but also include a heme group with bis(Met·S) axial ligation.⁵¹⁶ Hemosiderin is found mainly in animals and appears to store iron in a form similar to ferritin. The protein is usually located within the intracellular membrane and is of limited solubility. Lastly, we note the discerning comment by Theil and Raymond: “The structure of ferritin is the most complete paradigm for bioinorganic chemistry because of three features: the protein coat, the iron–protein interface, and the iron core.”⁵¹⁷

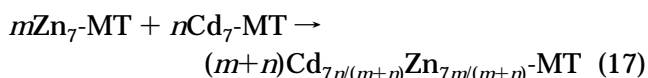
3. Metallothioneins

These proteins^{518–521} have been isolated from a variety of sources including mammals, crustaceans, and yeast. The mammalian proteins have been the most extensively studied. They typically have about 60 amino acid residues, one-third of which are cysteine. For example, rat liver metallothionein (MT) and human MT-2 have 61 residues, 20 of which are Cys. Not infrequently, proteins from a single organism occur as *isoforms*, sometimes differing by only a single amino acid residue. No other protein type has such a high Cys content. These residues bind a variable number of metal ions, with loadings of 4–12 metal ions per molecule rather common. Metal content depends on the organism and the extent of heavy metal exposure. While a number of functions have been ascribed to MT, those which are frequently associated with these proteins are homeostatic regulation of essential metals such as zinc, and detoxification by sequestration of physiologically adverse metals such as cadmium and mercury. For example, cadmium induces the biosynthesis of MT. As would be expected, apo-MT binds practically any transition metal ion, but their interactions with an array of soft metals including Zn(II), Cd(II), Hg(II), Cu(I), Ag(I), Au(I), and Pt(II) have been the most thoroughly examined. Numerous MTs have been isolated from natural sources, and others have been prepared from apo-MT and metal ions or by displacement of bound metal ions. However, there is at present only one MT crystal structure (Table 16), that of $\text{Cd}_5\text{Zn}_2\text{—MT-2}$ from rat liver. This structure has been described in detail in the original literature and subsequently.⁵²²

Rat liver MT-2 has been cleaved into two polypeptides. The β or N-terminal domain consists of residues 1–30, among which are 9 Cys. The α or C-terminal domain includes residues 33–61, of which 11 are Cys. These individual domains bind metals the same as does the intact protein.⁵²³ The metal sites of the rat liver protein divide into two polynuclear aggregates, which are depicted in Figure 32C. The two domains are not in contact and are separated by a short polypeptide linker (residues 30–32). All seven coordination sites are tetrahedral, as would be expected for four-coordinate Zn(II) and Cd(II); the 20 Cys residues are fully utilized in metal binding. The β domain cluster $[\text{CdZn}_2(\text{S}\cdot\text{Cys})_9]$ is a nonplanar six-membered ring with two bridge and two terminal bonds at each metal atom. The α

domain cluster $[\text{Cd}_4(\text{S}\cdot\text{Cys})_{11}]$ consists of two nonplanar six-membered rings with two common bonds, such that two cadmium atoms each have one terminal ligand. The protein is folded the same way in the crystal and in solution. The original crystal structure⁵⁰⁰ was not in agreement with the pattern of binding of Cys residues to the two clusters deduced from a solution NMR study of rat liver $\text{Cd}_7\text{-MT-2}$.⁵²⁴ A second X-ray determination⁵⁰¹ afforded the same molecular structure as in solution; the situation has been resolved.⁵²⁵ Apo-MT itself is a random coil polypeptide; the holoprotein achieves its tertiary structure by metal binding.

Except for its occurrence as the β domain cluster in MT, a separate $\text{M}_3(\mu\text{-SR})_3$ ring structure is unknown in zinc and cadmium thiolate chemistry. It has been established in $[\text{Fe}_3(\mu\text{-SR})_3\text{X}_6]^{3-}$ ($\text{X} = \text{Cl}^-$, Br^-), but in these complexes the rings are planar.⁵²⁶ However, this ring in the chair conformation occurs in the adamantane-like complexes $[\text{M}_4(\mu\text{-SR})_6\text{X}_4]^{2-}$ ($\text{X} = \text{halide}, \text{RS}^-$),⁵²⁷ including $[\text{M}_4(\text{SPh})_{10}]^{2-}$ with $\text{M} = \text{Zn}$ ⁵²⁸ and Cd .⁵²⁹ The α domain cluster is formally derivable from $\text{M}_4(\text{SR})_{10}$ by addition of thiolate at one metal site, thereby breaking one M-S(R)-M bridge under the constraint of tetrahedral coordination. The structural chemistry of MT has been greatly aided by perspicacious use of $^{111,113}\text{Cd}$ NMR,⁵³⁰ whose chemical shift sensitivity affords resolution of all seven cadmium atoms in a Cd_7 protein. The original recognition of tri- and tetranuclear aggregates came not from X-ray crystallography but from NMR.^{530a} Further, line broadening effects in NMR suggest that the clusters are fluxional, with $\text{Cys}\cdot\text{S}$ ligands moving between different metals and Cd(II) atoms exchanging sites in the β domain cluster faster than in the α domain cluster and between sites in different clusters.^{520,531} This behavior indicates binding lability, and is consistent with rapid substitution of zinc by external Cd^{2+} . The following qualitative order of replacement in MT holds: $\text{Zn(II)} < \text{Cd(II)} < \text{Cu(I)}, \text{Au(I)}, \text{Pt(II)}, \text{Ag(I)}, \text{Hg(II)}$.⁵³² Reactions are rapid compared to the often slow replacements of the metal in zinc enzymes. Native cluster compositions can be achieved by mixing appropriate quantities of $\text{Cd}_7\text{-MT}$ and $\text{Zn}_7\text{-MT}$ in the intermolecular metal exchange reaction 17.⁵³¹ This reaction favors cadmium binding



in the four-metal cluster and zinc binding in the three-metal cluster, leading to the suggestion that the two-domain structure allows the protein to function simultaneously as toxic metal scavenger (Cd(II) in the β domain) and in zinc metabolism (Zn(II) in the α domain).⁵³¹

Petering *et al.* have effectively summarized the functional aspects of MT related to metal ion homeostasis and sequestration of toxic metals: "Because of this unusual kinetic lability as well as the thermodynamic stability [owing to soft acid-soft base interactions] of the metallothionein species that are formed, metallothionein acts as a sink for the binding of a variety of essential and toxic metal ions which enter cells."⁵³²

H. Nonredox Enzymes

As the name implies, these enzymes catalyze reactions in which there is no net flow of electrons into or out of the active site. The majority of these are *hydrolytic* enzymes—peptidases/proteases, collagenases, phospholipases, phosphatases, ATPases, and lactamases, constituting the major categories.⁷¹ Also in this group are enzymes such as kinases, alcohol dehydrogenases, DNA polymerases, and urease. These enzymes generally employ Mg(II) or Zn(II) in their active sites, but nonnative metal ions can often be substituted with retention of (some) enzymatic activity. At present, urease, with a binuclear *nickel* site,²⁵ is a special case, although in nonredox enzymes binuclear catalytic sites are not exceptional. The large majority of enzymes utilize zinc. The body of mechanistic investigations of these enzymes is profuse, detailed, and occasionally contentious; its scope is beyond the purview of this article. Here we scrutinize the structural chemistry of the active sites of nonredox enzymes, with some note of structure/function relationships.

1. Structural Zinc

Before proceeding to the structures of zinc enzymes, we observe that Zn(II) has a very significant, purely structural role in metalloproteins in addition to serving as a catalytic metal. As noted in section III, the prototypical structural site is $[\text{Zn}(\text{S}\cdot\text{Cys})_4]$, such as that in alcohol dehydrogenase and shown in Chart 6A (p 2254). Among many other examples are those found in zinc fingers,^{533,534} proteins involved in gene regulation. Tetrahedral coordination by Zn(II) results in the folding of protein minidomains which are recognized and bound to DNA. In addition to the foregoing site, $[\text{Zn}(\text{N}\cdot\text{His})_2(\text{S}\cdot\text{Cys})_2]$ is a frequent structural unit in zinc fingers, and even binuclear $[\text{Zn}_2(\mu\text{-Cys}\cdot\text{S})_2(\text{S}\cdot\text{Cys})_4]$ has been encountered. Examples of structural zinc sites are included in Table 17.^{78,535-543} We note, however, a further role for $[\text{Zn}(\text{S}\cdot\text{Cys})_4]$ in at least one protein. The protein Ada from *E. coli* possesses a tightly bound Zn(II) atom that is essential for protein folding; it may be replaced by Cd(II) . From a combination of ^{113}Cd NMR and site mutagenesis experiments, the $[\text{M}(\text{S}\cdot\text{Cys})_4]$ site ($\text{M} = \text{Zn(II)}, \text{Cd(II)}$) was established.⁵⁸³ It was further shown that Ada recognizes and repairs DNA whose phosphate groups have become non-enzymatically methylated. The repair mechanism involves the nucleophilic attack by coordinated cysteinate on the methyl phosphotriester moiety, recovering the phosphate, and creating a methionine residue at the Zn(II) site.⁵⁸³ The reaction of $[\text{Zn}(\text{SPh})_4]^{2-}$ with $(\text{MeO})_3\text{PO}$ to afford quantitative conversion to PhSMe and $(\text{MeO})_2\text{PO}_2^-$ ⁵⁸⁴ lends considerable support to this picture.

2. Catalytic Zinc

Structurally characterized catalytic sites of zinc enzymes are summarized in Table 17.^{24,78,535,544-582} Other collections and discussions of zinc protein structures are available (Lipscomb, W. N.; Sträter, N.; this issue).^{77,585-588} It is emphasized that the actual body of structural data is much larger than

Table 17. Crystallographically Defined Structural and Catalytic Coordination Units of Zinc and Cadmium Enzymes

unit/enzyme	resolution (Å)	references (PDB code) ^a
Structural		
[Zn(S·Cys) ₄] alcohol dehydrogenase (horse liver) ^[6A]	2.4	78, 535 (6ADH)
aspartate transcarbamoylase (<i>Escherichia coli</i>)	3.0	536, 537 (2AT2)
[Zn(N·His) ₂ (S·Cys) ₂] tramtrack (Zn finger— <i>Drosophila melanogaster</i>)	2.8	538 (2DRP)
Zif268-DNA complex (Zn finger—mouse)	2.1	539
Co ^{II} -substituted	2.4	539
GLI-DNA complex (Zn finger—human)	2.6	540
[Zn ₂ (μ-S·Cys) ₂ (S·Cys) ₄] GAL4-DNA complex (Zn finger—yeast)	2.7	541
[Zn(N·His) ₃ Cl], [Zn(N·His) ₂ (OH ₂) ₂], [Zn(N·His) ₃ (OH ₂) ₃] 2-zinc insulin ^b (human; porcine)	1.6, 1.5	542 (1TRZ;3INS)
4-zinc insulin ^b (human)	1.85	543
Mononuclear Catalytic		
[Zn(N·His) ₃ (OH ₂)] adamalysin II (rattlesnake venom)	2.0	544
atrolysin C (rattlesnake venom)	2.3	545
carbonic anhydrase I (human erythrocyte)	2.0	546 (2CAB)
carbonic anhydrase II (human erythrocyte) ^[6C] pH 6.0; 7.8	2.0	547, 548 (4CAC)
mutants: Val143Gly, His, Phe, Tyr	1.67, 1.54	549 (2CBB, 2CBA)
Gln92Ala, Asn, Glu, Leu; Glu117Ala	2.1–2.8	550 (6CA2–9CA2)
carboxypeptidase DD (<i>Streptomyces albus</i>)	2.1–2.8	551 (1CNG-1CNK)
β-lactamase II (<i>Bacillus cereus</i>)	2.8	552 (1PTE)
Cd ^{II} -substituted form, apoprotein	3.5	553
[Zn(N·His) ₃ (O ₂ ·X)] ^c collagenase (human fibroblast, neurophil)	3.5	553
[Zn(N·His) ₃ (O ₂ C ^γ ·Asp)] collagenase (human fibroblast, neurophil)	1.6–2.4	554–559
[Zn(N·His) ₃ (O ₂ C ^γ ·Asp)(HOR)] adenosine deaminase (mouse) purine ribonucleotide (ROH)-bound form	1.6–2.4	554, 555, 558, 559
[Zn(N·His) ₃ (OH ₂)](HO·Tyr) ^d protease (<i>Serratia marcescens</i>)	2.4	560 (2ADA)
protease (<i>Pseudomonas aeruginosa</i>)	1.8	561
astacin (crayfish)	1.6	562
Co ^{II} , Cu ^{II} , Ni ^{II} , Hg ^{II} -substituted forms	1.8	563, 564
apoenzyme	2.2	564, 565
[Zn(N·His) ₂ (O ₂ C ^δ ·Glu)(OH ₂)] carboxypeptidase A (bovine pancreas) ^[6D]	2.4	564
carboxypeptidase B (bovine pancreas)	1.54	566 (5CPA)
phospholipase C ^e (<i>Bacillus cereus</i>)	2.8	567 (1CPB)
phosphate-bound form	1.5	569
thermolysin (<i>Bacillus thermoproteolyticus</i>)	2.1	570
Mn ^{II} , Fe ^{II} , Co ^{II} , Cd ^{II} -substituted forms	1.6	571, 572, 573 (1LNF)
[Zn(N·His) ₂ (O ₂ C ^γ ·Asp)(OH ₂) ₂] P1 nuclease (<i>Penicillium citrinium</i>)	1.7–1.9	574
[Zn(N·His) ₂ (S·Cys)(OH ₂)] T7 lysozyme	2.8	575
[Zn(N·His)(S·Cys) ₂ (OH ₂)] alcohol dehydrogenase (horse liver) ^[6B]	2.2	568
apoprotein	2.4	78, 546 (6ADH)
	2.4	546 (8ADH)
Binuclear Catalytic		
[(His·N) ₂ (Asp ^γ CO ₂)Zn(μ-η ¹ :η ¹ -PO ₄)Zn(N·His)(O ₂ C ^γ ·Asp)(O ₂ C ^δ ·Glu)] alkaline phosphatase ^f (<i>E. coli</i>), phosphate-bound	2.0	576 (1ALK)
Cd ^{II} -substituted, phosphate-bound	2.5	576
Asp101Ser mutant	2.5	577
[(His·N)(Asp ^γ CO ₂)Zn(μ-η ¹ :η ¹ -O ₂ C ^γ ·Asp)(μ-OH ₂)Zn(N·His)(O ₂ C ^δ ·Glu)] aminopeptidase (<i>Aeromonas proteolytica</i>) ^[6E]	1.8	578 (1AMP)
[(His·N) ₂ (Asp ^γ CO ₂)Zn(μ-η ¹ :η ¹ -O ₂ C ^γ ·Asp)(μ-OH ₂)Zn(N·His)(NH·Trp)OC·Trp)] phospholipase C (<i>Bacillus cereus</i>)	1.5	569
P1 nuclease (<i>Penicillium citrinium</i>)	2.8	575
[(Asp ^γ CO ₂)(Asp·CO)Zn(μ-η ² -O ₂ C ^δ ·Glu)(μ-η ¹ :η ¹ -O ₂ C ^γ ·Asp)(μ-OH ₂)Zn(O ₂ C ^γ ·Asp)(εNH ₂ ·Lys)] leucine aminopeptidase (bovine lens)	1.6	579, 580, 581 (1BPN)
[(His·N) ₂ (Asp ^γ CO ₂)Cd(μ-η ¹ :η ¹ -O ₂ CNH·Lys)(μ-OH ₂)Cd(N·His) ₂ (OH ₂) ₂] phosphotriesterase ^g (<i>Pseudomonas diminuta</i>)	2.0	24
apoprotein	2.1	582

^a See footnote in Table 5. ^b Insulin in a hormone; 2-zinc form has the 6-coordinate site only. ^c Coordinated by two oxygen atoms of an inhibitor molecule. ^d Weak ligand at 2.5–2.8 Å; state of protonation not specified. ^e Two aquo ligands. ^f The active site of this enzyme is a [Mg(O₂C^γ·Asp)(O₂C^δ·Glu)(HO·Thr)(OH₂)₃] unit. ^g One bridge is a carbamylated lysine residue.

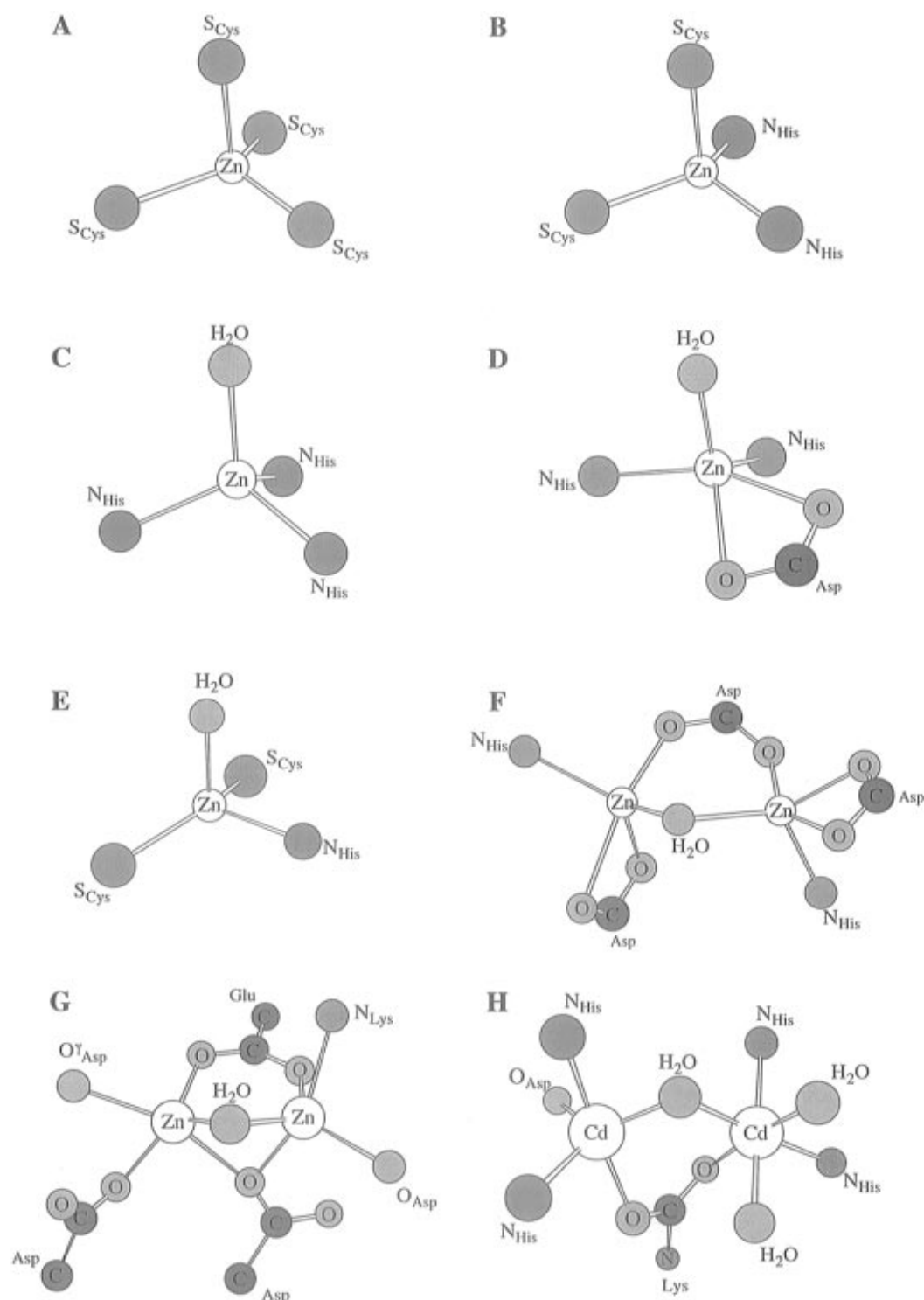


Figure 33. Structures of biological Zn(II) and Cd(II) sites: structural sites in alcohol dehydrogenase (A) and a zinc finger (B); catalytic sites in carbonic anhydrase (C), carboxypeptidase A (D), alcohol dehydrogenase (E), aminopeptidase (F), leucine aminopeptidase (G), and phosphotriesterase (H).

that in Table 17, which does not include numerous structures with substrate and transition-state analogues, inhibitors, and exogenous anions. These may be retrieved from the PDB.⁷ One example is the endopeptidase thermolysin, where a structural basis for the catalytic mechanism has been derived from extensive crystallographic studies of the native enzyme and its inhibitors.⁵⁸⁹ The mechanisms of action of a number of zinc enzymes and related structural considerations have been dealt with at length (Lipscomb, W. N.; Sträter, N.; this issue).^{71,537,588-592}

Catalytic sites are mainly mononuclear, but may also involve two or three Zn(II) atoms (Table 17). Some of these sites are illustrated in Chart 6 (p 2254); a larger set is available in Figure 33. All four-coordinate sites are tetrahedral, and nearly all, in the forms studied, contain one or sometimes two coordinated water ligand(s). The leading reactions catalyzed by these enzymes are summarized in Table 18.

Mononuclear zinc sites are of the general type $[\text{Zn}(\text{N}\cdot\text{His})_{3-n}\text{L}_n(\text{OH}_2)]$ in which L is a protein ligand ($\text{Cys}\cdot\text{S}$, $\text{X}\cdot\text{CO}_2$) and $n = 1, 2$. The most prevalent sites

Table 18. Reaction Types of Nonredox Enzymes^a

Peptidase	
$\text{H}_2\text{N}-\underset{\text{R}_1}{\text{CH}}-\overset{\text{O}}{\parallel}{\text{C}}-\text{NH}-\underset{\text{R}_2}{\text{CH}}-\overset{\text{O}}{\parallel}{\text{C}}-\text{NH}-\underset{\text{R}_3}{\text{CH}}-\overset{\text{O}}{\parallel}{\text{C}}-\text{NH}-\underset{\text{R}_4}{\text{CH}}-\text{COOH}$	
exopeptidase leucine aminopeptidase (R ₁ = CH ₂ CHMe ₂) aminopeptidase (A. proteolytica)	exopeptidase carboxypeptidase A (R ₄ hydrophobic) B (R ₄ basic) DD (R ₃ = R ₄ = Me)
endopeptidase adamalysin II atrolysin C astacin collagenase neutral protease (B. cereus) thermolysin	
Hydration of CO₂	
$\text{CO}_2 + \text{H}_2\text{O} \rightleftharpoons \text{HCO}_3^- + \text{H}^+$ carbonic anhydrase	
Alcohol Dehydrogenase	
$\text{RCH}_2\text{OH} + \text{NAD}^+ \rightleftharpoons \text{RCHO} + \text{NADH} + \text{H}^+$	
Phosphatase	
$\text{ROPO}_3^{2-} + \text{H}_2\text{O} \longrightarrow \text{HPO}_4^{2-} + \text{ROH}$	
Phosphotriesterase	
$(\text{RO})_3\text{PO} + \text{H}_2\text{O} \longrightarrow (\text{RO})_2\text{PO}_2^- + \text{ROH} + \text{H}^+$	
Lactamase	
Urease^b	
$\text{H}_2\text{N}-\overset{\text{O}}{\parallel}{\text{C}}-\text{NH}_2 + \text{H}_2\text{O} \longrightarrow 2\text{NH}_3 + \text{CO}_2$	

^a Examples from the enzymes in Tables 17 and 19. ^b Ni enzyme.

are [Zn(N·His)₃(OH₂)_{1,2}] (Chart 6C, p 2254), which have been established in carbonic anhydrase and a number of endopeptidases. Those enzymes which exhibit a characteristic sequence motif involving the three histidyl ligands are considered to form a "superfamily" of zinc peptidases.^{587,588} This site may also apply to collagenase, whose only available structure contained an inhibitor molecule bound to the metal. Collagenase additionally contains the structural site [Zn(N·His)₃(O₂C⁻·Asp)]. Sites with two His·N ligands take the forms [Zn(N·His)₂(O₂C⁻·X)(OH₂)_{1,2}] and occur in exo- and endopeptidases and at least one nuclease. The carboxylate group is unidentate in the tetrahedral thermolysin site, but bidentate in carboxypeptidase A (Chart 6D, p 2254) leading to a five-coordinate structure. The formulation [Zn(N·His)₂(S·Cys)(OH₂)] is entirely probable for the native site of cytidine deaminase; in known structures the putative water molecule is replaced by an oxygen atom from a transition state analogue molecule.⁵⁹³ The tetrahedral site [Zn(N·His)(S·Cys)₂(OH₂)] (Chart 6B, p 2254) has been encountered thus far only with alcohol dehydrogenase.

Binuclear zinc sites all have at least one His·N ligand at each metal subsite. The remaining coordination positions are taken up by carboxylate and water, which are also the prevalent bridging ligands. The active site of *A. proteolytica* aminopeptidase (Chart 6E, p 2254) is among the simpler binuclear structures; this and others are illustrated in Figure 33. Whereas mononuclear sites are structurally unexceptional, the binuclear sites exhibit several

features rarely observed with biological coordination units: binding by the amino group of lysine and bridging by *one* oxygen atom of a carboxylate group (aspartate) in leucine aminopeptidase (Figure 33G), the occurrence of and bridging by a carbamylated lysine residue (-CH₂NH-CO₂⁻) in a Cd₂ phosphotriesterase (Figure 33H), and interaction with an amido nitrogen atom in phospholipase C and P1 nuclease. Actually, the active-site regions of these two enzymes contain three zinc atoms (Table 17). In P1 nuclease, the separations are Zn(1)-Zn(3) = 3.2 Å, Zn(1)-Zn(2) = 5.8 Å, and Zn(2)-Zn(3) = 4.7 Å. The bridged Zn(1)Zn(3) pair is tabulated as such; the Zn(2) site is not directly bridged to this pair. Current evidence suggests that all three zinc atoms are required for activity,⁵⁷⁵ but the role of each metal center remains to be elucidated. Vallee and Auld⁵⁸⁵ term sites with two or more Zn(II) atoms in close proximity *cocatalytic*. Fenton and Okawa⁵⁹⁴ have called attention to "trinuclear constellations" in metallobiomolecules, which, in addition to these two enzymes, include cuboidal [Fe₃S₄(S·Cys)₃] clusters (Figure 4), the Zn₂-Mg grouping in *E. coli* alkaline phosphatase, the trinuclear cluster in metallothionein (Figure 30C), and the tricopper array in ascorbate oxidase (Chart 4C, p 2253, Figure 27). Binuclear hydrolytic enzymes have been treated by Wilcox (this issue).

Among transition elements in biology, zinc is second only to iron in pervasiveness. In the context of nonredox enzymes, the question "Why zinc?" has been often raised.⁵⁹⁵ Without speculating on the means of natural selection of zinc, but rather considering its intrinsic chemical properties, the salutary features of the element are clearly apparent. (i) The Zn²⁺ ion readily undergoes ligand substitution, the aquo exchange rate of [Zn(OH₂)₆]²⁺ being *ca.* 10⁷ s⁻¹,⁵⁹⁶ at least 1 order of magnitude higher than for hexaquo ions of other divalent first transition series ions except [Cu(OH₂)₆]²⁺ (*k* ≈ 10⁹ s⁻¹),⁵⁹⁷ whose axial sites are labilized by a Jahn-Teller distortion. (ii) Zn(II) is not subject to the effects of LFSE (Table 2), meaning that its coordination number (nearly always 4 or 5 in proteins) and stereochemistry are entirely set by ligand charge and size. Further, there is no LF activation energy for the substitution reactions in *i* nor for intramolecular ligand rearrangement (known to be facile for Zn(II)⁵⁹⁸). (iii) Zn(II) is a borderline hard-soft acid, and thus has a developed affinity for soft ligands like Met·S and Cys·S and harder ligands like X·CO₂, His·N, and H₂O/OH⁻. Its hard ligand affinity extends to the binding of carbonyl oxygen atoms in protein side chains and backbones and in substrates and inhibitors; carbonyl oxygen ligands are not uncommon at zinc sites but are only occasionally encountered in binding sites of other transition metals. (v) Zn(II) is entirely resistant to redox changes at biological potentials, cannot be oxidized by dioxygen, and cannot itself generate radicals. (vi) Its charge:radius ratio (3.3 and 2.9 in tetrahedral and five-coordinate, respectively (Table 2)) is such as to allow it to function as an effective Lewis acid in polarizing carbonyl groups subject to nucleophilic attack. Further, coordinated water can be deprotonated to hydroxide at or near physiological pH, generating an internal nucleophile for attack at

a bound or otherwise adjacent substrate. Consequently, biological Zn(II) is a redox-stable, (often) coordinately unsaturated, substitutionally and stereochemically labile, Lewis-acidic metal center capable of binding and activating substrate and releasing product efficiently. This combination of features potentiates the "hydroxide-carbonyl" mechanism, whereby bound hydroxide nucleophilically attacks a carbonyl group activated by coordination to the same (or a bridged) Zn(II) center.

3. Nonnative Metals

Other divalent ions can be substituted at Zn(II) sites by displacement of the native metal or by reaction with apoprotein.⁵⁹⁹ As noted earlier, substitution is often for the purpose of introducing a spectroscopic probe. Moreover, an associated issue is the effect on enzymatic activity by a nonnative metal ion of variant size and possibly different stereochemical preference in the presence of sufficient ligands (protein, water) to satisfy a coordination number up to 6 (Table 2). We briefly consider the cases of two endopeptidases, astacin and thermolysin (Tables 17 and 18). For both, placement of divalent ions other than Zn(II) in the binding site of the latter causes structural changes of note only in the close vicinity of the catalytic site. In addition to the native Zn(II) form, the structures of the Co(II), Cu(II), Ni(II), and Hg(II) variants of astacin are known,⁵⁶⁵ of which the latter two are inactive ($\leq 5\%$ activity). The site $[\text{Hg}(\text{N}\cdot\text{His})_3(\text{O}\cdot\text{Tyr})]$ lacks a catalytic water molecule. The site $[\text{Ni}(\text{N}\cdot\text{His})_3(\text{O}\cdot\text{Tyr})(\text{OH}_2)_2]$ contains two *cis* water ligands which may be insufficiently labile for efficient substrate substitution ($k \approx 10^4 \text{ s}^{-1}$ for $[\text{Ni}(\text{OH}_2)_6]^{2+}$ ligand exchange⁵⁹⁶) and/or insufficiently acidic for development of a coordinated hydroxide nucleophile. On the other hand, the sites $[\text{M}(\text{N}\cdot\text{His})_3(\text{O}\cdot\text{Tyr})(\text{OH}_2)]$ ($\text{M} = \text{Co(II), Cu(II)}$) have the same trigonal-bipyramidal structure of the Zn(II) enzyme, with a water ligand in the equatorial plane which is hydrogen bonded to a glutamate carboxylate group. These substituted forms of the enzyme have 37% (Cu(II)) and 140% (Co(II)) of the activity of the native enzyme,⁵⁶⁵ presumably because they possess a catalytic water and can achieve a substrate-bound intermediate stereochemistry resembling that of the Zn(II) enzyme. Thermolysin has been substituted with Mn(II), Fe(II), Co(II), and Cd(II) and the structures of the substituted enzymes determined.⁵⁷⁴ The Cd(II) form has no activity, a behavior seemingly consistent with the structural change embodied in the six-coordinate site $[\text{Cd}(\text{N}\cdot\text{His})_2(\text{O}_2\text{C}^\delta\cdot\text{Glu})_2(\text{OH}_2)_2]$ (monodentate carboxylates) compared to the native tetrahedral unit $[\text{Zn}(\text{N}\cdot\text{His})_2(\text{O}_2\text{C}^\delta\cdot\text{Glu})(\text{OH}_2)]$. The Mn(II) (10%) and Fe(II) (60%) sites are four- and five-coordinate, respectively, and their enzymes have the indicated activities.⁶⁰⁰ However, the enzyme containing the five-coordinate site $[\text{Co}(\text{N}\cdot\text{His})_2(\text{O}_2\text{C}^\delta\cdot\text{Glu})(\text{OH}_2)_2]$ (monodentate carboxylate) exhibits 200% activity. Relative activities can be strongly dependent on reaction conditions and the substrate itself, and must be carefully determined to be strictly comparable.

While there is no universal metal activity order for metallopeptidases, overall—with a few exceptions—it

has been found that Co(II) is the most efficient substitution, following from an activity criterion at parity of substrate.⁵⁹⁹ In addition to the results for astacin and thermolysin, Co(II) induces 50% activity in carbonic anhydrase,⁶⁰¹ comparable activity in alcohol dehydrogenase,⁶⁰² and 110–1100% activity in carboxypeptidases A, depending on the enzyme and substrate.⁵⁹⁹ Thus, in some instances, Co(II) substitution leads to a hyperactive enzyme; there is no case reported where this substitution results in $< 50\%$ activity of the native enzyme. The entire body of structure/activity relationships is difficult to interpret in terms of size or stereochemical preference based on LFSE, especially given that fact that Shannon radii (Table 2) are "best-fit" values deduced from a variety of compounds. Nonetheless, several points can perhaps be raised. High-spin Mn(II), as Zn(II), has no intrinsic stereochemical preference. However, with coordination numbers 4, 5, and 6 it does have a decisively larger radius and consequently should not afford as good a stereochemical fit in resting or intermediate state structures as the native site, assuming the latter is somewhere near optimal in this regard. Cd(II) has an even more accentuated size mismatch. Atoms in the sequence Fe(II)–Cu(II) have preferential stereochemistries and favor octahedral coordination with access to sufficient ligands. There is little to differentiate them on this basis except for the decided octahedral preference of Ni(II). While possibly more apparent than real, the radii of Co(II) and Zn(II) in four-, five-, and six-coordination are closely matched. It may be for this reason that nearly congruent ground and intermediate/transition state configurations can be achieved, accompanied by comparable acidities of coordinated water, to generate enzymes of activity commensurate with or larger than that of the native form.

4. Miscellaneous Enzymes

Collected in Table 19^{603–613} are metal site structures for nonredox enzymes which contain zinc and other metals. It is convenient to include jack bean concanavalin A in this tabulation. Concanavalin A is not an enzyme but a glycoprotein (*lectin*) that recognizes saccharides containing glucosyl and mannosyl residues. The jack bean protein features six-coordinate Mn(II) and seven-coordinate Ca(II) sites at a distance of 4.2 Å and bridged by two aspartate carboxylate groups. One carboxylate is chelated to Ca(II) and utilizes one oxygen atom in the bridge, while the other carboxylate forms one terminal ligand bond to each metal. The metals in this protein are structural in nature; their removal abolishes binding ability. The metals Ni(II), Co(II), and Cd(II) substitute isomorphously at the octahedral Mn(II) site; the calcium coordination units remain unchanged. However, in examining cadmium-substituted concanavalin A, a third metal site containing octahedral Cd(II) (Table 19) was discovered.

Urease, with *D. gigas* hydrogenase (Table 14), are the only two nickel-containing enzymes of known structure. Urease hydrolyzes urea (Table 18); it utilizes a binuclear Ni(II) site in which the metal atoms are separated by 3.5 Å and are bridged by the two carboxylate oxygen atoms of a carbamylated lysine residue. One Ni(II) atom is five-coordinate

Table 19. Crystallographically Defined Catalytic and Structural Coordination Units in Isomerases, Purple Acid Phosphatase, a Transferase, Urease, and Concanavalin

protein	resolution (Å)	references (PDB Code) ^a
D-xylose (glucose) isomerase ^b		
<i>Actinoplanes missouriensis</i> [(Asp ^γ ·CO ₂) ₂ (Glu ^δ ·CO ₂)Co ^{II} (μ-η ¹ :η ¹ -O ₂ C ^δ ·Glu)Co ^{II} (N·His)(O ₂ C ^γ ·Asp) ₂ (OH ₂)] apoprotein	2.2 2.4	603 (1XIM-9XIM, 1XIN-5XIN) 603
<i>Streptomyces rubiginosus</i> [(H ₂ O) ₂ (Asp ^γ ·CO ₂) ₂ (Glu ^δ ·CO ₂)Mn ^{II} (μ-η ¹ :η ¹ -O ₂ C ^δ ·Glu)Mn ^{II} (N·His)(O ₂ C ^γ ·Asp) ₃ (OH ₂)]	1.6	604,605 (1XIB)
purple acid phosphatase (kidney bean) [(His·N)(Asp ^γ ·CO ₂)(Tyr ^γ ·O)(HO)Fe ^{III} (μ-O ₂ C ^γ ·Asp)(μ-OH)Zn ^{II} (N·His) ₂ (OC ^γ ·Asn)(OH ₂)] ^c	2.9	606
galactose-1-phosphate uridylyltransferase (<i>E. coli</i>) [Fe ^{II} (N·His) ₂ (O ₂ C ^δ ·Glu)] [Zn ^{II} (N·His) ₂ (S·Cys) ₂]	1.8	607 (1HXP)
urease (<i>Klebsiella aerogenes</i>) [(His·N) ₂ Ni ^{II} (μ-η ¹ :η ¹ -O ₂ CNH·Lys)Ni ^{II} (N·His) ₂ (O ₂ C ^γ ·Asp)(OH ₂)] ^d	2.2	25
concanavalin A (jack bean) [(H ₂ O) ₂ (His·N)(Asp ^γ ·CO ₂)(Glu ^δ ·CO ₂)Mn ^{II} (μ-η ¹ :η ¹ -O ₂ C ^γ ·Asp)(μ-η ¹ -O ₂ C ^γ ·Asp)Ca(OC ^γ ·Asn)(OC·Tyr)(OH ₂) ₂] Co ^{II} -substituted (for Mn ^{II}) Ni ^{II} -substituted (for Mn ^{II}) Cd ^{II} -substituted (for Mn ^{II}) [Cd(OH ₂) ₂ (O ₂ C ^γ ·Asp)(O ₂ C ^δ ·Glu) ₂] ^e	1.75 1.6 2.0 2.0	608–611 (2CTV) 612 (1SCS) 612 (1SCR) 613

^a See footnote in Table 5. ^b Same structure with Mg(II). ^c Hydroxo and aquo ligands modeled, not directly located. ^d Bridging ligand is a carbamylated Lys residue. ^e Mononuclear 6-coordinate site in addition to the CdCa binuclear site.

while the other is described as “pseudotetrahedral with a weakly occupied fourth ligand”.²⁵ The fourth ligand may be a water molecule disordered over two or three positions but primarily a terminal ligand to the five-coordinate Ni(II) atom. Urease is considered in detail elsewhere (Wilcox, D. F.; this issue).

D-Xylose isomerases catalyze the isomerization of the aldose D-xylose to the ketose D-xylulose, and of D-glucose to D-fructose. These enzymes contain bridged binuclear sites and are activated by divalent ions such as Mg²⁺, Mn²⁺, and Co²⁺, and inhibited by Cu²⁺, Zn²⁺, and Ca²⁺. The forms of the enzyme that have been structurally defined contain Mg(II), Co(II), or Mn(II) (Table 19). In the *A. missouriensis* enzyme the structural Co(II) atom is tetrahedrally coordinated by four unidentate carboxylate oxygen atoms and is bridged at ca. 5 Å by a single carboxylate group to a catalytic Co(II) site. Octahedral coordination is completed at that site by uni- and bidentate Asp^γ·CO₂ groups, His·N, and a water molecule. The *S. rubiginosus* enzyme contains two octahedral Mn(II) sites bridged at 4.9 Å by a single carboxylate group. Structures are also available for enzyme-substrate and enzyme-inhibitor complexes,^{603–605,614–616} including enzymes mutated at or near the active site.^{603,616} Collectively, these studies point to a metal-mediated 1,2-hydride shift mechanism^{605,614} whereby hydrogen is transferred from C(2) of D-xylose or D-glucose to C(1) of D-xylulose or D-fructose in a process demonstrated to occur without exchange with solvent.⁶¹⁷ The labilization of hydride is presumably accomplished by formation of an intermediate C(2) alkoxide stabilized by binding to the two Mn(II) atoms followed by concerted development of a C(2) keto group and attack of hydride on the C(1) carbonyl group activated by coordination to Mn(II) and hydrogen bonding to a protonated lysine residue. Further details are available elsewhere,^{605,614} including a depiction of the hydride transfer part of the overall reaction pathway (Lipscomb, W. N.; Sträter, N.; this issue).

Galactose-1-phosphate uridylyltransferase catalyzes nucleotide exchange between uridine 5'-diphos-

phate hexoses and hexose-1-phosphates,⁶¹⁸ and thus participates in the Leloir pathway of galactose metabolism. The enzyme from *E. coli* as examined crystallographically contains a tetrahedral Zn(II) and a five-coordinate Fe(II) site (Table 19). However, Mn(II), Co(II), and Cd(II) when substituted in the enzyme afford activities of 40–50% of the FeZn enzyme. This retention of activity is considered suggestive of a structural, rather than a catalytic, role of the metal sites.⁶¹⁸

Purple acid phosphatases^{212b,619} (PAPs) catalyze the hydrolysis of aryl phosphate esters, phosphoric anhydrides, and phosphoroproteins with serine residues. They are readily distinguished from alkaline phosphatase and other mammalian acid phosphatases by their low pH optima (4–6) for activity, their insensitivity to inhibition by tartrate (a powerful inhibitor of other acid phosphatases), and their intense pink or violet coloration. PAPs have been isolated from a variety of bacterial, plant, and mammalian sources. Two of the most thoroughly investigated PAPs are those from porcine uterus (uteroferrin) and bovine spleen. Molecular weights are in the 25–35 kD range; the amino acid sequences of the porcine and bovine enzymes are highly conserved (>90%). These enzymes contain an antiferromagnetically coupled binuclear iron site with the accessible oxidation states Fe^{III}Fe^{III} and Fe^{III}Fe^{II}. Spectroscopic data suggest a minimal formulation [(H₂O)(His·N)(X·CO₂)-Fe^{II}(μ-OH)(μ-X·CO₂)Fe^{III}(N·His)(O₂C·X)(O·Tyr)] for the catalytic oxidation state; the color arises from a Tyr·O→Fe^{III} LMCT band near 560 nm. Because the structure of the diiron PAP site has not been established crystallographically, considerable interest has greeted the structure determination of kidney bean PAP (α₂, M_r 110 000 kD). This enzyme contains an FeZn binuclear active site (Table 19, Chart 6F, p 2254) in which the metal atoms are separated by 3.1 Å and bridged by one oxygen atom of Asp^γ·CO₂ and a putative hydroxide group. The latter, a terminal hydroxide group assigned to Fe(III), and a water molecule placed on Zn(II) were not directly located at 2.9 Å resolution, but were satisfactorily modeled

in the refinement.⁶⁰⁶ In this formulation, both metals are six-coordinate. The current mechanism^{620,621} of the phosphatase reaction (Table 18) involves unidentate binding of the ester ROPO_3^- to Zn(II) by displacement of the apparent water ligand, attack by the adjacent $\text{Fe}^{\text{III}}\text{-OH}^-$ nucleophile to generate a pentacoordinate phosphorus intermediate, and cleavage of the P–O bond most nearly opposite the attacking nucleophile to release HPO_4^{2-} and ROH. This sequence is consistent with the observed inversion at phosphorus.⁶²⁰ The low pH optima presumably are due to the generation of the $\text{Fe}^{\text{III}}\text{-OH}^-$ group in acidic solution. The mechanism was originally framed for $\text{Fe}^{\text{III}}\text{Fe}^{\text{II}}$ enzymes. However, replacement of Zn(II) with Fe(II) in kidney bean PAP affords an enzyme with 125% of the activity of zinc enzyme,⁶²² suggesting that Zn(II) and Fe(II) are surrogate metals in PAPs. Lastly, when considering phosphatases and other enzymes where a metal-bound nucleophile reacts with a ligand containing an electrophilic center (whether or not on the same metal), it is appropriate to place in context the classic experiments of Sargeson and co-workers.⁶²³ These investigators proved such reactions in well-defined systems containing metal complexes nonlabile with respect to binding of the nucleophilic and electrophilic components.

IV. Prospectus

In this article we have endeavored to present a comprehensive treatment of the five types of metal sites in biology, with exclusion of heme and corrin prosthetic groups. The large majority of protein crystallographic data on these metal sites has been summarized. Structure/function relationships are developed where feasible and not treated comparably in this issue or in the recent literature. It has been our intent to provide an introduction to sites in metalloproteins which is assimilable by students and persons entering the field of bioinorganic chemistry, and at the same time to make available a concise structure database together with interpretive views (our own and others) of the function of selected sites.

It is not inconsequential to observe that evolution has selected elements for tasks that are entirely consistent with chemical experience uncoupled to biology; e.g., iron and copper—with two stable oxidation states—for electron transfer, binding and activation of dioxygen, and oxidation–reduction of substrates; molybdenum—with three stable oxidation states—for oxygen atom transfer; zinc with its flexible stereochemistry for nonredox catalysis; nickel and cobalt for catalysis involving formation and rupture of metal–carbon bonds. Perhaps it could not have been any other way. However, within these and other examples, the evolutionarily dictated organization of metal ions with each other and with endogenous and exogenous ligands has produced a remarkable array of structures, often unpredicted but increasingly anticipated by spectroscopic interpretation and directed at the accomplishment of function. One prominent example is the remarkable family of iron–sulfur redox centers, each member of which has a different intrinsic potential, with each such potential subject to modulation by the protein environment. In this way, one-electron transfers can be

accomplished at a rather fine grid of potentials within the interval of *ca.* +300 to –500 mV. This family of protein sites has been synthesized, a result that has the effect of directing attention and research effort toward those sites not yet achieved in the laboratory—*inter alia*, the P-cluster and cofactor cluster of nitrogenase, the delicate entatic blue copper sites, the tricopper array of multicopper oxidases, the copper–iron dioxygen binding site of heme-copper oxidases, the mononuclear iron sites of non-heme oxygenases, the binuclear iron site of methane monooxygenase, the nickel-iron site of hydrogenase, monooxo $\text{Mo}^{\text{VI}}/\text{W}^{\text{VI}}$ atom transfer groups and the entire pterin cofactor of oxotransferases, and the Brobdignagian—but discrete—iron oxide cluster of ferritin. When seeking further challenges in research, one need only contemplate the specific byproduct-free reactions of enzymes such as hydrogenase, nitrogenase, sulfite reductase, and copper and iron oxygenases and oxidases, and our current inability to assemble the essential catalyst and otherwise to control and manipulate the overall biological reaction. The chemist will eventually be defeated in this pursuit only if the three-dimensional organization of protein structure, with its ability to influence metal site structure, to contribute to the binding and orientation of substrate, and to control proton and electron flux to or from the catalytic site of redox enzymes, is mandatory.

Spectroscopy is directed at the disclosure of ground and excited states and electron distributions of metalloproteins active sites in order to elucidate electronic structure, which is an integral aspect of reactivity. Insights into geometric structure can also be obtained. Crystallography aims for the definitive establishment of geometric structure. These approaches are obviously complementary and essential by reason of the simple axiom: no structure, no [rigorous] reaction mechanism! If explication of function at the atomic level is the ultimate goal with any metalloprotein, the initiation point is, irreducibly, a knowledge of geometric and electronic structure. With ever-improving X-ray sources and means of data collection and analysis, and the advent of time-resolved protein crystallography, the rate of acquisition of protein structures will clearly increase rapidly. Indeed, that trend is already upon us, as demonstrated by the availability of an impressive array of structures, including many of the key metalloproteins active sites in biology. Consequently, metalloproteins will remain most attractive systems for investigation in the foreseeable future as they present manifold challenges in electronic structure, reactivity, kinetics and mechanism, and synthesis. It is hoped that this article may also engage the interest of those with presently only a peripheral awareness of the experimental activity and intellectual excitement in bioinorganic research.

Abbreviations

This list excludes amino acid, organism, and common biochemical nomenclature; see also Tables 4 and 12.

AO	ascorbate oxidase
Az	azurin
CEP	ceruloplasmin

co	cofactor
CT	charge transfer
DA	donor-acceptor
EDTA	ethylenediamine- <i>N,N,N,N</i> -tetraacetate(4-)
ET (et)	electron transfer
Fd	ferredoxin
Hc	hemocyanin
HEDTA	<i>N</i> -(hydroxyethyl)ethylenediamine- <i>N,N,N</i> -triacetate(3-)
HiPIP	high-potential iron protein
Hr	hemerythrin
IPNS	isopenicillin N-synthase
kD	kilodalton
L	ligand (generalized)
LC	laccase
LMCT	ligand-to-metal charge transfer
LUMO	lowest unoccupied molecular orbital
M	metal (generalized)
MMO	methane monooxygenase
MO	molecular orbital
MT	metallothionein
NHE	normal hydrogen electrode
mnt	maleonitriledithiolate(2-)
PAP	purple acid phosphatase
PDB	protein databank (Brookhaven)
Pc	plastocyanin
Rd	rubredoxin
RDPR	ribonucleotide diphosphate reductase
SCE	standard calomel electrode
SOD	superoxide dismutase
X	amino acid residue (generalized)

Acknowledgments

We are indebted to J. Bolin, A. Volbeda and J. C. Fontecilla-Camps, D. Dooley and H. C. Freeman, J. S. Valentine and P. J. Hart, B. Krebs, and S. Yoshikawa, who kindly supplied structural information prior to publication. We thank C. K. Ryder for editorial assistance. Bioinorganic research at Harvard University is supported by NIH Grant GM 28856 and NSF Grant 94-23830, and at Stanford University by NIH Grants GM 40392 and DK 31450 and by NSF Grants MCB 93-16768 and CHE 95-28250.

V. References

- Chan, M. K.; Kim, J.; Rees, D. C. *Science* **1993**, *260*, 792.
- Iwata, S.; Ostermeier, C.; Ludwig, B.; Michel, H. *Nature* **1995**, *376*, 660.
- Tsukihara, T.; Aoyama, H.; Yamashita, E.; Tomikazi, T.; Yamaguchi, H.; Shinzawa-Ittoh, K.; Nakashima, R.; Yaono, R.; Yoshikawa, S. *Science* **1995**, *269*, 1069.
- Crane, B. R.; Siegel, L. M.; Getzoff, E. D. *Science* **1995**, *270*, 59.
- Zaitsev, I.; Zaitseva, V.; Card, V.; Moshkov, K.; Bax, B.; Ralph, A.; Lindley, P. J. *Biol. Inorg. Chem.* **1996**, *1*, 1.
- (a) Armstrong, W. H. In *Metal Clusters in Proteins*, ACS Symposium Series No. 372; American Chemical Society: Washington, DC, 1988; Chapter 1. (b) Creighton, T. E. *Proteins: Structures and Molecular Properties*, 2nd ed.; Freeman: New York, 1993; Appendix 2.
- (a) Bernstein, T.; Koetzle, T. F.; Williams, G. J. B.; Meyer, E. F.; Brice, M. D.; Rodgers, J. R.; Kennard, O.; Shimanouchi, T.; Tasumi, M. The Protein Data Bank: A Computer-based Archival File for Macromolecular Structures. *J. Mol. Biol.* **1977**, *112*, 535. (b) Abola, E. E.; Bernstein, F. C.; Bryant, S. H.; Koetzle, T. F.; Weng, J. Protein Data Bank. In *Crystallographic Databases - Information Content, Software Systems, and Scientific Applications*; Allen, F. H., Bergerhoff, G., Sievers, R., Eds.; Data Commission of the International Union of Crystallography: Bonn, 1987; pp 107-132.
- Cantor, C. R.; Schimmel, P. R. *Biophysical Chemistry. Part 1, The Conformation of Biological Macromolecules*; W. H. Freeman & Co.: New York, 1980; pp 42-51.
- Fee, J. A.; Phillips, W. D. *Biochim. Biophys. Acta* **1975**, *412*, 26.
- (a) Sillén, L. G.; Martell, A. E. *Stability Constants of Metal Ion Complexes*, 2nd ed.; The Chemical Society: London, 1964; Section 2; 1971, Supplement no. 1, Part 2. (b) Smith, R. M.; Martell, A. E. *Critical Stability Constants*, Vol. 6; Plenum Press: New York, 1989; Supplement no. 2, and earlier volumes in this series.
- (a) Slater, J. C. *Phys. Rev.* **1930**, *36*, 57. (b) Clementi, E.; Raimondi, D. L. *J. Chem. Phys.* **1963**, *38*, 2686. (c) Shannon, R. D. *Acta Crystallogr.* **1976**, *A32*, 576.
- Ballhausen, C. J.; Jørgensen, C. K. *Kgl. Danske Videnskab. Selskab. Mat. fys. Medd.* **1955**, *29* (No. 14). Ballhausen, C. J. *Kgl. Danske Videnskab. Selskab. Mat. fys. Medd.* **1954**, *29* (No. 4).
- Basolo, F.; Pearson, R. G. *Mechanisms of Inorganic Reactions*; Wiley: New York, 1967; Chapter 3.
- Lin, J.; Jones, P. M.; Lowery, M. D.; Gay, R. R.; Cohen, S. L.; Solomon, E. I. *Inorg. Chem.* **1992**, *31*, 686.
- Christianson, D. W. *Adv. Protein Chem.* **1991**, *42*, 281.
- Glusker, J. P. *Adv. Protein Chem.* **1991**, *42*, 1.
- Guckert, J. A.; Lowery, M. D.; Solomon, E. I. *J. Am. Chem. Soc.* **1995**, *117*, 2817.
- Margerum, D. W.; Wong, L. F.; Bossu, F. P.; Chellappa, K. L.; Czarnecki, J. J.; Kirksey, S. T., Jr.; Neubecker, T. A. *Adv. Chem. Ser.* **1977**, *162*, 281.
- Lowery, M. D.; Solomon, E. I. *Inorg. Chim. Acta* **1992**, *198-200*, 233.
- Carrell, C. J.; Carrell, H. L.; Erlebacher, J.; Glusker, J. P. *J. Am. Chem. Soc.* **1988**, *110*, 8651.
- Campochiaro, C.; Hanson, M. A.; Solomon, E. I. Unpublished results.
- Penfield, K. W.; Gewirth, A. A.; Solomon, E. I. *J. Am. Chem. Soc.* **1985**, *107*, 4519.
- Chakrabarti, P. *Biochemistry* **1989**, *28*, 6081.
- Benning, M. W.; Kuo, J. M.; Raushel, F. M.; Holden, H. M. *Biochemistry* **1995**, *34*, 7973.
- Jabri, E.; Carr, M. B.; Hausinger, R. P.; Karplus, P. A. *Science* **1995**, *268*, 998.
- Baldwin, M. J.; Root, D. E.; Pate, J. E.; Fujisawa, K.; Kitajima, N.; Solomon, E. I. *J. Am. Chem. Soc.* **1992**, *114*, 10421.
- Baes, C. F., Jr.; Mesmer, R. E. *The Hydrolysis of Cations*; Wiley: New York, 1984; Chapters 10, 12, and 13.
- Sigel, H.; McCormick, D. B. *Acc. Chem. Res.* **1970**, *3*, 201.
- Hille, R. *Biochim. Biophys. Acta* **1994**, *1184*, 143.
- Schultz, B. E.; Hille, R.; Holm, R. H. *J. Am. Chem. Soc.* **1995**, *117*, 827.
- Van Holde, K. E.; van Bruggen, E. F. J. In *Subunits in Biological Systems, Part A*; Timasheff, S. N., Fasman, G. D., Eds.; Marcel Dekker: New York, 1971; pp 1-53.
- Structure and Function of Hemocyanin*; Bannister, J. V., Ed.; Springer-Verlag: Berlin, 1977.
- Messerschmidt, A.; Rossi, A.; Ladenstein, R.; Huber, R.; Bolognesi, M.; Gatti, G.; Marchesini, A.; Petruzzelli, R.; Finazzi-Agro, A. *J. Mol. Biol.* **1989**, *206*, 513.
- Cole, J. L.; Ballou, D. B.; Solomon, E. I. *J. Am. Chem. Soc.* **1991**, *113*, 8544.
- Colman, P. M.; Freeman, H. C.; Guss, J. M.; Murata, M.; Norris, V. A.; Ramshaw, J. A. M.; Venkatappa, M. P. *Nature* **1978**, *272*, 319.
- Sykes, A. G. *Struct. Bonding* (Berlin) **1991**, *75*, 177.
- Yington, J. C.; Gaffney, B. J.; Amzel, L. M. *Science* **1993**, *260*, 1482.
- Holmes, M. A.; Stenkamp, R. E. *J. Mol. Biol.* **1991**, *220*, 723.
- Mure, M.; Klinman, J. P. *J. Am. Chem. Soc.* **1995**, *117*, 8698, 8707.
- Banci, L.; Bertini, I., et al. Results to be published.
- (a) Vallee, B. L.; Williams, R. J. P. *Proc. Natl. Acad. Sci. U.S.A.* **1968**, *59*, 498. (b) Williams, R. J. P. *Eur. J. Biochem.* **1995**, *234*, 363.
- Malmström, B. G. *Eur. J. Biochem.* **1994**, *223*, 711.
- Carlin, R. L. *Magnetochemistry*; Springer-Verlag: Berlin, 1986.
- Day, E. P.; Kent, T. A.; Lindahl, P. A.; Munck, E.; Orme-Johnson, W. H.; Roder, H.; Roy, A. *Biophys. J.* **1987**, *52*, 837.
- Day, E. P. *Methods Enzymol.* **1993**, *227*, 437.
- Gütlich, P.; Link, R.; Trautwein, A. X. *Mössbauer Spectroscopy and Transition Metal Chemistry*; Springer-Verlag: Berlin, 1978.
- Münck, E. *Methods Enzymol.* **1978**, *54*, 346.
- McGarvey, B. R. In *Transition Metal Chemistry*; Carlin, R. E., Ed.; Marcel Dekker: New York, 1967; Vol. 3, pp 89-201.
- (a) Pilbrow, J. R.; Hansen, G. R. *Methods Enzymol.* **1993**, *227*, 330. (b) Brudvig, G. W. *Methods Enzymol.* **1995**, *246*, 536.
- Hendrich, M. P.; Debrunner, P. G. *Biophys. J.* **1989**, *56*, 489.
- Schweiger, A. *Struct. Bonding* (Berlin) **1982**, *51*, 1.
- DeRose, V.; Hoffman, B. M. *Methods Enzymol.* **1995**, *246*, 554.
- Mims, W. B.; Peisach, J. In *Advanced EPR*; Hoff, A. J., Ed.; Elsevier: Amsterdam, 1989; pp 1-55.
- Bertini, I.; Luchinat, C. *NMR of Paramagnetic Molecules in Biological Systems*; Benjamin/Cummings Publishing Co.: New York, 1986.
- Bertini, I.; Turano, P.; Villa, A. J. *Chem. Rev.* **1993**, *93*, 2833.
- Nakamoto, K. *Infrared Spectra of Inorganic and Coordination Compounds*, 4th ed.; Wiley: New York, 1986.
- Solomon, E. I. *Comments Inorg. Chem.* **1984**, *3*, 225.
- Piepho, S. B.; Schatz, P. N. *Group Theory and Spectroscopy*; Wiley-Interscience: New York, 1983.
- Stephens, P. J. *Annu. Rev. Phys. Chem.* **1974**, *25*, 201.

- (60) Thomson, A. J.; Cheesman, M. R.; George, S. J. *Methods Enzymol.* **1993**, *226*, 199.
- (61) Gillard, R. D. In *Physical Methods in Advanced Inorganic Chemistry*; Hill, H. A. O., Day, P., Eds.; Interscience: New York, 1968; pp 167–213.
- (62) Mason, S. F. *Molecular Optical Activity and the Chiral Discriminations*; Cambridge University Press: New York, 1982.
- (63) Clark, R. J. H.; Stewart, B. *Struct. Bonding (Berlin)* **1979**, *36*, 1.
- (64) (a) Loehr, T. M.; Sanders-Loehr, J. *Methods Enzymol.* **1993**, *226*, 431. (b) Spiro, T. G.; Czernuszewicz, R. S. *Methods Enzymol.* **1995**, *246*, 416.
- (65) Cramer, S. P.; Hodgson, K. O. *Prog. Inorg. Chem.* **1979**, *25*, 1.
- (66) Yachandra, V. K. *Methods Enzymol.* **1995**, *246*, 638.
- (67) Kau, L.-S.; Spira-Solomon, D. J.; Penner-Hahn, J. E.; Hodgson, K. O.; Solomon, E. I. *J. Am. Chem. Soc.* **1987**, *109*, 288.
- (68) Shadle, S. E.; Penner-Hahn, J. E.; Schugar, H. J.; Hedman, B.; Hodgson, K. O.; Solomon, E. I. *J. Am. Chem. Soc.* **1993**, *115*, 767.
- (69) Didziulis, S. V.; Cohen, S. L.; Gewirth, A. A.; Solomon, E. I. *J. Am. Chem. Soc.* **1988**, *110*, 250.
- (70) Ballhausen, C. J. *Introduction to Ligand Field Theory*; McGraw-Hill: New York, 1962.
- (71) Bertini, I.; Luchinat, C. In *Bioinorganic Chemistry*; Bertini, I., Gray, H. B., Lippard, S. J., Valentine, J. S., Eds.; University Science Books: Mill Valley, CA, 1994; Chapter 2.
- (72) Ludwig, M. L.; Metzger, A. L.; Patridge, K. A.; Stallings, W. C. *J. Mol. Biol.* **1991**, *219*, 335.
- (73) Penner-Hahn, J. E. In *Manganese Redox Enzymes*; Pecoraro, V. L., Ed.; VCH Publishers: New York, 1992; Chapter 2.
- (74) Sauer, K.; Yachandra, V. K.; Britt, D. B.; Klein, M. P. In *Manganese Redox Enzymes*; Pecoraro, V. L., Ed.; VCH Publishers: New York, 1992; Chapter 8.
- (75) Glusker, J. P.; Lewis, M.; Rossi, M. *Crystal Structure Analysis for Chemists and Biologists*; VCH Publishers: New York, 1994; Chapter 9.
- (76) McPhalen, C. A.; Strynadka, N. C. J.; James, M. N. G. *Adv. Protein Chem.* **1991**, *42*, 77.
- (77) Forsén, S.; Kördel, J. In *Bioinorganic Chemistry*; Bertini, I., Gray, H. B., Lippard, S. J., Valentine, J. S., Eds.; University Science Books: Mill Valley, CA, 1994; Chapter 3.
- (78) Eklund, H.; Nordström, B.; Zeppezauer, E.; Söderlund, G.; Ohlsson, I.; Boiwe, T.; Söderberg, B.-O.; Tapia, O.; Brändén, C.-I.; Åkeson, Å. *J. Mol. Biol.* **1976**, *102*, 27.
- (79) Matsubara, H.; Saeki, K. *Adv. Inorg. Chem.* **1992**, *38*, 223.
- (80) Cammack, R. *Adv. Inorg. Chem.* **1992**, *38*, 281.
- (81) Sykes, A. G. *Met. Ions Biol. Syst.* **1991**, *1*, 291.
- (82) Watenpugh, K. D.; Sieker, L. C.; Jensen, L. H. *J. Mol. Biol.* **1979**, *131*, 509; **1980**, *138*, 615.
- (83) Stenkamp, R. E.; Sieker, L. C.; Jensen, L. H. *Proteins* **1990**, *8*, 352.
- (84) Frey, M.; Sieker, L.; Payan, F.; Haser, R.; Bruschi, M.; Pepe, G.; LeGall, J. *J. Mol. Biol.* **1987**, *197*, 525.
- (85) Dauter, Z.; Sieker, L. C.; Wilson, K. S. *Acta Crystallogr.* **1992**, *B48*, 42.
- (86) Day, M. W.; Hsu, B. T.; Joshua-Tor, L.; Park, J.-B.; Zhou, Z. H.; Adams, M. W. W.; Rees, D. C. *Protein Sci.* **1992**, *1*, 1494.
- (87) Rypniewski, W. R.; Breiter, D. R.; Benning, M. M.; Wesenberg, G.; Oh, B.-H.; Markley, J. L.; Rayment, I.; Holden, H. M. *Biochemistry* **1991**, *30*, 4126.
- (88) Holden, H. M.; Jacobson, B. L.; Hurley, J. K.; Tollin, G.; Oh, B.-H.; Skjeldal, L.; Chae, Y. K.; Cheng, H.; Xia, B.; Markley, J. M. *J. Bioenerg. Biomembr.* **1994**, *26*, 67.
- (89) Jacobson, B. L.; Chae, Y. K.; Markley, J. L.; Rayment, I.; Holden, H. M. *Biochemistry* **1993**, *32*, 6788.
- (90) Tsukihara, T.; Fukuyama, K.; Mizushima, M.; Harioka, T.; Kusunoki, M.; Katsube, Y.; Hase, T.; Matsubara, H. *J. Mol. Biol.* **1990**, *216*, 399.
- (91) Ikemizu, S.; Bando, M.; Sato, T.; Morimoto, Y.; Tsukihara, T.; Fukuyama, K. *Acta Crystallogr.* **1994**, *D50*, 167.
- (92) Sussman, J. L.; Brown, J. H.; Shoham, M. In *Iron-Sulfur Protein Research*; Matsubara, H., Katsube, Y., Wada, K., Eds.; Springer-Verlag: New York, 1987; pp 69–81.
- (93) Sussman, J. L.; Shoham, M.; Harel, M. *Prog. Clin. Biol. Res.* **1989**, *289*, 171.
- (94) Tsukihara, T.; Fukuyama, K.; Tahara, H.; Katsube, Y.; Matsubara, H.; Tanaka, N.; Kakudo, M.; Wada, K.; Matsubara, H. *J. Biochem. (Tokyo)* **1978**, *84*, 1645.
- (95) Fukuyama, K.; Hase, T.; Matsumoto, S.; Tsukihara, T.; Katsube, Y.; Tanaka, N.; Kakudo, M.; Wada, K.; Matsubara, H. *Nature* **1980**, *286*, 522.
- (96) Tsukihara, T.; Fukuyama, K.; Nakamura, M.; Katsube, Y.; Tanaka, N.; Kakudo, M.; Wada, K.; Hase, T.; Matsubara, H. *J. Biochem. (Tokyo)* **1981**, *90*, 1763.
- (97) Fukuyama, K.; Ueki, N.; Nakamura, H.; Tsukihara, T.; Matsubara, H. *J. Biochem. (Tokyo)* **1995**, *117*, 1017.
- (98) (a) Dugad, L. B.; La Mar, G. N.; Banci, L.; Bertini, I. *Biochemistry* **1990**, *29*, 2263. (b) Im, S.-C.; Lam, K.-Y.; Lim, M.-C.; Ooi, B.-L.; Sykes, A. G. *J. Am. Chem. Soc.* **1995**, *117*, 3635.
- (99) Fee, J. A.; Findling, K. L.; Yoshida, T.; Hille, R.; Tarr, G. E.; Hearschen, D. O.; Dunham, W. R.; Day, E. P.; Kent, T. A.; Münck, E. *J. Biol. Chem.* **1984**, *259*, 124.
- (100) (a) Gurbiel, R. J.; Batie, C. J.; Sivaraja, M.; True, A. E.; Fee, J. A.; Hoffman, B. M.; Ballou, D. P. *Biochemistry* **1989**, *28*, 4861. (b) Gurbiel, R. J.; Ohnishi, T.; Robertson, D. E.; Daldal, F.; Hoffman, B. M. *Biochemistry* **1991**, *30*, 11579.
- (101) Britt, R. D.; Sauer, K.; Klein, M. P.; Knaff, D. B.; Kriauciunas, A.; Yu, C.-A.; Yu, L.; Malkin, R. *Biochemistry* **1991**, *30*, 1892.
- (102) Verhagen, M. F. J. M.; Link, T. A.; Hagen, W. R. *FEBS Lett.* **1995**, *361*, 75.
- (103) Kissinger, C. R.; Adman, E. T.; Sieker, L. C.; Jensen, L. H. *J. Am. Chem. Soc.* **1988**, *110*, 8721.
- (104) Kissinger, C. R.; Sieker, L. C.; Adman, E. T.; Jensen, L. H. *J. Mol. Biol.* **1991**, *219*, 693.
- (105) (a) Stout, G. H.; Turley, S.; Sieker, L. C.; Jensen, L. H. *Proc. Natl. Acad. Sci. U.S.A.* **1988**, *85*, 1020. (b) Merritt, E. A.; Stout, G. H.; Turley, S.; Sieker, L. C.; Jensen, L. H. *Acta Crystallogr.* **1993**, *D49*, 272.
- (106) Stout, C. D. *J. Biol. Chem.* **1988**, *263*, 9256.
- (107) Stout, C. D. *J. Mol. Biol.* **1989**, *205*, 545.
- (108) Martin, A. E.; Burgess, B. K.; Stout, C. D.; Cash, V. L.; Dean, D. R.; Jensen, G. M.; Stephens, P. J. *Proc. Natl. Acad. Sci. U.S.A.* **1990**, *87*, 598.
- (109) Soman, J.; Iismaa, S.; Stout, C. D. *J. Biol. Chem.* **1991**, *266*, 21558.
- (110) Shen, B.; Jollie, D. R.; Diller, T. C.; Stout, C. D.; Stephens, P. J.; Burgess, B. K. *Proc. Natl. Acad. Sci. U.S.A.* **1995**, *92*, 10064.
- (111) Stout, C. D. *J. Biol. Chem.* **1993**, *268*, 25920.
- (112) Robbins, A. H.; Stout, C. D. *Proteins* **1989**, *5*, 289.
- (113) (a) Zhou, J.; Holm, R. H. *J. Am. Chem. Soc.* **1995**, *117*, 11353. (b) Zhou, J.; Hu, Z.; Münck, E.; Holm, R. H. *J. Am. Chem. Soc.* **1996**, *118*, 1966.
- (114) (a) Iismaa, S. E.; Vázquez, A. E.; Jensen, G. M.; Stephens, P. J.; Butt, J. N.; Armstrong, F. A.; Burgess, B. K. *J. Biol. Chem.* **1991**, *266*, 21563. (b) Shen, B.; Martin, L. L.; Butt, J. N.; Armstrong, F. A.; Stout, C. D.; Jensen, G. M.; Stephens, P. J.; La Mar, G. N.; Gorst, C. M.; Burgess, B. K. *J. Biol. Chem.* **1993**, *268*, 25928. (c) Armstrong, F. A.; George, S. J.; Thomson, A. J.; Yates, M. G. *FEBS Lett.* **1988**, *234*, 107.
- (115) Tong, J.; Feinberg, B. A. *J. Biol. Chem.* **1994**, *269*, 24920.
- (116) Holm, R. H. *Adv. Inorg. Chem.* **1992**, *38*, 1.
- (117) (a) Srivastava, K. K. P.; Surerus, K. K.; Conover, R. C.; Johnson, M. K.; Park, J.-B.; Adams, M. W. W.; Münck, E. *Inorg. Chem.* **1993**, *32*, 927. (b) Moreno, C.; Macedo, A. L.; Moura, I.; LeGall, J.; Moura, J. J. G. *J. Inorg. Biochem.* **1994**, *53*, 219. (c) Butt, J. N.; Niles, J.; Armstrong, F. A.; Berton, J.; Thomson, A. J. *Nature Struct. Biol.* **1994**, *1*, 427. (d) Finnegan, M. G.; Conover, R. C.; Park, J.-B.; Zhou, Z. H.; Adams, M. W. W.; Johnson, M. K. *Inorg. Chem.* **1995**, *34*, 5358.
- (118) Armstrong, F. A. *Adv. Inorg. Chem.* **1992**, *38*, 117.
- (119) (a) Fukuyama, K.; Matsubara, H.; Tsukihara, T.; Katsube, Y. *J. Mol. Biol.* **1989**, *210*, 383. (b) Fukuyama, K.; Nagahara, Y.; Tsukihara, T.; Katsube, Y.; Hase, T.; Matsubara, H. *J. Mol. Biol.* **1989**, *210*, 183.
- (120) Carter, C. W., Jr.; Kraut, J.; Freer, S. T.; Xuong, N.-H.; Alden, R. A.; Bartsch, R. G. *J. Biol. Chem.* **1974**, *249*, 4212.
- (121) Carter, C. W., Jr.; Kraut, J.; Freer, S. T.; Alden, R. A. *J. Biol. Chem.* **1974**, *249*, 6339.
- (122) Freer, S. T.; Alden, R. A.; Carter, C. W., Jr.; Kraut, J. *J. Biol. Chem.* **1975**, *250*, 46.
- (123) Duée, E. D.; Fanchon, E.; Vicat, J.; Sieker, L. C.; Meyer, J.; Moulis, J.-M. *J. Mol. Biol.* **1994**, *243*, 683.
- (124) Séry, A.; Housset, D.; Serre, L.; Bonicel, G.; Hatchikian, C.; Frey, M.; Roth, M. *Biochemistry* **1994**, *33*, 15408.
- (125) Breiter, D. R.; Meyer, T. E.; Rayment, I.; Holden, H. M. *J. Biol. Chem.* **1991**, *266*, 18660.
- (126) Benning, M. M.; Meyer, T. E.; Rayment, I.; Holden, H. M. *Biochemistry* **1994**, *33*, 2476.
- (127) Adman, E. T.; Sieker, L. C.; Jensen, L. H. *J. Biol. Chem.* **1973**, *248*, 3987; **1976**, *251*, 3801.
- (128) Backes, G.; Mino, Y.; Loehr, T. M.; Meyer, T. E.; Cusanovich, M. A.; Sweeney, W. V.; Adman, E. T.; Sanders-Loehr, J. *J. Am. Chem. Soc.* **1991**, *113*, 2055.
- (129) Rayment, I.; Wesenberg, G.; Meyer, T. E.; Cusanovich, M. A.; Holden, H. M. *J. Mol. Biol.* **1992**, *228*, 672.
- (130) (a) Berg, J. M.; Holm, R. H. In *Iron-Sulfur Proteins*; Spiro, T. G., Ed.; Wiley: New York, 1982; Chapter 1. (b) O'Sullivan, T.; Millar, M. M. *J. Am. Chem. Soc.* **1985**, *107*, 4096.
- (131) Carney, M. J.; Papaefthymiou, G. C.; Frankel, R. B.; Holm, R. H. *Inorg. Chem.* **1989**, *28*, 1497.
- (132) Bertini, I.; Ciurli, S.; Luchinat, C. *Struct. Bonding (Berlin)* **1995**, *83*, 1.
- (133) (a) Banci, L.; Bertini, I.; Ciurli, S.; Ferretti, S.; Luchinat, C.; Piccoli, M. *Biochemistry* **1993**, *32*, 9387. (b) Babini, E.; Bertini, I.; Borsari, M.; Capozzi, F.; Dikly, A.; Eltis, L. D.; Luchinat, C. *J. Am. Chem. Soc.* **1996**, *118*, 75.
- (134) Guss, J. M.; Freeman, H. C. *J. Mol. Biol.* **1983**, *169*, 521.
- (135) Garrett, T. P. J.; Clingeffer, D. J.; Guss, J. M.; Rogers, S. J.; Freeman, H. C. *J. Biol. Chem.* **1984**, *259*, 2822.

- (136) Church, W. B.; Guss, J. M.; Potter, J. J.; Freeman, H. C. *J. Biol. Chem.* **1986**, *261*, 234.
- (137) Guss, J. M.; Harrowell, P. R.; Murata, M.; Norris, V. A.; Freeman, H. C. *J. Mol. Biol.* **1986**, *192*, 361.
- (138) Redinbo, M. R.; Cascio, D.; Choukair, M. K.; Rice, D.; Merchant, S.; Yeats, T. O. *Biochemistry* **1993**, *32*, 10560.
- (139) Collyer, C. A.; Guss, J. M.; Sugimura, Y.; Yoshizaki, F.; Freeman, H. C. *J. Mol. Biol.* **1990**, *211*, 617.
- (140) Inoue, T.; Kai, Y.; Harada, S.; Kasai, N.; Ohshiro, Y.; Suzuki, S.; Kohzuma, T.; Tobari, J. *Acta Crystallogr.* **1994**, *D50*, 517.
- (141) Adman, E. T.; Turley, S.; Bramson, R.; Petratos, K.; Banner, D.; Tsernoglou, D.; Beppu, T.; Watanabe, H. *J. Biol. Chem.* **1989**, *264*, 87.
- (142) Petratos, K.; Dauter, Z.; Wilson, K. S. *Acta Crystallogr.* **1988**, *B44*, 628.
- (143) Vakoufari, E.; Wilson, K. S.; Petratos, K. *FEBS Lett.* **1994**, *347*, 203.
- (144) Guss, J. M.; Merritt, E. A.; Phizackerley, R. P.; Hedman, B.; Murata, M.; Hodgson, K. O.; Freeman, H. C. *Science* **1988**, *241*, 806.
- (145) Kukimoto, M.; Nishiyama, M.; Murphy, M. E. P.; Turley, S.; Adman, E. T.; Horinouchi, S.; Beppu, T. *Biochemistry* **1994**, *33*, 5246.
- (146) Murphy, M. E. P.; Turley, S.; Kukimoto, M.; Nishiyama, N.; Horinouchi, S.; Sasaki, H.; Tanokura, M.; Adman, E. T. *Biochemistry* **1995**, *34*, 12107.
- (147) Kim, E. E.; Wyckoff, H. W. *J. Mol. Biol.* **1991**, *218*, 449.
- (148) Godden, J. W.; Turley, S.; Teller, D. C.; Adman, E. T.; Liu, M. Y.; Payne, W. J.; Le Gall, J. *Science* **1991**, *253*, 438.
- (149) Nar, H.; Messerschmidt, A.; Huber, R.; van de Kamp, M.; Canters, G. W. *J. Mol. Biol.* **1991**, *221*, 765.
- (150) Adman, E. T.; Stenkamp, R. E.; Sieker, L. C.; Jensen, L. H. *J. Mol. Biol.* **1978**, *123*, 35.
- (151) Adman, E. T.; Jensen, L. H. *Isr. J. Chem.* **1981**, *21*, 8.
- (152) Nar, H.; Messerschmidt, A.; Huber, R.; van de Kamp, M.; Canters, G. W. *J. Mol. Biol.* **1991**, *218*, 427.
- (153) Moratal, J. M.; Romero, A.; Salgado, J.; Perales-Alarcón, A.; Jiménez, H. R. *Eur. J. Biochem.* **1995**, *228*, 653.
- (154) Nar, H.; Huber, R.; Messerschmidt, A.; Filippou, A. C.; Barth, M.; Jaquinod, M.; van de Kamp, M.; Canters, G. W. *Eur. J. Biochem.* **1992**, *205*, 1123.
- (155) Norris, G. E.; Anderson, B. F.; Baker, E. N. *J. Am. Chem. Soc.* **1986**, *108*, 2784.
- (156) Baker, E. N. *J. Mol. Biol.* **1988**, *203*, 1071.
- (157) Shepard, W. E. B.; Anderson, B. F.; Lewandoski, D. A.; Norris, G. E.; Baker, E. N. *J. Am. Chem. Soc.* **1990**, *112*, 7817.
- (158) Hart, P. J.; Nersissian, A. M.; Valentine, J. S.; Eisenberg, D. Manuscript in preparation.
- (159) Romero, A.; Hottink, C. W. G.; Nar, H.; Huber, R.; Messerschmidt, A.; Canters, G. W. *J. Mol. Biol.* **1993**, *229*, 1007.
- (160) Shepard, W. E. B.; Kingston, R. L.; Anderson, B. F.; Baker, E. N. *Acta Crystallogr.* **1993**, *D49*, 331.
- (161) Wilmanns, M.; Lappalainen, P.; Kelly, M.; Sauer-Eriksson, E.; Saraste, M. *Proc. Natl. Acad. Sci. U.S.A.* **1995**, *92*, 11955.
- (162) Penfield, K. W.; Gay, R. R.; Himmelwright, R. S.; Eickman, N. C.; Norris, V. A.; Freeman, H. C.; Solomon, E. I. *J. Am. Chem. Soc.* **1981**, *103*, 4382.
- (163) Bergman, C.; Gandvik, E.-K.; Nyman, P. O.; Strid, L. *Biochem. Biophys. Res. Commun.* **1977**, *77*, 1052.
- (164) (a) Messerschmidt, A.; Huber, R. *Eur. J. Biochem.* **1990**, *187*, 341. (b) Messerschmidt, A. *Adv. Inorg. Chem.* **1993**, *40*, 121.
- (165) (a) Kroneck, P. H. M.; Antholine, W. E.; Riester, J.; Zumft, W. G. *FEBS Lett.* **1988**, *242*, 70. (b) Antholine, W. E.; Kastrau, D. H. W.; Steffens, G. C. M.; Buse, G.; Zumft, W. G.; Kroneck, P. H. M. *Eur. J. Biochem.* **1992**, *209*, 875. (c) Lappalainen, P.; Saraste, M. *Biochim. Biophys. Acta* **1994**, *1187*, 222. (d) Malmström, B. G.; Aasa, R. *FEBS Lett.* **1993**, *325*, 49.
- (166) Blackburn, N. J.; Barr, M. E.; Woodruff, W. H.; van der Oost, J.; de Vries, S. *Biochemistry* **1994**, *33*, 10401.
- (167) Robin, M. B.; Day, P. *Adv. Inorg. Chem. Radiochem.* **1967**, *10*, 247.
- (168) Bair, R. A.; Goddard, W. A., III. *J. Am. Chem. Soc.* **1978**, *100*, 5669.
- (169) Langen, R.; Jensen, G. M.; Jacob, U.; Stephens, P. J.; Warshel, A. *J. Biol. Chem.* **1992**, *267*, 25625.
- (170) Hagen, K. S.; Watson, A. D.; Holm, R. H. *J. Am. Chem. Soc.* **1983**, *105*, 3905.
- (171) Xu, F.; Shin, W.; Brown, S. H.; Wahleitner, J.; Sundaram, U. M.; Solomon, E. I. *Biochim. Biophys. Acta* **1996**, in press.
- (172) (a) Bursten, B. E.; Green, M. R. *Prog. Inorg. Chem.* **1988**, *36*, 393. (b) Lever, A. B. P. *Inorg. Chem.* **1990**, *29*, 1271.
- (173) Nikles, D. E.; Powers, M. J.; Urbach, F. L. *Inorg. Chem.* **1983**, *22*, 3210.
- (174) Knapp, S.; Keenan, T. P.; Zhang, X.; Fikar, R.; Potenza, J. A.; Schugar, H. J. *J. Am. Chem. Soc.* **1990**, *112*, 3452.
- (175) Maelia, L. E.; Millar, M.; Koch, S. A. *Inorg. Chem.* **1992**, *31*, 4594.
- (176) Butcher, K. D.; Didziulis, S. V.; Briat, B.; Solomon, E. I. *Inorg. Chem.* **1990**, *29*, 1626.
- (177) Norman, J. G., Jr.; Jackels, S. C. *J. Am. Chem. Soc.* **1975**, *97*, 3833.
- (178) (a) Butcher, K. D.; Didziulis, S. V.; Briat, B.; Solomon, E. I. *J. Am. Chem. Soc.* **1990**, *112*, 2231. (b) Butcher, K. D.; Gebhard, M. S.; Solomon, E. I. *Inorg. Chem.* **1990**, *29*, 2067.
- (179) Marcus, R. A.; Sutin, N. *Biochim. Biophys. Acta* **1985**, *811*, 265. (See Appendix I for evaluation of the term Ao^2 in eq 2).
- (180) Newton, M. D. *J. Phys. Chem.* **1988**, *92*, 3049.
- (181) Sykes, A. G. *Adv. Inorg. Chem.* **1991**, *36*, 377.
- (182) Jacks, C. A.; Bennett, L. E.; Raymond, W. N.; Lovenberg, W. *Proc. Natl. Acad. Sci. U.S.A.* **1974**, *71*, 1118.
- (183) Berg, J. M. Private communication.
- (184) Rao, K. K.; Evans, M. C. W.; Cammack, R.; Hall, D. O.; Thompson, C. L.; Jackson, P. J.; Johnson, C. E. *Biochem. J.* **1972**, *129*, 1063.
- (185) Logan, J.; Newton, M. D.; Noell, J. O. *Int. J. Quantum Chem. (Chem. Symp.)* **1984**, *18*, 213.
- (186) Gephirth, A. A.; Solomon, E. I. *J. Am. Chem. Soc.* **1988**, *110*, 3811.
- (187) Hopfield, J. J. *Proc. Natl. Acad. Sci. U.S.A.* **1974**, *71*, 3640.
- (188) (a) Beratan, D. N.; Onuchic, J. N. *Photosynthesis* **1989**, *22*, 173. (b) Beratan, D. N.; Onuchic, J. N.; Betts, J. N.; Bowler, B. E.; Gray, H. B. *J. Am. Chem. Soc.* **1990**, *112*, 7915.
- (189) Langen, R.; Colón, J. L.; Casimiro, D. R.; Karpishin, T. R.; Winkler, J. R.; Gray, H. B. *J. Biol. Inorg. Chem.* **1996**, *1*, 221.
- (190) Lowery, M. D.; Guckert, J. A.; Gebhard, M. S.; Solomon, E. I. *J. Am. Chem. Soc.* **1993**, *115*, 3012.
- (191) (a) Dunham, W. R.; Bearden, A. J.; Salmeen, I. T.; Palmer, G.; Sands, R. H.; Orme-Johnson, W. H.; Beinert, H. *Biochim. Biophys. Acta* **1971**, *253*, 134. (b) Dunham, W. R.; Palmer, G.; Sands, R. H.; Bearden, A. J. *Biochim. Biophys. Acta* **1971**, *253*, 373.
- (192) Rawlings, J.; Wherland, S.; Gray, H. B. *J. Am. Chem. Soc.* **1977**, *99*, 1968.
- (193) Noodleman, L.; Case, D. A. *Adv. Inorg. Chem.* **1992**, *38*, 423.
- (194) Bertini, I.; Gaudemer, A.; Luchinat, C.; Piccioli, M. *Biochemistry* **1993**, *32*, 12887.
- (195) Ramirez, B. E.; Malmström, B. G.; Winkler, J. R.; Gray, H. B. *Proc. Natl. Acad. Sci. U.S.A.* **1995**, *92*, 11949.
- (196) Kurtz, D. M., Jr. In *Advances in Comparative and Environmental Physiology. Blood and Tissue O₂ Carriers*; Magnum, C. P., Ed.; Springer-Verlag: New York, 1992; Vol. 13, pp 151–171.
- (197) Stenkamp, R. E. *Chem. Rev.* **1994**, *94*, 715.
- (198) Magnus, K. A.; Ton-That, H.; Carpenter, J. E. *Chem. Rev.* **1994**, *94*, 727.
- (199) (a) Magnus, K.; Ton-That, H. *J. Inorg. Biochem.* **1992**, *47*, 20. (b) Magnus, K. A.; Hazes, B.; Ton-That, H.; Bonaventura, C.; Bonaventura, J.; Hol, W. G. *J. Proteins* **1994**, *19*, 302.
- (200) Hazes, B.; Magnus, K. A.; Bonaventura, J.; Dauter, Z.; Kalk, K. H.; Hol, W. G. *J. Protein Sci.* **1993**, *2*, 597.
- (201) Gaykema, W. P. J.; Volbeda, A.; Hol, W. G. *J. Mol. Biol.* **1985**, *187*, 255.
- (202) Gaykema, W. P. J.; Hol, W. G. J.; Vereijken, J. M.; Soeter, N. M.; Bak, H. J.; Beintema, J. *J. Nature* **1984**, *309*, 984.
- (203) Volbeda, A.; Hol, W. G. *J. Mol. Biol.* **1989**, *209*, 249.
- (204) Holmes, M. A.; Le Trong, I.; Turley, S.; Sieker, L. C.; Stenkamp, R. E. *J. Mol. Biol.* **1991**, *218*, 583.
- (205) Stenkamp, R. E.; Sieker, L. C.; Jensen, L. H.; McCallum, J. D.; Sanders-Loehr, J. *Proc. Natl. Acad. Sci. U.S.A.* **1985**, *82*, 713.
- (206) Stenkamp, R. E.; Sieker, L. C.; Jensen, L. H. *J. Am. Chem. Soc.* **1984**, *106*, 618.
- (207) Stenkamp, R. E.; Sieker, L. C.; Jensen, L. H. *Acta Crystallogr.* **1983**, *B39*, 697.
- (208) Sheriff, S.; Hendrickson, W. A.; Smith, J. L. *J. Mol. Biol.* **1987**, *197*, 273.
- (209) Stenkamp, R. E.; Sieker, L. C.; Jensen, L. H. *Acta Crystallogr.* **1982**, *B38*, 784.
- (210) Reem, R. C.; Solomon, E. I. *J. Am. Chem. Soc.* **1984**, *106*, 8323.
- (211) Dawson, J. W.; Gray, H. B.; Hoenig, H. E.; Rossman, G. R.; Schredder, J. M.; Wang, R.-H. *Biochemistry* **1972**, *11*, 461.
- (212) (a) Kurtz, D. M., Jr. *Chem. Rev.* **1990**, *90*, 585. (b) Que, L., Jr.; True, A. E. *Prog. Inorg. Chem.* **1990**, *38*, 97.
- (213) Brown, C. A.; Remar, G. J.; Musselman, R. L.; Solomon, E. I. *Inorg. Chem.* **1995**, *34*, 688.
- (214) Shiemke, A. K.; Loehr, T. M.; Sanders-Loehr, J. *J. Am. Chem. Soc.* **1984**, *106*, 4951; **1986**, *108*, 2437.
- (215) Reem, R. C.; McCormick, J. M.; Richardson, D. E.; Devlin, F. J.; Stephens, P. J.; Musselman, R. L.; Solomon, E. I. *J. Am. Chem. Soc.* **1989**, *111*, 4688.
- (216) (a) Kitajima, N.; Fujisawa, K.; Moro-oka, Y. *J. Am. Chem. Soc.* **1989**, *111*, 8975. (b) Kitajima, N.; Fujisawa, K.; Fujimoto, C.; Moro-oka, Y.; Hashimoto, S.; Kitagawa, T.; Toriumi, K.; Tatsumi, K.; Nakamura, A. *J. Am. Chem. Soc.* **1992**, *114*, 1277.
- (217) Perutz, M. F. *Proc. R. Soc. London, Ser. B* **1980**, *208*, 135.
- (218) Himmelwright, R. S.; Eickman, N. C.; LuBien, C. D.; Lerch, K.; Solomon, E. I. *J. Am. Chem. Soc.* **1980**, *102*, 7339.
- (219) Sullivan, B.; Bonaventura, J.; Bonaventura, C. *Proc. Natl. Acad. Sci. U.S.A.* **1974**, *71*, 2558.
- (220) Jekel, P. A.; Bak, H. J.; Soeter, N. M.; Vereijken, J. M.; Beintema, J. *Eur. J. Biochem.* **1988**, *178*, 403.
- (221) van Breeman, J. F. L.; Schuurds, G. J.; van Bruggen, E. F. In *Structure and Function of Haemocyanin*; Bannister, J. V., Ed.; Springer-Verlag: Berlin, 1977, pp 13–21.

- (222) Richardson, D. E.; Reem, R. C.; Solomon, E. I. *J. Am. Chem. Soc.* **1983**, *105*, 7781.
- (223) Richardson, D. E.; Emad, M.; Reem, R. G.; Solomon, E. I. *Biochemistry* **1987**, *26*, 1003.
- (224) Zhang, J.-H.; Kurtz, D. M., Jr. *Biochemistry* **1991**, *30*, 9121.
- (225) Brouwer, M.; Bonaventura, C.; Bonaventura, J. *Biochemistry* **1978**, *17*, 2148.
- (226) Monod, J.; Wyman, J.; Changeux, J.-P. *J. Mol. Biol.* **1965**, *12*, 88.
- (227) Lamy, J.; Lamy, J. *Invertebrate Oxygen Binding Proteins: Structure, Active Site, and Function*; Marcel Dekker: New York, 1981.
- (228) Hwang, Y. T.; Andrews, L. J.; Solomon, E. I. *J. Am. Chem. Soc.* **1984**, *106*, 3832.
- (229) Zhang, K.; Stern, E. A.; Ellis, F.; Sanders-Loehr, J.; Shiemke, A. K. *Biochemistry* **1988**, *27*, 7470.
- (230) Eickman, N. C.; Himmelfwright, R. S.; Solomon, E. I. *Proc. Natl. Acad. Sci. U.S.A.* **1979**, *76*, 2094.
- (231) Bonaventura, C.; Sullivan, B.; Bonaventura, J.; Bourne, S. *Biochemistry* **1974**, *13*, 4784.
- (232) van der Deen, H.; Hoving, H. *Biophys. Chem.* **1979**, *9*, 169.
- (233) Momenteau, M.; Reed, C. A. *Chem. Rev.* **1994**, *94*, 659.
- (234) (a) Goddard, W. A., III; Olafson, B. D. *Proc. Natl. Acad. Sci. U.S.A.* **1975**, *72*, 2335. (b) Case, D. A.; Huynh, B. H.; Karplus, M. *J. Am. Chem. Soc.* **1979**, *101*, 4433.
- (235) Solomon, E. I. In *Copper Proteins*; Spiro, T. G., Ed.; Wiley: New York, 1981; Chapter 2.
- (236) Karlin, K. D.; Cruse, R. W.; Gultneh, Y.; Farooq, A.; Hayes, J. C.; Zubieta, J. *J. Am. Chem. Soc.* **1987**, *109*, 2668.
- (237) Pate, J. E.; Cruse, R. W.; Karlin, K. D.; Solomon, E. I. *J. Am. Chem. Soc.* **1987**, *109*, 2624.
- (238) Karlin, K. D.; Ghosh, P.; Cruse, R. W.; Farooq, A.; Gultneh, Y.; Jacobson, R. R.; Blackburn, N. J.; Strange, R. W.; Zubieta, J. *J. Am. Chem. Soc.* **1988**, *110*, 6769.
- (239) Tuzcek, F.; Solomon, E. I. *J. Am. Chem. Soc.* **1994**, *116*, 6916.
- (240) Ross, P. K.; Solomon, E. I. *J. Am. Chem. Soc.* **1990**, *112*, 5871; **1991**, *113*, 3246.
- (241) Stenkamp, R. E.; Sieker, L. C.; Jensen, L. H. *Proc. Natl. Acad. Sci. U.S.A.* **1976**, *73*, 349.
- (242) Gay, R. R.; Solomon, E. I. *J. Am. Chem. Soc.* **1978**, *100*, 1972.
- (243) Solomon, E. I.; Tuzcek, F.; Root, D. E.; Brown, C. A. *Chem. Rev.* **1994**, *94*, 827.
- (244) McCord, J. M.; Fridovich, I. *J. Biol. Chem.* **1969**, *244*, 6049.
- (245) Valentine, J. S. In *Bioinorganic Chemistry*; Bertini, I., Gray, H. B., Lippard, S. J., Valentine, J. S., Eds.; University Science Books: Mill Valley, CA, 1994; Chapter 5.
- (246) (a) Vilter, H. *Phytochemistry* **1984**, *23*, 1387. (b) de Boer, E.; van Kooyk, Y.; Tromp, M. G. M.; Plat, H.; Wever, R. *Biochim. Biophys. Acta* **1986**, *869*, 48.
- (247) Butler, A.; Walker, J. V. *Chem. Rev.* **1993**, *93*, 1937.
- (248) Vilter, H. *Met. Ions Biol. Syst.* **1995**, *31*, 326.
- (249) Lah, M. S.; Dixon, M. L.; Patridge, K. A.; Stallings, W. C.; Fee, J. A.; Ludwig, M. L. *Biochemistry* **1995**, *34*, 1646.
- (250) Stallings, W. C.; Powers, T. B.; Patridge, K. A.; Fee, J. A.; Ludwig, M. L. *Proc. Natl. Acad. Sci. U.S.A.* **1983**, *80*, 3884.
- (251) Cooper, J. B.; Driessen, H. P. C.; Wood, S. P.; Zhang, Y.; Young, D. *J. Mol. Biol.* **1994**, *235*, 1156.
- (252) Cooper, J. B.; McIntyre, K.; Badasso, M. O.; Wood, S. P.; Zhang, Y.; Garbe, T. R.; Young, D. *J. Mol. Biol.* **1995**, *246*, 531.
- (253) Stoddard, B. L.; Howell, P. L.; Ringe, D.; Petsko, G. *Biochemistry* **1990**, *29*, 8885.
- (254) Ringe, D.; Petsko, G. A.; Yamamura, F.; Suzuki, K.; Ohmori, D. *Proc. Natl. Acad. Sci. U.S.A.* **1983**, *80*, 3879.
- (255) Stoddard, B. L.; Ringe, D.; Petsko, G. A. *Protein Eng.* **1990**, *4*, 113.
- (256) Stallings, W. C.; Patridge, K. A.; Strong, R. K.; Ludwig, M. L. *J. Biol. Chem.* **1985**, *260*, 16424.
- (257) Parker, M. W.; Blake, C. C. F. *J. Mol. Biol.* **1988**, *199*, 649.
- (258) Borgstahl, G. E.; Parge, H. E.; Hickey, M. J.; Beyer, W. F., Jr.; Hallewell, R. A.; Tainer, J. A. *Cell* **1992**, *71*, 107; **1993**, *72*, 476.
- (259) Kitagawa, Y.; Tanaka, N.; Hata, Y.; Kusunoki, M.; Lee, G.-P.; Katsube, Y.; Asada, K.; Aibara, S.; Morita, Y. *J. Biochem. (Tokyo)* **1991**, *109*, 477.
- (260) Djinovic, K.; Gatti, G.; Coda, A.; Antolini, L.; Pelosi, G.; Desideri, A.; Falconi, M.; Marmocchi, F.; Rotilio, G.; Bolognesi, M. *Acta Crystallogr.* **1991**, *B47*, 918.
- (261) Djinovic, K.; Gatti, G.; Coda, A.; Antolini, L.; Pelosi, G.; Desideri, A.; Falconi, M.; Marmocchi, F.; Rotilio, G.; Bolognesi, M. *J. Mol. Biol.* **1992**, *225*, 791.
- (262) Djinovic, K.; Carugo, K.; Coda, A.; Battistoni, A.; Carri, M. T.; Polticelli, F.; Desideri, A.; Rotilio, G.; Wilson, K. S.; Bolognesi, M.; results to be published.
- (263) Deng, H.-X.; Hentati, A.; Tainer, J. A.; Iqbal, Z.; Cayabyab, A.; Hung, W.-Y.; Getzoff, E. D.; Herzfeldt, B.; Roos, R. P.; Warner, C.; Deng, G.; Soriano, E.; Smyth, C.; Parge, H. E.; Ahmed, A.; Roses, A. D.; Hallewell, R. A.; Pericak-Vance, M. A.; Siddique, T. *Science* **1993**, *261*, 1047.
- (264) Parge, H. E.; Hallewell, R. A.; Tainer, J. A. *Proc. Natl. Acad. Sci. U.S.A.* **1992**, *89*, 6109.
- (265) Tainer, J. A.; Getzoff, E. D.; Beem, K. M.; Richardson, J. S.; Richardson, D. C. *J. Mol. Biol.* **1982**, *160*, 181.
- (266) Tainer, J. A.; Getzoff, E. D.; Richardson, J. S.; Richardson, D. C. *Nature* **1983**, *306*, 284.
- (267) Banci, L.; Bertini, I.; Bruni, B.; Carloni, P.; Luchinat, C.; Mangani, S.; Orioli, P. L.; Piccoli, M.; Rypniewski, W. R.; Wilson, K. S. *Biochem. Biophys. Res. Commun.* **1994**, *202*, 1088.
- (268) Rypniewski, W. R.; Mangani, S.; Bruni, B.; Orioli, P. L.; Casati, M.; Wilson, K. S. *J. Mol. Biol.* **1995**, *251*, 282.
- (269) Roberts, V. A.; Fisher, C. L.; Redford, S. M.; McRee, D. E.; Parge, H. E.; Getzoff, E. D.; Tainer, J. A. *Free Radical Res. Commun.* **1990**, *12*, 269.
- (270) Smith, C. D.; Carson, M.; van der Woerd, M.; Chen, J.; Ischiropoulos, H.; Beckman, J. S. *Arch. Biochem. Biophys.* **1992**, *299*, 350.
- (271) McRee, D. E.; Redford, S. M.; Getzoff, E. D.; Lepock, J. R.; Hallewell, R. A.; Tainer, J. A. *J. Biol. Chem.* **1990**, *265*, 14234.
- (272) Djinovic, K.; Coda, A.; Antolini, L.; Pelosi, G.; Desideri, A.; Falconi, M.; Rotilio, G.; Bolognesi, M. *J. Mol. Biol.* **1992**, *226*, 227.
- (273) Messerschmidt, A.; Wever, R. *Proc. Natl. Acad. Sci. U.S.A.* **1996**, *93*, 392.
- (274) Banci, L.; Bencini, A.; Bertini, I.; Luchinat, C.; Piccoli, M. *Inorg. Chem.* **1990**, *29*, 4867.
- (275) Roe, J. A.; Butler, A.; Scoller, D. M.; Valentine, J. S.; Marky, L.; Breslauer, K. *Biochemistry* **1988**, *27*, 950.
- (276) (a) Blumberg, W. E.; Peisach, J.; Eisenberg, P.; Fee, J. A. *Biochemistry* **1978**, *17*, 1842. (b) Blackburn, N. J.; Hasnain, S. S.; Binsted, N.; Diakun, G. P.; Garner, C. D.; Knowles, P. F. *Biochem. J.* **1984**, *219*, 985.
- (277) Stallings, W. C.; Bull, C.; Fee, J. A.; Lah, M. S.; Ludwig, M. L. In *Molecular Biology of Free Radical Scavenging Systems*; Scandalious, J. G., Ed.; Cold Spring Harbor Laboratory Press: Plainview, NY, 1992; pp 193–211.
- (278) Penner-Hahn, J. E.; In *Manganese Redox Enzymes*; Pecoraro, V. L., Ed.; VCH Publishers: New York, 1992; Chapter 2.
- (279) (a) Vainshtein, B. K.; Melik-Adamyam, W. R.; Barynin, V. V.; Vagin, A. A.; Grebenko, A. I. *Proc. Int. Symp. Biomol. Struct. Interact., Suppl. J. Biosci.* **1985**, *8*, 471. (b) Barynin, V. V.; Vagin, A. A.; Melik-Adamyam, W. R.; Grebenko, A. I.; Khangulov, S. V.; Popov, A. N.; Andrianova, M. E.; Vainshtein, B. K. *Dokl. Akad. Nauk SSSR* **1986**, *228*, 877.
- (280) Wieghardt, K. *Angew. Chem., Int. Ed. Engl.* **1989**, *28*, 1153.
- (281) Sawyer, D. T.; Valentine, J. S. *Acc. Chem. Res.* **1981**, *14*, 393.
- (282) (a) Rabani, J.; Nielson, S. O. *J. Phys. Chem.* **1969**, *73*, 3736. (b) Koppelen, W. H. In *Oxygen and Oxy-Radicals in Chemistry and Biology*; Rodgers, M. A.; Powers, E. L., Eds.; Academic Press: New York, 1981; pp 671–674.
- (283) (a) Joester, K. E.; Jung, G.; Weber, U.; Weser, U. *FEBS Lett.* **1972**, *25*, 25. (b) Paschen, W.; Weser, U. *Biochim. Biophys. Acta* **1973**, *327*, 217. (c) Klug-Roth, D.; Rabani, J. *J. Phys. Chem.* **1976**, *80*, 588. (d) Weinstein, J.; Bielski, B. H. J. *J. Am. Chem. Soc.* **1980**, *102*, 4916. (e) O'Young, C.-L.; Lippard, S. J. *J. Am. Chem. Soc.* **1980**, *102*, 4920.
- (284) Fielden, E. M.; Roberts, P. B.; Bray, R. C.; Lowe, D. J.; Mautner, G. N.; Rotilio, G.; Calabrese, L. *Biochem. J.* **1974**, *139*, 49.
- (285) Fee, J. A.; McClune, G. J.; O'Neill, P.; Fielden, E. M. *Biochem. Biophys. Res. Commun.* **1981**, *100*, 377.
- (286) McAdam, M. E.; Fox, R. A.; Lavelle, F.; Fielden, E. M. *Biochem. J.* **1977**, *165*, 71.
- (287) (a) Sharp, K.; Fine, R.; Honig, B. *Science* **1987**, *236*, 1460. (b) Getzoff, E. D.; Tainer, J. A.; Weiner, P. K.; Kollman, P. A.; Richardson, J. S.; Richardson, D. C. *Nature* **1983**, *306*, 287.
- (288) Banci, L.; Carloni, P.; La Penna, G.; Orioli, P. L. *J. Am. Chem. Soc.* **1992**, *114*, 6994.
- (289) Carloni, P.; Blöchl, P. E.; Parrinello, J. *Phys. Chem.* **1995**, *99*, 1338.
- (290) Fee, J. A.; Bull, C. *J. Biol. Chem.* **1986**, *261*, 13000.
- (291) Pantoliano, M. W.; Valentine, J. S.; Burger, A.; Lippard, S. J. *J. Inorg. Biochem.* **1982**, *17*, 325.
- (292) Whittaker, J. W.; Solomon, E. I. *J. Am. Chem. Soc.* **1988**, *110*, 5329.
- (293) Sawyer, D. T. *Oxygen Chemistry*; Oxford University Press: New York, 1991; p 21.
- (294) (a) Fee, J. A.; DiCorleto, P. E. *Biochemistry* **1973**, *12*, 4893. (b) St. Clair, C. S.; Gray, H. B.; Valentine, J. S. *Inorg. Chem.* **1992**, *31*, 925.
- (295) Barrette, W. C., Jr.; Sawyer, D. T.; Fee, J. A.; Asada, K. *Biochemistry* **1983**, *22*, 624.
- (296) Lawrence, G. D.; Sawyer, D. T. *Biochemistry* **1979**, *18*, 3045.
- (297) *Standard Potentials in Aqueous Potentials*; Bard, A. J.; Parsons, R., Jordan, J., Eds.; Marcel Dekker: New York, 1985.
- (298) Bull, C.; McClune, G. J.; Fee, J. A. *J. Am. Chem. Soc.* **1983**, *105*, 5290.
- (299) Stein, J.; Fackler, J. P., Jr.; McClune, G. J.; Fee, J. A. *Inorg. Chem.* **1979**, *18*, 3511.
- (300) Miller, A.-F. Personal communication.
- (301) Ose, D. E.; Fridovich, I. *Arch. Biochem. Biophys.* **1979**, *194*, 360.
- (302) Poulos, T. L. In *Cytochrome P-450: Structure, Mechanism, and Biochemistry (B)*; Ortiz de Monellano, P. R., Ed.; Plenum: New York, 1986; pp 505–523.
- (303) Khangulov, S. V.; Pessiki, P. J.; Barynin, V. V.; Ash, D. E.; Dismukes, G. C. *Biochemistry* **1995**, *34*, 2015.

- (304) Waldo, G. S.; Yu, S.; Penner-Hahn, J. E. *J. Am. Chem. Soc.* **1992**, *114*, 5869.
- (305) Gamelin, D. R.; Kirk, M. L.; Stemmler, T. L.; Pal, S.; Armstrong, W. H.; Penner-Hahn, J. E.; Solomon, E. I. *J. Am. Chem. Soc.* **1994**, *116*, 2392.
- (306) de Boer, E.; Boon, K.; Wever, R. *Biochemistry* **1988**, *27*, 1629.
- (307) (a) van Schijndel, J. W. P. M.; Barnett, P.; Roelse, J.; Vollenbroek, E. G. M.; Wever, R. *Eur. J. Biochem.* **1994**, *225*, 151. (b) Soedjak, H. S.; Walker, J. V.; Butler, A. *Biochemistry* **1995**, *34*, 12689.
- (308) Everett, R. R.; Butler, A. *Inorg. Chem.* **1989**, *28*, 393.
- (309) Ohlendorf, D. H.; Lipscomb, J. D.; Weber, P. C. *Nature* **1988**, *336*, 403.
- (310) Howard, J. D.; Rees, D. C. *Adv. Protein Chem.* **1991**, *42*, 199.
- (311) Ohlendorf, D. H.; Orville, A. M.; Lipscomb, J. D. *J. Mol. Biol.* **1994**, *244*, 586.
- (312) Han, S.; Eltis, L. D.; Timmis, K. N.; Muchmore, S. W.; Bolin, J. T. *Science*, to be published.
- (313) Senda, T.; Sugiyama, K.; Narita, H.; Yamamoto, T.; Kimbara, K.; Fukuda, M.; Sato, M.; Yano, K.; Mitsui, Y. *J. Mol. Biol.* **1996**, *255*, 735.
- (314) Minor, W.; Steczko, J.; Bolin, J. T.; Otwinowski, Z.; Axelrod, B. *Biochemistry* **1993**, *32*, 6320.
- (315) Roach, P. L.; Clifton, I. J.; Fülöp, V.; Harlos, K.; Barton, G.; Hajdu, J.; Andersson, I.; Schofield, C. J.; Baldwin, J. E. *Nature* **1995**, *375*, 700.
- (316) Rosenzweig, A. C.; Frederick, C. A.; Lippard, S. J.; Nordlund, P. *Nature* **1993**, *366*, 537.
- (317) Rosenzweig, A. C.; Lippard, S. J. *Acc. Chem. Res.* **1994**, *27*, 229.
- (318) Rosenzweig, A. C.; Nordlund, P.; Takahara, P. M.; Frederick, C. A.; Lippard, S. J. *Chem. Biol.* **1995**, *2*, 409.
- (319) Nordlund, P.; Eklund, H. *J. Mol. Biol.* **1993**, *232*, 123.
- (320) Atta, M.; Nordlund, P.; Åberg, A.; Eklund, H.; Fontcave, M. J. *Biol. Chem.* **1992**, *267*, 20682.
- (321) Åberg, A.; Nordlund, P.; Eklund, H. *Nature* **1993**, *361*, 276.
- (322) Parsons, M. R.; Convery, M. A.; Wilmot, C. M.; Yadav, K. D. S.; Blakeley, V.; Corner, A. S.; Phillips, S. E. V.; McPherson, M. J.; Knowles, P. F. *Structure* **1995**, *3*, 1171.
- (323) Cumar, V.; Guss, J. M.; McGuirl, M. A.; Dooley, D. M.; Freeman, H. C. *Structure*, to be published.
- (324) Ito, N.; Phillips, S. E. V.; Yadav, K. D. S.; Knowles, P. F. *J. Mol. Biol.* **1994**, *238*, 794.
- (325) Ito, N.; Phillips, S. E. V.; Stevens, C.; Ogel, Z. B.; McPherson, M. J.; Keen, J. N.; Yadav, K. D. S.; Knowles, P. F. *Nature* **1991**, *350*, 87.
- (326) Messerschmidt, A.; Ladenstein, R.; Huber, R.; Bolognesi, M.; Avigliano, L.; Petruzzelli, R.; Rossi, A.; Finazzi-Agró, A. *J. Mol. Biol.* **1992**, *224*, 179.
- (327) Messerschmidt, A.; Luecke, H.; Huber, B. *J. Mol. Biol.* **1993**, *230*, 997.
- (328) Messerschmidt, A.; Steigemann, W.; Huber, R.; Lang, G.; Kroeck, P. M. H. *Eur. J. Biochem.* **1992**, *209*, 597.
- (329) Lipscomb, J. D.; Orville, A. M. *Met. Ions Biol. Syst.* **1992**, *28*, 243.
- (330) Que, L., Jr. In *Iron Carriers and Iron Proteins*; Loehr, T. M., Ed.; VCH Publishers: New York, 1989; Chapter 6.
- (331) Shu, L.; Chiou, Y.-M.; Orville, A. M.; Miller, M. A.; Lipscomb, J. D.; Que, L., Jr. *Biochemistry* **1995**, *34*, 6649.
- (332) Pavlosky, M. A.; Zhang, Y.; Westre, T. E.; Gan, Q.-F.; Hedman, B.; Hodgson, K. O.; Solomon, E. I. *J. Am. Chem. Soc.* **1995**, *117*, 4316.
- (333) Schilstra, M. J.; Veldink, G. A.; Vliegthart, J. F. G. *Biochemistry* **1994**, *33*, 3974.
- (334) Zhang, Y.; Gebhard, M. S.; Solomon, E. I. *J. Am. Chem. Soc.* **1991**, *113*, 5162.
- (335) Scarrow, R. C.; Trimitsis, M. G.; Buck, C. P.; Grove, G. N.; Cowling, R. A.; Nelson, M. J. *Biochemistry* **1994**, *33*, 15023.
- (336) Penner-Hahn, J. E. *Basic Life Sci.* **1989**, *51*, 177.
- (337) Gassner, G. T.; Ballou, D. P.; Landrum, G. A.; Whittaker, J. W. *Biochemistry* **1993**, *32*, 4820.
- (338) Pavel, E. G.; Martins, L. J.; Ellis, W. R., Jr.; Solomon, E. I. *Chem. Biol.* **1994**, *1*, 173.
- (339) Ruettinger, R. T.; Griffith, G. R.; Coon, M. J. *Arch. Biochem. Biophys.* **1977**, *183*, 528.
- (340) Dix, T. A.; Bollag, G. E.; Domanico, P. L.; Benkovic, S. J. *Biochemistry* **1985**, *24*, 2955.
- (341) Baldwin, J. E.; Lloyd, M. D.; Wha-Son, B.; Schofield, C. J.; Elson, S. W.; Baggaley, K. H.; Nicholson, N. H. *J. Chem. Soc., Chem. Commun.* **1993**, 500.
- (342) (a) Salowe, S. P.; Marsh, E. N.; Townsend, C. A. *Biochemistry* **1990**, *29*, 6499. (b) Salowe, S. P.; Krol, W. J.; Iwata-Reuyl, D.; Townsend, C. A. *Biochemistry* **1991**, *30*, 2281.
- (343) Baldwin, J. E.; Bradley, M. *Chem. Rev.* **1990**, *90*, 1079.
- (344) Orville, A. M.; Chen, V. J.; Kriauciunas, A.; Harpel, M. R.; Fox, B. G.; Münck, E.; Lipscomb, J. D. *Biochemistry* **1992**, *31*, 4602.
- (345) Stubbe, J.; Kozarich, J. W. *Chem. Rev.* **1987**, *87*, 1107.
- (346) Loeb, K. E.; Zaleski, M. J.; Westre, T. E.; Guajardo, R. J.; Mascharak, P. K.; Hedman, B.; Hodgson, K. O.; Solomon, E. I. *J. Am. Chem. Soc.* **1995**, *117*, 4545.
- (347) (a) Burger, R. M.; Peisach, J.; Horwitz, S. B. *J. Biol. Chem.* **1981**, *256*, 11636. (b) Burger, R. M.; Horwitz, S. B.; Peisach, J.; Wittenberg, J. B. *J. Biol. Chem.* **1979**, *254*, 12299.
- (348) Atkin, C. L.; Thelander, L.; Reichard, P.; Lang, G. *J. Biol. Chem.* **1973**, *248*, 7464.
- (349) Fox, B. G.; Froland, W. A.; Dege, J.; Lipscomb, J. D. *J. Biol. Chem.* **1989**, *264*, 10023.
- (350) (a) DeRose, V. J.; Liu, K. E.; Kurtz, D. M.; Hoffman, B. M.; Lippard, S. J. *J. Am. Chem. Soc.* **1993**, *115*, 6640. (b) Thomann, H.; Bernardo, M.; McCormick, J. M.; Pulver, S.; Andersson, K. K.; Lipscomb, J. D.; Solomon, E. I. *J. Am. Chem. Soc.* **1993**, *115*, 8881.
- (351) (a) Scarrow, R. C.; Maroney, M. J.; Palmer, S. M.; Que, L., Jr.; Roe, A. L.; Salowe, S. P.; Stubbe, J. *J. Am. Chem. Soc.* **1987**, *109*, 7857. (b) Bunker, G.; Peterson, L.; Sjöberg, B.-M.; Sahlín, M.; Chance, M.; Chance, B.; Ehrenberg, A. *Biochemistry* **1987**, *26*, 4708. (c) Sjöberg, B.-M.; Loehr, T. M.; Sanders-Loehr, J. *Biochemistry* **1987**, *21*, 96.
- (352) Pulver, S. C.; Thong, W. H.; Bollinger, J. M.; Stubbe, J.; Solomon, E. I. *J. Am. Chem. Soc.* **1995**, *117*, 12664.
- (353) Rardin, R. L.; Tolman, W. B.; Lippard, S. J. *New J. Chem.* **1991**, *15*, 417.
- (354) Ling, J.; Sahlín, M.; Sjöberg, B.-M.; Loehr, T. M.; Sanders-Loehr, J. *J. Biol. Chem.* **1994**, *269*, 5595.
- (355) Pulver, S.; Froland, W. A.; Fox, B. G.; Lipscomb, J. D.; Solomon, E. I. *J. Am. Chem. Soc.* **1993**, *115*, 12409.
- (356) Libby, E.; Averill, B. A. *Biochem. Biophys. Res. Commun.* **1992**, *187*, 1529.
- (357) Janes, S. M.; Klinman, J. P. *Methods Enzymol.* **1995**, *258*, 20.
- (358) Knowles, P. F.; Dooley, D. M. *Met. Ions Biol. Syst.* **1994**, *30*, 362.
- (359) Whittaker, J. W. *Met. Ions Biol. Syst.* **1994**, *30*, 316.
- (360) Clark, K.; Penner-Hahn, J. E.; Whittaker, M.; Whittaker, J. W. *Biochemistry* **1994**, *33*, 12553.
- (361) Brenner, M. C.; Klinman, J. P. *Biochemistry* **1989**, *28*, 4664.
- (362) (a) Klinman, J. P.; Krueger, M.; Brenner, M.; Edmondson, D. E. *J. Biol. Chem.* **1984**, *259*, 3399. (b) Brenner, M. C.; Murray, C. J.; Klinman, J. P. *Biochemistry* **1989**, *28*, 4656.
- (363) (a) Reedy, B. J.; Blackburn, J. M. *J. Am. Chem. Soc.* **1994**, *116*, 1924. (b) Merkler, D. J.; Kulathila, R.; Ash, D. E. *Arch. Biochem. Biophys.* **1995**, *317*, 93.
- (364) Wilcox, D. E.; Porras, A. G.; Hwang, Y. T.; Lerch, K.; Winkler, M. E.; Solomon, E. I. *J. Am. Chem. Soc.* **1985**, *107*, 4015.
- (365) (a) Allendorf, M. D.; Spira, D. J.; Solomon, E. I. *Proc. Natl. Acad. Sci. U.S.A.* **1985**, *82*, 3063. (b) Spira-Solomon, D. J.; Allendorf, M. D.; Solomon, E. I. *J. Am. Chem. Soc.* **1986**, *109*, 5318.
- (366) Nguyen, H.-H. T.; Shiemke, A. K.; Jacobs, S. J.; Hales, B. J.; Lidstrom, M. E.; Chan, S. I. *J. Biol. Chem.* **1994**, *269*, 14995.
- (367) Villafranca, J. J.; Freeman, J. C.; Kotchevar, A. In *Bioinorganic Chemistry of Copper*; Karlin, K. D.; Tyeklar, Z., Eds.; Chapman & Hall: New York, 1993; pp 439-446.
- (368) Cole, J. L.; Tan, G. O.; Yang, E. K.; Hodgson, K. O.; Solomon, E. I. *J. Am. Chem. Soc.* **1990**, *112*, 2243.
- (369) (a) Rydén, L. *Proc. Natl. Acad. Sci. U.S.A.* **1982**, *79*, 6767. (b) Ortel, T. L.; Takahashi, N.; Putnam, F. W. *Proc. Natl. Acad. Sci. U.S.A.* **1984**, *81*, 4761.
- (370) Babcock, G. T.; Wikström, M. *Nature* **1992**, *356*, 301.
- (371) (a) Calhoun, M. W.; Thomas, J. W.; Gennis, R. B. *Trends Biochem. Sci.* **1994**, *19*, 325. (b) Garcia-Horsman, J. A.; Barquera, B.; Rumbley, J.; Ma, J.; Gennis, R. B. *J. Bacteriol.* **1994**, *176*, 5587.
- (372) Lappalainen, P.; Saraste, M. *Biochim. Biophys. Acta* **1994**, *1187*, 222.
- (373) Day, E. P.; Peterson, J.; Sendova, M. S.; Schoonover, J. S.; Palmer, G. *Biochemistry* **1993**, *32*, 7855.
- (374) (a) DeGroot, J. J. M. C.; Veldink, G. A.; Vliegthart, J. F. G.; Boldingh, J.; Wever, R.; Van Gelder, B. F. *Biochim. Biophys. Acta* **1975**, *377*, 71. (b) Nelson, M. J.; Cowling, R. A.; Seitz, S. P. *Biochemistry* **1994**, *33*, 4966.
- (375) Corey, E. J.; Nagata, R. *J. Am. Chem. Soc.* **1987**, *109*, 8107.
- (376) Jang, H. G.; Cox, D. D.; Que, L., Jr. *J. Am. Chem. Soc.* **1991**, *113*, 9200.
- (377) Shin, W.; Sundaram, U. M.; Cole, J. L.; Zhang, H. H.; Hedman, B.; Hodgson, K. O.; Solomon, E. I. *J. Am. Chem. Soc.* **1996**, *118*, in press.
- (378) Westre, T. E.; Loeb, K. E.; Zaleski, J. M.; Hedman, B.; Hodgson, K. O.; Solomon, E. I. *J. Am. Chem. Soc.* **1995**, *117*, 1309.
- (379) Sam, J. W.; Tang, X.-J.; Peisach, J. *J. Am. Chem. Soc.* **1994**, *116*, 5250.
- (380) Burger, R. M.; Kent, T. A.; Horwitz, S. B.; Münck, E.; Peisach, J. *J. Biol. Chem.* **1984**, *258*, 1559.
- (381) (a) Liu, K. E.; Wang, D.; Huynh, B. H.; Edmondson, D. E.; Salifoglou, A.; Lippard, S. J. *J. Am. Chem. Soc.* **1994**, *116*, 7465. (b) Liu, K. E.; Valentine, A. M.; Qiu, D.; Edmondson, D. E.; Appelman, E. H.; Spiro, T. G.; Lippard, S. J. *J. Am. Chem. Soc.* **1995**, *117*, 4997.
- (382) (a) Lee, S.-K.; Fox, B. G.; Froland, W. A.; Lipscomb, J. D.; Münck, E. *J. Am. Chem. Soc.* **1993**, *115*, 6450. (b) Lee, S.-K.; Nesheim, J. C.; Lipscomb, J. D. *J. Biol. Chem.* **1993**, *268*, 21569.
- (383) (a) Ravi, N.; Bollinger, M. J., Jr.; Huynh, B. H.; Edmondson, D. E.; Stubbe, J. *J. Am. Chem. Soc.* **1994**, *116*, 8007. (b) Bollinger, J. M., Jr.; Tong, W. H.; Ravi, N.; Huynh, B. H.; Edmondson, D. E.; Stubbe, J. *J. Am. Chem. Soc.* **1994**, *116*, 8024. (c) Bollinger, J. M., Jr.; Tong, W. H.; Ravi, N.; Huynh, B. H.; Edmondson, D. E.; Stubbe, J. *J. Am. Chem. Soc.* **1994**, *116*, 8015.

- (384) Ravi, N.; Bominaar, E. L. *Inorg. Chem.* **1995**, *34*, 1040.
- (385) Burdi, D.; Sturgeon, B. E.; Tong, W. H.; Stubbe, J.; Hoffman, B. M. *J. Am. Chem. Soc.* **1996**, *118*, 281.
- (386) Palmer, G.; Reedijk, J. *Eur. J. Biochem.* **1991**, *200*, 599.
- (387) Robbins, A. H.; Stout, C. D. *Proc. Natl. Acad. Sci. U.S.A.* **1986**, *86*, 3639.
- (388) Kuo, C.-F.; McRee, D. E.; Fisher, C. L.; O'Handley, S. F.; Cunningham, R. P.; Tainer, J. A. *Science* **1992**, *258*, 434.
- (389) Smith, J. L.; Zaluzec, E. J.; Wery, J.-P.; Niu, L.; Switzer, R. L.; Zalkin, H.; Satow, Y. *Science* **1994**, *264*, 1427.
- (390) Volbeda, A.; Charon, M.-H.; Piras, C.; Hatchikian, E. C.; Frey, M.; Fontecilla-Camps, J. C. *Nature* **1995**, *373*, 580.
- (391) Georgiadis, M. M.; Komiya, H.; Chakrabarti, P.; Woo, D.; Kornuc, J. J.; Rees, D. C. *Science* **1992**, *257*, 1653.
- (392) (a) Kim, J.; Rees, D. C. *Science* **1992**, *257*, 1677. (b) Kim, J.; Rees, D. C. *Nature* **1992**, *360*, 553.
- (393) Kim, J.; Woo, D.; Rees, D. C. *Biochemistry* **1993**, *32*, 7104.
- (394) (a) Bolin, J. T.; Campobasso, N.; Muchmore, S. W.; Morgan, T. V.; Mortenson, L. E. In *Molybdenum Enzymes, Cofactors, and Model Systems*, ACS Symposium Series 535; Stiefel, E. I., Coucouvanis, D.; Newton, W. E., Eds.; American Chemical Society: Washington, DC, 1993; pp 186–195. (b) Bolin, J. T.; Ronco, A. E.; Morgan, T. V.; Mortenson, L. E.; Xuong, N.-H. *Proc. Natl. Acad. Sci. U.S.A.* **1993**, *90*, 1078.
- (395) Bolin, J. T. Private communication.
- (396) Correll, C. C.; Batie, C. J.; Ballou, D. P.; Ludwig, M. L. *Science* **1992**, *258*, 1604.
- (397) McRee, D. E.; Richardson, D. C.; Richardson, J. S.; Siegel, L. M. *J. Biol. Chem.* **1986**, *261*, 10277.
- (398) Lim, L. W.; Shamala, N.; Mathews, F. S.; Steenkamp, D. J.; Hamlin, R.; Xuong, N. H. *J. Biol. Chem.* **1986**, *261*, 15140.
- (399) Cammack, R. *Adv. Inorg. Chem.* **1988**, *32*, 297.
- (400) (a) Fauque, G.; Peck, H. D., Jr.; Moura, J. J. G.; Huynh, B. H.; Berlier, Y.; DerVartanian, D. V.; Teixeira, M.; Przybyla, A. E.; Lospinat, P. A.; Moura, I.; LeGall, J. *FEMS Microbiol. Rev.* **1988**, *54*, 299. (b) Voordouw, G. *Adv. Inorg. Chem.* **1992**, *38*, 397.
- (401) Adams, M. W. W. *Biochim. Biophys. Acta* **1990**, *1020*, 115.
- (402) Cammack, R. In *Bioinorganic Catalysis*; Reedijk, J., Ed.; Marcel Dekker: New York, 1993; Chapter 7.
- (403) Fu, W.; Drozdowski, P. M.; Morgan, T. V.; Mortenson, L. E.; Juszczak, A.; Adams, M. W. W.; He, S.-H.; Peck, H. D., Jr.; DerVartanian, D. V.; LeGall, J.; Johnson, M. K. *Biochemistry* **1993**, *32*, 4813.
- (404) Long, J. R.; Holm, R. H. *J. Am. Chem. Soc.* **1994**, *116*, 9989. (This article contains a listing of structurally defined Fe-S clusters.)
- (405) Wang, G.; Benecky, M. J.; Huynh, B. H.; Cline, J. F.; Adams, M. W. W.; Mortenson, L. E.; Hoffman, B. M.; Münck, E. *J. Biol. Chem.* **1984**, *259*, 14328.
- (406) Telsner, J.; Benecky, M. J.; Adams, M. W. W.; Mortenson, L. E.; Hoffman, B. M. *J. Biol. Chem.* **1986**, *261*, 13536.
- (407) Telsner, J.; Benecky, M. J.; Adams, M. W. W.; Mortenson, L. E.; Hoffman, B. M. *J. Biol. Chem.* **1987**, *262*, 6589.
- (408) Rusnak, F. M.; Adams, M. W. W.; Mortenson, L. E.; Münck, E. *J. Biol. Chem.* **1987**, *262*, 38.
- (409) Papaefthymiou, V.; Girerd, J.-J.; Moura, I.; Moura, J. J. G.; Münck, E. *J. Am. Chem. Soc.* **1987**, *109*, 4703.
- (410) Adams, M. W. W.; Eccleston, E.; Howard, J. B. *Proc. Natl. Acad. Sci. U.S.A.* **1989**, *86*, 4932.
- (411) Zambrano, I. C.; Kowal, A. T.; Mortenson, L. E.; Adams, M. W. W.; Johnson, M. K. *J. Biol. Chem.* **1989**, *264*, 20974.
- (412) Thomann, H.; Bernardo, M.; Adams, M. W. W. *J. Am. Chem. Soc.* **1991**, *113*, 7044.
- (413) Meyer, J.; Gagnon, J. *Biochemistry* **1991**, *30*, 9697.
- (414) George, G. N.; Prince, R. C.; Stokley, K. E.; Adams, M. W. W. *Biochem. J.* **1989**, *259*, 597.
- (415) Goh, C.; Weigel, J. A.; Holm, R. H. *Inorg. Chem.* **1994**, *33*, 4861.
- (416) Kim, J.; Rees, D. C. *Biochemistry* **1994**, *33*, 393.
- (417) (a) Marritt, S. J.; Farrar, J. A.; Breton, J. L. J.; Hagen, W. R.; Thomason, A. J. *Eur. J. Biochem.* **1995**, *232*, 501. (b) de Vocht, M. L.; Kooter, I. M.; Bulsink, Y. B. M.; Hagen, W. R.; Johnson, M. K. *J. Am. Chem. Soc.* **1996**, *118*, 2766.
- (418) Payne, M. J.; Chapman, A.; Cammack, R. *FEBS Lett.* **1993**, *317*, 101.
- (419) Smith, E. T.; Adams, M. W. W. *Biochim. Biophys. Acta* **1994**, *1206*, 105.
- (420) Przybyla, A. E.; Robbins, J.; Menon, N.; Peck, H. D., Jr. *FEMS Microbiol. Rev.* **1992**, *88*, 109.
- (421) Albracht, S. P. J. *Biochim. Biophys. Acta* **1994**, *1188*, 167.
- (422) (a) Teixeira, M.; Moura, I.; Xavier, A. V.; Huynh, B. H.; DerVartanian, D. V.; Peck, H. D., Jr.; LeGall, J.; Moura, J. J. G. *J. Biol. Chem.* **1985**, *260*, 8942. (b) Cammack, R.; Patil, D. S.; Hatchikian, E. C.; Fernandez, V. M. *Biochim. Biophys. Acta* **1987**, *912*, 98. (c) Huynh, B. H.; Patil, D. S.; Moura, I.; Teixeira, M.; Moura, J. J. G.; DerVartanian, D. V.; Czechowski, M. H.; Prickril, B. C.; Peck, H. D., Jr.; LeGall, J. *J. Biol. Chem.* **1987**, *262*, 795. (d) Moura, I.; Xavier, A. V.; Moura, J. J. G.; LeGall, J.; DerVartanian, D. V.; Peck, H. D., Jr.; Huynh, B. H. *J. Biol. Chem.* **1989**, *264*, 16435. (e) Guigliarelli, B.; More, C.; Fournel, A.; Asso, M.; Hatchikian, E. C.; Williams, R.; Cammack, R.; Bertrand, P. *Biochemistry* **1995**, *34*, 4781.
- (423) Scott, R. A.; Wallin, S. A.; Czechowski, M.; DerVartanian, D. V.; LeGall, J.; Peck, H. D., Jr.; Moura, I. *J. Am. Chem. Soc.* **1984**, *106*, 6864.
- (424) (a) Garondeau, D. P.; Roberts, L. M.; Lindahl, P. A. *J. Am. Chem. Soc.* **1994**, *116*, 3442. (b) Roberts, L. M.; Lindahl, P. A. *Biochemistry* **1994**, *33*, 14339. (c) Roberts, L. M.; Lindahl, P. A. *J. Am. Chem. Soc.* **1995**, *117*, 2565.
- (425) van der Swaan, J. W.; Albracht, S. P.; Fontijn, R. D.; Slater, E. C. *FEBS Lett.* **1985**, *179*, 271.
- (426) Whitehead, J. P.; Gurbel, R. J.; Bagyinka, C.; Hoffman, B. M.; Maroney, M. J. *J. Am. Chem. Soc.* **1993**, *115*, 5629.
- (427) Fan, C.; Teixeira, M.; Moura, J.; Moura, I.; Huynh, B.-H.; LeGall, J.; Peck, H. D., Jr.; Hoffman, B. M. *J. Am. Chem. Soc.* **1991**, *113*, 20.
- (428) Maroney, M. J. *Comments Inorg. Chem.* **1995**, *6*, 347.
- (429) Maroney, M. J.; Colpas, G. J.; Bagyinka, C.; Baidya, N.; Mascharak, P. K. *J. Am. Chem. Soc.* **1991**, *113*, 3962.
- (430) Bagyinka, C.; Whitehead, J. P.; Maroney, M. J. *J. Am. Chem. Soc.* **1993**, *115*, 3576.
- (431) Surerus, K. K.; Chen, M.; van der Zwaan, J. W.; Rusnak, F. M.; Kolk, M.; Duin, E. C.; Albracht, S. P. J.; Münck, E. *Biochemistry* **1994**, *33*, 4980.
- (432) Bryant, F. O.; Adams, M. W. W. *J. Biol. Chem.* **1989**, *264*, 5070.
- (433) Orme-Johnson, W. H. *Annu. Rev. Biophys. Biophys. Chem.* **1985**, *14*, 419.
- (434) *New Horizons in Nitrogen Fixation*; Palacios, R.; Mora, J., Newton, W. E., Eds.; Kluwer Academic Publishers: Dordrecht, 1993.
- (435) Eady, R. R.; Leigh, G. J. *J. Chem. Soc., Dalton Trans.* **1994**, 2739.
- (436) (a) Rees, D. C.; Chan, M. K.; Kim, J. *Adv. Inorg. Chem.* **1994**, *40*, 89. (b) Howard, J. B.; Rees, D. C. *Annu. Rev. Biochem.* **1994**, *63*, 235.
- (437) Burgess, B. K. *Chem. Rev.* **1990**, *90*, 1377.
- (438) Lindahl, P. A.; Day, E. P.; Kent, T. A.; Orme-Johnson, W. H.; Münck, E. *J. Biol. Chem.* **1985**, *260*, 11160.
- (439) Carney, M. J.; Papaefthymiou, G. C.; Spartalian, K.; Frankel, R. B.; Holm, R. H. *J. Am. Chem. Soc.* **1988**, *110*, 6084.
- (440) Thorneley, R. N. F.; Ashby, G. A.; Fisher, K.; Lowe, D. J. In *Molybdenum Enzymes, Cofactors, and Models*; Stiefel, E. I., Coucouvanis, D., Newton, W. E., Eds.; American Chemical Society: Washington, DC, 1993; pp 290–302.
- (441) Wolle, D.; Dean, D. R.; Howard, J. B. *Science* **1992**, *258*, 992.
- (442) Bolin, J. T.; Ronco, A. E.; Mortenson, L. E.; Morgan, T. V.; Williamson, M.; Xuong, N.-H. In *Nitrogen Fixation: Achievements and Objectives. Proceedings of the 8th International Congress on Nitrogen Fixation Research*; Gresshoff, P. M., Roth, L. E., Stacy, G., Newton, W. E., Eds.; Chapman & Hall: New York, 1990; pp 117–122.
- (443) Shah, V. K.; Brill, W. J. *Proc. Natl. Acad. Sci. U.S.A.* **1977**, *74*, 5468.
- (444) (a) Pierik, A. J.; Wassink, H.; Haaker, H.; Hagen, W. R. *Eur. J. Biochem.* **1993**, *212*, 51. (b) Tittsworth, R. C.; Hales, B. J. *J. Am. Chem. Soc.* **1993**, *115*, 9763.
- (445) (a) Stack, T. D. P.; Carney, M. J.; Holm, R. H. *J. Am. Chem. Soc.* **1989**, *111*, 1670. (b) Challen, P. R.; Koo, S.-M.; Dunham, W. R.; Coucouvanis, D. *J. Am. Chem. Soc.* **1990**, *112*, 2455.
- (446) Cai, L.; Segal, B. M.; Long, J. R.; Scott, M. J.; Holm, R. H. *J. Am. Chem. Soc.* **1995**, *117*, 8863.
- (447) (a) Hoover, T. R.; Imperial, J.; Ludden, P. W.; Shah, V. K. *Biochemistry* **1989**, *28*, 2768. (b) Imperial, J.; Hoover, T. R.; Madden, M. S.; Ludden, P. W.; Shah, V. K. *Biochemistry* **1989**, *28*, 7796.
- (448) Krüger, T.; Krebs, B.; Henkel, G. *Angew. Chem., Int. Ed. Engl.* **1989**, *28*, 61.
- (449) Nordlander, E.; Lee, S. C.; Cen, W.; Wu, Z. Y.; Natoli, C. R.; Di Cicco, A.; Filippini, A.; Hedman, B.; Hodgson, K. O.; Holm, R. H. *J. Am. Chem. Soc.* **1993**, *115*, 5549.
- (450) Cen, W.; MacDonnell, F. M.; Scott, M. J.; Holm, R. H. *Inorg. Chem.* **1994**, *33*, 5809.
- (451) MacDonnell, F. M.; Ruhlandt-Senge, K.; Ellison, J.; Holm, R. H.; Power, P. P. *Inorg. Chem.* **1995**, *34*, 1815.
- (452) (a) Chen, J.; Christiansen, J.; Campobasso, N.; Bolin, J. T.; Tittsworth, R. C.; Hales, B. J.; Rehr, J. J.; Cramer, S. P. *Angew. Chem., Int. Ed. Engl.* **1993**, *32*, 1592. (b) Chen, J.; Christiansen, J.; Tittsworth, R. C.; Hales, B. J.; George, S. J.; Coucouvanis, D.; Cramer, S. P. *J. Am. Chem. Soc.* **1993**, *115*, 5509.
- (453) Christiansen, J.; Tittsworth, R. C.; Hales, B. J.; Cramer, S. P. *J. Am. Chem. Soc.* **1995**, *117*, 10017.
- (454) Eliezer, D.; Frank, P.; Gillis, N.; Newton, W. E.; Doniach, S.; Hodgson, K. O. *J. Biol. Chem.* **1993**, *268*, 20953.
- (455) Liu, H. I.; Filippini, A.; Gavini, N.; Burgess, B. K.; Hedman, B.; Di Cicco, A.; Natoli, C. R.; Hodgson, K. O. *J. Am. Chem. Soc.* **1994**, *116*, 2418.
- (456) Conradson, S. D.; Burgess, B. K.; Newton, W. E.; Di Cicco, A.; Filippini, A.; Wu, Z. Y.; Natoli, C. R.; Hedman, B.; Hodgson, K. O. *Proc. Natl. Acad. Sci. U.S.A.* **1994**, *91*, 1290.
- (457) (a) Ma, L.; Gavini, N.; Liu, H. I.; Hedman, B.; Hodgson, K. O.; Burgess, B. K. *J. Biol. Chem.* **1994**, *269*, 18007. (b) Ma, L.; Brosius, M. A.; Burgess, B. K. *J. Biol. Chem.* **1996**, *271*, 10528.
- (458) Holm, R. H.; Simhon, E. D. In *Molybdenum Enzymes*; Spiro, T. G., Ed.; Wiley: New York, 1985; Chapter 1.

- (459) Demadis, K. D.; Coucouvanis, D. *Inorg. Chem.* **1995**, *34*, 436.
- (460) Demadis, K. D.; Campana, C. F.; Coucouvanis, D. *J. Am. Chem. Soc.* **1995**, *117*, 7832.
- (461) Deng, H.; Hoffmann, R. *Angew. Chem., Int. Ed. Engl.* **1993**, *32*, 1062.
- (462) Thorneley, R. N. F.; Lowe, D. J. *Molybdenum Enzymes*; Spiro, T. G., Ed.; Wiley: New York, 1985; Chapter 5.
- (463) Dance, I. G. *Aust. J. Chem.* **1994**, *47*, 979.
- (464) Leigh, G. J. *Eur. J. Biochem.* **1995**, *229*, 14.
- (465) (a) Coucouvanis, D.; Mosier, P. E.; Demadis, K. D.; Patton, S.; Malinak, S. M.; Kim, C. G.; Tyson, M. A. *J. Am. Chem. Soc.* **1993**, *115*, 12193. (b) Laughlin, L. J.; Coucouvanis, D. *J. Am. Chem. Soc.* **1995**, *117*, 3118. (c) Malinak, S. M.; Demadis, K. D.; Coucouvanis, D. *J. Am. Chem. Soc.* **1995**, *117*, 3126.
- (466) Bray, R. C. *Q. Rev. Biophys.* **1988**, *21*, 299.
- (467) Enemark, J. H.; Young, C. G. *Adv. Inorg. Chem.* **1994**, *40*, 1.
- (468) Romão, M. J.; Archer, M.; Moura, I.; Moura, J. J. G.; LeGall, J.; Engh, R.; Schneider, M.; Hof, P.; Huber, R. *Science* **1995**, *270*, 1170.
- (469) (a) Chan, M. K.; Mukund, S.; Kletzin, A.; Adams, M. W. W.; Rees, D. C. *Science* **1995**, *267*, 1463. (b) Schindelin, H.; Kisker, C.; Hilton, J.; Rajagopalan, K.; Rees, D. C. *Science* **1996**, *272*, 1615.
- (470) George, G. N.; Prince, R. C.; Mukund, S.; Adams, M. W. W. *J. Am. Chem. Soc.* **1991**, *114*, 3521.
- (471) (a) Rajagopalan, K. V. *Adv. Enzymol. Relat. Areas Mol. Biol.* **1991**, *64*, 215. (b) Rajagopalan, K. V.; Johnson, J. L. *J. Biol. Chem.* **1992**, *267*, 10199.
- (472) Cramer, S. P.; Wahl, R.; Rajagopalan, K. V. *J. Am. Chem. Soc.* **1981**, *103*, 7721.
- (473) Hille, R.; George, G. N.; Eidsness, M. K.; Cramer, S. P. *Inorg. Chem.* **1989**, *28*, 4018.
- (474) Cramer, S. P.; Solomonson, L. P.; Adams, M. W. W.; Mortenson, L. E. *J. Am. Chem. Soc.* **1984**, *106*, 1467.
- (475) George, G. N.; Kipke, C. A.; Prince, R. C.; Sunde, R. A.; Enemark, J. H.; Cramer, S. P. *Biochemistry* **1989**, *28*, 5075.
- (476) George, G. N.; Turner, N. A.; Bray, R. C.; Morpeth, F. F.; Boxer, D. H.; Cramer, S. P. *Biochem. J.* **1989**, *259*, 693.
- (477) George, G. N.; Hilton, J.; Rajagopalan, K. V. *J. Am. Chem. Soc.* **1996**, *118*, 1113.
- (478) Hille, R.; Sprecher, H. *J. Biol. Chem.* **1987**, *262*, 10914.
- (479) Hilton, J. C.; Rajagopalan, K. V. *Arch. Biochem. Biophys.* **1996**, *325*, 139.
- (480) Holm, R. H.; Berg, J. M. *Acc. Chem. Res.* **1986**, *19*, 363.
- (481) Holm, R. H. *Coord. Chem. Rev.* **1990**, *100*, 183.
- (482) (a) Schultz, B. E.; Gheller, S. F.; Muetterties, M. C.; Scott, M. J.; Holm, R. H. *J. Am. Chem. Soc.* **1993**, *115*, 2714. (b) Schultz, B. E.; Holm, R. H. *Inorg. Chem.* **1993**, *32*, 4244.
- (483) (a) Das, S. K.; Chaudhury, P. K.; Biswas, D.; Sarkar, S. *J. Am. Chem. Soc.* **1994**, *116*, 9061. (b) Donahue, J. P.; Holm, R. H. Results to be published.
- (484) (a) Xiao, Z.; Young, C. G.; Enemark, J. H.; Wedd, A. G. *J. Am. Chem. Soc.* **1992**, *114*, 9194. (b) Oku, H.; Ueyama, N.; Kondo, M.; Nakamura, A. *Inorg. Chem.* **1994**, *33*, 209. (c) Laughlin, L. J.; Young, C. G. *Inorg. Chem.* **1996**, *35*, 1050.
- (485) Donahue, J. P.; Holm, R. H. *Polyhedron* **1993**, *12*, 571.
- (486) Das, S. K.; Biswas, D.; Maiti, R.; Sarkar, S. *J. Am. Chem. Soc.* **1996**, *118*, 1387.
- (487) Sarker, S.; Das, S. K. *Proc. Indian Acad. Sci. (Chem. Sci.)* **1992**, *104*, 533.
- (488) (a) Yoshinaga, N.; Ueyama, N.; Okamura, T.; Nakamura, A. *Chem. Lett.* **1990**, 1655. (b) Boyde, S.; Ellis, S. R.; Garner, C. D.; Clegg, W. *J. Chem. Soc., Chem. Commun.* **1986**, 1541. (c) Ueyama, N.; Oku, H.; Nakamura, A. *J. Am. Chem. Soc.* **1992**, *114*, 7310.
- (489) Bailey, S.; Evans, R. W.; Garratt, R. C.; Gorinsky, B.; Hasnain, S.; Horsburgh, C.; Jhoti, H.; Lindley, P. F.; Mydin, A.; Sarra, R.; Watson, J. L. *Biochemistry* **1988**, *27*, 5804.
- (490) Sarra, R.; Garratt, R.; Gorinsky, B.; Jhoti, H.; Lindley, P. *Acta Crystallogr.* **1990**, *B46*, 763.
- (491) Anderson, B. F.; Baker, H. N.; Dodson, E. J.; Norris, G. E.; Rumball, S. V.; Waters, J. M.; Baker, E. N. *Proc. Natl. Acad. Sci. U.S.A.* **1987**, *84*, 1769.
- (492) Anderson, B. F.; Baker, H. N.; Norris, G. E.; Rice, D. W.; Baker, E. N. *J. Mol. Biol.* **1989**, *209*, 711.
- (493) Shongwe, M. S.; Smith, C. A.; Ainscough, E. W.; Baker, H. M.; Brodie, A. M.; Baker, E. N. *Biochemistry* **1992**, *31*, 4451.
- (494) Day, C. L.; Anderson, B. F.; Tweedie, J. W.; Baker, E. N. *J. Mol. Biol.* **1993**, *232*, 1084.
- (495) Smith, C. A.; Anderson, B. F.; Baker, H. M.; Baker, E. N. *Biochemistry* **1992**, *31*, 4527.
- (496) Anderson, B. F.; Baker, H. N.; Norris, G. E.; Rumball, S. V.; Waters, J. M.; Baker, E. N. *Nature* **1990**, *344*, 784.
- (497) Lindley, P. F.; Bajaj, M.; Evans, R. W.; Garratt, R. C.; Hasnain, S. S.; Jhoti, H.; Kuser, P.; Neu, M.; Patel, K.; Sarra, R.; Strange, R.; Walton, A. *Acta Crystallogr.* **1993**, *D49*, 292.
- (498) Dewan, J. C.; Mikami, B.; Hirose, M.; Sacchettini, J. C. *Biochemistry* **1993**, *32*, 11963.
- (499) Lawson, D. W.; Artymiuk, P. J.; Yewdall, S. J.; Smith, J. M. A.; Livingstone, J. C.; Treffry, A.; Luzzago, A.; Levi, S.; Arosio, P.; Cesarini, G.; Thomas, C. D.; Shaw, W. V.; Harrison, P. M. *Nature* **1991**, *349*, 541.
- (500) Furey, W. F.; Robbins, A. H.; Clancy, L. L.; Winge, D. R.; Wang, B. C.; Stout, C. D. *Science* **1986**, *231*, 704.
- (501) Robbins, A. H.; McRee, D. E.; Williamson, M.; Collett, S. A.; Xuong, N. H.; Furey, W. F.; Wang, B. C.; Stout, C. D. *J. Mol. Biol.* **1991**, *221*, 1269.
- (502) (a) Harris, D. C.; Aisen, P. In *Iron Carriers and Iron Proteins*; Loehr, T. M., Ed.; VCH Publishers: New York, 1989; Chapter 3. (b) Aisen, P. In *Iron Carriers and Iron Proteins*; Loehr, T. M., Ed.; VCH Publishers: New York, 1989; Chapter 4.
- (503) Baker, E. N. *Adv. Inorg. Chem.* **1994**, *41*, 389.
- (504) Kretchmar, S. A.; Reyes, Z. E.; Raymond, K. N. *Biochim. Biophys. Acta* **1988**, *956*, 85.
- (505) Aisen, P. In *Iron in Biochemistry and Medicine*; Jacobs, A., Worwood, M., Eds.; Academic Press: New York, 1980; Vol. II, pp 87–129.
- (506) Harris, W. R.; Pecoraro, V. L. *Biochemistry* **1983**, *22*, 292.
- (507) Harris, W. R. *Biochemistry* **1983**, *22*, 3920; *J. Inorg. Biochem.* **1986**, *27*, 41.
- (508) Thiel, E. C. *Annu. Rev. Biochem.* **1987**, *56*, 298.
- (509) Harrison, P. M.; Lilley, T. H. In *Iron Carriers and Iron Proteins*; Loehr, T. M., Ed.; VCH Publishers: New York, 1989; Chapter 2.
- (510) Harrison, P. M.; Andres, S. C.; Artymiuk, P. J.; Ford, G. C.; Guest, J. R.; Hirtzmann, J.; Lawson, D. M.; Livingstone, J. C.; Smith, J. M. A.; Treffry, A.; Yewdall, S. J. *Adv. Inorg. Chem.* **1991**, *36*, 449.
- (511) Lawson, D. M.; Treffry, A.; Artymiuk, P. J.; Harrison, P. M.; Yewdall, S. J.; Luzzago, A.; Cesareni, G.; Levi, S.; Arosio, P. *FEBS Lett.* **1989**, *254*, 207.
- (512) Harrison, P. M.; Fischbach, F. M.; Hoy, T. G.; Haggis, G. H. *Nature* **1967**, *216*, 1188.
- (513) (a) Mann, S.; Williams, J. M.; Treffry, A.; Harrison, P. M. *J. Mol. Biol.* **1987**, *198*, 405. (b) Mann, S.; Bannister, J. V.; Williams, R. J. P. *J. Mol. Biol.* **1986**, *188*, 225.
- (514) Towe, K. M.; Bradley, W. F. *J. Colloid Interface* **1967**, *24*, 384.
- (515) (a) Sayers, D. E.; Theil, E. C.; Rennick, R. J. *J. Biol. Chem.* **1983**, *258*, 14076. (b) Yang, C.-Y.; Meagher, A.; Huynh, B. H.; Sayers, D. E.; Theil, E. C. *Biochemistry* **1987**, *26*, 497.
- (516) Cheesman, M. R.; Thomson, A. J.; Greenwood, C.; Moore, G. R.; Kadir, F. *Nature* **1990**, *346*, 771.
- (517) Theil, E. C.; Raymond, K. N. In *Bioinorganic Chemistry*; Bertini, I., Gray, H. B., Lippard, S. J., Valentine, J. S., Eds.; University Science Books: Mill Valley, CA, 1994; Chapter 1.
- (518) (a) *Metallothionein*; Kägi, J. H. R.; Nordberg, M., Eds.; Birkhauser Verlag: Basel, 1979. (b) *Metallothionein II*; Kägi, J. H. R., Kokima, Y., Eds.; Birkhauser Verlag: Basel, 1985.
- (519) (a) Hamer, D. H. *Annu. Rev. Biochem.* **1986**, *55*, 913. (b) Kägi, J. H. R.; Schäfer, A. *Biochemistry* **1988**, *27*, 8509.
- (520) Otvos, J. D.; Petering, D. H.; Shaw, C. F. *Comments Inorg. Chem.* **1989**, *9*, 1.
- (521) *Metallothioneins*; Stillman, M. J., Shaw, C. F., III, Suzuki, K. T., Eds.; VCH Publishers: New York, 1992.
- (522) Robbins, A. H.; Stout, C. D. In ref 521, Chapter 3.
- (523) (a) Winge, D. R.; Miklossy, K. A. *J. Biol. Chem.* **1982**, *257*, 3471. (b) Nielson, K. B.; Winge, D. R. *J. Biol. Chem.* **1984**, *259*, 4941.
- (524) Schultze, P.; Wörgötter, E.; Braun, W.; Wagner, G.; Vašák, M.; Kägi, J. H. R.; Wüthrich, K. *J. Mol. Biol.* **1988**, *203*, 251.
- (525) Braun, W.; Vašák, M.; Robbins, A. H.; Stout, C. D.; Wagner, G.; Kägi, J. H. R.; Wüthrich, K. *Proc. Natl. Acad. Sci. U.S.A.* **1992**, *89*, 10124.
- (526) Whitener, M. A.; Bashkin, J. K.; Hagen, K. S.; Girerd, J.-J.; Gamp, E.; Edelstein, N.; Holm, R. H. *J. Am. Chem. Soc.* **1986**, *108*, 5607.
- (527) Dean, P. A. W.; Vittal, J. J. In ref 521, Chapter 14.
- (528) Hencher, J. L.; Khan, M.; Said, F. F.; Tuck, D. G. *Polyhedron* **1985**, *4*, 1263.
- (529) Hagen, K. S.; Holm, R. H. *Inorg. Chem.* **1983**, *22*, 3171.
- (530) (a) Otvos, J. D.; Armitage, I. M. *Proc. Natl. Acad. Sci. U.S.A.* **1980**, *77*, 7094. (b) Dalgarno, D. C.; Armitage, I. M. *Met. Ions. Biol. Syst.* **1984**, *6*, 113. (c) Otvos, J. D.; Engeseth, H. R.; Wehrli, S. *Biochemistry* **1985**, *24*, 6735.
- (531) Nettersheim, D. G.; Engeseth, H. R.; Otvos, J. D. *Biochemistry* **1985**, *24*, 6744.
- (532) Petering, D. H.; Krezoski, S.; Chen, P.; Pattanaik, A.; Shaw, C. F., III. In ref 521, Chapter 7.
- (533) Klug, A.; Schwabe, J. W. R. *FASEB J.* **1995**, *9*, 597.
- (534) Berg, J. M.; Shi, Y. *Science* **1996**, *271*, 1081.
- (535) Eklund, H.; Brändén, C.-I. In *Zinc Enzymes*; Spiro, T. G., Ed.; Wiley: Interscience: New York, 1983; Chapter 4.
- (536) Honzatko, R. B.; Crawford, J. L.; Monaco, H. L.; Ladner, J. E.; Edwards, B. F. P.; Evans, D. R.; Warren, S. G.; Wiley, D. C.; Ladner, R. C.; Lipscomb, W. N. *J. Mol. Biol.* **1982**, *160*, 219.
- (537) Lipscomb, W. N. *Adv. Enzymol. Relat. Areas Mol. Biol.* **1994**, *68*, 67.
- (538) Fairall, L.; Schwabe, J. W. R.; Chapman, L.; Finch, J. T.; Rhodes, D. *Nature* **1993**, *366*, 483.
- (539) Pavletich, N. P.; Pabo, C. O. *Science* **1991**, *252*, 809.
- (540) Pavletich, N. P.; Pabo, C. O. *Science* **1993**, *261*, 1701.
- (541) Marmorstein, R.; Carey, M.; Ptashne, M.; Harrison, S. C. *Nature* **1992**, *356*, 408.

- (542) Bordas, J.; Dodson, G. G.; Grewe, H.; Koch, M. H. J.; Krebs, B.; Randall, J. *Proc. R. Soc. London* **1983**, B219, 21.
- (543) (a) Smith, G. D.; Swenson, D. C.; Dodson, E. G.; Dodson, G. G.; Reynolds, C. D. *Proc. Natl. Acad. Sci. U.S.A.* **1984**, 81, 7093. (b) Sowadski, J. M.; Handschumaker, M. D.; Krishna Murthy, H. M.; Foster, B. A.; Wyckoff, H. W. *J. Mol. Biol.* **1985**, 186, 417.
- (544) (a) Gomis-Rüth, F. X.; Kress, L. F.; Bode, W. *EMBO J.* **1993**, 12, 4157. (b) Gomis-Rüth, F. X.; Kress, L. F.; Kellermann, J.; Mayr, I.; Lee, X.; Huber, R.; Bode, W. *J. Mol. Biol.* **1994**, 239, 513.
- (545) Zhang, D.; Botos, I.; Gomis-Rüth, F.-X.; Doll, R.; Blood, C.; Njoroge, F. G.; Fox, J. W.; Bode, W.; Meyer, E. F. *Proc. Natl. Acad. Sci. U.S.A.* **1994**, 91, 8447.
- (546) Kannan, K. K.; Notstrand, B.; Fridborg, K.; Lövgren, S.; Ohlsson, A.; Petef, M. *Proc. Natl. Acad. Sci. U.S.A.* **1975**, 72, 51.
- (547) Liljas, A.; Kannan, K. K.; Bergstén, P.-C.; Waara, I.; Fridborg, K.; Strandberg, B.; Carlsson, U.; Järup, L.; Lövgren, S.; Petef, M. *Nature New Biol.* **1972**, 235, 131.
- (548) Eriksson, A. E.; Jones, T. A.; Liljas, A. *Proteins* **1988**, 4, 274.
- (549) Håkansson, K.; Carlsson, M.; Svensson, L. A.; Liljas, A. *J. Mol. Biol.* **1992**, 227, 1192.
- (550) Alexander, R. S.; Nair, S. K.; Christianson, D. W. *Biochemistry* **1991**, 30, 11064.
- (551) Lesburg, C. A.; Christianson, D. W. *J. Am. Chem. Soc.* **1995**, 117, 6838.
- (552) Dideberg, O.; Charlier, P.; Dive, G.; Joris, B.; Frère, J. M.; Ghuysen, J. M. *Nature* **1982**, 299, 469.
- (553) Sutton, B. J.; Artymiuk, P. J.; Cordero-Borboa, A. E.; Little, C.; Phillips, D. C.; Waley, S. G. *Biochem. J.* **1987**, 248, 181.
- (554) Borkakoti, N.; Winkler, F. K.; Williams, D. H.; D'Arcy, A.; Broadhurst, M. J.; Brown, P. A.; Johnson, W. H.; Murray, E. J. *Nature Struct. Biol.* **1994**, 1, 106.
- (555) Bode, W.; Reinemer, P.; Huber, R.; Kleine, T.; Schmierer, S.; Tschesche, H. *EMBO J.* **1994**, 13, 1263.
- (556) Lovejoy, B.; Hassell, A. M.; Luther, M. A.; Weigl, D.; Jordan, S. R. *Biochemistry* **1994**, 33, 8207.
- (557) Lovejoy, B.; Cleasby, A.; Hassell, A. M.; Longley, K.; Luther, M. A.; Weigl, D.; McGeehan, G.; McElroy, A. B.; Drewry, D.; Lambert, M. H.; Jordan, S. R. *Science* **1994**, 263, 375.
- (558) Spurlino, J. C.; Smallwood, A. M.; Carlton, D. D.; Banks, T. M.; Vavra, K. J.; Johnson, J. S.; Cook, E. R.; Falvo, J.; Wahl, R. C.; Pulvino, T. A.; Wendoloski, J. J.; Smith, D. L. *Proteins* **1994**, 19, 98.
- (559) Stams, T.; Spurlino, J. C.; Smith, D. L.; Wahl, R. C.; Ho, T. F.; Qoronfleh, M. W.; Banks, T. M.; Rubin, B. *Nature Struct. Biol.* **1994**, 1, 119.
- (560) Wilson, D. K.; Rudolph, F. B.; Quijcho, F. A. *Science* **1991**, 252, 1278.
- (561) Baumann, U. *J. Mol. Biol.* **1994**, 242, 244.
- (562) Baumann, U.; Wu, S.; Flaherty, K. M.; McKay, D. B. *EMBO J.* **1993**, 12, 3357.
- (563) Bode, W.; Gomis-Rüth, F. X.; Huber, R.; Zwilling, R.; Stöcker, W. *Nature* **1992**, 358, 164.
- (564) Gomis-Rüth, F. X.; Stöcker, W.; Huber, R.; Zwilling, R.; Bode, W. *J. Mol. Biol.* **1993**, 229, 945.
- (565) Gomis-Rüth, F. X.; Grams, F.; Yiallourous, I.; Nar, H.; Küsthardt, U.; Zwilling, R.; Bode, W.; Stöcker, W. *J. Biol. Chem.* **1994**, 269, 17111.
- (566) Rees, D. C.; Lewis, M.; Lipscomb, W. N. *J. Mol. Biol.* **1983**, 168, 367.
- (567) Schmid, M. F.; Herriott, J. R. *J. Mol. Biol.* **1976**, 103, 175.
- (568) Cheng, X.; Zhang, X.; Pflugrath, J. W.; Studier, F. W. *Proc. Natl. Acad. Sci. U.S.A.* **1994**, 91, 4034.
- (569) Hough, E.; Hansen, L. K.; Birknes, B.; Jynge, K.; Hansen, S.; Horvik, A.; Little, C.; Dodson, E.; Derewenda, Z. *Nature* **1989**, 338, 357.
- (570) Hansen, S.; Hansen, L. K.; Hough, E. *J. Mol. Biol.* **1992**, 225, 543; **1993**, 231, 870.
- (571) Colman, P.; Jansonius, J. N.; Matthews, B. W. *J. Mol. Biol.* **1972**, 70, 701.
- (572) Matthews, B. W.; Weaver, L. H.; Kester, W. R. *J. Biol. Chem.* **1974**, 249, 8030.
- (573) Holmes, M. A.; Matthews, B. W. *J. Mol. Biol.* **1982**, 160, 623.
- (574) Holland, D. R.; Hausrath, A. C.; Juers, D.; Matthews, B. W. *Protein Sci.* **1995**, 4, 1955.
- (575) Volbeda, A.; Lahm, A.; Sakiyama, F.; Suck, D. *EMBO J.* **1991**, 10, 1607.
- (576) Kim, E. E.; Wyckoff, H. W. *J. Mol. Biol.* **1991**, 218, 449.
- (577) Chen, L.; Neidhardt, D.; Kohlbrenner, W. M.; Mandecki, W.; Bell, S.; Sowadski, J.; Abad-Zapatero, C. *Protein Eng.* **1992**, 5, 605.
- (578) Chevrier, B.; Schalk, C.; D'Orchymont, H.; Rondeau, J.-M.; Moras, D.; Tarnus, C. *Structure* **1994**, 2, 283.
- (579) Burley, S. K.; David, P. R.; Sweet, R. M.; Taylor, A.; Lipscomb, W. N. *J. Mol. Biol.* **1992**, 224, 113.
- (580) Kim, H.; Lipscomb, W. N. *Proc. Natl. Acad. Sci. U.S.A.* **1993**, 90, 5006.
- (581) Sträter, N.; Lipscomb, W. N. *Biochemistry* **1995**, 34, 9200, 14792.
- (582) Benning, M. W.; Kuo, J. M.; Raushel, F. M.; Holden, H. M. *Biochemistry* **1994**, 33, 15001.
- (583) Myers, L. C.; Terranova, M. P.; Ferentz, A. E.; Wagner, G.; Verdine, G. L. *Science* **1993**, 261, 1164.
- (584) Wilker, J. J.; Lippard, S. J. *J. Am. Chem. Soc.* **1995**, 117, 8682.
- (585) Vallee, B. L.; Auld, D. S. *Biochemistry* **1990**, 29, 5647; *Acc. Chem. Res.* **1993**, 26, 543.
- (586) (a) *Zinc Enzymes*; Spiro, T. G., Ed.; Wiley-Interscience: New York, 1983. (b) *Zinc Enzymes*; Bertini, I.; Luchinat, C.; Maret, W.; Zeppezauer, M., Eds.; Birkhäuser Verlag: Basel, 1986.
- (587) Stöcker, W.; Gomis-Rüth, F.-X.; Bode, W.; Zwilling, R. *Eur. J. Biochem.* **1993**, 214, 215.
- (588) Stöcker, W.; Grams, F.; Baumann, U.; Reinemer, P.; Gomis-Rüth, F.-X.; McKay, D. B.; Bode, W. *Protein Sci.* **1995**, 4, 823.
- (589) Matthews, B. W. *Acc. Chem. Res.* **1988**, 21, 333.
- (590) Christianson, D. W.; Lipscomb, W. N. *Acc. Chem. Res.* **1989**, 22, 62.
- (591) Kim, H.; Lipscomb, W. N. *Adv. Enzymol. Relat. Areas Mol. Biol.* **1994**, 68, 153.
- (592) Silverman, D. N.; Lindskog, S. *Acc. Chem. Res.* **1988**, 21, 30.
- (593) (a) Betts, L.; Xiang, S.; Short, S. A.; Wolfenden, R.; Carter, C. W., Jr. *J. Mol. Biol.* **1994**, 235, 635. (b) Xiang, R.; Short, S. A.; Wolfenden, R.; Carter, C. W., Jr. *Biochemistry* **1995**, 34, 4516.
- (594) Fenton, D. E.; Okawa, H. *J. Chem. Soc., Dalton Trans.* **1993**, 1349.
- (595) For one exploration of this question, see: Fraústo da Silva, J. J. G.; Williams, R. J. P. *The Biological Chemistry of the Elements*; Clarendon Press: Oxford, 1991; Chapters 6 and 11.
- (596) Frey, C. M.; Stuehr, J. *Met. Ions Biol. Syst.* **1974**, 1, 69.
- (597) Lincoln, S. F.; Merbach, A. E. *Adv. Inorg. Chem.* **1995**, 42, 2.
- (598) Eaton, S. S.; Holm, R. H. *Inorg. Chem.* **1971**, 10, 1446. (This work provides several examples of fluxional Zn(II) complexes.)
- (599) Auld, D. S. *Methods Enzymol.* **1995**, 248, 228.
- (600) Holmquist, B.; Vallee, B. L. *J. Biol. Chem.* **1974**, 249, 4601.
- (601) Lindskog, S. *Adv. Inorg. Biochem.* **1982**, 4, 115.
- (602) Dunn, M. F.; Dietrich, H.; MacGibbon, A. K. H.; Koerber, S. C.; Zeppezauer, M. *Biochemistry* **1982**, 21, 354.
- (603) Jenkins, J.; Janin, J.; Rey, F.; Chiadmi, M.; von Tilbeurgh, H.; Lasters, I.; De Maeyer, M.; Van Belle, D.; Wodak, S. J.; Lauwereys, M.; Stanssens, P.; Mrabet, N. T.; Snauwaert, J.; Matthyssens, G.; Lambeir, A.-M. *Biochemistry* **1992**, 31, 5449.
- (604) Carrell, H. L.; Glusker, J. P.; Burger, V.; Manfre, F.; Tristsch, D.; Biellmann, J.-F. *Proc. Natl. Acad. Sci. U.S.A.* **1989**, 86, 4440.
- (605) Whitlow, M.; Howard, A. J.; Finzel, B. C.; Poulos, T. L.; Winborne, E.; Gilliland, G. *Proteins* **1991**, 9, 153.
- (606) Sträter, N.; Klabunde, T.; Tucker, P.; Witzel, H.; Krebs, B. *Science* **1995**, 268, 1489.
- (607) Wedekind, J. E.; Frey, P. A.; Rayment, I. *Biochemistry* **1995**, 34, 11049.
- (608) Becker, J. W.; Reeke, G. N., Jr.; Wang, J. L.; Cunningham, B. A.; Edelman, G. M. *J. Biol. Chem.* **1975**, 250, 1513.
- (609) Reeke, G. N., Jr.; Becker, J. W.; Edelman, G. M. *J. Biol. Chem.* **1975**, 250, 1525.
- (610) Hardman, K. D.; Agarwal, R. C.; Freiser, M. J. *J. Mol. Biol.* **1982**, 157, 69.
- (611) Weisgerber, S.; Helliwell, J. R. *J. Chem. Soc., Faraday Trans.* **1993**, 89, 2667.
- (612) Emmerich, C.; Helliwell, J. R.; Redshaw, M.; Naismith, J. H.; Harrop, S. J.; Reffery, J.; Kalb (Gilboa), A. J.; Yariv, J.; Dauter, Z.; Wilson, K. S. *Acta Crystallogr.* **1994**, D50, 749.
- (613) Naismith, J. H.; Habash, J.; Harrop, S.; Helliwell, J. R.; Hunter, W. N.; Kalb (Gilboa), A. J.; Yariv, J. *Acta Crystallogr.* **1993**, D49, 561.
- (614) Collyer, C. A.; Henrick, K.; Blow, D. M. *J. Mol. Biol.* **1990**, 212, 211.
- (615) (a) Farber, G. K.; Glasfeld, A.; Tiraby, G.; Ringe, D.; Petsko, G. A. *Biochemistry* **1989**, 28, 7289. (b) Collyer, C. A.; Blow, D. M. *Proc. Natl. Acad. Sci. U.S.A.* **1990**, 87, 1362. (c) Carrell, H. L.; Hoier, H.; Glusker, J. P. *Acta Crystallogr.* **1994**, D50, 113.
- (616) van Tilbeurgh, H.; Jenkins, J.; Chiadmi, M.; Janin, J.; Wodak, S. J.; Mrabet, N. T.; Lambeir, A.-M. *Biochemistry* **1992**, 31, 5467.
- (617) (a) Rose, I. A.; O'Connell, E. L.; Mortlock, R. P. *Biochim. Biophys. Acta* **1969**, 179, 376. (b) Bock, K. B.; Meldal, M.; Meyer, B.; Wiebe, L. *Acta Chem. Scand.* **1983**, B37, 101.
- (618) Ruzicka, F. J.; Wedekind, J. E.; Kim, J.; Rayment, I.; Frey, P. A. *Biochemistry* **1995**, 34, 5610.
- (619) (a) Doi, K.; Antanaitis, B. C.; Aisen, P. *Struct. Bonding* (Berlin) **1988**, 70, 1. (b) Vincent, J. B.; Olivier-Lilley, G. L.; Averill, B. A. *Chem. Rev.* **1990**, 90, 1447.
- (620) Mueller, E. G.; Crowder, M. W.; Averill, B. A.; Knowles, J. R. *J. Am. Chem. Soc.* **1993**, 115, 2974.
- (621) (a) Dietrich, M.; Münstermann, M.; Suerbaum, H.; Witzel, H. *Eur. J. Biochem.* **1991**, 199, 105. (b) Aquino, M. A. S.; Lim, J.-S.; Sykes, A. G. *J. Chem. Soc., Dalton Trans.* **1984**, 429.
- (622) Suerbaum, H.; Körner, M.; Witzel, H.; Althaus, E.; Mosel, B.-D.; Müller-Warmuth, W. *Eur. J. Biochem.* **1993**, 214, 313.
- (623) Hendry, P.; Sargeson, A. M. *Prog. Inorg. Chem.* **1990**, 38, 201, and references therein.